Estimating groundwater recharge from alley farming systems in the southern Murray Basin Australia

Tim Ellis

Submitted as requirement in full for the degree of Doctor of Philosophy

June 2001

Department of Agronomy and Farming Systems

University of Adelaide

Abstract

The clearing of natural vegetation for agricultural purposes in southern Australia has increased groundwater recharge rates by orders magnitude. This has led to large areas of land being affected or threatened by secondary dryland salinity. Alley farming systems, comprising alternate belts of trees and crops, have been proposed for reducing recharge and mitigating salinity. There is a need to be able to estimate the recharge reduction expected from alley farming systems.

This thesis reviews methods for measuring and modelling recharge, and identifies the difficulties associated with modelling tree belts using conventional methods. The major knowledge gaps identified relate to: methods for quantifying the land area occupied by the tree belts; and information regarding the manner in which the belts hydrologically occupy that area.

A new concept for an Equivalent Recharge Zone *ERZ* is therefore presented; *ERZ* is used to introduce the Equivalent No Recharge *ENOR* concept for describing the zone of occupation of a tree belt root zone. A hypothesis is presented such that *ENOR* can be scaled to the leaf area index *LAI* (m^2 m^{-2}) of the belt, relative to the *LAI* of local natural vegetation. It is then shown mathematically that the width *B* (m) of the *ENOR* can be estimated from the leaf area of the tree belt, per unit length of belt *LLA* (m^2 m^{-1}), divided by the *LAI* of local natural vegetation.

The approach is tested by comparing *B* predicted from leaf area, with *B* determined from recharge measurements, at six sites spread across a climate gradient (300 to 700 mm annual average rainfall) between the northern Eyre Peninsula of South Australia and south western Victoria. In a separate experiment in South Australia, predicted *B* was compared with *B* determined from a year of water balance measurements. Both of these experiments showed that the *ENOR* approach could be used to estimate the area hydrologically occupied by a belt of trees. Relative recharge *RR* from an alley farm (relative to recharge from a cropping system) is shown to equal $1 - B/W$, where *W* is the centre-to-centre tree belt spacing. This is called the *ENOR* model, and requires no input parameters from below ground.

Two methods are then developed for estimating *LAI* (from a climate wetness index) and *LLA* (from a survey of farm tree belts), for application of the *ENOR* model to hypothetical alley farms, or where data is not available. Detailed procedures and worked examples are given for applying the *ENOR* model, within the Murray Darling Basin, to estimate

recharge from hypothetical alley farms, and to design alley farms to result in a prescribed recharge.

Users of the techniques can expect an error in *RR* no greater than 20%, when using measured *LLA* and *LAI*. A larger error should be expected where *LLA* and *LAI* are estimated using the methods derived. The thesis concludes that the *ENOR* model will be a useful tool in the development of catchment management plans for addressing dryland salinity from paddock to regional scales.

Statement of originality and consent to photocopying

This work contains no material which has been accepted for the award of any other degree or diploma in any university or other tertiary institution and, to the best of my knowledge and belief, contains no material previously published or written by another person, except where due reference has been made in the text.

I give consent to this copy of my thesis, when deposited in the University Library, being available for loan and photocopying.

Signed

Timothy W. Ellis

This 26th day of June 2001

Acknowledgements

I thank my supervisors Ian Nuberg and Tom Hatton for giving me the space and encouragement to think 'outside the box'; for their admirable mentorship in matters scientific, administrative, political and personal; for having a great sense of humour (i.e. they put up with mine); and for their patience whenever I rejected their advice (quite often and usually unwisely). I am also grateful to Ian for championing the project, and for obtaining the research funding.

Both the University of Adelaide (UA) and CSIRO Land and Water have provided workspace for me, and have generously met all my requests for resources. In this regard I am particularly grateful to David Mathew (UA) and Greg Foster (CSIRO).

The Murray Darling Basin Commission (MDBC) provided the main source of funds for this study, and I thank John Powell for attending to my questions during the early stages of the project. As part of a larger research team of the MDBC project "Low rainfall alley farming systems", I am indebted to Lisa Robins for managing the project (in the latter stages) as well as other team members for their administrative support, for their organisation of agroforestry tours, and for their general encouragement. For this I thank Primary Industries and Resources staff Alex Knight; Greg Dalton; Peter Bullman; Phil Beale; and John Bourne; as well as John Williamson (Department of Natural Resources and Environment, Victoria) and Ivan Mock (Agriculture Victoria).

My presentation of a paper at Envirowater99 Conference in Lausanne, Switzerland in 1999 was funded by: The Wilf Crane Memorial Award; The University of Adelaide; The Cooperative Research Centre for Catchment Hydrology; and The RIRDC/LWRRDC/FWPRDC Joint Venture Agroforestry Program.

During the development of my central concepts, a number of scientists took part in the many associated discussions. These discussions were often intense and sometimes heated. For this I firstly thank my (then) fellow UA student Peter Taylor who, in the early days of the project, acted as a much-needed and discerning 'sounding board' (with sparkling wit and a homonym for every occasion). In the latter stages Richard Silberstein, Mike Raupach, and Lu Zhang (all from CSIRO) filled this role. Especially I thank Richard Stirzaker (CSIRO) for his dogged dissection of, and challenges to my ideas, which undoubtedly helped me to clarify and focus them. Peter Taylor and Isa Yunusa (UA) as well as Warrick Dawes, John Knight, Warren Bond, Mirko Stauffacher, Val Snow, Rob Vertessy, Ian Jolly, Peter Hairsine, Joe Walker, Zahra Paydar, Tim McVicar, and Glen

Walker (all from CSIRO) provided specific and critical information and comment on experimental technique, interpretation of data and mathematical analysis.

Ray Evans and Anthony Stephenson (Australian Geographic Survey Organisation) provided advice regarding the use of hydrogeologic information. Neil McKenzie and Phil Ryan provided information for, and critical appraisal of, site and landform descriptions. Isa Yunusa (Agriculture Victoria), Peter Richardson (CSIRO) and Sandra Roberts (Melbourne University) kindly provided extra climatological and leaf area data.

Many people assisted in the collection and processing of soil and leaf samples, often under difficult weather conditions. In this regard Rebecca Sherman deserves the greatest acknowledgement for her work in the field and laboratory, for her colourful and inspiring friendship, and for her talent in finding offbeat coffee shops in country towns. For field and laboratory work I also thank: Shaun Upton; Adrian Upton; Warwick Donaldson; Christopher Donaldson; Mark Turner; Tommy Wellington; Martyn Ellis; Peter Ellis; Karen Petersen; Colin Rivers (UA); Mr Thompson; Anastasia Dallzeil; Steve Mylius (UA); Rachelle Nevin; James Margules; and Daniel Figucio. Of course no data collection would have been possible without access to farmland. I therefore thank: Robert Selleck; Ian Rice (UA); Mrs Hazeldeane; Mr and Mrs Wakefield; the Verner family; Mr Anderson and Ms Murphy; Mr Simpson; the Bulle family; O.C and D.E. Killalea; W. Anderson; N. Boyer; H. Friend; P. O'Connor; N. Passelaqua; A. Hart; G, C. and R, Davis; W. Esler; D. and L. Kohlhegen; H. Sharkie; D. Daniels; and B. and R. Ross.

I thank CSIRO's Andrew Bradford and Mat Gilfedder for GIS and graphics support; Peter Hairsine for operational and scientific advice; Frances Marston and Sue Cuddy for advice on methods of document construction. Natasha Herron provided valuable ideas on the structure of the final chapter of the thesis.

I am grateful to Michael and Hannah Ellis (Figure 1) who stalwartly endured relative poverty during the Ph.D. period, which has amounted to a significant proportion of their lives (respectively, 0.36 and 0.46). This situation would not have been manageable without the unfaltering generosity of Peter and Jacinta Ellis, who provided us with accommodation for a large part of this time.

For her well-qualified empathy, support and patience I thank Sharon Davis (Figure 2) who also encouraged me to publish my work before writing my thesis – a process that made the latter all the more focussed and satisfying.

Richard Ellis deserves special thanks for agreeing to proof read the penultimate draft, at short notice, and for pointing out that split infinitives are more commonly considered to be acceptable these days.

Figure 1 Hannah and Michael Ellis in 1997, wondering when their father will finish his thesis (only 4 more years).

Figure 2 Sharon Davis off enjoying herself (having already finished her thesis).

Finally I thank George and Floyd, two dogs (*Canis familiaris)* who made life bearable during the long, long hours of neutron moisture meter field measurements.

I recall the whole of my Ph.D. experience (almost without exception) as both enjoyable and rewarding. Undoubtedly this would not have been the case without the input of those mentioned above.

Table of contents

List of figures

List of tables

List of symbols used in the *ENOR* approach and related calculations

A	Equivalent No Recharge area, m^2.
B	Equivalent No Recharge width, m.
C_d	Average annual chloride concentration of groundwater recharge, mg L^{-1}.
C_p	Average annual chloride concentration of precipitation and dryfall, mg L^{-1}.
D	Average annual groundwater recharge, mm yr^{-1}.
d	Distance from coast, km.
E	Evaporation from soil, mm yr^{-1}.
E_0	Average annual pan evaporation, m yr^{-1}.
ENOR	Equivalent No Recharge zone, m^2 or m.
ET	Annual evapotranspiration from a landscape, m yr^{-1}.
I	Interception, L or L m^{-1} tree belt.
L	Leaf area, m^2.
LAI	Leaf Area Index, m^2 m^{-2}.
LLA	Lineal Leaf Area of agroforestry belt, m^2 m^{-1}.
λ	Latent heat of vaporisation of water = 2.4 M J m^{-3}.
P	Average annual rainfall, mm yr^{-1}, m yr^{-1}.
R	Annual net radiation flux, G J m^{-2} yr^{-1}.
RR	Relative recharge; alley farm compared to agricultural land.
ΔS	Change in soil water storage, mm yr^{-1}.
T	Transpiration, L or L, m^{-1} tree belt, or mm or mm yr^{-1}.
W	Alley farm centre-to-centre belt spacing, m.

List of equations

Note: All equations in the thesis are listed below and numbered in order of their first appearance in the text. Key equations have been named. The page number indicates the first reference to the equation in the text. The descriptions, origins and/or derivations of the equations and symbols can be obtained from the text.

Number	Equation	Name	Page
1.	$q = \frac{-K_{sat}\Delta H}{\Delta z}$	Darcy's Law (saturated flow)	32
2.	$q = \frac{-K_{\theta}[\Delta h_{\theta} + \Delta z]}{\Delta z}$	Darcy's Law (unsaturated flow)	32
3.	$\Delta h = \frac{R}{Sy}$		34
4.	$D = \frac{PC_p}{C_d}$	Chloride mass balance	37
5.	$EC_a = EC_w\theta_v T + EC_s$		39
6.	$D = \alpha(P - P_{thr})$		48
7.	$\frac{A_3}{A_2} = \frac{LAI_2}{LAI_1}$		60
8.	$A_3 = \frac{A_2 \times LAI_2}{LAI_1}$		60
9.	$A_2 \times LAI_2 = L_2$		60
10.	$A_3 = \frac{L_2}{LAI_1}$		60
11.	$A = \frac{L}{LAI}$	*ENOR* area	61
12.	$B = \frac{LLA}{LAI}$	*ENOR* width (for tree belt)	61
13.	$RR = \frac{\text{recharge from alley farm}}{\text{recharge from conventional farm}} = 1 - \frac{B}{W}$	Relative Recharge (words and algebraic)	63
14.	$RR = 1 - \frac{B}{W}$	Relative Recharge (algebraic)	63
15.	$RA = RC \times RR$	Actual recharge	63

16.	$A = \frac{T + I}{P - E - \Delta S}$	*ENOR* area (water balance)	83
17.	$B = \frac{T + I}{P - E - \Delta S}$	*ENOR* width (water balance)	83
18.	$\left(\frac{T + I}{P - E}\right)_{isolated} = \left(\frac{T + I}{P - E}\right)_{non-isolated}$	Water balance condition	84
19.	$E_\theta = \frac{s}{b} n \sqrt{\left(\frac{1}{c} + \frac{1}{w}\right)}$	NMM random count error	92
20.	$B(P - E - \Delta S) - T - I = 0$		104
21.	$\frac{R}{\lambda P} \approx \frac{E_0}{P}$	Budyko's index of dryness	110
22.	$k = 0.0045 + \frac{71.57}{E_0}$	Specht's *k*	111
23.	$LAI = 3.5 \frac{P}{E_0}$	*LAI* climate versus index of wetness	118
24.	$ET = \frac{R}{\lambda} \tanh \frac{\lambda P}{R}$	Budyko's evapotranspiration	119
25.	$P = \frac{R}{\lambda} \tanh^{-1} \frac{\lambda ET}{R}$		119
26.	$LAI = 0.0028P - 0.33$	LAI versus rainfall	119
27.	$Module\,area(m^2) = \frac{average\,area\,of\,sub\,samples(m^2) \times total\,mass\,of\,leaf\,(g)}{100}$		198
28.	$C_p = \frac{0.99}{\sqrt[4]{d - 0.23}}$	Chloride concentration in rainfall	203
29.	$PC_p = DC_d$		204
30.	$D = 0.9 \times \frac{PC_p}{C_d}$	Corrected chloride mass balance	204
31.	$\int_0^{Zcf} \theta \, dz = \int_0^{Zd} \theta (1 - \frac{C}{C_d}) \, dz$	Transient chloride front	205
32.	$K = K_s (\frac{\theta}{\theta_s})^{2b+3}$		223

33.	$b = \frac{1}{[-0.25\log(\%clay) + 0.5]}$	Smettem expression for Campbell exponent	223
34.	$K_s = 9.7\times10^9\, a.h_b^{-2}$	Smettem and Bristow saturated hydraulic conductivity	223
35.	$h_b = 43.5\times b$	Bubbling pressure	223
36.	$K = 9.7\times10^9.ah_b^{-2}(\frac{\theta}{\theta_s})^{2b+3}$	Derived unsaturated hydraulic conductivity	224
37.	$V_h = \frac{x_1 + x_2}{2t_0}$		227
38.	$V'_h = a_0 + a_1V_h + a_2V_h^2$		228
39.	$V_s = aV'_h$		228
40.	$V_s = V'_h\left(0.505F_m + F_w\right)$	Sap velocity	228
41.	$Q = \overline{V}_s A_s$	Sap flow	229

Publications arising from this work

Ellis, T.W., T. J. Hatton and I.K. Nuberg, (1999) A simple method for estimating recharge from low rainfall agroforestry systems. *In* (Eds A. Musey, L. Santos Pereira and m. Fritsch) *Envirowater99, 2nd Inter-Regional Conference on Environment-Water, 1-4 September, Laussane*, Switzerland. Presses Polytechnique et Universitaires Romandses, Laussane, 1999.

Ellis, T.W., T. J. Hatton and I.K. Nuberg (in press) An ecological optimality approach for predicting deep drainage from alley farming systems in water-limited environments, submitted to *Water Resources Research*, 2002.

Ellis, T.W., and T.J. Hatton (in press) Relating *LAI* of natural vegetation to climate indices in southern Australia, *Australian Journal of Botany*, submitted March 2002.

Ellis, T.W. and Y. Bessard, (2001) Estimating recharge from alley farms: applying the *ENOR* model within the Murray-Darling Basin –Full Report, CSIRO Land and Water Technical Report 3/01.

Other publications involving this work

Stirzaker, R.J., T.W. Ellis and E.C. Lefroy, (2002) Mixing trees with crops and pastures, *In* Stirzaker, R.J., Vertessy, R.A. and Sarre A. (Eds), *Trees, Water and Salt: an Australian guide for using trees to achieve healthy catchments and productive farms*, RIRDC/LWRRDC/FWPRDC Joint Venture Agrofrestry Program.

Stirzaker, R.J., E.C. Lefroy and T.W. Ellis, (2002) Belts of trees in the cropping landscape; the tradeoff between drainage and yield, *Agricultural Water Management*, 53:187-199.

Walker, G.R. Zhang, L., Ellis, T. W., Hatton, T.J. and C. Petheram, (2001) Towards a predictive framework for estimating recharge under different land uses: review of modelling and other approaches, *Hydrogeology*, 10:68-90.

Dunin, F. X., White D. A., Hatton T. J. and T. W. Ellis (2001) Evapotranspiration characteristics of woody communities, natural and exotic, across southern Australia, *In Proceedings of the MODSIM Conference*, Canberra, August 2001.

Chapter 1

Introduction

Context

This thesis covers the development of a static model for estimating the groundwater recharge expected from alley farming systems. Alley farming is an agroforestry system that comprises belts of trees, alternated across the landscape with strips of crop or pasture (Lefroy and Scott, 1994). Groundwater recharge (hereafter referred to as 'recharge') is the amount of infiltrated water that reaches a specific groundwater system (Walker *et al.*, 2001) and is a significant contributing factor to secondary dryland salinity; a more specific working definition of recharge is given in Chapter 3. Alley farms have been proposed as an alternative to conventional farming systems, with the aim of reducing recharge, and mitigating salinisation of the Murray-Darling Basin, Australia (Stirzaker *et al.*, 2000).

The Murray-Darling Basin covers 84.6 million ha spread across the states of Queensland, New South Wales, Victoria and South Australia, from which is derived 41% of Australia's gross value of agricultural production (Crab, 1997). Large areas of natural vegetation in the basin were cleared for agriculture, mainly during the 1920s and 1950s (Walker *et al.*, 1993), and has been shown to cause groundwater recharge to increase by at least two orders of magnitude (Allison *et al.*, 1990; Kennett-Smith *et al.*, 1992b). In areas where annual rainfall <700 mm, soil profiles contain ancient salt stores, of aeolian origin, and increased recharge in these areas is the principal cause of the salinisation of large areas of

land, and significant inland water supplies (Wood, 1924; Barnett, 1989; Williamson, 1998). Currently, an estimated 2.5 million ha of land is affected by salinity, with the potential for this to increase to 15 million ha over coming decades (PMSEIC, 1999). The exact costs of salinisation is uncertain, but is estimated to be $100 million per year for lost agricultural production alone, and is predicted to double in the next 40 years (PMSEIC, 1999). Annual damage to infrastructure and environmental assets is estimated in the tens of millions of dollars. In South Australia, at the lower end of the Basin, at least 20% of surface water is above recommended salinity limits for human consumption. There is therefore, interest in reducing recharge from agricultural systems in the Murray Basin (Williams *et al.*, 1998; Stirzaker *et al.*, 2000).

In southern Australia, annual crops and pastures, because of their shallow root systems and winter/spring growing seasons, offer little scope for reducing recharge (Walker *et al.*, 1999). Perennial pastures provide greater hope in this regard (Smettem, 1998), but only trees appear to possess the rooting depth and perenniallity to reduce recharge to desired levels for salinity mitigation (Nulsen *et al.*, 1986; Kennet-Smith *et al.*, 1992b; Petheram *et al.*, 2000; Petheram *et al.*, 2001). Unfortunately, salinity-prone areas generally lack the rainfall for commercial forestry. Agroforestry systems therefore, are increasingly being considered as methods for incorporating tree species into agriculture to reduce recharge and mitigate salinsation.

In 1996 The Murray Darling Basin Commission (MDBC) funded the Low Rainfall Alley Farming LRAF research project No. D9005, to investigate the feasibility of alley farming in the 300 mm to 450 mm rainfall zone (Figure 133) of the Murray-Darling Basin (MDBC, 2000). Trial sites were established in 1996 to investigate cultural, agronomic, and productivity aspects of alley farming at: Pallamana, South Australia; Walpeup and Bridgewater, Victoria. A Ph.D. scholarship (this thesis) was also commissioned at the same time. While the original LRAF project was restricted to low-rainfall areas, the scope of this thesis was widened to include higher rainfall areas. This has allowed: interpretation of data over a wider range of climatic conditions (and a more confident validation of the approach); and the development of a model that is applicable to other parts of the Basin.

Aims of this study

This study aims to develop a model for:

1. Predicting recharge from alley farming systems in the Murray Basin;
2. Designing alley farms that will result in a prescribed or 'target' recharge reduction.

Over the next ten years, targets for levels of land and stream salinity will be set and monitored in 20 to 50 major catchments in the around Australia (Agriculture, Forests and Fisheries, 2000); six of these catchments are in the southern Murray Basin. Target setting will be a first stage of the development of catchment management plans for the large-scale management of dryland salinity. This thesis describes the development and testing of a model that can fulfil the above aims, and within a catchment management context.

Thesis structure

To provide a physiographic context for the study, Chapter 2 describes the stratigraphy and hydrogeology of the Murray Basin. Dryland salinity is then defined, and the processes of secondary dryland salinity and stream salinisation are explained with respect to land use change. The temporal and spatial aspects of catchment response to hydrologic perturbations are illustrated with reference to catchment type. Chapter 3 provides a working definition of recharge, reviews recharge measurement and modelling techniques, discusses the problems associated with applying conventional hydrological models to agroforestry systems, and concludes that there is a need for a new approach.

In light of this, a new approach is derived in Chapter 4; a central hypothesis is proposed; and an alley farm recharge model (*ENOR* – Equivalent No Recharge) is constructed. The main input parameters for the model are: Leaf Area Index *LAI* (m^2 m^{-2}) of natural vegetation; and Lineal Leaf Area *LLA* (m^2 m^{-1}) of tree belts. Chapters 5 and 6 describe experiments used to test the model using direct recharge measurements (chloride method - Allison and Hughes, 1983; Walker *et al.*, 1991), and from a water balance perspective. Chapter 7 covers the derivation of a method for estimating *LAI* of natural vegetation; in Chapter 8 a scheme is developed for estimating *LLA* of tree belts. These estimation methods can be used where speed of application of the *ENOR* model is required, or where *LAI* and *LLA* data is not available. Chapter 9 gives procedures for applying the *ENOR* model to hypothetical alley farms within the Murray Darling Basin. Chapter 9 also presents a discussion on the use of the *ENOR* model (within the context of catchment plans), and the limitations and errors associated with its application.

The thesis closes with Chapter 10, which summarises the findings of the thesis with reference to the aims (this Chapter). The experimental hypotheses and their underlying assumptions are reviewed, and in light of this study, three main areas are suggested for future research. The final remarks, while recognising the limitations of the *ENOR* model, conclude that it fulfils the aims of the study and provides a means to estimate the recharge from alley farms, and to design alley farms to result in a prescribed recharge reduction.

Appendices 1 to 5 contain respectively: site descriptions; example calculations; calibrations; error analyses; and maps of elevation, rainfall and evaporation of the Murray Darling Basin.

Chapter 2

The Murray Basin and dryland salinity

Introduction

This chapter defines the study area and provides stratigraphic and hydrogeologic context for salinisation of land and streams in the Murray Basin. The stratigraphy provides an appreciation of the geometry of the Murray Basin and the degree to which its large, relatively flat shape and shallow sediments influence the expression of dryland salinity. A time line of significant tectonic and eustatic events and resulting strata emphasises the geological antiquity of the basin and explains the vertical and horizontal distribution of the sediments forming the key aquifers. The Basin hydrogeology is then summarised and the three provinces identified: Scotia Province; the Riverine Province; and the Murray-Limestone Province – the latter encompasses the Mallee region of the Basin. The aquifers of the Murray-Limestone Province are described in more detail, along with the flow direction, relative magnitude and salinity of the associated groundwater flow systems. At this point salinity in Australia is briefly described and the key contributing factors are discussed: climate; salt stores; hydrogeology; and land cover with particular attention to the latter and its effect on recharge. It is noted that, of the factors contributing to dryland salinity, land cover is the only one that can be effectively manipulated by humans. This has been demonstrated most dramatically by the increases in recharge following the

removal of natural vegetation during the last century (Walker *et al.,* 1993), and the subsequent spread of dryland salinity.

The saline pollution of groundwater and streams are shown to be the major expressions of nature of dryland salinity in the Murray Mallee region, with an associated current and forecast cost of tens of millions of dollars per year. The methods for mitigating dryland salinity are outlined and the distinction is made between 'discharge' and 'recharge' solutions. Because increased recharge has caused the modern increases in salinity, recharge reduction is the logical long-term solution. Three options for reducing recharge over large areas of agricultural land are examined: 1) reduce the recharge from conventional farming systems; 2) replace agriculture with plantation forestry; 3) develop new agricultural systems that control recharge. Conventional farming systems have limited recharge reduction potential and plantation forestry, while it could control recharge, would eliminate valuable agricultural production (Walker *et al.*, 1999). This has prompted interest in new methods of farming such as agroforestry, which incorporate trees in the rural landscape and maintain some agricultural production (Stirzaker *et al.*, 2000). Alley farming systems comprise alternate belts of trees and crops, and are suited to low to medium rainfall, broad acre areas (Lefroy and Scott, 1994). It has been proposed that such spaced tree belts could displace less cropping land than plantations, but reduce recharge over a proportionally larger area because tree roots extend laterally from the belts.

Using real examples of alley plantings in discharge areas on southern Australia, it is emphasised that, these can only ever have a local hydrologic impact, and add little to addressing dryland salinity at a catchment scale.

The chapter therefore concludes there is a need to estimate, *a priori*, the recharge reduction from alley farming systems (in recharge areas) and to be able to design alley farms that result in a prescribed recharge reduction target.

Stratigraphy

The Murray Basin covers about 30 million ha of the southern Murray-Darling Basin. It is the catchment area for the Murray River, which is fed by the Lachlan and Murrumbidgee rivers from the northeast; and the Ovens, Goulburn and Loddon rivers from the south (Figure 3). The average slope of the land surface over much of the 600 km wide Basin is about 0.1%. Brown (1989), Evans and Kellett (1989) describe the Basin as "low-lying" and "saucer-shaped", flanked by subdued mountain ranges, and almost entirely separated from the sea. Brown (1989) noted that the sedimentary sequence is "*extremely thin, consisting of a veneer of platform cover sediments, rather than a 'conventional' basinal*

succession". Basin sediments reach a maximum depth of 600 m and are frequently less than 200 m deep. They are generally saturated, with little remaining storage capacity (Brown, 1989) and, because of the low relief, have low average hydraulic gradients.

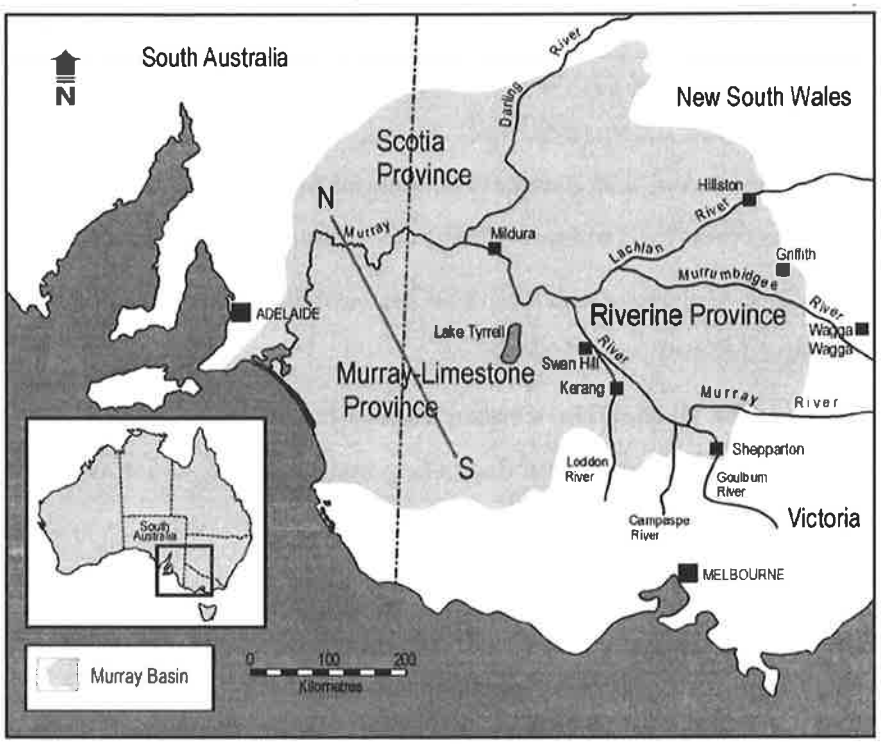

Figure 3 The Murray Basin, southern Australia (modified from Herzceg *et al.*, 2001) showing the three hydrogeologic provinces. The transect NS marks the position of the cross section (Figure 4) of the aquifers of the Murray-Limestone Province which underlie most of the Mallee Region.

The Basin geometry has meant that subtle movements of the Cainozoic basement have had large effects on the sedimentation of the basin and the resulting groundwater systems (Brown, 1989). In a comprehensive geological study of the Murray Basin, Brown and Stephenson (1991) describe and date the geological and geomorphic events that produced the sediments that dictate the hydrogeologic nature of the modern Murray Basin. The Murray Basin has existed as a geological entity since the Late Paleocene, and developed following the break up of Australia and Antarctica. Tectonics has provided the primary control on the Basin development although eustatic and climate changes have also played a part. The most significant events and periods, together with the associated strata, are summarised below, modified from Stephenson and Brown (1989) and Brown and Stephenson (1991).

- *Late Eocene-earliest Oligocene* (35 – 40 Ma) The ancestral Murray River emptied into the sea, probably via a number of estuarine zones, penetrating deep into the basin.

These now form the Renmark Beds, part of the Renmark Group aquifer. Closest to the sea in the southwest, marine sediment formed the Buccleuch Beds.

- *Late Oligocene-early Middle Miocene* (15 – 30 Ma) A marine incursion flooded the western part of the basin, forming the ancient Murravian Gulf. During this time 150 m of bryozoal limestone was deposited in the western parts (limestone formations of the Murray Group) over the marine marl Ettrick Formation. Progressively eastwards, (shorewards) marls were laid down (Winnambool Formation), tidal flats (Geera Clay) and fluvial deltas and flood plains (Olney Formation of the Renmark Group).
- *Late Middle late Miocene* (~10 Ma) The sea retreated from most of the Basin, and tributary valleys became entrenched.
- *Latest Miocene* (5 – 10 Ma) The western Murray Basin was once again invaded by the sea, backfilling entrenchments and depositing marine sands, which were derived from reworking of the underlying sandy limestones.
- *Early Pliocene* (5 Ma) The sea retreated once more, leaving a strand plain of north-westerly trending beach ridges and inter-ridge fluvial deposits (Pliocene Loxton-Parilla Sands). This dune-swale system has been well preserved and can been seen in the modern landscape of north western Victoria and adjacent parts of South Australia.
- *Late Pliocene* (2.5 Ma) A short-lived marine transgression/regression briefly flooded the Murray River valley, but did not affect the rest of the landscape. More influential however, was the tectonic uplift of the Pinnaroo Block, which dammed the Murray River near the modern town of Mannum, about 2.5 Ma ago (Stephenson, 1986). This formed the huge inland Lake Bungunnia, which remained for at least 1.8 Ma and covered 3.3 million ha. The most significant formations resulting from lake depositions are the Bungunnia Limestone and the much more extensive Blanchetown Clay. The lake boundary fluctuated widely, and parts of the Blanchetown Clay are fluvial, rather than lacustrine, but in general, modelling by Stephenson (1986) concluded that the overall climate was at least twice as wet as today. Further to the east on the flood plain, fluvio-lacustrine sediments were forming the basis for the Shepparton Formation.
- *Late Pliocene to Recent* (~1 Ma) The draining of Lake Bungunnia commenced at about 0.7 Ma leaving aeolian-fluvio-lacustrine sediments in the Mallee region. Some remnants of the lake exist today, including Lakes Tyrrell and Hindmarsh (Stephenson, 1986), although they are now maintained mainly by groundwater rather than river influx.

- *Recent* The alternate flooding and draining of the Murray Mallee, resulted in the deposition and reworking of dunal landscapes by both wind and water. The Recent dominant Quaternary morphostratigraphic units of the western parts of the Basin are the Woorinen (sand) Formation and the Molineaux-Lowan Sands, which were formed by aeolian reworking of the Woorinen Formation. The modern Murray Mallee region therefore, comprises largely dune-swale land systems, of which there are several types (Rowan and Downes, 1963; Laute *et al.*, 1977; Brown and Stephenson, 1991) and are covered in the experimental site descriptions, Appendix 1.

Hydrogeology

Murray Basin

The Murray Basin has three regional aquifer provinces (Evans and Kellett, 1989): the Riverine Province, underlying the Riverine Plain and the eastern Mallee region in New South Wales and Victoria; the Scotia Province underlying the arid regions the northern parts of the Basin in South Australia and New South Wales; and the Mallee-Limestone Province underlying the Mallee region in South Australia, and the Mallee and Wimmera regions of western Victoria. All groundwater flow from the provinces discharges to the Murray River, the only outlet from the Basin (Evans and Kellett, 1989), apart from minor potential flow over the Padthaway Ridge in the south west of the Basin (Stephenson and Brown, 1989).

The aquifers hold approximately 4600 000 ML of groundwater, two thirds of which is useful to humans. Accompanying this is an enormous salt load in the aquifers and aquitards of about 100 000 million tonnes. At present rates of groundwater-surface water interaction, it would take 25 000 years to transport this load from the Basin via the Murray River (Evans and Kellet, 1989).

The major aquifers within the provinces are: the Renmark Group (assemblage of Warina Sand Olney Formation and minor Buccleuch Beds in the west); Murray Group (limestone); Pliocene Sands (Loxton-Parilla sands); and the Shepparton Formation (complex assemblage of fluvio-lacustrine sediments restricted to the Riverine Province). The Oligocene Winambool/Geera Clay Formation extends in an arc about 100 km wide, through the centre of the Basin, roughly separating the Mallee-Limestone and the Riverine Provinces. This low permeability formation represents a major impediment to both lateral flow and is one of the factors controlling the distribution of groundwater discharge zones within the basin (Evans and Kellett, 1989).

Mallee-Limestone province

The Mallee-Limestone province contains the deepest sediments in the Basin, sequentially with age these are (see Figure 4): the Renmark Group; the Ettrick Formation aquitard; the Murray Group; the Winnambool and Geera Clay aquitard formations (not shown in the NS cross section); the Loxton-Parilla Sands; and the Plioscene Sands. The province underlies most of the Murray Mallee region in South Australia and Victoria, and is bounded in the southwest by the Padthaway ridge. Groundwater flows tend generally northwest from the Wimmera Region, then west towards the Murray River. A small amount of groundwater flows over the Padthaway Ridge to the Upper Southeast Region of South Australia (Evans and Kellett, 1989). Groundwater quality in the older, lower aquifers is generally good, and often fit for human consumption (<1500 $\mu S\ cm^{-1}$). In the more recent sediments however, salinity levels can be as high as high as seawater (50 000 to 60 000 $\mu S\ cm^{-1}$).

The lowest aquifer of the Mallee-Limestone Province is the Renmark Group, and is generally 150 m below the land surface and about 150 m thick (Figure 4). From this aquifer groundwater discharges to the north west by upward flow through the lower confining layer (Ettrick Formation) of the overlying Murray Group limestone aquifer, and into the lower reaches of Murray River. Further north there is some mixing with groundwater from the Riverine Province (Stephenson and Brown, 1989). The geometry of groundwater flows is complex. Evans and Kellet (1989) collated groundwater quality information for Murray basin aquifers and it is displayed graphically on a Preliminary Shallow Groundwater Map of the Murray Basin (Evans, 1988). Salinity of groundwater in the Renmark group ranges from about 1500 $\mu S\ cm^{-1}$ (1000 mg L^{-1}) in the southern recharge areas to 4500 $\mu S\ cm^{-1}$ towards the northern and western boundaries of the province. Salinity increases towards the north eastern and western boundaries of the Renmark Group, due to intrusions from the Riverine province, and flow over the Padthaway Ridge, respectively. On the northern boundary near the Murray River, there is an abrupt increase to 35 000 $\mu S\ cm^{-1}$.

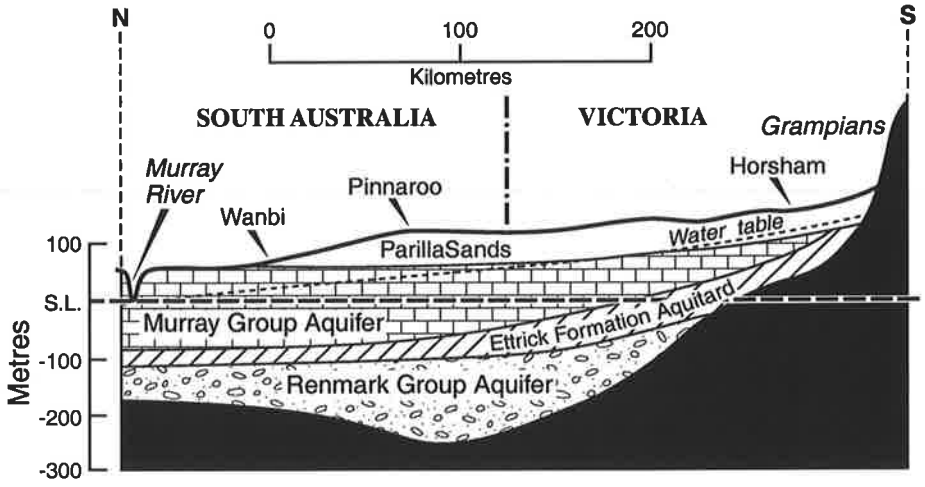

Figure 4 Cross section of the aquifers of the Murray-Limestone Province underlying the Mallee Region. *Source*: CSIRO.

Overlying the Renmark Group is the Murray Group aquifer (Figure 4), comprising middle Tertiary marine limestone and calcarenite and is the most intensively exploited regional aquifer in the Basin (Evans and Kellett, 1989). The aquifer generally underlies an upper confining layer in the central and western parts of the province, but becomes semi-confined in the southern and eastern areas where it is overlain by clay-marl (mainly the Winnambool Formation and Geera Clay) and the Loxton-Parilla Sands, respectively. Significant recharge occurs in both these areas, and aquifer discharge occurs in zones along the Murray River to the north. Groundwater of good quality and generally less than 1500 $\mu S\ cm^{-1}$ in the south; about 9500 $\mu S\ cm^{-1}$ in the north west; and 1900 $\mu S\ cm^{-1}$ on the eastern boundary, grading into the low-permeability Winambool Formation (Evans and Kellett, 1989). In the north there is also thought to be upward discharge to the Murray Group aquifer from the Renmark Group, raising the salinity, and downward leakage from the overlying Loxton-Parilla Sands to the Murray Group aquifer in the south of the province.

The Pliocene Sands aquifer is the shallowest aquifer in the Murray Limestone province. It is largely unconfined and is recharged by downward percolation; sands are saturated only in the eastern parts of the province. The sands are discontinuous in the central west of the province and the Murray Group aquifer becomes unconfined as it does in the west (Figure 4). Groundwater flow is in the same direction as, and eventually coincides with, that in the Murray Group aquifer, discharging directly to the Murray River. A large amount of groundwater is lost from the aquifer, on its way to the Murray River, by evaporation from

discharge zones at the land surface. The salinity of the groundwater in the Pliocene Sands aquifer is generally high (45 000 to 60 000 μS cm $^{-1}$) but can be much higher near the discharge zones. The water table is 30 m to 60 m below the land surface over most of the Mallee region (Evans, 1988). There is therefore a time delay between increased recharge at the surface and the resulting pressure front adding to the water table. Jolly *et al.* (1989) showed that, in a Mallee soil where the water table was 60 m below the surface, the post-clearing pressure front would take about 80 years to reach the water table. The implications for this with respect to the response of a catchment to such a perturbation, and the subsequent salinisation of land and streams is discussed in the next section.

Salinity in southern Australia

Saline streams and discharge areas occur naturally in much of Australia, principally in low to medium rainfall zones and such phenomena are often referred to as primary salinity. However it is secondary salinity, induced by landscape changes, that is of concern over large areas of southern Australia, and very recently, Queensland (PMSEIC, 1999). Secondary salinity has numerous definitions (Taylor, 1996) but the one most useful to this thesis is "*adverse changes in salinity of soils and waters due to human activities*". It is also important to make the distinction here between irrigation salinity, which is not dealt with in this thesis, and dryland salinity. Irrigation salinity results form either the use of saline water for irrigating crops or from the alteration of water table height and/or salinity levels by irrigation practices. Dryland salinity occurs in non-irrigated areas where changes in land–use perturb hydrologic equilibria. This severe form of land degradation is not confined to the Murray Basin and is generally a problem on agricultural land in Australia where the average annual rainfall is less than 700 mm (Williamson, 1998), which is insufficient to flush salt from the aquifer. It is now clear that degradation of agricultural land is only one of the costs of secondary salinity. Equal, and in some case larger, in magnitude are the costs associated with: damage to rural roads, buildings and towns; loss of ecosystem and habitat; pollution of urban water supplies; and loss of production form irrigated agriculture. The basic processes behind secondary dryland salinity in Australia have been known for many decades (Wood, 1924). It is only in recent decades, however, that both the scale and the possible consequences of increasing salinity have been appreciated by scientists and land managers (Peck, 1977; Barnett, 1989; Barnett *et al.*, 1996; George *et al.*, 1999). It was only very recently that it has caught the attention of the wider community (PMSEIC, 1999). The expression of secondary salinity can vary but

each case requires three basic ingredients: a source of salt; mobilisation of the salt; discharge of the salt.

The process

Recharge is the amount of infiltrated water that reaches a specific groundwater system; increased recharge has, in most cases, been the primary cause of secondary dryland salinity in southern Australia. Before land clearing, groundwater systems were in (or close to) equilibrium such that recharge equalled groundwater discharge, either subsurface to streams, or the land surface if water tables were shallow. Salt stores in the regolith, before clearing, were also stable because they generally existed below the root zone (Peck, 1977), below which recharge was very small. If recharge is increased then so too must discharge, although there will be a delay dependent on the size and type of the groundwater system. Increased discharge at the land surface can only be accommodated by larger discharge area. The increased recharge also remobilises the salt store.

Secondary dryland salinity can occur following the salinisation of a water table that discharges to the land surface, or by the raising of an already saline water table so that surface discharge occurs. Stream salinity can be increased by sub-surface addition of saline water or surface wash-off from saline discharge areas. Salt accumulates in saline discharge areas, limiting plant growth, or completely eliminating it in severe cases.

Coram *et al.*, (2000) list four key factors contributing to dryland salinity as:

- The amount of water input to the catchment surface through rainfall and removed through evaporation (climate);
- The amount of water that can infiltrate from the catchment surface to the groundwater system (land cover);
- The amount of salt stored in the catchment and available for mobilisation by groundwater (salt stores);
- The structural and geomorphic features of the catchment that determine how much groundwater can be stored, how far it will flow, and what will cause the discharge.

Coram *et al.* (2000) note that these factors are interrelated: the first two determining whether dryland salinity can occur; and the second two determine the inherent susceptibility of the catchment to dryland salinity. The authors address each key factor briefly; I have addressed the issues similarly, under the same headings, together with additional issues specific to the Murray Mallee region and this thesis.

Climate

It is somewhat paradoxical that dryland salinity, one of the most significant forms of land and water degradation, occurs in areas of relatively low annual rainfall (400 mm – 700 mm), and is due principally to an 'excess' of water.

The southern Australian climate is characterised by a winter-dominant rainfall (Australian Bureau of Meteorology, 2000) at which time rainfall exceeds evaporative demand, and often the storage capacity of the soil. The latter is somewhat dependent on the soil depth considered and the methods of redistribution of water in the root zone (Nulsen *et al.*, 1986). Where excess water cannot be used during the cooler months (because of low atmospheric demand), nor stored and utilised over summer, recharge occurs on a regular basis.

Coram *et al.* (2000) noted that climate, therefore, in part explains the widespread occurrence of dryland salinity in southern agricultural lands, especially where annual rainfall exceeds 400 mm. Australian rainfall is typically strongly episodic (Lewis, 1998; Zhang *et al.*, 1999), meaning it is distributed as infrequent, significant events (Barnes *et al*, 1994; 'significant', in this case, refers to the relative magnitude of the recharge event) and has a large bearing on the frequency and magnitude of recharge episodes. As a consequence, recharge in the Mallee region is also generally regarded to be episodic. In areas where rainfall is either evenly distributed throughout the year, or occurs mainly in summer (as is the case in northern New South Wales and Southern Queensland) it is episodicity, rather than a mismatch of rainfall and atmospheric demand, that can induce dryland salinity. Zhang *et al.* (1999) modelled recharge from fallow, crops and pastures at two sites where annual rainfall was 564 mm and 351 mm. The authors showed that 10% of the annual events accounted for 25 – 85% of the total recharge, up to 130 mm yr^{-1}. Because of the many influencing factors however, such as: antecedent soil moisture; magnitude and duration of the rainfall episodes; winter rainfall or summer storms; or presence or absence of, or even growth stage of a crop, it is difficult to give typical characteristic of rainfall events that cause recharge.

Land cover

Much of the natural vegetation in the Basin was cleared for agriculture in the 1920s and 1950s (Walker *et al.*, 1993; Figure 5). Natural vegetation has a large perennial component that prospers in the Australian climate because of: conservative water use to ensure survival through drought periods, most likely evolving in a way similar to that suggested by Eagleson (1982); deeper rooting depth and the ability to store excess water deep in the

profile (Nulsen *et al.*, 1986); perennial growth, allowing use of water, over the dry summer, that was stored during the winter, or following large rainfall episodes. In the large majority of soil types therefore, undisturbed natural vegetation systems evaporates almost all the rainfall, and recharge is very small (Petheram *et al.*, 2000). Carbon *et al.* (1982) however, measured recharge below native banksia heath land was 43% of the 775 mm annual rainfall on deep sand plains in Western Australia, but this is not typical for southern Australia.

Annual crops and pastures generally lack all of the above attributes, and consequently often cannot use all the rainfall. Zhang *et al.* (1999) used computer modelling to predict recharge from typical Mallee land uses practices: bare fallow; wheat (*Triticum aestivum*) and oats crops (*Avena sativa*); lucerne (*Medicago sativa*) and medic (*Medicago spp.*) pasture. They concluded that while deeper-rooted plants such as lucerne can reduce the mean annual recharge, they are not likely to eradicate the largest recharge events. Excess water therefore moves through the soil profile beyond the root zone, increasing rates of recharge by up to one hundred times that under native vegetation (Allison *et al*, 1990; Smettem, 1998; Petheram, 2000). The increased recharge causes water tables to rise, bringing salt stored in the regolith, eventually discharging at the land surface, or increasing discharge to streams.

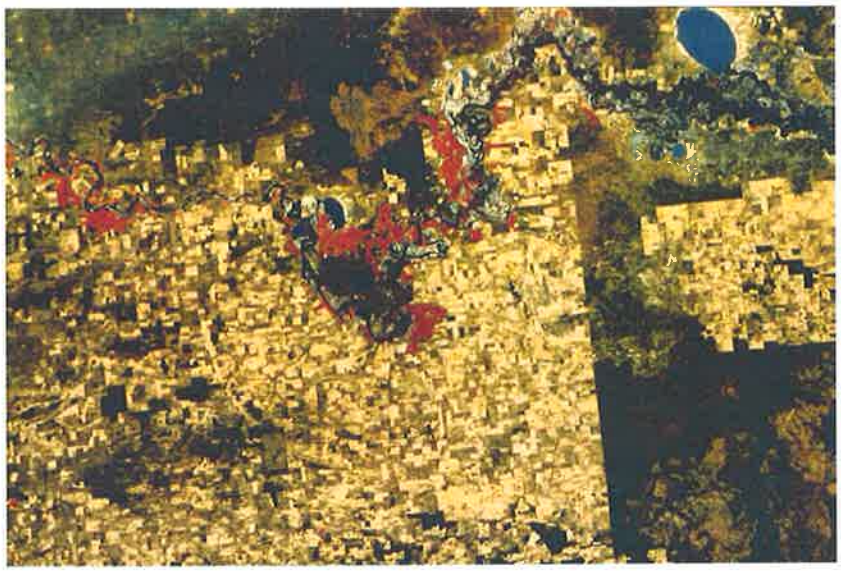

Figure 5 Satellite image showing the Murray River and the South Australian – Victorian border. Light areas are farm land and dark areas are natural vegetation. The different clearing patterns are due to legislative differences between the two states. *Source:* Murray Darling Basin Commission.

Salt stores

Soluble salts that occur in soils consist of various proportions of the cations - sodium; calcium, magnesium, and potassium; and anions – chloride, sulphate, bicarbonate and nitrate. The origin of salts has been a topic for some debate in the past (Hutton and Leslie, 1958; Hingston and Gailitis, 1976; Gunn and Richardson, 1979). Some carbonate and sulphate salts originate from the deep weathering of sedimentary and granitic parent rock and ancient marine sediments, respectively (Gunn and Richardson, 1979). Sodium chloride however is derived principally from the sea, carried by wind and rain (Hutton and Leslie, 1958; Hingston and Gailitis, 1976). Herczeg *et al.* (2001) evaluated four hypotheses for the origin of salt in the Murray Basin aquifers these being: a) mixing with original seawater; b) dissolution of salt deposits; c) weathering of aquifer minerals; and d) acquisition of solutes via rainfall. The authors concluded: "*About 1.5 million tons of new salt is deposited in the Murray Basin each year by rainfall. The groundwater chemistry has evolved by a combination of atmospheric fallout of marine and continentally derived solutes and the removal of water by evapotranspiration over tens of thousands of years of relative aridity*".

Rainfall has a very low salt concentration of about 5 mg L^{-1} (Hutton, 1976). Plants transpire the water, concentrating the salt in the soil profile (Peck, 1977). Soil water in the unsaturated zone beneath native Mallee vegetation has salt concentrations between 15 000 and 40 000 mg L^{-1} (Cook *et al.*, 1993). This is therefore flushed into the largely unconfined Loxton-Parilla Sands aquifer, and following that, water of <300 mg L^{-1} salt concentration (Jolly *et al.*, 1989).

Hydrogeology

Groundwater flow systems can comprise one, or an assemblage of, aquifers. Each aquifer can be thought of, very simplistically, as a vessel. They are filled in recharge areas, they have some finite storage capacity, and they drain via discharge zones. Aquifers occur in a range of sizes; a description of the three major classes of groundwater flow systems is reproduced below from Coram (1998).

- ***Regional groundwater flow systems*** *are characterised by laterally extensive aquifers, which may be thicker than 300 m, and recharge and discharge areas separated by distances of 50 km or more. They occur in areas of low relief such as alluvial plains. The aquifers in regional systems are usually wholly or partly confined, and can be overlain by local or intermediate systems. The time for groundwater discharge to*

occur following post-clearing increases in groundwater recharge may be as great as one hundred years.

- ***Intermediate groundwater flow systems*** *are intermediate in extent between local and regional systems, generally occurring within individual catchments but also sometimes flowing between smaller sub-catchments. They tend to occur in valleys, and typically occur over a horizontal extent of 5 km to 10 km.*
- ***Local groundwater flow systems*** *have recharge and discharge areas within a few kilometres of one another. They tend to occur within individual sub-catchments, in areas of higher relief such as foothills to ranges. These systems exhibit dryland salinity within a decade or so of clearing.*

The Murray Mallee is classified as a regional groundwater flow system (Figure 6), therefore having a hydraulic response time in the order of hundreds of years, which must be kept in mind when assessing costs and benefits of attempts to mitigate salinity.

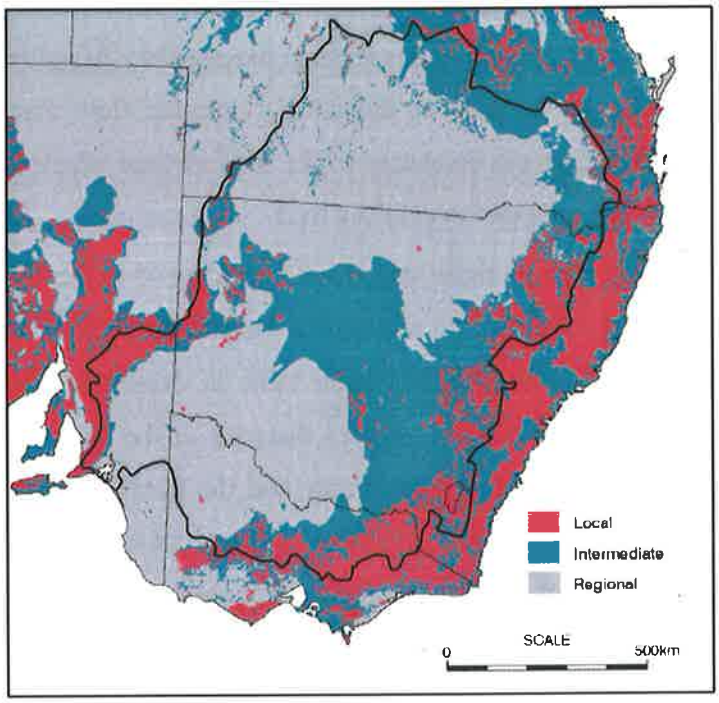

Figure 6 Groundwater flow systems of southeast Australia as categorised by Coram *et al.* (2000). *Source:* National Land and Water Audit.

Recharge to aquifers can be from rainfall, as with the Loxton-Parilla Sands aquifer and the Murray Group limestone aquifer where it is unconfined. Where the water table is close to the land surface, recharge and discharge zones can occupy the same space, although actual recharge and discharge events are usually separated in time. Such situations occur in the low-lying areas of the Murray Mallee near Lakes Tyrrell and Hindmarsh, as well as closer

to the Murray River and east of the Padthaway Ridge. Although these interactions are important, this thesis is focussed on the processes of recharge via rainfall and deals only with recharge in pure recharge areas, where water tables are deep and inaccessible to vegetation. This is discussed further at the end of this chapter.

For a given climate and vegetation cover, the groundwater recharge rates are determined by principles governing all fluid mechanics (Duncan *et al.*, 1970) and Darcy's Law for the movement of fluids through porous media (Marshall *et al* (1996). Cook (1990) showed that recharge rates in the Murray Mallee was highly dependent on soil clay content, and give average values for sandy loams and sands of 5 mm yr^{-1} and 35 mm yr^{-1}, respectively. This led Good (1994) to list dune soils as a higher priority for recharge reduction measures in the Mallee.

Recharge to unconfined aquifers in the Mallee usually occurs via unsaturated soil water flow below the root zone, except following extreme episodic events and where the water table is shallow. Where water tables are shallow, discharge can occur via capillary rise to the land surface or, if the water table is deeper than the capillary fringe but within reach of plant roots, by transpiration or gaseous diffusion. Saturated flow discharge occurs via subsurface flow to streams, or via discharge to the land surface where the potentiometric head coincides with, or exceeds the level of the land.

Episodic recharge events such as those described by Zhang *et al.* (1999) move relatively slowly in the unsaturated state. For an event of a specific magnitude, the delay between leaving the root zone and adding to the water table is determined by the unsaturated hydraulic conductivity of the soil and vertical distance to the water table (Jolly *et al.*, 1989). The soil saturated hydraulic conductivity and the potentiometric head determine saturated flow discharge rates. Discharge from shallow water tables is controlled by: available energy and/or plant leaf conductance (Monteith and Unsworth, 1990); soil hydraulic properties (Marshal *et al.*, 1996); gaseous diffusivity of the soil (Monteith and Unsworth, 1990).

For a given rate of recharge, the area over which it occurs determines the actual recharge flux. Similarly, the discharge flux is dependent on the transmissivity of the aquifer, or its thickness and the hydraulic conductivity. For a given recharge flux, an aquifer will transmit water according to its transmissivity (Coram *et al.*, 2000). If recharge is increased, discharge will also increase, the speed of response depending on the extent of the groundwater flow system, the geological structure of the catchment, and the geomorphological/topographical setting of the catchment (Coram, 1998; Coram *et al.*,

2000). When recharge increases beyond the transmissivity of the aquifer, new flow patterns are formed to accommodate an increase in discharge, and surface discharge areas can increase.

Groundwater in confined aquifers becomes pressurised and can be forced upwards through confining layers as with the Renmark Group. If restrictions occur low in the catchment, water may discharge to the land surface higher in the catchment. In the case of the unconfined Loxton-Parilla Sands aquifer, the potentiometric surface is raised, increasing lateral flow towards the Murray River, as well as the land surface discharge area (northern parts of the Murray-Limestone province) and increasing downward leakage into the Murray Group aquifer. Geological features can also change the transmissivity of aquifers and, the case of the Murray Mallee, effect discharge patterns and the likely future increases. Geological fault or constrictions in the regolith depth reduce transmissivity and change groundwater flow directions. The Morgan, Murrayville and Danyo Fault lines have a significant effect on the location of subsurface discharge to the Murray River and discharge at the land surface in the north of the province. The Padthaway Ridge similarly determines the fate of much of the low-lying areas in the southwest of the Basin (Evans, 1988)

Dryland salinity in the Murray Mallee

Barnett (1989) predicted with finite element computer modelling (25 km grid size) that there would be two deleterious effects of rising water tables in the Murray Mallee. Firstly, the low-lying areas of land to the southwest of the Mallee region will be salinised. This process has already begun and has the potential to affect all below 20 m, Australian Height Datum (AHD) in by 2040. At 1989 values, Barnett estimated lost land value to be in the order of $60 million and about $20 million loss of agricultural production, annually. Secondly, 50 years after the Murray group aquifer begins responding to the increased recharge, salinity of water in the Murray River near the town of Morgan is predicted to increase by 70 $\mu S\ cm^{-1}$ and cost $4.9 million annually. Barnett (1990) undertook additional modelling but using higher recharge rates estimated by Cook (1989). Cook *et al.* (1993) confirmed that there is no doubt that the groundwater below the Murray Mallee (Loxton-Parilla Sands aquifer) will be salinised in coming decades. There is also some evidence that the unconfined parts of the Murray Group (limestone) aquifer are already being salinised in the Mallee region. These trends were also confirmed by Barnett *et al.* (2000). This could eventually render the upper part of the aquifer unusable for domestic purposes and the entire aquifer unusable for irrigation.

Good (1994) used finite element modelling, but with a 7 km grid size, to simulate various revegetation scenarios on river salinity, as well as the effects of a large irrigation area in the northern part of the South Australian Mallee. Good (1994) predicted continual reductions in salt inputs to the Murray River for 200 years after revegetation of farming areas takes effect and, due mainly to the relatively deep watertable, 300 to 1000 years before land salinisation occurs in the central and southern Mallee. As part of the Murray-Darling Basin Salinity Audit (MDBC, 2000) Barnett *et al.* (2000) again modelled the effect of revegetation of the Mallee on salinity trends in the Murray River, assuming no change to recharge from irrigation areas. The authors used finite element grid cell sizes of mostly 500 m, allowing better tests for sensitivity to revegetation strategies. The authors also attempted to model flood plain processes as they significantly affect the rate and timing of salt loads entering the main river channel. Barnett *et al.* (2000) predicted the total cost of river salinity increased due solely to clearing would be: \$8.3 million yr^{-1}; \$16.7 million yr^{-1}; and \$24.6 million yr^{-1} in 2020, 2050 and 2100, respectively.

Mitigating dryland salinity in the Murray Mallee

Having established the need to reduce recharge to address dryland salinity, this section discusses the potential of three land management options: current farming systems; revegetation; new land use systems.

Current farming systems

Williams *et al.* (1998) give a summary review of how recharge from current farming systems has caused much of the dryland salinity problem in Australia. Many believe that since current farming systems are the cause of the problem, they cannot be used to solve the problem. Others believe that crops and pasture systems can be modified, with addition of perennial species, early sowing and double cropping, to reduce recharge to levels that will achieve useful mitigation of salinity (Dunin *et al*, 1999; Ringrose-Voase *et al.*, 1999; Ringrose-Voase and Cresswell, 2000). The greatest scope for doing so is where soil profiles can store a lot of water at depths that is still accessible to subsequent crops, and where rainfall is more evenly distributed throughout the year, rather than winter-dominated. This is the case for areas New South Wales such as the Liverpool Plains (Ringrose-Voase and Cresswell, 2000). The Mallee region however mostly lacks both of these properties. Good (1994) and Barnett *et al.* (2000) list several options for reducing recharge from agricultural land by modifying current farming practices; these generally involve increasing water use. This can be achieved by: earlier sowing of crops; improving fertiliser application; establishment of perennial pasture, chenopods and native pastures

suited to the conditions. This is a step in the right direction and will undoubtedly be an important component in future strategies for reducing recharge on agricultural land. Where reductions in recharge are required to approximate pre-clearing values however, it is likely that no manner of reorganisation of timing, combination of species or improved yields will achieve this. Farming systems using 'conventional' species will always be limited in their ability to control recharge by rooting depth and/or their lack of perenniality (Zhang *et al*, 1999).

Revegetation

Barnett (1990), Good (1994) and Barnett *et al.* (2000), following testing of various revegetation scenarios for the Murray Mallee, emphasised the efficacy of completely revegetating strips of land 5 km to 40 km wide adjacent to the Murray River. Barnett (1990) found that completely revegetating a strip 40 km wide would reduce river salinity increases at the town of Morgan by 50%. Good (1994) predicted that 20 km of vegetation would at least halve the salt load entering the river. Barnett *et al.* (2000), using a more sensitive model, showed that a revegetated strip of only 5 km wide will reduce increases in river salinity by 55% in the next 20 years, and strips of 10 km and 20 km wide achieve only 7% and 10% greater reduction, respectively. The modelling also indicated that about 70% of future groundwater discharge to the river will originate from the south, and therefore revegetation of land north of the river will have a small effect.

The authors note that the modelling assumed instantaneous reduction of recharge, following revegetation, to pre-clearing values in 2000. However, in reality, such a reduction would take decades. Also, saline inflow to the river will gradually increase again after 150 to 200 years due to water table rise outside the revegetated zones. Longer-term reductions would therefore require recharge to be reduced over larger portions of the Mallee region.

Further groundwater flow modelling work is planned for this region (Barnett pers. comm.) to more accurately predict saline groundwater influx to the Murray River in time and space. This will allow more specific design of revegetation strategies for land close to the river. The new work will include time delays between revegetation and recharge reduction that will reflect both the establishment phase for the new vegetation and variation in depth to water table.

New land-use systems

George *et al.* (1999) suggests that to reduce recharge levels in Western Australia sufficiently to reduce dryland salinity, 70% to 80% of the landscape will need to be

revegetated. This is likely to be impractical due to both the sheer enormity of the task and the opportunity costs associated with the displacement of agricultural production. This is, of course, unless the species used for revegetation have intrinsic value approaching that of conventional agriculture. To this end, several scientific projects aim to identify new plant species for southern Australia (Cooperative Research Centre for Plant-Based Management of Dryland Salinity, 2001; RIRDC, 1999). Stirzaker *et al.* (2000) summarised all of the current and likely future options for agricultural systems in areas affected or threatened by dryland salinity. Of these, only three 'new' systems: companion farming; low rainfall trees; and agroforestry are both applicable to the Murray Mallee region, and have the potential to reduce recharge. Companion farming is the practice of incorporating perennial species (such as lucerne) into annual crops and pastures. This would achieve a recharge reduction similar to that demonstrated by Zhang *et al.*, (1999) with perennial lucerne. Low rainfall trees, if grown in the Mallee region, are likely to reduce recharge to very low values. However, as with new agricultural plants, there is currently no low rainfall tree species with a product that has financial returns comparable to cropping and grazing.

Agroforestry systems offer potential for significant recharge reduction while maintaining some agricultural production (RIRDC, 2000). They may comprise discrete plantings such as wood lots and windbreaks which take up small parts of the landscape, or can be rotated in time with other crops as proposed by Harper (see "Phase farming with trees", RIRDC, 2000; Stirzaker *et al.*, 2000). Also known as 'short rotation agroforestry' this system involves planting fast-growing tree species such as *Eucalyptus globulus* in areas where there is fresh groundwater close to the surface or where there is water stored in the soil profile. Once the trees have depleted the moisture reserves, they are harvested to make way for conventional crops. The rotation is then repeated elsewhere on the farm, thereby intermittently reducing recharge to zero in discrete areas, but also significantly reducing overall recharge from the farm.

Alley farming

Alley farming is an agroforestry system that mixes belts of trees with crops and pastures, allowing conventional agriculture to take place in the intervening areas (Figure 7). This system was originally developed for tropical landscapes to promote a diversification of plant species in the production system and also to help stabilise steep slopes (Kang *et al.*, 1990; Nuberg and Evans, 1993). Alley farming was also often alleged to have significant overall productivity advantages over conventional systems. However, initial trial results were subsequently shown to be misleading due to the confounding influence of tree root

invasion into control plots, lowering crop yields and creating an impression of a higher relative yield from the alley system (Ong and Ong, 1994). About the same time, however, the promise of higher productivity and the simultaneous advantages of wind protection, higher water use and greater bio-diversity made the alley farming concept attractive for parts of southern Australia (Francis, 1992; Lefroy and Scott, 1994). There was a significant level of interest from Australian farmer groups for whom alley farming offered solutions to a range of problems including wind erosion, lack of stock shelter and rising water tables (Agriculture Western Australia, 2001). An added attraction was early reports of yield increases of field crops (Bicknell, 1991; Burke, 1991). However subsequent reviews and exhaustive experimental studies have concluded that shelter-induced yield improvements in field crops are generally not as high nor as frequent as first thought (Nuberg, 1998; Cleugh *et al*, 1998; Cleugh and Prinsley, 1998) although wind breaks can significantly reduce damage from extreme wind events.

Growing concern regarding salinity has maintained the interest in alley farming (Figure 7) as a means for reducing recharge (Stirzaker and Lefroy, 1997). It was generally thought that such systems would eliminate recharge beneath the belts of trees, and reduce recharge significantly for some distance either side of the belts. The overall effect was a reduction in the average recharge from the landscape. These values, however, had been neither measured nor modelled. For planning and design purposes there was a need for a means of predicting both the width of influence of the tree belts and the reduced (equivalent diffuse) recharge expected from an entire alley farm.

Figure 7 Alley farming systems using single rows of *Eucalyptus occidentalis* in Western Australia (left) and an aerial view 2 m wide belts of *Acacia saligna* in South Australia (right; *Source*: Alex Knight).

The case for alley farming in recharge areas, not discharge areas

When discussing dryland salinity in the Murray Basin, I stressed the need to reduce recharge, and because it is recharge increases that have brought about increases in dryland

salinity, it makes sense to address the problem, not increased catchment discharge, which is a symptom. There will be situations where it is a good idea to vegetate discharge areas for production reasons, possibly with alleys, but this will usually only occur where groundwater is fresh.

If a discharge area is a relatively fresh and accessible (shallow) water source, trees are likely to grow well, an increase in evaporation from the discharge area by growing trees can never significantly change the catchment water balance, because discharge is limited by aquifer transmissivity (Coram *et al.*, 2000). Any hydrologic effects will be very local only; and, if the groundwater is fresh, then there is no salinity problem. If the discharge area were saline, there would be even less incentive to vegetate it. Trees growing over shallow saline water tables either accumulate salt in their root zone until they eventually cannot survive, or they live on fresh water from rainfall, which floats on top of the (more dense) saline water (Strizaker, 2001). In the latter situation, the trees are still only accessing rainfall and, although it would better to have trees than no trees, they will not change the salinisation trajectory of the catchment. To illustrate this point I have included Figure 8 and Figure 9 which show young alley farms planted in a discharge zone at Cook Plains, and in the Upper South East Region of South Australia.

Figure 8 A pit dug to expose an extremely saline (60 000 µS cm $^{-1}$) water table 1.5 m below a eucalypt alley farm in a discharge area of the Cook Plains, South Australia. The water table is rising slowly; in the long-term the trees are likely to die as they cannot use the water; their presence in no way will protect any land from dryland salinity. This graphically illustrates the hopelessness of trying to address dryland salinity by vegetating discharge areas.

Figure 8 shows a large pit that has been dug between eucalypt belts to expose the water table which is about 1.5 m below the surface and extremely saline (60 000 μS cm $^{-1}$), too saline to be used by the trees. While ever the watertable remains at the level shown the trees may survive on the rainfall, or they may accumulate salt in their root zone and die. Piezometer measurements (Alex Knight, unpublished data) have shown that the water table at this site, although fluctuating, is rising slowly on average.

Figure 9 shows acacia belts planted on undulating ground, below which there is also a saline water table. The belt near the centre of the picture crosses a hollow; as the soil surface dips closer to the water table the trees become stunted and eventually non-existent. Groundwater in shallow water tables in the Murray Basin is usually saline; fresh shallow groundwater is rare. In the situations of both Figure 8 and Figure 9, the alley plantings are not significantly affecting the catchment water balance, and cannot reduce dryland salinity, except (possibly) very locally.

Figure 9 *Acacia saligna* alley farm planted over a saline water table in South Australia. The soil surface dips closer to the water table in the center of the photograph, stunting and killing the trees.

Conclusion

The increases of dryland salinity have been brought about principally by increases in recharge following the replacement of natural vegetation with cropping and pasture systems. Trying to increase catchment discharge by planting trees in discharge areas is unlikely to mitigate dryland salinity, as it is the hydraulic characteristics of aquifers that

determine discharge rates. Alley farming has been promoted as an alternative to conventional crop and pasture systems because it can potentially reduce recharge, and at the same time maintain some level of agricultural production. There is a need, therefore, for a modelling technique that can determine *a priori* the effects of alley farms on recharge (in recharge areas) of the Murray Basin.

Summary

This chapter has described the underlying stratigraphy of the Murray Basin as the most significant and immutable factor governing the expression and mitigation of dryland salinity. Specifically, the Basin is a shallow dish-like formation about 600 km across, but with sediments of only about 200 to 600 m deep, with very little slope, and connected to the sea by only the channel of the Murray River. The spatial arrangement of sediments, and the resulting aquifers is complex, and reflects the numerous tectonic movements, sea level and climatic changes over the last 40 million years. The large stores of salt in the aquifers of the basin has been conclusively attributed to the deposition from rainfall over tens of thousands of years. During this time the climate was relatively arid, and almost all rainfall was evaporated or transpired by plants. Deep drainage was small and therefore salt has built up in groundwater or in the overlying regolith.

Land cover is the only factor contributing the dryland salinity that can be significantly influenced by humans. The spatial and temporal distribution of vegetation has a large effect on deep drainage and hence the leaching of salt from the soil profile and the recharge of aquifers. The clearing of natural vegetation has greatly increased recharge rates and the mobilisation of salt in the Basin. In the eastern and south western regions of the Basin, saline groundwater comes close to the land surface, limiting plant growth and degrading land. However, the most serious effects of dryland salinity in the Mallee region of the Basin are the pollution of potable groundwater and increases in the subsurface discharge of saline groundwater to the lower reaches Murray River.

The discharge rate of an aquifer is determined by aquifer thickness, hydraulic conductivity and hydraulic head. There is little scope, therefore, to reduce the dryland salinity by attempting to increase aquifer discharge. Groundwater pumping and/or growing trees in discharge areas may lower water tables, but the effects are very localised and are often small in comparison the scale of an aquifer (Norman, 1995; Hatton and Salama, 1998). In addition, discharge areas are often saline; plant growth and therefore water use is therefore reduced (Slavich *et al.* 1999; Zhang *et al.* 1999).

Recharge reduction via manipulation of land cover over large areas is seen as the only long-term solution to the problem. The options for doing this are examined using conventional cropping systems, revegetation, new plant species and agroforestry. Alley farming, an agroforestry system comprising a spaced belts of trees is described a method for reducing recharge and, at the same time, maintaining some agricultural production. The chapter concludes with the observation: to be able to assess the usefulness of alley farming in such an application, a method is required for estimating its effect on recharge.

The following chapter reviews methods for measuring and modelling recharge, outlines the additional challenges associated with doing this for agroforestry systems, shows the need for a new method and lists its desired attributes.

Chapter 3

Measuring and modelling recharge from agroforestry systems

Introduction

The previous chapter demonstrated the need to model recharge from alley farming systems to assess their role in salinity mitigation in the southern Murray Basin. This chapter presents the rationale for the new modelling approach that is central to this study, and is described in the following chapter.

A working definition of recharge is given and the methods for measuring recharge are outlined. Special consideration is then given to the additional challenges associated with tree belts and agroforestry systems due to the lateral spread of tree roots and the problems associated with measuring the complex variation (both spatially and temporally) of plant/soil/water process within that zone. At this point an assertion is made: rather than attempting to describe the physical processes (and the spatial and temporal distribution thereof) involved in the production of recharge from alley farms, it would be better to avoid them altogether. The effort and resources required to measure recharge form an alley farm are illustrated with reference to a previous study undertaken in southwestern Australia.

Recharge modelling methods are then reviewed in brief, highlighting the combined problems of: the (typically) small magnitude of recharge in Australia; and the number of physical processes that need to be described to model it. It is noted that there is a trade-off

between the use of simple models that generate errors from their simplifying assumptions, and complex models that accumulate errors from a larger number of input parameters. An overview is given of agroforestry modelling, highlighting some relevant recommendations from recent reviews. Previous relevant agroforestry modelling studies are then outlined and comments are made with regard to their suitability for modelling recharge from alley farms in the southern Murray Basin.

A second assertion is made that a practically applicable alley farm recharge model cannot be assembled using the above experimental techniques and the modelling methods alone. I therefore propose that a new approach is required. The chapter concludes by listing the main knowledge gaps, followed by the desired attributes of a new modelling approach.

Recharge – a working definition

It is important to make the distinction between the terms recharge, deep drainage, and potential recharge (Walker *et al.*, 2001).

1. *Recharge (or groundwater recharge)* is the amount of infiltrated water that reaches a specific groundwater system;
2. *Deep drainage* is the flux of water that moves past the root zone of vegetation. Deep drainage only becomes recharge when there are no impeding layers, which prevent water moving down to the groundwater system;
3. *Potential (groundwater) recharge* becomes future recharge. Where there is a change of land use, there is a time delay for the recharge associated with the new land use to reach the water table (e.g. Jolly *et al.* 1989).

Although in specific cases, distinction between the above is essential, for convenience and for the purposes of this study, the term 'recharge' will be used to cover all three of the above terms. I justify this on the following grounds: 1) recharge is the process by which land use systems most significantly affect dryland salinity (Coram *et al.*, 2000), depending on salt stores; 2) deep drainage does not always become recharge, depending on the presence or absence of confining layers and proximity to streams however, land use induced increases in recharge do result from deep drainage; 3) in the majority of cases the southern Murray Basin, deep drainage will inevitably become recharge (see Chapter 2).

Measuring recharge

Recharge is difficult to measure; it is typically the smallest fraction of the total water balance (Walker and Zhang, 2001; Walker *et al.,* 2001), and it occurs below the root zone where it is difficult to access.

In a comprehensive review of recharge and discharge, Zhang and Walker (*Eds,* 1998) have compiled an unequalled resource on the topic in relation to Australian conditions. Within this compendium are described all significant methods of recharge measurement: *soil physical methods* (Bond, 1998); *groundwater responses* (Armstrong and Narayan, 1998); *soil water tracers* Walker (1998); and *electromagnetic induction* (Cook and Williams, 1998). Each of these methods are summarised below and comments are included regarding their suitability for use in alley farming studies.

Soil physical methods

Bond (1998) observed that the statement of Wagenet (1986) '*there currently does not exist a direct [routine] measurement technique for [soil] water flux on a field basis'* still holds. He then describes four soil physical methods for estimating recharge that can be used given the absence of a direct method: *Zero Flux Plane Method*; the *Unit Gradient and Measured Gradient methods based on Darcy's Law*; and *Lysimetry*. All of these methods apply only where matrix flow of water in soil is a valid assumption, and should not be applied where 'preferred pathway' or 'bypass flow' are significant processes. That is, the soil is assumed to be "*a continuous distribution of pores of various sizes, and measurements made at conventional scales (of the order of a few cm) relate to a representative sample of them"* Bond (1998). The role of macro pores (such as root channels, worm holes and shrinkage cracks), therefore, in soil water movement is assumed to be small. Although care must be taken in the application of these assumptions to Australian soils (e.g. the assumptions are not valid for swelling soils under certain combinations of soil moisture contents and wetting conditions), it is generally safe to do so, especially below crop root zones. This is often not so, however, in the case of tree root zones, especially given that natural species have evolved to survive drought periods by concentrating excess rainfall in root channels and storing it deep in the profile for use in subsequent 'dry' periods (Nulsen *et al.,* 1986). The implications of the possibility of preferential and bypass flow in tree root zones requires careful consideration and is discussed in more detail later in this chapter.

Where soil matrix flow is assumed, Darcy's Law can be applied

$$q = \frac{-K_{sat}\Delta H}{\Delta z}, \qquad (1)$$

where q is flow rate (mm d^{-1}) and is directly proportional to hydraulic gradient $\Delta H/\Delta z$; K_{sat} is saturated hydraulic conductivity (mm d^{-1}) for the soil. For unsaturated flow conditions, Bond (1998) gives Darcy's Law

$$q = \frac{-K_{\theta}[\Delta h_{\theta} + \Delta z]}{\Delta z}. \qquad (2)$$

The subscript θ here represents soil water content; K_{θ} and h_{θ} are hydraulic conductivity and suction, both are dependent on water content.

The *Zero Flux Plane ZFP Method* identifies the position in the soil profile, above which the soil water flux is upward (due to evaporation or extraction by plants) and below which the flux is downward (due to drainage). The flux at this point therefore must be zero. Thus, as time progresses, the *ZFP* following a rainfall or irrigation event, moves down the profile as evaporation and drainage continue. Changes in water content above this point are due to evaporation or extraction by plants; changes below this point are due to drainage. If there is a water table below this point, drainage becomes recharge.

Darcy's Law (Equations 1 and 2), although not applied directly in the *ZFP* method, is invoked to show that soil water flux is zero when the hydraulic gradient is zero. Tensiometers (Cassell and Klute, 1986; Hutchinson and Bond, 2001) are then used at regular depth intervals to measure suction and to determine at what point $\Delta H/\Delta z$ is zero.

Soil water content must also be measured simultaneously with suction, and usually on a daily basis, for the calculation of drainage. Drainage is calculated as the change in soil water content within a certain depth interval below the *ZFP*; the magnitude of the 'drainage' will of course vary with the depth interval chosen, and is unlikely to equal recharge unless the entire depth interval between the *ZFP* and the water table is considered.

Factors limiting the application of the *ZFP* method to alley farms include the large resource requirement for soil water and soil suction measurements. These would need to be repeated daily, and distributed vertically throughout the profile (at least replicated once, both within and outside the tree root zone). For estimates of long-term average drainage this must be continued for at least a year. Approximation of recharge using the *ZFP* method is impractical wherever the water table is deep, which is the case for most of the Murray Mallee (see Chapter 2).

The Unit Gradient Method, outlined by Bond (1998) can be used under special circumstances where, once drainage is established, the hydraulic gradient is unity and does not need to be measured (Equation 1 and 2). The soil water flow rate q is then equal to the soil hydraulic conductivity at the prevailing soil water content. This method requires that soil hydraulic properties must be measured, and must be uniform over the interval of measurement. This often limits the application of the technique, especially for alley farms since trees have deep root zones and are very likely to intersect changes in soil physical conditions. Although uniform, deep sands existed at the alley farm experimental site of Lefroy *et al.*, (2001), such conditions are the extreme exception in the Murray Basin. Bond (1998) warns that for layered soils, errors of up to 900% can occur when using the method to estimate drainage. Despite this, I have used the *Unit Gradient Method* to obtain an estimate of the order of magnitude of drainage in the tree root zone (Chapter 6 and Appendix 2) to validate an assumption of negligible recharge. In this case, because of the extremely small magnitude of q, the likely error associated with the use of the *Unit Gradient Method* is not an issue.

The *Measured Gradient Method* is often employed when the *Unit Gradient Method* cannot be used due to changing soil physical conditions. This method requires the application of Darcy's Law (Equations 1 or 2) and therefore the simultaneous measurement of K_θ, and h_θ and their variation with depth. The resource requirements for this method are similar and often greater than the *Unit Gradient Method*, and the greatest errors stem from the measurement of K_θ, which can yield large uncertainties at high suctions. While this method may be useful for point measurements, in my opinion, the labour involved makes it unsuitable for describing a zone as large and as complex as a tree root zone.

Lysimeters are usually best suited to measure evapotranspiration (Bond, 1998) although they can be adapted to measure recharge both directly and indirectly. Tanner (1967) describes a lysimeter as '*a device in which a volume of soil, which may be planted to vegetation, is located in a container to isolate it hydrologically from the surrounding soil'*. With suitable instrumentation, the operator can have complete knowledge of all the components of the water balance. Lysimeters are classified as 'weighing' and 'non-weighing', and as the names imply, refer to the whether or not water storage is determined by measuring the mass of the lysimeter. Where lysimeters need to be large (e.g. for trees) water storage are determined from other, usually non-destructive, methods such as a neutron probe. The main assumption is that the conditions inside lysimeters represent those of the surrounding undisturbed paddock (or forest), and this is often the most limiting factor to their confident application. Taking large, undisturbed soil samples is a

large and difficult task, as is hydrologically isolating them from the surrounding soil and then instrumenting them. Excavating and repacking lysimeters immutably changes soil physical conditions and can defeat the purpose of using them. Add to this, for agroforestry studies, the need to grow trees, and lysimeter methods rapidly become unwieldly. Sometimes local impermeable soil layers eliminate some of the physical structure required to isolate the soil hydrologically (Oke, 1978; Dunin *et al*, 1985) but the problem remains of needing to separately monitor the 'interface' zone in an agroforestry study.

Using groundwater responses to infer recharge

A change in groundwater level can be the most conclusive proof that recharge has changed; it would therefore seem to be an attractive option to work backwards from a measured groundwater response to quantify the recharge that caused it. As with the adage: "*The proof of the pudding is in the eating.*" (Anon), the effect of land use changes on recharge will ultimately be judged by groundwater responses. For groundwater signals to be used this way, they must be representative of the effects of the land use change, for which there are two prerequisites: 1) the land use system must have 'matured' (requiring years to decades in the case of alley farms); 2) the groundwater flow system must have reached a new equilibrium, either static or dynamic (requiring decades to centuries for most groundwater flow systems associated with dryland salinity; see Chapter 2). The use of groundwater responses for estimating recharge is therefore better suited to long-term studies or where the water table is not very far below the soil surface. An advantage of the technique is that groundwater response represents a spatial average of recharge over the catchment. A limitations to the technique is the availability of data from which to describe the specific yield, transmissivity and geometry of the aquifer (Dawes *et al.*, 2001).

Armstrong and Narayan (1998) summarise the use of groundwater response to infer recharge from the basic principle

$$\Delta h = \frac{R}{Sy}, \tag{3}$$

where Δh is the rise in water table level (m); R is the depth of recharge ($m^3\ m^{-2}$); and Sy is the specific yield of the aquifer ($m^3\ m^{-3}$). I have omitted a detailed discussion of the use of groundwater response because of the restrictions associated with applying such techniques in the Murray Basin, due principally to time taken for increases in recharge to reach the water table (25 to 80 yr, Jolly *et al.* 1989; Allison *et al.* 1990). Groundwater flow systems in the Murray Basin (see Chapter 2) with suitably shallow water tables (several metres below the surface) occur almost exclusively in 'local' scale flow systems, which do not

accumulate salt, or in discharge areas. There is little point focusing this study on such sites as they poorly represent the general case in the southern Murray Basin, and plantings in discharge areas can never reduce recharge. I therefore deemed groundwater response techniques to be of little use here. Until such time that there are significant areas of sufficiently mature alley farms in a catchment for which there is a long-term record of groundwater levels (both before and after alley planting), groundwater responses cannot be used to assess the effect of alley farms on recharge.

Using soil water tracers to estimate recharge

Most of the definitive work on recharge in the Murray Basin has been undertaken using soil water tracers (Allison and Hughes, 1972, 1978, 1983; Allison *et al.,* 1990; Jolly *et al.,* 1989; Walker *et al.,* 1991; Kennett-Smith *et al.,* 1992a, 1992b). A tracer is a soluble substance that is moved through the soil by water, and of which the concentration can be determined, usually by laboratory analysis of field samples. The spatial and temporal distributions (concentrations) of the tracer are used to infer the water movement that would cause such distributions, rather than measuring the water movement directly. Walker (1998), who has provided a comprehensive collation of the use of tracer methods, gives reasons for the popularity of tracer methods

1. *"The movement of tracers is governed mainly by the long-term mean soil water fluxes that lead to recharge"* compared to soil physical methods which measure fluxes on unnecessarily short time scales to give recharge estimates;
2. Tracer methods do not require frequent visits to the field;
3. It is possible to estimate smaller [long-term average] fluxes using tracers rather than other methods.

Walker (1998) also notes that there is often no alternative.

Tracer methods can be divided into those that use *Artificial, Historical,* or *Environmental Tracers.* An *Artificial* tracer (e.g. bromide) used for recharge studies is one that is applied by the investigator and its motion through the soil profile is then subsequently monitored. *Historical* tracers used in recharge studies (e.g. tritium; ^{36}Cl) are isotopes that originate mainly from atomic tests conducted in the Southern Hemisphere during the 1950s. High concentrations of the tracers were deposited on the soil surface around the time of the event and subsequently leached downward through the soil profile over long periods. Using historical tracers avoids the demanding application procedures required for artificial tracers and the safety precautions needed when handling concentrated isotopes. When using historical tracers, decay rates and mixing with 'background' levels of the isotopes

(^{36}Cl also occurs naturally) must also be taken into account. Due to its relatively short half-life of 12.4 years, tritium concentrations in soil water have decayed to levels similar to those in rainfall. By comparison, ^{36}Cl has a half-life of 3 million years and remains a useful artificial tracer. The cost of extraction of isotopic tracers from soil samples is usually large ($80Aus to $1000Aus per sample, 1997 prices; Walker, 1998) compared to other types of tracers and will often be the main cost where only shallow sampling is required. Deep-drilling costs, however, can be extreme where specialist machinery is required (~$200Aus m^{-1}) and it is often necessary to drill to depth greater than 10 m. Where soil conditions are not extremely hard, and where there are no rock layers, hand augering is much cheaper and often faster than the specialist drilling machinery required to retrieve uncontaminated samples from known depths (wire-lining technique; see Figure 129).

Environmental tracers are those that exist naturally in the landscape, and are numerous. Chloride occurs naturally in rainfall (Hutton, 1976) and has proven to be the most useful environmental tracer for recharge studies in Australia (Allison and Hughes, 1972, 1978, 1983; Allison *et al.,* 1990; Jolly *et al.,* 1989; Walker *et al.,* 1991; Kennett-Smith *et al.,* 1992a, 1992b).

In most parts of southern Australia plant growth is water limited; chloride is delivered to the soil surface via rainfall and, following evapotranspiration of the water, remains in the root zone and becomes concentrated. In naturally vegetated landscapes of the Murray Basin, chloride usually reaches a peak concentration (often called the chloride 'front') at 1 – 3 m below the soil surface. Although drainage below the root zone (and hence recharge) is extremely small (often <1% rainfall) in most natural landscapes, it can never be zero if the plants are to survive in the long term. Recharge is the mechanism by which salts (also delivered in rainfall, see Chapter 2) are continually leached below the root zone. For this reason, long-term average recharge (although small) below a natural plant community (that is in equilibrium with its environment) is essential, and relatively constant with time. As a result, the concentration of chloride in the soil profile below this point is relatively constant with depth. Allison and Hughes (1978) used this and applied a simple mass balance to show that if the (input) rainfall rate P (mm yr^{-1}) and chloride concentration C_p (mg L^{-1}) is known, and the (output) recharge chloride concentration C_d (mg L^{-1}) is also known, then the (output) recharge rate D (mm yr^{-1}) below the natural vegetation can be calculated

$$D = \frac{PC_p}{C_d} \quad (4)$$

Allison and Hughes (1978, 1983) and Allison *et al.* (1990) subsequently showed that the peak chloride concentration below cleared agricultural land occurred lower in the profile (the 'new' depth) compared to that below natural vegetation (the 'old' depth). Further, it was shown the vertical downward displacement was caused by higher recharge rates leaching chloride down through the soil profile. The authors then measured the soil water (mm) stored between the 'new' depth of the chloride peak in the agricultural land, and the 'old' depth before clearing (estimated from undisturbed sites nearby). The average recharge rate (mm yr^{-1}) from the agricultural land is simply the soil water (mm) stored between the 'old' and the 'new' positions, divided by the number of years since the land was cleared.

This is called the 'chloride front displacement method' and can be used to calculate recharge wherever definite chloride 'fronts' can be detected below both undisturbed and cleared land, and where 'piston' flow of the soil water is a valid assumption. Often these conditions are not met, so Walker *et al.* (1991) developed the generalized version of the chloride front displacement method, often referred to as the 'transient chloride front displacement method'. The name reflects the fact that the technique addresses chloride concentration profiles that are 'transient' between two equilibria. Strictly speaking, a new equilibrium will not be reached under such circumstances until the old chloride front is flushed through the entire soil profile to the water table and a new C_d is established. Where the water table is deep this can take many decades (Jolly *et al.,* 1989).

The leaching process described here occur almost exclusively (except following large episodic events) under conditions of unsaturated flow and is therefore very slow. The vertical difference (m) between the 'old' and the 'new' positions of the chloride front is critical to the calculation of recharge, and is a function of recharge rate, time and soil physical properties. The vertical increments of soil sampling must be adjusted to ensure sufficient resolution to estimate the 'old' and 'new' positions accurately; smaller vertical increments (~0.25 m) are required for fine-textured soils compared to coarse-textured soils (up to 1.0 m). The (slow) speed of the solute leaching process also means that chloride methods are unsuited for detecting relatively short-term (one to a few years) changes in recharge, and should only be used to compare the effects of different land use changes that are separated by years or decades. The accompanying advantage, however, is that properly

applied chloride methods integrate seasonal variability (and episodicity) and yield relatively accurate long-term average values of recharge.

Due largely to these reasons, chloride methods were chosen to be the most appropriate for this study; chloride results are described in Chapter 5; and detailed worked examples are given in Appendix 2, along with their application to tree root zones and a detailed error analysis.

Probably the two most significant issues affecting the interpretation of chloride methods, tracers in general, and in fact any point measurement technique are: the consequences of preferred pathway flow; and spatial variability of recharge, especially below agricultural land (Cook *et al.,* 1989). These are discussed in more detail later. To some degree *Electromagnetic induction techniques* (next section), are less sensitive to these issues although they have other limitations.

Groundwater chemical methods

Groundwater chemical methods (Cook and Herczeg, 1998), like groundwater response methods are largely unsuited for this study for the same reasons, but are well suited to longer-term studies. As with environmental soil water tracer methods, groundwater chemical methods use naturally occurring tracers (^{3}H, ^{2}H, ^{18}O, chloride) to infer recharge rates from mass balances. Another approach estimates the age or residence time of the groundwater by measuring the activity of radioactive 'bomb' tracers (^{14}C, ^{14}N), which resulted from atomic testing in the 1950s.

Electromagnetic induction techniques

Compared to other techniques, *Electromagnetic (EM) induction techniques* sample a larger volume of soil with each measurement. In this way they can avoid some of the problems associated with spatial variability of recharge over very short distances (less than a few metres), and can also facilitate the statistical description of spatial variability at the paddock scale (as undertaken by Cook and Williams, 1998).

EM techniques are particularly well suited to mapping gradual changes in recharge with horizontal distance as would be expected below a tree belt. Cook and Williams (1998) provide an overview of EM techniques and divide them into two categories: *Frequency-domain methods* (FEM); and *Time-domain methods* (TEM). Both methods employ an energised transmitter coil (placed at the ground surface) which induces eddy currents in the subsurface material, which in turn induces a secondary magnetic field, the characteristics of which are used to infer the electrical conductivity EC_a (dS m^{-1}) of the soil. EC_a is proportional to the electrical conductivity of the soil solids EC_s, the electrical

conductivity of the soil solution EC_w, volumetric soil water content θ_v and the tortuosity T, a property of the soil matrix and θ_v

$$EC_a = EC_w \theta_v T + EC_s \quad (5)$$

and is generally found to be lower in areas of high recharge (due to leaching of salts) than in low recharge areas. EC_a can therefore be used as a surrogate to measure either relative recharge, or absolute recharge, with suitable calibration against another method of recharge measurement (usually a chloride profile method).

FEM uses a transmitter coil energised with an alternating current. A receiver coil, placed on the ground a short distance away, measures both the primary and secondary (induced) magnetic fields; the ratio of which is directly proportional to EC_a. The TEM measures the transient response of the decaying secondary field after the transmitter is rapidly switched off; the decay rate of the secondary field is inversely proportional to EC_a.

Both FEM and TEM have been adapted and used successfully to survey large areas rapidly from aircraft but still require some calibration. The main attraction of EM compared to other techniques is their ability to take many measurements rapidly (Cook *et al.,* 1989); if only relative recharge values are required then minimal calibration is needed.

Spatial variability and preferred pathway flow

Cook *et al.* (1989) used EM techniques to show that there can be a high degree of variability in recharge at the paddock scale. In most cases recharge measurement methods are limited to providing only point estimates; EM techniques are a slight improvement in this regard as they sample a larger volume of soil, and also allow multiple measurements to be taken rapidly for statistical analysis. Groundwater techniques represent the ultimate in spatial averaging of recharge over a catchment but there are significant time delays associated. Cook *et al.* (1989) concluded that recharge rates in the western Murray Basin were log-normally distributed with the mean and variance of the log-transformed values equal to 2.65 and 0.831, respectively. This implied that 86% of the recharge occurred through 60% of the land area; and 41% of the recharge occurred through 20% of the land area. The authors approximated the spatial structure of the distribution using a spherical semivariogram with an auto correlation scale of 120 m (note: a similar spatial scale to tree belt spacing in alley farms). This variability will be a concern for studies or predictions made at this scale, but since the spatial variability of recharge is random, it becomes less of a problem over large areas and can be neglected at the paddock scale, as long as a representative recharge value is available. The most significant implications for the spatial variability of recharge values relates to predictions made regarding the eventual

salinisation of the watertable following the downward remobilisation of salt. Cook *et al.* (1989) note that a lower spatial variability will result in a more sudden impact (and general) on the watertable than would occur with a high spatial variability.

There is little that can be done regarding the inherent spatial variability of the landscape other than to be aware of the implications when collecting and using recharge measurements. In most cases the costs of field measurements prohibit a sampling density sufficient to rigorously analyse and allow for spatial variability however the work of Cook *et al.* (1989) can be used as a guide.

Preferred pathway flow considered here refers to discontinuities at the pedal scale that may result in non-matrix flow, such as cracks; biopores; root channels etc. I have highlight it because of the manner in which eucalypt mallee species concentrate rainfall via stem flow and store it deep in the soil profile, apparently in the soil surrounding the root channels Nulsen *et al.* (1986). The authors showed that this can occur to depths of 26 m, far greater than the average depth of the chloride front beneath undisturbed vegetation (1 – 3 m). The implications of this on recharge measurements must be explored, but first I consider the evidence of preferred pathway flow in recharge studies.

Walker (1998) gives a comprehensive discussion on the topic and cites studies from Western Australia (Johnson, 1987) as evidence that preferred pathways in a lateritic soil play a significant role in conducting water to the watertable. Walker (1998) also cites the studies of Cook *et al.* (1990) and of Allison and Hughes (1978) that show little evidence for preferred pathway flow in the South Australian Mallee. In addition, Walker (1998) notes that observed wetting fronts in the Mallee are often sharply defined, indicating little movement of water ahead of the front as would be the case if preferred pathway flow was significant and concludes that the use of tracers such as chloride give meaningful and robust measurements of recharge.

However, I now return to the issue of trees actively using preferred pathway flow as a survival mechanism, and the implications for the chloride technique. The characteristic chloride concentration peak (front) at a depth of 1 to 3 m (Figure 101) is an established phenomenon for natural (water-limited) vegetation in southern Australia, yet it is much shallower than the maximum rooting depth of eucalypts (Nulsen *et al.,* 1986). Many studies have shown that the front is displaced downward by increased recharge following land clearing, yet we are happy with the notion that water is routinely transported past this point by eucalypts Nulsen *et al.,* (1986), *before* clearing. How can this be? I am not aware of any studies that address this (potential) contradiction however I offer my interpretation

below, given that eucalypt root architecture is strongly dimorphic (Knight, 1999), having both shallow roots and deep tap roots.

If water is concentrated and stored in root channels below the chloride front and extracted later by tap roots, this means:

1. A relatively small ground area is covered by taproots and is therefore involved in the vertical transport of 'preferred pathway' water below the chloride front. This leaves most of the ground area to conduct water via matrix flow (although the fate of drainage following large episodic events is uncertain);
2. Because the 'preferred pathway' water is extracted from the soil again it does not become recharge and does not need to be considered here, even though it passes below the chloride front;
3. The (shallow) chloride front commonly measured below natural vegetation is a result of matrix flow processes occurring within the zone of the 'shallow' roots only, however (because of 2, above) it is still representative of the average vertical movement of water in the entire root zone.

Tree belts and lateral roots in alley farms

The previous section briefly described what is involved in measuring recharge in one-dimensional systems such as pure crop or pure forest. This section looks at the additional considerations required when investigating agroforestry systems. These are primarily related to the spatial heterogeneity of alley farms (i.e. trees belts and alleys of crops), but more specifically, the spread of lateral tree roots into adjacent land and the resulting 'interface' zone. Knight (1999) reviewed the morphology of tree roots in Australia and concluded that they were strongly dimorphic (especially for eucalypts) having both deep taproots and dense surface roots that can extend laterally for up to 30 m.

Where both the tree belts and alleys are very wide (say 200 m; much wider than 'interface' zone) the tree belts and alleys can be thought of as separate, one-dimensional, 'forest' and 'crop/pasture' elements. In southern Australia, although alley (crop/pasture) widths can be in the range of 100 to 200 m, tree belts are typically about 10 m wide, meaning the spread of lateral tree roots and the associated interface zone is often larger than the belt width. This zone therefore becomes a significant, often dominant, feature of such systems. In this 'interface' zone of an alley farm, water movement occurs in both vertical (crop transpiration, soil evaporation, infiltration, recharge) and horizontal (extraction by tree

roots) directions. In addition, the processes vary spatially in both vertical and horizontal directions, as well as temporally.

Other than investigations of windbreak effects (Bicknell, 1991, Nuberg, 1998, Cleugh *et al.,* 1998; Cleugh and Prinsley, 1998), there have been only a few field studies on this zone in Australia (Albertson, *et al.,* 2000; Hall *et al.,* 2000; Lefroy *et al.,* 2001a and b). Owing to the greater prevalence of alley farming in other parts of the world, tree/crop interactions has received more attention in other countries. VanDenBeldt *et al.,* (1990) reviewed tree/crop interactions in agroforestry situations, both below and above ground, and point to the (then) recent experimental evidence that trees do not always benefit nearby crops but can compete with them in many situations. The authors stress the importance of endeavouring to separate such interactions in experiments. Schroth (1999), in a comprehensive review of below ground interactions in agroforestry, explores the interactions of root systems under different environmental conditions and outlines the vertical, horizontal and temporal stratification such interactions. While the focus of the review is on the management options for optimising the results of root interactions, it serves to illustrate the complex nature of such interactions. Schroth (1999) concludes that while the interactions are many and varied, only a few of these can be quantified in reality due to the *"notoriously difficult and cumbersome"* nature of field root studies. A feeling for just how 'difficult and cumbersome' this is can be gained from the thorough review on root measurement techniques edited by Bohm (1979).

The principal interaction of concern to this study is the competition for water between trees and crops and the subsequent effects on recharge. Below, I have used photographs taken during this study to illustrate the effects of the lateral spread of tree belt roots into agricultural land. The orientation of the belts is such that the observed affects are likely to be due entirely to competition for below ground resources, rather than shading. Crop growth next to trees, in these cases, serves as an indicator of some of the below ground interactions, and also the likely spatial distribution of tree roots. Due to the sensitivity of annual crops to seasonal conditions, using crops in this way tends to reflect the recent, rather than the long-term, competition effects.

Figure 10 Suppression of a wheat (*Triticum aestivum)* crop due to competition for resources by *E. occidentalis* (left) and *E. leucoxylon* (right) tree belt. The two sites were in the same paddock at Roseworthy, South Australia, but at different stages of crop development. Such examples show that the influence of lateral tree roots can vary both spatially and temporally, and are often species dependent.

Trees usually compete aggressively with crops for resources, and in southern Australian water limited conditions, water is usually the most critical. Crop growth in the 'interface' zone is often suppressed because of this (Figure 10; Figure 11), but can sometimes be unaffected (Figure 12) or can be enhanced (Figure 13), although this is relatively uncommon in southern Australia.

Figure 11 Severe suppression of a pea (*Pisum sativum)* crop next to a belt of *E. occidentalis* at Roseworthy, South Australia. *E. occidentalis* was notorious for its pronounced effects on crop growth compared to other tree species at this site. During crop germination there was little discernable influence from the trees; in the subsequent weeks as soil conditions dried and there was little rain, seedlings growing in the tree root zone became water stressed and died.

Figure 12 An alley farm at Narrogin, Western Australia, showing pasture growth apparently unaffected by the presence of single rows of *E. cornuta*.

Figure 13 A relatively rare example (for southern Australia) where crop growth is enhanced close to trees. In this case barley (*Hordeum vulgare*) was under sown in spring with lucerne (*Medicago sativa*) in a clay soil near Bordertown, South Australia. Waterlogged conditions killed lucerne seedlings except near the trees (*E. microcarpa*) where the soil was drier.

Similar competitive effects have been reported in southern Australia (Albertson *et al.*, 2000; Hall *et al.*, 2000) and also in a temperate climate in the USA (Jose *et al.*, 2000). They are often site and species dependent, and vary both spatially and temporally. The mapping of the spatial distribution and intensity of the underlying processes represents a significant challenge. Since the review of Bohm (1979), less labour intensive methods

have been developed for tree root investigations using fractal techniques (Van Noordwjik *et al.*, 1995). Ong *et al.*, (1999) used similar methods and sap flow to investigate below ground complementarity in agroforestry. They developed an index relating tree size, and the diameter of tree roots close to the stem, to crop competition. Although fractal methods greatly reduce the labour required to describe tree root systems, it requires the exposure and measurement of tree roots close to the bole of each tree. This is still relatively labour intensive, somewhat destructive, and provides little or no information regarding the horizontal extent on the root system.

Rather than dwelling on the difficulties associated with this, I use it here as a reason to try and avoid having to describe below ground processes, and especially their distribution. This point is taken up again when proposing a new approach to modelling recharge.

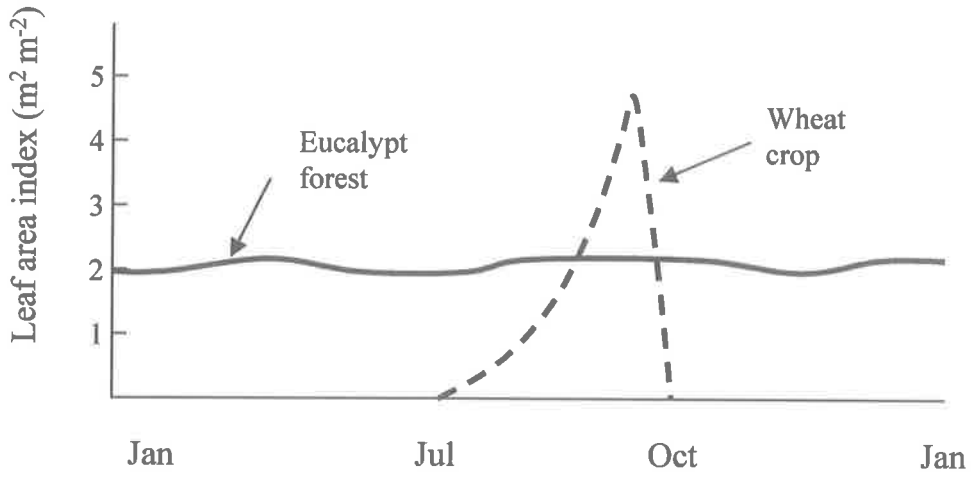

Figure 14 The leaf area index of a eucalypt forest and a wheat crop in southern Australia, modified from Hatton and Dawes (1993) computer simulations. Eucalypt trees are evergreen but wheat growth occurs over a relatively small portion of the year.

It should be noted also, that the above photographs are representative of dryland farming conditions in southern Australia where most of the rainfall (and the growing season) occurs between about April and October. It is only for about half of this period that crop leaf area is significant and for the remaining portion of the year there is no crop or pasture growth (Figure 14). The trees, therefore, have a dominant influence within the zone they hydrologically occupy, and this allows the use of an important simplifying assumption for this thesis (see Chapter 4).

Measuring recharge from an alley farm - previous work

The only thorough measurement of recharge from an alley farm in Australia, previous to this study, was undertaken in southwestern Australia (Lefroy *et al.*, 2001a and b). The authors describe a very detailed, replicated experiment comparing the water use of crops and of tagasate (*Chamaecytisus proliferus*), in both block and alley farm geometries, growing in a deep sand over a shallow (accessed by the trees), fresh water table. The main aim of the study was to test the effectiveness of alley farms for reducing recharge, and thereby assess the proportion of landscape under trees, and the spacing required, to meet a particular drainage reduction target. The situation of a fresh water table accessible to trees is unusual for southern Australia.

Crops were grown between the tree belts; Lefroy *et al.*, (2001b) noted the difficulty of accounting for the fate of rainfall in mixed plant communities and therefore employed four different measurement approaches: replicated neutron moisture metre measurements at 0.2 m depth intervals to a depth of 3.7 m, spaced at 0, 1, 2, 4, 8, and 15 m either side of tree rows; time domain reflectometry was used at depths 0.2, 0.75, 1.5, 2.3, 2.75 and 3.6 m for fine scale continuous (hourly intervals) water content measurements; transpiration was measured for a total of 27 stems using a combination of sapflow and heat ratio methods, and was used to assist in the partitioning of soil water loss between transpiration and drainage; stable isotope analysis was used to partition tree water use between soil and groundwater sources. In addition, 11 wells (distributed across the 8 ha site) were used to monitor the water table level.

The soil was (conceptually) divided into seven zones on the basis of the presence of tree roots, crop roots, both or neither (Figure 15). The divisions were established to quantify the interactions between the trees and the crops, however the authors note that "*Complete quantification of all the transfers occurring within and between the these zones was not possible as there was insufficient instrumentation to measure drainage and evapostranspiration at the crop interface. Emphasis was placed instead on measuring tree water uptake from soil and groundwater in the alley crop treatment, and drainage in the sole crop treatment and, from this, inferring drainage across the alley treatment.*". From this, recharge from the crop to the watertable was estimated to be 193 mm over a year, and was estimated to be reduced to 32 mm under the alley layout.

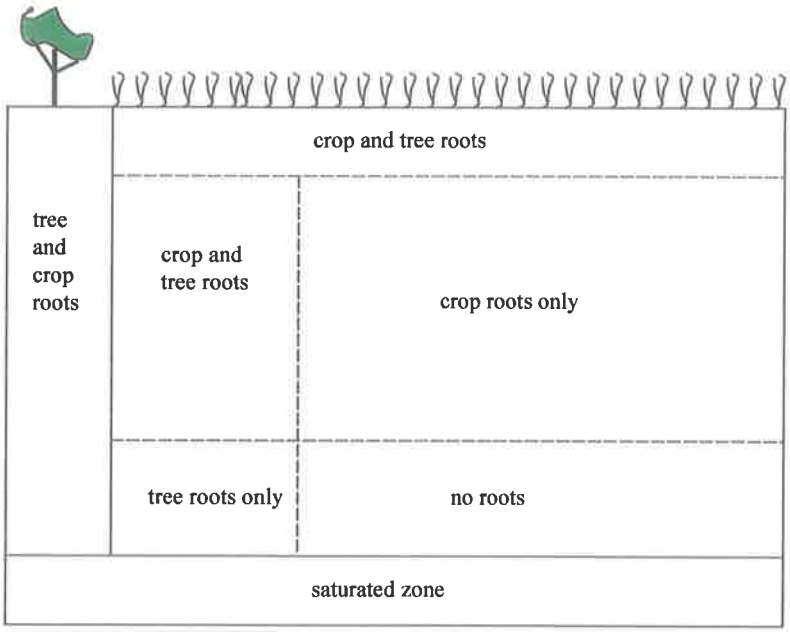

Figure 15 Schematic representation of the interaction between trees and crops in an alley system below ground environment. Seven zones are identified that are occupied by either: crop roots only; tree roots only; both crop and tree roots; or no roots. Redrawn from Lefroy *et al.* (2001b).

The authors also concluded that in this particular case, there was no yield/recharge reduction advantage afforded by the alley system, and that segregated monocultures of trees and crops would be more appropriate. This was a pivotal study in that it highlighted some limitations of alley farming for recharge control (although under unusual site conditions) and also illustrated the large resources required just to obtain an *estimate* of recharge from an alley farm (Richard Stirzaker pers. Comm.). The deep sands at this site represent possibly some of the best conditions for soil sampling and instrumentation; a greater effort could therefore be required if the experiment were to be undertaken on other soil types.

Modelling recharge

This section looks in brief at methods that are traditionally used to model recharge from land use systems. All methods consider the systems to be one-dimensional, although in some cases a protocol may be employed to move water landscape between cells to account for three dimensional flow (Dawes *et al.,* 1997). Often the purpose for modelling recharge to derive recharge inputs to groundwater models for scenario testing (e.g. Barnett, *et al.,* 2000). Hatton (1998) gives an overview of this process applied at the catchment scale, describing case studies undertaken in the Murray Mallee and the Loddon-Campaspe

catchments of the Murray Basin. Although, with regard to alley farms, we eventually want to know the effect of alley farms at the catchment scale for the same reasons, the dominant characteristic of alley farms is their spatial heterogeneity at the plot to paddock scales (tens to hundreds of metres). I therefore focus on methods of modelling recharge at the smaller scales, for which Walker and Zhang (2001) provide a comprehensive overview with particular reference to the choice and use of specific models. Walker et al., (2001) also described the same modelling approaches with view to developing a predictive framework for different land use systems.

Walker and Zhang (2001) provide an overview of numerous plot-scale soil-water-vegetation (SWV) models, how they can be best-used gauging recharge, and some of the dangers of misuse. The following section presents the salient features of such models and the consequences of trying to model recharge processes at different levels of complexity, both with respect to the resulting errors and the input parameters required.

Simple models

Walker and Zhang (2001) used Figure 16 to illustrate the components of the water balance associated with vegetated land, the interactions of which are extremely complex in reality. Recharge is usually the smallest component, and is often of a similar magnitude to the errors involved in the determination of the other components; it is this dilemma that makes accurate modelling of recharge a significant challenge.

As with many exercises involving the complex interactions of numerous processes, it is important to focus on describing the process of interest, in this case recharge, rather than using a model that may include recharge, but has been developed to more accurately describe other parts of the water balance. This may be a truism, but in the face of the temptation to use and adapt existing models for a new application, rather than rethinking the problem, it is worth keeping mind. Learning to use sophisticated soil-water-vegetation models can require full-time dedication for up to six months; in the process it is possible to stray from one's original objective. The danger of this occurring tends to increase with increasing model complexity.

Walker and Zhang (2001) give the simplest expression for recharge from a SWV system

$$D = \alpha(P - P_{thr}) \tag{6}$$

where D is recharge, P is precipitation, α is a fitted parameter and P_{thr} is a threshold precipitation and is also fitted. The threshold relationship lends itself to be represented using a 'tipping bucket' analogy (Figure 17); the bucket capacity being the difference

between field capacity and permanent wilting point of the soil and is fitted to field data. Water in excess of the bucket capacity is counted as recharge.

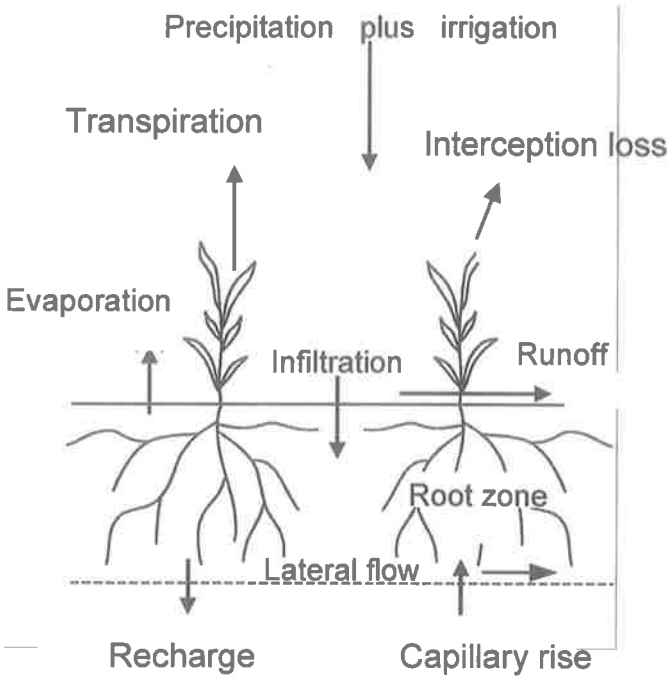

Figure 16 Schematic diagram of the water balance of a soil-water-vegetation system. Modified from Walker and Zhang (2001).

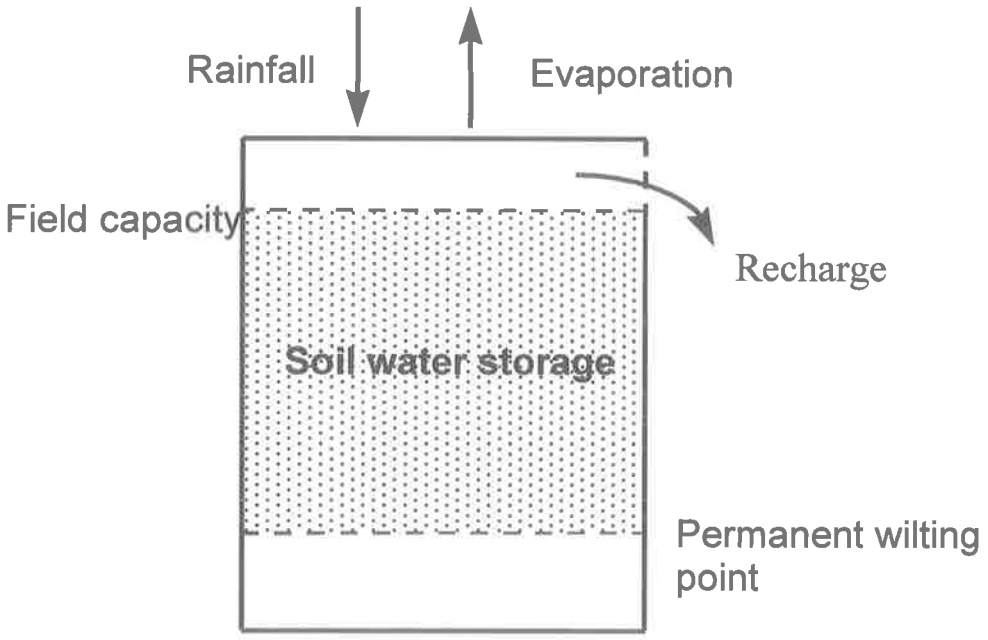

Figure 17 Schematic diagram of a tipping bucket model, as it would be used to represent a soil-vegetation system (Figure 10). Source: Walker and Zhang (2001).

Increasing complexity

The simple analogy (Figure 17) forms the basis for most water balance models; the levels of complexity increase as descriptions of additional processes are added such as: run-off; infiltration; drainage constraints; partitioning between runoff and drainage. Such equations are myriad, ranging from simple coefficients to empirically derived equations or mechanistic flow equations with simplified boundary conditions. The Richards equation (Richards, 1931) is often used in the more complex models like TOPOG (Dawes *et al.*, 1997). The growth and water use of vegetation has a dominant influence on recharge and is governed by the vegetation parameters including: Root distribution; Perenniality; Rainfall interception; Leaf area.

Root distribution determines the capacity of the root zone to buffer against recharge and to extract stored water; *Perenniality* determines the seasonal temporal distribution of the plant water use; *Rainfall interception* represents a significant proportion of the water balance and is approximately proportional to leaf area; *Leaf area* determines the upper limit of transpiration of available water for a given atmospheric demand, and hence has a major influence on plant growth. Space does not permit a complete account of all the processes involved in plant growth and water use (and I have omitted some) but my point is that it is a very complex process to model.

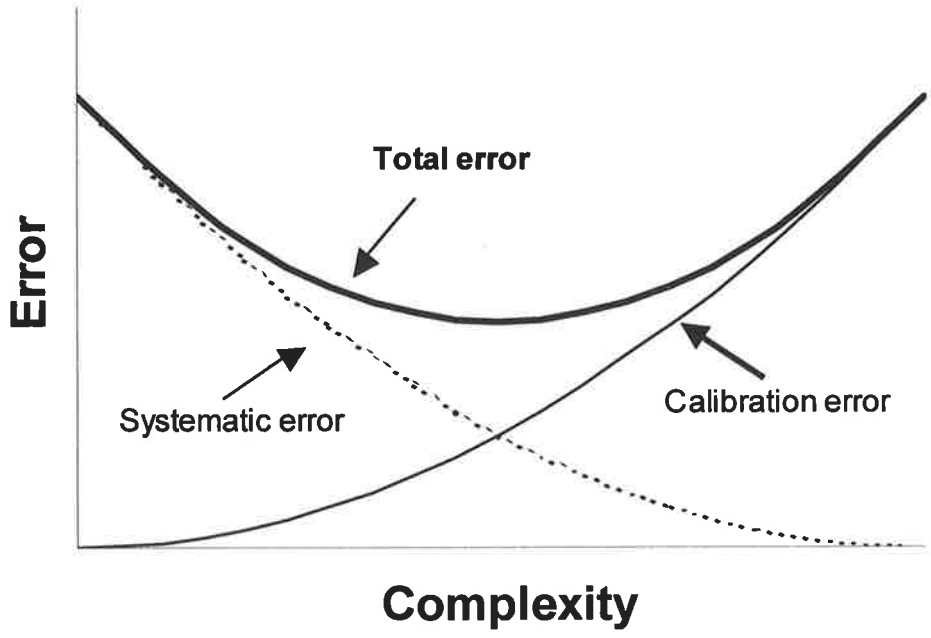

Figure 18 Representation of total modelling error as the sum of 'systematic error' (arising from simplifying assumptions) and 'calibration error' (arising from using incorrect parameters. *Source:* Walker and Zhang (2001).

There is a trade-off between simplicity and complexity, and it is reflected in model out put errors (Figure 18; Walker and Zhang, 2001). Simple models tend towards large 'systematic' errors because of inaccurate assumptions (e.g. runoff is small) whereas more complex models tend to include more 'calibration' errors since they require more input parameters. At some point between simplicity and complexity (although it is difficult to know exactly where) the total error, the sum of the systematic and the calibration error, should be at a minimum (Figure 18). Complex models such as WAVES (Zhang and Dawes, 1998) can require up to 50 input parameters, many of them from below ground. Hatton *et al.,* (1994), in short review of spatial models and their role of in predicting the impact of land use on salinity, asserted that the input parameter requirement for such process-based models has become extreme and compromises both the accuracy of predictions and the practicality of application of the models.

Hatton *et al.,* (1994) also alluded to the concept of the a trade-off between simplicity and complexity, and conclude strongly: *"Model development should emphasise elegance and parsimony over realism..."*. In addition to the dangers of a high level of complexity leading to large errors, one must also consider the extra resources required to obtain large numbers of parameters, especially those from below-ground. It is worth a reminder at this point that recharge in southern Australia is not only the smallest component of the water balance, but is similar in magnitude to the experimental errors involved in the measurement of the remaining components.

The next section shows how modelling agroforestry systems, because of lateral spread of tree roots and interactions between species (both above and below ground) is even more complex. I make the case that, rather than trying to account for this additional complexity in models by attempting to describe the underlying processes, it would be better to invest in new conceptual methods that *avoid* having to describe the processes, but retain their overall effects.

Modelling agroforestry systems

This section firstly lists relevant findings and recommendations of four reviews of agroforestry modelling, and then presents the results of some key agroforestry modelling studies dealing with plant/soil/water relations. The methodologies and findings of the studies are then discussed in relation to modelling recharge from alley farms.

Previous agroforestry modelling has been undertaken principally to answer questions relating to the ecology, productivity or economics of such systems. The interest in using agroforestry for recharge control is relatively recent. The reviews therefore identify the

issues relating these aspects and make little mention of hydrologic issues, and no mention of recharge. They do however, unanimously refer to the measurement and modelling problems associated with the complex spatial and temporal distributions of roots as identified above. Muetzelfeldt and Sinclair (1993) list this as a topic for future research and note that the "*complexity and interdisciplinary nature of agroforestry creates major problems that hamper the construction, use and dissemination of relevant models, and thereby restrict both the cost effectiveness and scientific rigor of modelling in agroforestry*". Anderson *et al.* (1993) present a strategy for the integration and experimental work in agroforestry and, drawing on Anderson and Sinclair, 1993, list problems associated with "*the complexity of agroforestry systems, the representation of a set of individuals, combining effects of multiple influencing factors...* ". Seven key areas of weakness in understanding were identified: nutrient cycling; hydrology; erosion; organic matter; competition; genetics; and productivity. They recommend the development of simple models for the tree-crop interface and that the highest priority research topic is root architecture. A common theme of both Anderson *et al.* (1993) and Muetzelfeldt and Sinclair (1993) is the large costs associated with the development, testing and training of people to use agroforestry models. Gregory (1996) highlights the major limitation to developing water and nutrient uptake models is the "*lack of adequate measurements and conceptual models for describing the distribution of roots spatially and temporally*". Gregory (1996) also notes that there is a need to adopt a range of approaches capable of utilizing limited amounts of data available, and that different problems will require attention at different scales.

Previous relevant studies in agroforestry modelling

McJannette (1999) simulated the water use and growth of tree belts on a hillslope in Victoria, Australia, using the model TOPOG (Dawes *et al.,* 1997), but assumed no tree roots extended laterally from the belts. Theoretical process-based models have been written to describe the lateral spread of roots and water extraction of isolated trees (Landsberg and McMurtrie, 1984) and tree/crop competition (McMurtrie and Wolf, 1983). Lawson *et al.* (1995) coupled existing tree and crop models to form an agroforestry interface model. Simunek *et al.,* (1999) developed a two-dimensional model for simulating water and solute transport, in variably saturated media. The model has a facility for simulating water extraction by plant roots and could be adapted to describe a tree belt. These models are quite complex and (I believe) best suited to site-specific studies because of number of below ground parameters required. There are also simpler conceptual models for describing interactions between trees and other species (Walker *et al.*, 1989) and

approximate solutions for placing trees in the landscape to control dryland salinity (Stirzaker *et al.*, 1999; Taylor, 1999). Recently, two-dimensional models have been employed to investigate water, nutrient and light capture (Van Noordwijk and Lusiana, 1999) and root interactions for water (Sillon *et al.*, 2000).

The Ecological Field Theory (EFT) of Walker *et al.* (1989) provided a different approach to the interactions between plant species of different sizes with the concept of 'pulsating geometric zones' of influence surrounding individual plants. The domain and intensity of the zones of influence vary with seasonal conditions and, where they overlap, sum to represent the dual, or multi, demand on resources. The EFT (Walker *et al.*, 1989), while providing a simpler conceptualisation of species interactions, also remains insufficiently focussed for the purpose of modelling recharge (Joe Walker pers. comm.).

Taylor (1999) investigated the use of, and provided design suggestions for (wide) belts of trees for the interception of subsurface water for salinity mitigation in the Upper South East of South Australia. Taylor (1999) measured the enhancement of transpiration at the edges of belts (due to advected energy) but did not investigate any effects relating to the lateral spread of roots.

Stirzaker *et al.* (1999) provided some approximate solutions for where to plant trees in the landscape for controlling dryland salinity; they partition the soil into zones that are either 'shared' or 'not-shared' by trees and crops and also introduce the concept of a 'capture zone' up to a few metres wide, beyond the periphery of the tree root zone. Although not alluded to by the authors, this capture zone would, in reality, pulsate with seasonal conditions as predicted by EFT. The approximate solutions were further developed by Lefroy and Stirzaker (1999) who investigated the possibilities for gaining a recharge reduction that is proportionally larger than the land occupied by the trees and at the same time placing trees so that they use the water that is excess to the requirements of the crops. In doing this, the authors considered the opportunities for moving the excess water laterally to the trees, either under the influence of gravity (lateral subsurface flow on a hillslope) or by allowing the spread of tree roots into cropping land to access more water. These approaches make useful contributions to simplifying the problem of modelling spatially heterogeneous systems, however they still require large numbers of soil and root parameters, and focus on tree water use, rather than recharge.

Van Noordwijk and Lusiana (1999) outline the WaNulCAS model of water, nutrient, and light interactions in agroforestry. WaNulCAS was developed to deal with a wide range of agroforestry conditions including alley farms and is an impressive model. The authors

show simulation runs of alley geometries of different spacings and pruning regimes and drainage/rainfall fractions. However, with respect to its application for modelling recharge (although the authors did not develop it with such a use in mind), I identify the following shortcomings:

1. The model uses a four-layered soil profile that is divided into a further four horizontally spaced zones. Zone dimensions are specified by the user, as are the associated root length densities. Thus, the user needs a lot of below ground data.
2. The model needs a relationship between soil water potential and soil water content, for each soil layer. These either need to be measured (which is a lot of work) or estimated using pedotransfer functions (Arah and Hodnett, 1997). The latter can lead to gross errors at the high matric suctions that are likely to govern the recharge process under unsaturated flow.
3. Only the vertical transport of water is described.

The drainage/rainfall fractions were quite high (0.1 to 0.3 for a rainfall of about 500 mm) and do not reflect typical southern Australian conditions. However, I believe WaNulCAS would be extremely useful for investigating recharge from alley farms if the below ground data in 1), above, was available. The time required to learn to run the model and to analyse outputs needs to be considered. In addition, careful thought is required to limit the parameter space to minimise the number of permutations possible.

Sillon *et al.* (2000) also describe a two-dimensional model for the daily root interactions for water of a tropical shrub and grass alley cropping system. Soil-root water transport functions were solved for discrete volumes of cells, the size of which can be altered to any desired horizontal or vertical resolution. The model was tested on 0.9 m deep soil profile, 1.5 m wide and 0.75 m long. Vertical root maps of the two species were made at four locations by applying a 2 cm x 2cm mesh over a trench wall. Sillon *et al.* (2000) were able to simulate, quite well, the vertical and horizontal distribution of soil water potential. Although the authors did not estimate recharge, it would be possible using either the *Unit Gradient Method* or the *Measured Gradient Method* (as described above by Bond, 1998) together with the simulated water potential profiles. Again, with respect to the application of the model for recharge estimation from alley farming systems, it remains a plot-scale tool due to the resources required to obtain the required below ground parameters.

The case for a new approach

At this point I assert that a suitably practical method for estimating recharge from alley farms, over large areas in the southern Murray Basin, cannot be assembled using the above experimental techniques and the modelling methods alone. A new approach is required. Firstly though, I focus the issue by listing the main knowledge gaps, and then the desired attributes of a new approach.

Main knowledge gaps

1. There is very little data on the extent of tree belt root zones and the root distributions within them;
2. Virtually nothing is known about the spatial and temporal variation of recharge below a tree belt;
3. It is not known how the domain or intensity (Walker *et al.,* 1989) of a tree belt can be related to easily measured parameters;
4. There is little data and no methods for predicting the effects of different soil types on tree root architecture;
5. There is no simple method for describing the hydrology of (and within) tree root zones.

The knowledge gaps listed here pertain principally to the tree belt data and application of models for the modelling of recharge from agroforestry systems, rather than the measurement techniques themselves, or to the models. An obvious knowledge gap is the lack of a routine and simple method for measurement, but that is not the focus of this project (which is therefore constrained to work with the methods available). I do not see that there are 'knowledge gaps' as such within the models available for agroforestry systems. I believe that existing process-based modelling methods could be used for this project but the resources required would be large, the modelling procedure would be very complex, the outputs would be very site specific, and the errors would be difficult to quantify.

I see the main, overall, knowledge gap as being a conceptual one. There is a need for a new approach that does not require large amounts of data, and for which the errors are easily quantified.

Desirable attributes of a new approach

A new approach must satisfy the two aims of the study (see Chapter 1). In light of the above-mentioned knowledge gaps it must also:

1. account for the processes occurring in the interface zone;
2. be simple to apply;
3. not rely on the small-scale description of complex processes like tree/crop interactions;
4. be transferable between bio-climatic zones;
5. require minimal below-ground measurements;
6. have acceptable and easily measurable errors;
7. have minimal calibration requirement;
8. must be compatible with practical methods of validation.

Summary

This chapter describes the field techniques available for measuring recharge and their suitability for application to an alley farms study. Particular attention is given to chloride profile techniques (Allison and Hughes, 1983; Walker *et al.,* 1991) because they are used in Chapter 5 to test the new modelling approach developed in Chapter 4. Conventional methods of modelling recharge are reviewed briefly in order to give an appreciation of the complexities involved in a one-dimensional application of the models to 'pure' crop or forest systems. The added complexities associated with the spatial heterogeneity of alley farms is described in terms of the 'interface' zone that is shared by both trees and crops, and the difficulties surrounding the representation of soil water movement in that zone using process-based models. The case is made that a new approach is required for modelling recharge from alley farms; the desired attributes of a new approach are listed with reference to the perceived knowledge gaps surrounding the root zone and hydrological influence of tree belts.

Chapter 4

A new modelling approach

A summary of this chapter was presented at the *Envirowater99 – 2nd Inter-Regional Conference on Environment, Water* (see Ellis *et al.*, 1999). The contents of this chapter are also described in a manuscript submitted for publication to *Water Resources Research* (see Ellis *et al.*, in press).

Introduction

Chapter 2 outlined the proposal of alley farming systems for the mitigation of groundwater recharge and the requirement to evaluate the effect of alley farming on recharge. Chapter 3 reviewed methods for measuring and modelling recharge, described the problems associated with the small magnitude of recharge and the associated complexities of alley farms, and concluded that a new approach is needed. This chapter presents new concepts and a new approach, developed here in response to the need for ways to avoid having to describe the physical processes involved in the production of recharge, but at the same time retain their overall effects at the tree belt scale.

Equivalent Recharge Zone *ERZ* and Equivalent No Recharge zone *ENOR* concepts are explained and used to conceptually simplify the complex effects of tree belts on recharge. A hypothesis is then formulated from eco-hydrological optimality considerations

(Eagleson, 1982), to allow the prediction of *ENOR* for a belt of trees from leaf area measurements. Finally, it is shown how the *ENOR* can be used in a simple linear expression to estimate the long-term reduction in recharge expected, at the paddock scale, from an alley farming system.

Equivalent Recharge Zone *ERZ*

The *ERZ* concept is used here to introduce the *ENOR* concept that is central to the new modelling approach developed in this chapter. The *ENOR* concept is used to describe the zone hydrologically occupied by isolated tree belts. Both concepts are equally applicable to either: isolated trees; isolated belts or; isolated groups of trees and I refer to all of these collectively as 'isolated tree elements'. I then move from the general case and derive an expression for *ENOR* that is specific to tree belts, and hence alley farms.

Difficulties arise when trying to quantify the hydrologic contribution of an isolated tree element because of the unknown size and nature of the area of hydrologic occupation, due principally to the lateral spread of roots into adjacent land. Figure 19a schematically depicts a tree root zone and the likely, complex manner in which recharge, D, might vary spatially. This complex real zone can be simplified to an equivalent abstract zone A (Figure 19b), within which recharge is a constant value. A is therefore called the Equivalent Recharge Zone *ERZ* and makes a hydrologic contribution, at the paddock scale or catchment scale, equivalent to the hydrologic contribution of the real zone.

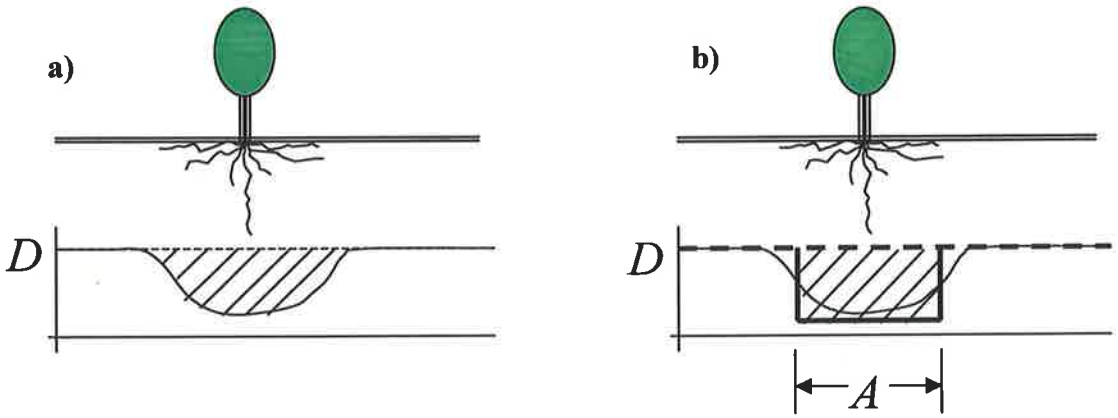

Figure 19 a) Schematic representation of actual recharge *D* below an isolated tree. b) The actual recharge profile can be simplified to an *ERZ* (Equivalent, Recharge Zone) *A* within which recharge is a constant value. For the hydrologic effects to be equivalent, the shaded area in a) must equal the shaded area in b).

That is, the 'recharge deficit' below the tree, compared to the ambient paddock recharge (shaded area Figure 19a) is equal to the recharge deficit from the *ERZ* zone *A* (shaded area

Figure 19b). The *ERZ* provides a simple method for describing the zones occupied by agroforestry isolated tree element. The next section uses hydro-ecological optimality theory (Eagleson, 1982) considerations to provide a means for predicting *ERZ*.

Eco-hydrological optimality theory

From ecologically-based premises (Specht, 1972; Specht and Specht, 1989; Eagleson and Segarra, 1985; Eagleson, 1982) it is logical that vegetation, in water limited environments, will grow to maturity in a way that is related to climate wetness. It follows that, given similarities in average leaf efficiency – transpiration per unit leaf area (Hatton *et al.*, 1997; Landsberg, 1999) - general relationships can be derived between leaf area index of vegetation communities and rainfall or some water balance index. Such relationships have been demonstrated (Specht, 1972; Specht and Specht, 1989; Grier and Running, 1977) and open the door for the investigation of possible analogous generalisations with respect to isolated tree elements.

Agroforestry tree elements in most of southern Australia are usually discrete patches of perennial vegetation, surrounded for some of the year by an annual crop or pasture. Except in the wetter climates, understorey is minimal to non-existent (see Chapter 3). In the zone shared by trees and crops, crop and pasture growth is partly or wholly suppressed compared to open paddock conditions, depending on the season. Over an annual time scale, the plant community within this boundary is overwhelmingly dominated by the perennial tree component. This allows a simpler representation of tree elements in southern Australia, and avoids the need to consider interactions between the trees and the crop or pasture. It follows therefore, that the mature structure of a tree canopy, in some way would reflect the size of its zone of hydrologic occupation.

Hypothesis

Eagleson (1982) hypothesised

> *"..water limited natural vegetal systems at any seral (i.e. successional) stage will develop a canopy density that produces minimum water demand stress under local climate conditions. A necessary condition for minimum stress is that soil moisture takes on the maximum value possible".*

Useful corollaries to this hypothesis are:

1. Isolated tree elements develop a canopy structure that produces minimum water demand stress equal to that of trees in a block.

2. The average leaf efficiency (transpiration per unit leaf area; Hatton *et al.,* 1997) is the same for isolated tree elements as it is for trees in a block.

Any changes in leaf efficiency of isolated trees due to greater nutrition from adjacent agricultural land are likely to be negated in water limited conditions (Landsberg and Waring, 1997). Also, under water-limited conditions, the enhancement of transpiration from advected (wind) energy is likely to be small (Thornley and Johnson, 1990; Taylor *et al.*, 2001; Smith *et al.,* 1997).

The hypothesis for the new approach is therefore:

The hydrologic effect of an isolated tree element in the landscape is equivalent to the hydrologic effect of a certain area of uniform vegetation within a block. The size of that area can be scaled to the LAI, or the leaf area L, of the isolated tree element, relative to the LAI of the uniform block.

Hypothesis in terms of Leaf Area Index *LAI*

Under water-limited conditions, the *LAI* of the isolated tree element is usually higher than that for a nearby forest or 'mature' plantation because roots extend laterally into unoccupied ground beyond the canopy. On a canopy area basis, therefore, the isolated tree element has access to more water than a forest or plantation tree. The isolated tree element usually reflects this by supporting more leaf and hence its *LAI* is often higher than that of a forest or plantation.

From Figure 20 this can be written mathematically

$$\frac{A_3}{A_2} = \frac{LAI_2}{LAI_1}, \tag{7}$$

where: A_3 is the area of hydrologic occupation of the tree belt, A_2 is the projected canopy area of the tree belt, LAI_2 is the leaf area index of the belt and LAI_1 is the leaf area index of the nearby block. Therefore:

$$A_3 = \frac{A_2 \times LAI_2}{LAI_1}, \tag{8}$$

but

$$A_2 \times LAI_2 = L_2, \tag{9}$$

where L_2 is the leaf area (m^2) occupying A_2. Substituting Equation 9 into Equation 8 gives

$$A_3 = \frac{L_2}{LAI_1}. \tag{10}$$

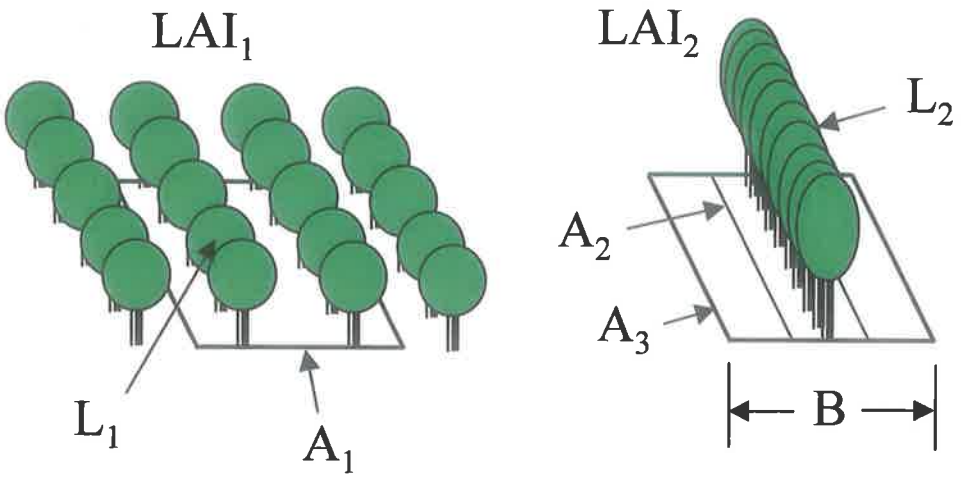

Figure 20 The leaf area index of an isolated tree element LAI_2 is usually higher than the average leaf area index of nearby (non-isolated) forest LAI_1. My hypothesis states that ratio of the equivalent area of hydrologic occupation to canopy projected area A_3/A_2 is equal to the ratio LAI_2/LAI_1. In which case A_3 is equal to L_2/LAI_1 and B (the width of A_3) is equal to LLA/LAI.

Hypothesis in terms of leaf area *L*

Consider Figure 20 with an area of leaf L_1 in a block and an equal area of leaf L_2 in a belt such that $L_1 = L_2$. My hypothesis says that the hydrologic effect of the leaf area is the same in both cases. In the block it unambiguously occupies area A_1, which must be equal to A_3 in the belt. By definition $A_1 = L_1/LAI_1$. Since $A_1 = A_3$ and $L_1 = L_2$ then $A_3 = L_2/LAI_1$ as with Equation 10.

The general form of the equation is therefore

$$A = \frac{L}{LAI}, \tag{11}$$

where: A is the equivalent recharge area (m^2); L is the leaf area of the agroforestry tree element (m^2); LAI is the leaf area index (m^2 m-2) of the block. The recharge flux in the defined area A, and in the block, are equal. This area, defined by this method, has the same hydrologic effect, at the paddock scale, as does the more complex, real hydrologically occupied zone. This general form (11) can be modified to more conveniently address alley farming geometries (Equation 12), using leaf area per unit length of belt.

$$B = \frac{LLA}{LAI}, \tag{12}$$

Where: *B* is the width (Figure 20) of the equivalent recharge zone (m); *LLA* is the lineal leaf area of the agroforestry belt (m^2 m^{-1} belt).

Equivalent No Recharge *ENOR*

The concept of 'equivalent recharge' can be taken a step further to 'Equivalent No Recharge', or *ENOR*. It allows the complex root zone hydrology of an agroforestry tree element to be expressed as a simple area, or width, of zero recharge (Figure 21).

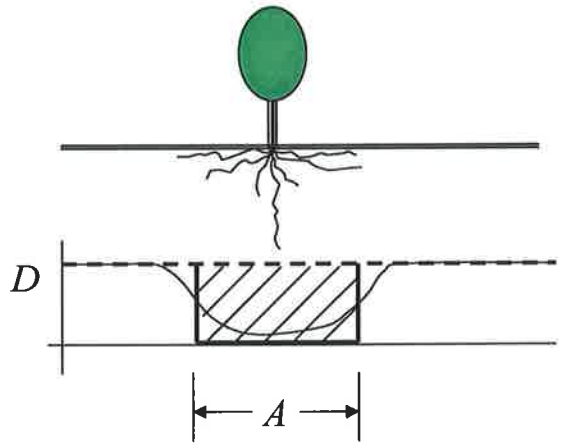

Figure 21 A schematic representation of a real recharge *D* profile under an isolated tree, approximated by zone *A* (m^2), within which recharge is zero. This zone is an Equivalent No Recharge Zone (*ENOR*).

A zero recharge zone may not exist in reality and therefore would be hypothetical. However, as with *ERZ* this zone of zero recharge makes an equivalent contribution to recharge, at the paddock scale, as does the 'real' recharge profile beneath a tree element.

ENOR – an approximation

In the large majority of water limited cases in southern Australia, steady state recharge from mature vegetation is very small (Allison *et al.*, 1990; Cook *et al.*, 1992; Kennett-Smith *et al.*, 1992a; Kennett-Smith *et al.*, 1992b; Walker *et al.*, 1992). In most cases in Australia, recharge beneath remnant vegetation or mature plantations is one or two orders of magnitude lower than the ambient values for cleared, agricultural land. This allows the equivalent area (Equations 11 and 12) to be considered to approximate a 'no recharge' zone (*ENOR*) when compared to the ambient recharge values.

In higher rainfall areas or where the soil is highly transmissive, recharge under mature vegetation will not be close to zero, for example in sand plain banksia species (Carbon *et al.*, 1982) where recharge can be as high as 330 mm yr^{-1}, 43% of rainfall. In this study, such situations are considered unusual. In such cases Equations 11 and 12 would predict

ERZ, rather than *ENOR*. However, an *ENOR* could still be easily scaled to the *ERZ* if required.

Seasonal variation of *LLA* and *LAI*

The *LAI* of natural vegetation is known to vary depending on the season and can fall by up to 50% under drought conditions (Pook, 1985). This has implications for predictions made using the *ENOR* approach, depending on the timing of the individual *LLA* and *LAI* measurements. Implicit in the above hypothesis is the assumption that the isolated tree element and the block are subject to the same seasonal conditions, and that they are both water-limited. Their changes in leaf area due to seasonal variations (relative to the long-term average) should be similar. It therefore follows that predictions from Equation 12 are independent of seasonal conditions if the *LLA* and *LAI* values used in are measured under the *same* seasonal conditions. Errors may be significant if *LLA* and *LAI* are measured under different seasonal conditions.

A recharge model for an alley farm

The *ENOR* concept allows a simple calculation of a percent recharge reduction expected for the whole system, from the ratio of no recharge area to total area (Equation 13, Figure 22).

$$RR = \frac{\text{recharge from alley farm}}{\text{recharge from conventional farm}} = 1 - \frac{B}{W} \qquad (13)$$

where: *RR* is Relative Recharge; the recharge from the alley farm as a fraction of recharge from the paddock if it were managed conventionally with crops and pastures; *Z* is the area of the agroforestry system or representative unit (m^2).

For linear agroforestry systems such as alley farms, *ENOR* width *B* can replace *A* and belt spacing *W* can replace *Z* giving Equation 14, and will be hence forth referred to as the *ENOR* model.

$$RR = 1 - \frac{B}{W}. \qquad (14)$$

Equation 14 can be used to estimate the expected recharge from an alley farm compared with that from a crop or pasture system. If the magnitude of recharge from the conventional farming system *RC* is known, an average recharge from the alley farm *RA* can be calculated

$$RA = RC \times RR. \qquad (15)$$

Alternatively, Equation 14 can be rearranged and solved for W (m) to allow the design of an alley farm geometry that will result in a 'target' recharge reduction, for a given B (m).

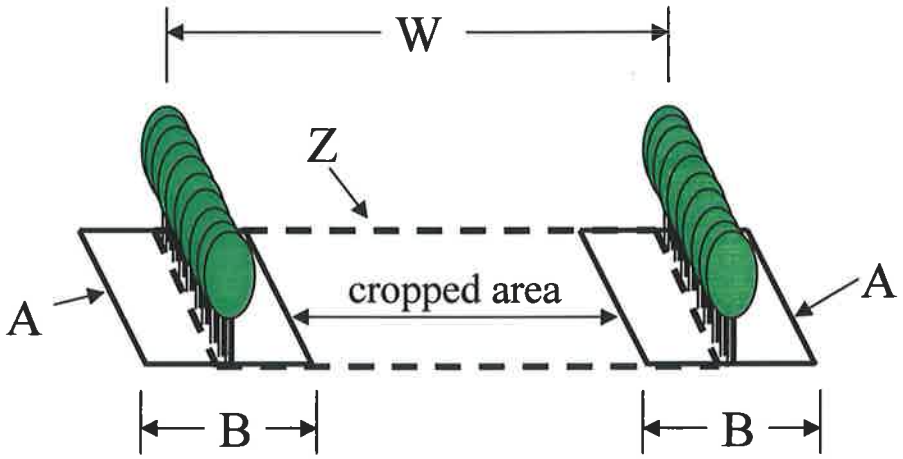

Figure 22 A schematic representation of an agroforestry system. *Z* is the total area or representative unit of the system. *A* is the *ENOR* area of the tree elements, *B* is the *ENOR* width and *W* is the belt spacing. The ratio *A/Z* gives the proportion of *ENOR* to crop/pasture area and is equivalent to *B/W*. Relative recharge reduction *RR* is therefore equal to 1 – B/W (Equation 14).

Conclusions

The new *ENOR* concept described in this chapter addresses the knowledge gaps identified in Chapter 3 in that it provides a simple method for describing the root zone of a tree belt, including the interface zone. The approach for predicting *ENOR* (Equation 12) using leaf area measurements satisfies the requirement for simple input parameters from above ground. The *ENOR* model (Equation 12) has the potential to fulfil the two aims of this study: 1) to estimate recharge from alley farms; 2) and to design alley farms to result in a prescribed or 'target' recharge. Attention should be paid to the conditions under which the *LLA* and *LAI* inputs are measured. If they are measured under similar seasonal conditions (preferably within days and kilometres of each other) then predictions should be insensitive to seasonal variations in the weather.

Summary

This chapter has introduced the concepts of Equivalent Recharge Zone *ERZ* and Equivalent No Recharge *ENOR* as means of simplifying the complex nature of tree belt root zones and the complex manner in which recharge is likely to vary within them. Mathematical expressions were then derived to show that, by considering the implications of eco-hydrological optimality theory (Eagleson, 1982), *ENOR* could be predicted from

leaf area measurements. The *ENOR* model for recharge from alley farms is then presented which represents alley farms as alternate *ENOR* zones and crop/pasture zones. The simple linear model can be rearranged to design an alley farm geometry to meet a given recharge target.

Chapter 5

Testing the *ENOR* approach using recharge measurements

Preliminary data from this chapter was presented at the *Envirowater99 – 2nd Inter-Regional Conference on Environment, Water* (see Ellis *et al.,* 1999). The contents of this chapter are also described in a manuscript submitted for publication to *Water Resources Research* (see Ellis *et al.,* in press).

Introduction

The previous chapter proposed a new approach and associated model for estimating the effect of alley farming on recharge, at paddock to catchment scales, or alternatively, for designing alley systems that would result in a specified recharge reduction. To be useful in the areas of southern Australia prone to dryland salinity, the model must also be applicable across a range of bio-climatic zones. The model used the *ENOR* with *B* (m) to describe the zone hydrologically occupied by tree belts. This chapter describes how predictions of *B,* made from leaf area measurements, were tested against measured recharge transects.

Following a statement of the aim of this chapter, the two methods used for the measurement of recharge and leaf area are outlined and then special attention is given to site selection and sampling. Selection criteria relate to the assumptions implicit in the *ENOR* approach, the methods used in the experiment, the need to collect data that is suitable to test the hypothesis, and the paucity of suitable tree belts sites.

To illustrate how the *ENOR* approach was tested, the results section presents, as examples, detailed data for 2 of the six sites (the remaining 4 are presented in Appendix 2). For each example site in turn, predicted *B* is calculated from leaf area and then compared with *B* measured from recharge transects. Predicted *B* for all six sites is then compared with measured *B* on a single graph.

Aim

To compare over a range of bio-climatic zones: values of *ENOR* width *B* (m) predicted from leaf area measurements (Equation 12) against *ENOR* width *B* (m) values calculated from measured recharge transects.

Methods

Recharge

Following a review of recharge measurement techniques (Chapter 3), the chloride profile methods (Allison and Hughes, 1978; Walker *et al.*, 1991) were determined to be most appropriate for this study. Chloride profile methods were chosen due to their ease of application and because they provide an average recharge flux, integrated over a long period. Although Electromagnetic (EM) techniques (Cook and Williams, 1998) would have also been a valid choice for use in this study, the main reasons they were not used include: the availability of equipment at the time of the field trips; and the requirement for EM to be calibrated at each site against a method such as the chloride front method. The calibration was likely to require just as many chloride profiles as were needed without using EM methods.

The chloride techniques were explained briefly in Chapter 3 and are explained in detail in Appendix 2 with accompanying calculations using data from sites used in this experiment. Generally, the mass balance technique (Allison and Hughes, 1978) was used to calculate the recharge flux where recharge was small, in remnant vegetation, old plantations, and in agricultural land close to trees. Where recharge flux was larger (towards the extremities of, and outside of tree root zones in agricultural land) the generalised chloride front displacement technique was used (Walker et. al., 1991). All soil was excavated using hand augers (Figure 23), placed in airtight containers and analysed for gravimetric water content and gravimetric chloride concentration (Beech, 1996). A soil bulk density of 1.5 g cm^{-3} was used for all soil (Jolly *et al.*, 1989) to convert gravimetric values to volumetric values.

Figure 23 Hand augers were used to extract soil samples for chloride profile technique, shown here at "Wakefield's" site, Parilla, South Australia. Note digging barrel about to be inserted in hole and handle near the top of the 6 m demountable shaft. This length represented less than half the depth of this hole.

Leaf area

Leaf areas used to calculate *LAI* (m^2 m^{-2}) and *LLA* (m^2 m^{-1}) were measured using the Adelaide (module) technique (Andrew *et al.*, 1979), in a similar manner to that described by Hatton *et al.* (1995). Two independent observers estimated the number of leaf modules (equivalent in size to a purposefully selected branch); the mean of the two estimates was then converted to leaf areas on the basis of the (single-sided) leaf area of the standard module, measured by electronic planimetry (Hatton *et al.* 1995).

As with Hatton *et al.* (1995) the method was tested against three trees with canopy areas: 14 m^2; 43 m^2; and 64 m^2 (Appendix 3). In a similar manner described by *Hatton et al.* [1995], the method was tested against three trees with canopy areas: 14 m^2; 43 m^2; and 64 m^2. These areas were determined by destructive sampling of the whole canopies. Linear

regression of the mean estimated values against known canopy leaf areas yielded y = 0.87 + 1.64 (r^2 = 0.99). Bias between observers was very small for a sample of 89 stems and r^2 = 0.98 (Figure 96).

The term lineal leaf area *LLA* (m^2 m^{-1}; leaf area per metre of belt) was used here as a convenient method to describe the canopy size of a linear agroforestry tree element like a belt or block edge (see next section), without needing to specify belt length. It also avoids the problem of needing to accurately measure the projected canopy area of belts (or block edges). This is usually difficult and prone to error because of the irregular shape of canopies. By measuring the leaf area of a known length of belt or block edge, *LLA* is calculated by dividing the leaf area (m^2) by the length of the row or the block edge (m). This gives a lineal leaf area, *LLA* (m^2 m^{-1}), as used in Equation 12. *LAI* (m^2 m^{-2}) was calculated by dividing the leaf area (m^2) measured within a marked quadrat, by the ground area (m^2) of that quadrat. Appendix 2 gives detailed descriptions of sampling methods and calculation of both *LAI* (m^2 m^{-2}) and *LLA* (m^2 m^{-1}).

Site selection and sampling

Recharge transects

Alley farming systems are a relatively recent phenomenon in southern Australia and there was a lack of suitably mature alley farming sites on which to test the approach. Isolated belts of trees on farming land were therefore chosen to represent a single unit of an alley system but were also extremely scarce.

Sites for recharge measurements were selected in 1997 at four locations (Figure 24; Table 1) over a climate gradient (Figure 133; Figure 134) using the following criteria: vegetation mainly composed of mature eucalypt trees; good tree health; immediately adjacent to agricultural land; at least 50 years since clearing of agricultural land; minimal understorey; minimal runoff; minimal wind erosion; ground water not accessible to trees (at least 30 m deep); and a relatively even tree growth along at least 20 m of the belt. Using these criteria, only two suitable tree belt sites were found and it was necessary to augment these by using the edges of blocks of vegetation, also selected using the above criteria. Edges of vegetation blocks in southern Australia exhibit a readily defined strip of enhanced growth. Of the four such edges measured, growth was enhanced by factors of about 1.5 to 3, relative to mid-block growth, and extending 5 – 15 m in from the edge stems. This phenomenon was obvious to the eye (Figure 27; Figure 28) and easily verified with leaf area measurement (Figure 29). Albertson *et al.*, (2000) and McJannet (1999) also reported this phenomenon in plantations. Table 1 gives basic characteristics of the two belts and

four block edges (one was a mature plantation); more detailed site descriptions are given in Appendix 1. Detailed soil descriptions were not recorded for these sites however generalised soil types, topography and site layout are given in Appendix 1.

The positions of soil profile holes in the transects were selected to adequately describe the change in recharge (from trees to paddock outside the tree root zone) with a minimum number of holes. The apparent extent of tree roots was often evident from above ground changes in soil appearance, crop or pasture stubble cover (if any), or from the absence of summer weeds. Greater soil hardness (judged by the difficulty of auguring), relative to open paddock conditions, and due to lower water content, was also used as an indicator that the hole was within the tree root zone. These methods proved to be reasonably effective for bracketing on the outer edge of the tree root zones although they tended to under estimate the maximum extent of the recharge reduction zone by several metres.

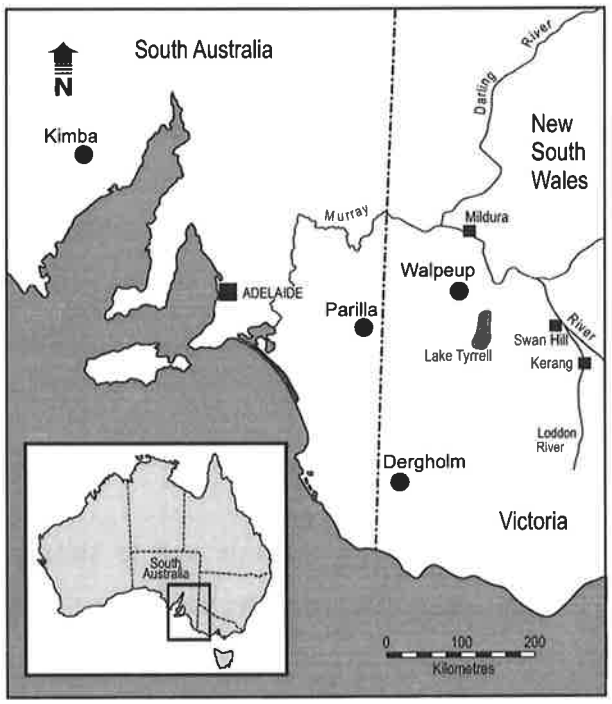

Figure 24 Southern South Australia and western Victoria. Two recharge transect sites were selected at both Kimba and Parilla; one site was selected at Walpeup and another at Dergholm (see Table 1).

Leaf Area Index *LAI* and Lineal Leaf Area *LLA*

LAI of natural vegetation was measured at the sites listed in Table 1 and shown in Figure 24, as close as possible to the recharge transect. Their proximity to the transects varied between immediately adjacent, and several kilometres away. They were selected on the following bases: good tree health; minimal disturbance; eucalypt dominated overstorey;

minimal run off; ground water not accessible by trees (at least 30 m deep), and minimal understorey. *LAI* quadrats were large to account for spatial variability; quadrat sides ranging from 20 – 50 m in length. *LLA* was averaged over at least 20 m length of belt or block edge; the ends of each belt or edge length were estimated to be mid-way between the adjacent canopies closest to the ends. As all *LLA* and accompanying *LAI* measurements were not separated significantly either temporally or spatially, it is safe to assume that the predictions made using the *ENOR* approach (Equation 12) would be free of any error associated with seasonal variation in climate.

Table 1 Basic characteristics of recharge transect sites.

Site	Vegetation type	Width of vegetation (m)	Edge growth enhancement relative to mid-block
Kimba	Remnant belt	7	NA
Kimba	Remnant block edge	6	1.5
Parilla	Remnant block edge	4	2
Parilla	Plantation edge	5	3
Walpeup	Remnant belt	8	NA
Dergholm	Remnant block edge	15	2

Explanatory notes for Table 1: 1) Width of vegetation for a belt is the width of the belt, measured stem to stem. 2) Width of vegetation for a block edge is the width of the strip of enhanced edge growth measured stem to stem. 3) NA = not applicable.

Results

Chloride profiles

Chloride profiles were used to calculate recharge and to subsequently map recharge transects. As an example, chloride profiles from the transect at the Walpeup site ($35^0$07'S, $141^0$59'E) are presented here in Figure 25 and the chloride profiles for the remaining sites are shown in Appendix 2. The Walpeup site was situated mid-slope, on a north-facing slope, of a Boigbeat dune-swale system (Rowan and Downes, 1963). The transect extended from within a north-south oriented, 8 m wide (stem to stem) belt of remnant white mallee (*Eucalyptus dumosa*).

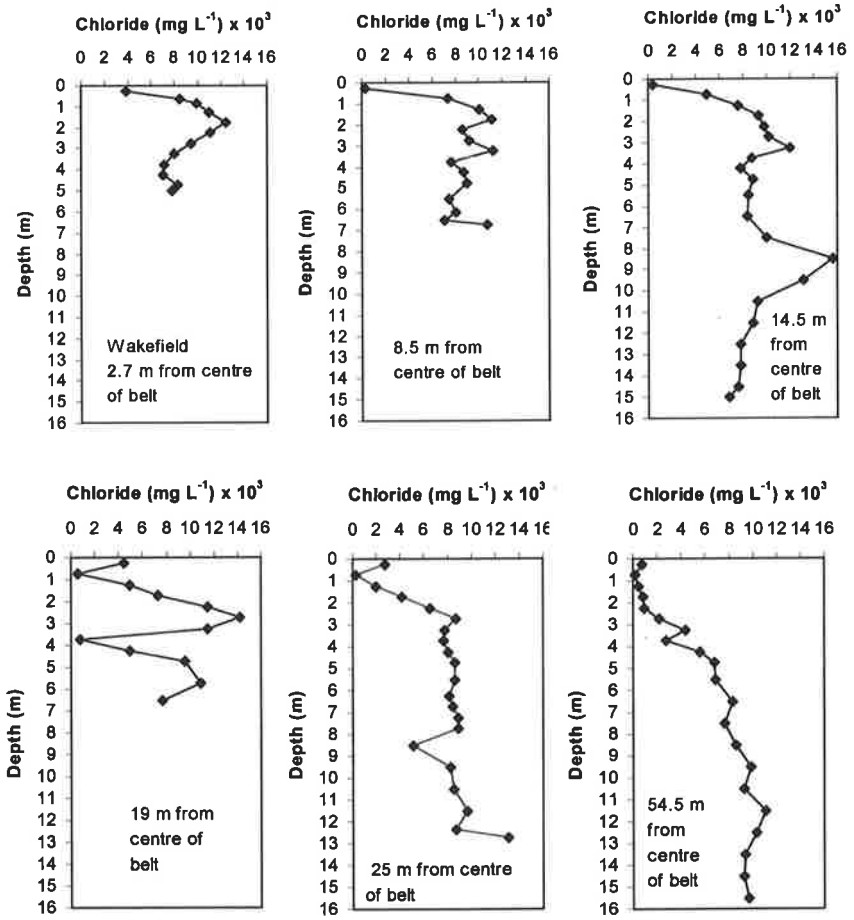

Figure 25 Soil water chloride concentration (mg L^{-1}) versus soil depth (m) from the Walpeup site, at six points between 2.7 m and 54.5 m from the centre of the belt.

The transect was perpendicular to the belt and in line with the dune, extending into adjacent agricultural land (Figure 23; Figure 88 gives an aerial view of the site). Figure 25 shows soil water chloride concentration versus soil depth for six points between 2.7 m and 54.5 m from the centre of the belt. Profiles 2.7 m, 8.5 m and 14.5 m from the centre of the belt of trees were typical of non-leached profiles beneath natural vegetation and showed a prominent chloride 'front' near to the surface. Recharge for these profiles was calculated using the mass balance method (Allison and Hughes, 1983). At 19 m, 25 m and 54.5 m solute profiles showed signs of leaching with a less pronounced chloride front lower in the profile. For leached profiles, recharge was calculated using the transient chloride method (Walker *et al.*, 1991). Appendix 2 gives worked examples of the calculation of recharge from both leached and non-leached profiles.

Predicted *ENOR* versus measured *ENOR*

This section presents, in detail, the results from two sites: the *remnant belt* at Walpeup; and the salmon gum *plantation block edge* at Parilla. *ENOR* width *B* (m) predictions from leaf area measurements are calculated and then compared with *B* (m) calculated from the recharge transects. Recharge transects from the remaining four sites are presented in Appendix 3. In the next section of this chapter the *B* (m) calculated from all six transects are presented together (Table 2; Figure 31) and compared with predictions.

The Walpeup *remnant belt B* value was predicted for the belt of remnant eucalypt mallee (*E. dumosa*) trees (Figure 24) by applying Equation 12. Using *LLA* of 25 m^2 m^{-1} and local *LAI* of 0.6 predicts an *ENOR* width *B* = 41.6 m for the belt (rounded up to 42 m). The recharge transect (Figure 26) for the belt was calculated from chloride profiles (Figure 25). Recharge flux below the belt is small (0.18 mm yr^{-1}), rising to the ambient value of 7.2 mm yr^{-1} beyond the influence of the tree roots. Given the order of magnitude difference, it was therefore valid to apply the *ENOR* approach. The vertical dashed line denotes the maximum lateral extent of the tree roots approximated from above ground observations, and is similar to observations from local land holders that eucalypt mallee can invade adjacent crops for up to 35 m.

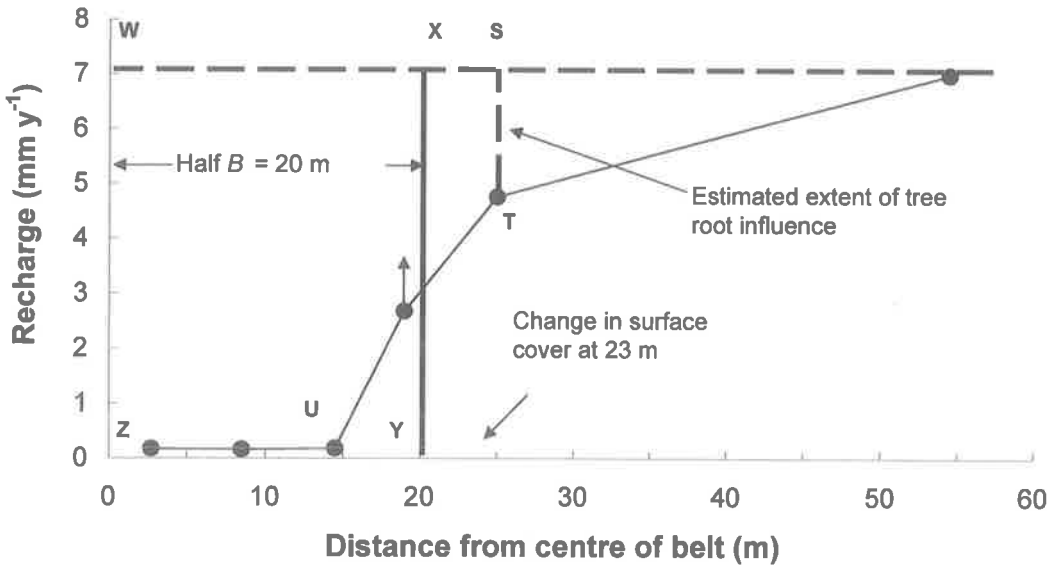

Figure 26 A recharge transect of an 8 m wide (stem to stem) belt of remnant eucalypt mallee (*Eucalyptus dumosa*) with a crown width of 10 m. *B* was calculated as the width of the rectangle WXYZ when its area is equal to the 'recharge deficit' rectangle WSTUZ.

The 'half-width' of *B* (Figure 26) is found from the width of rectangle WXYZ, the area of which is equal to the 'recharge deficit' above the actual recharge transect – the area of WSTUZ. That is, at the paddock scale, the measured transect provides a recharge reduction equivalent to a strip 20 m wide, within which recharge is zero. Since this is only half a complete transect, the *ENOR* width for the belt of trees is 40 m, if below ground effects are assumed symmetrical, and in this case it agrees well with the predicted value.

Figure 27 Aerial photograph of salmon plantation gum edge at Parilla, South Australia. A strip of enhanced growth can be seen close to the edge and correlates well with leaf area measurements and stem diameters (Figure 28 and Figure 29). The effect of the tree roots is reflected in the crop stubble. The effects ceased where the green weeds start; a distance of about 50 m, which correlates with the recharge transect from that site (Figure 28).

The salmon gum *plantation block edge* at Parilla (35^0 17' S; 140^0 39' E; Figure 27) is a classic example of enhanced edge growth due to the lateral extension of roots into the adjacent land. Figure 29 shows a row-by-row *LLA* transect that clearly indicates enhanced growth at the edge, reflecting greater access to resources, water probably being the most important. The row spacing was 2 m, and enhanced leaf growth was easily identified and associated with larger stem diameters; these were largest in the outer most row, falling to mid-plantation values by the fourth row from the edge. That is, the growing space of trees further than 5 m in from the edge was considered to be defined by their own projected areas. Whereas the growing space of trees within 5 m from the edge, was defined by the

horizontal extent of lateral roots into adjacent agricultural land as well as the ground area of the edge strip. Equation 12 was therefore applied to the three rows of enhanced growth having *LLAs* of 51.5, 7.7 and 11.8 m^2 m^{-1} respectively, giving a total *LLA* for the enhanced strip of 71 m^2 m^{-1} of edge. The mid-plantation *LAI* was 1.21, therefore Equation 12 predicts B =71/1.21 = 59 m. The *LAI* of the edge strip was about 3, although it was difficult to calculate accurately because of the problems associated with measuring the canopy projected area.

Figure 28 Stems of the salmon gum plantation showing significantly enhanced growth of the two outside rows (left to centre) relative to mid-plantation growth (right). The growth enhancement is illustrated in the aerial view (Figure 27) and leaf area measurements (Figure 29), which also shows that the growth of the third row is enhanced. Plantation grid spacing was 2 m. The higher *LAI* of about 3 near the edge (left to centre) is evident from the deeper shade compared to mid-plantation with *LAI* of 1.21 (right).

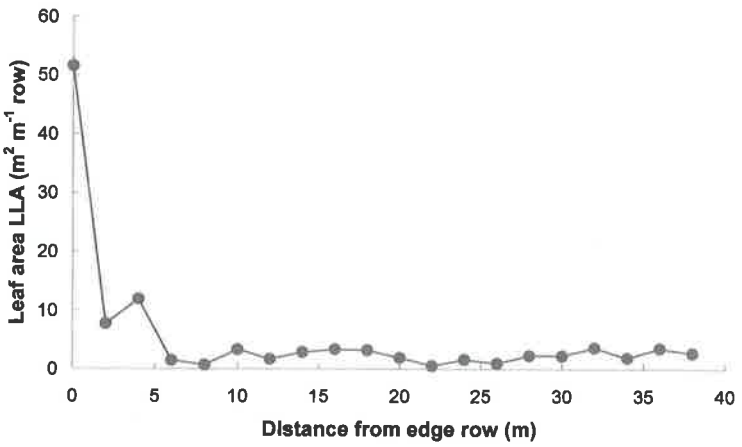

Figure 29 Lineal leaf area *LLA* of 20 rows (2 m row spacing) of a salmon gum (*Eucalyptus salmonophloia*) plantation. The transect extends from the edge row to 38 m inside the block where the average *LAI* was 1.21.

The recharge transect from the salmon gum site (Figure 30) extended from within the block, into the adjacent paddock, to beyond the tree root zone. From recharge measurements, *B* was calculated to be 60 m, equal to the width of the rectangle WXYZ, which is of equal area to the recharge deficit WSTU.

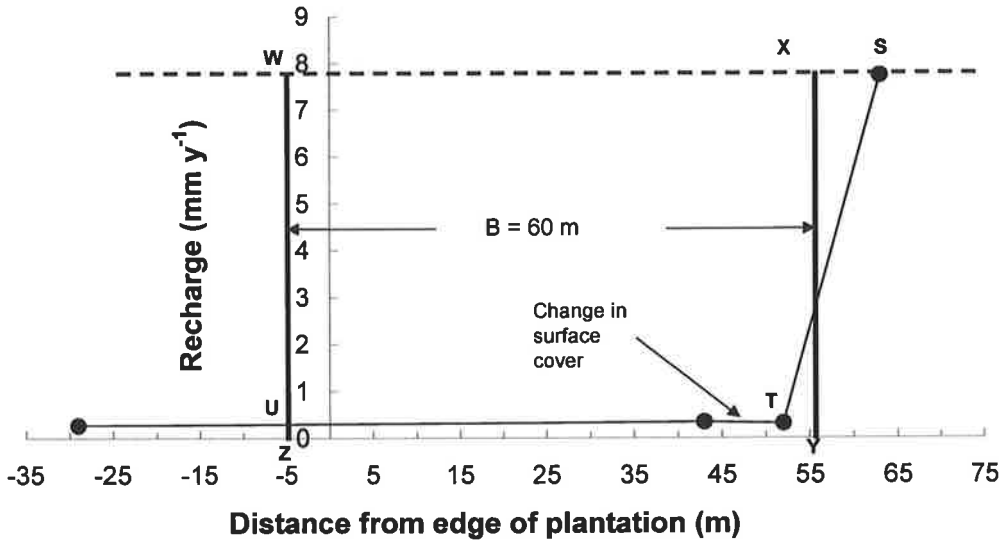

Figure 30 Recharge transect from the edge of a salmon gum (*Eucalyptus salmonophloia*) plantation at Parilla. The transect extended from within the plantation to outside the tree root zone. *B* was calculated to be 60 m, equal to the width of the rectangle WXYZ, which has the same area as the recharge deficit WSTU.

Testing predictions over a range of climates

This section presents the *ENOR* width *B* (m) for all six recharge transects sites and compares them with predicted *B* (m). The sites comprised two isolated tree belts and four block edges; for each of the isolated belts (see Table 1) a chloride transect was measured on one side of the belt only and assumed to be identical on the remaining side. For the four block edges, enhanced edge growth was easily identified and the *LLA* values from this strip were used in predictions (Equation 12). *B* calculated from recharge transects at block edges was considered to be associated with the strip of enhanced growth at the edge of the block.

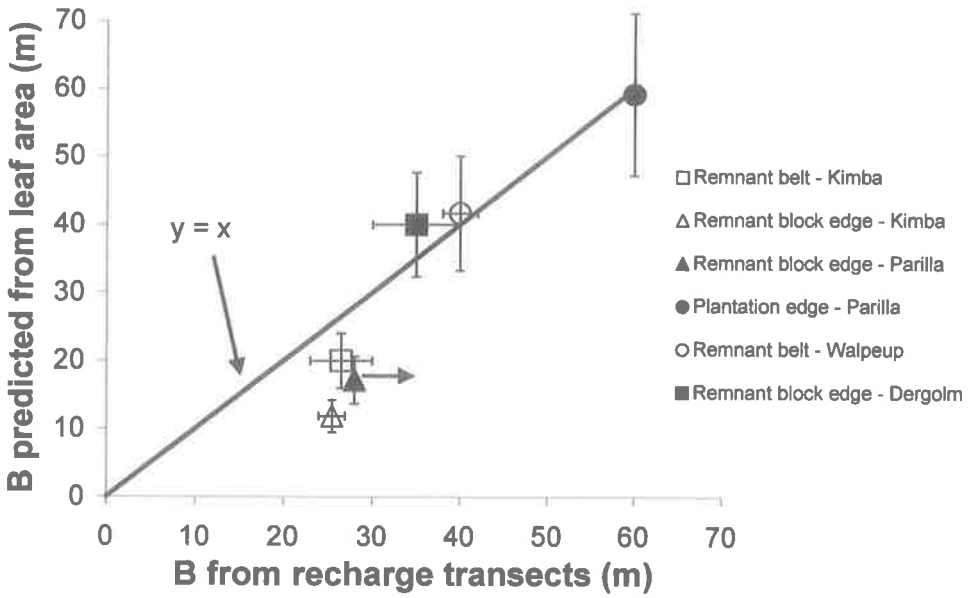

Figure 31 *B* predicted from leaf areas (Equation 12) versus *B* from recharge transects for two isolated belts and four block edges. Error bars represent the largest expected errors calculated in Appendix 2. At remnant block edge sites at Parilla ▲ and Kimba Δ, larger measured values correlate with likely runoff from these sites (see site descriptions Appendix 1). The arrow indicates that the data point for the Parilla remnant block edge represents a minimum measured *B* because the recharge transect did not extend past the end of the root zone (see Appendix 2).

B widths predicted from leaf areas were plotted against *B* calculated from recharge transects (Figure 31). Error bars displayed in the *y* direction show the worst-case errors expected in the prediction of *B* using a 10% error in both *LLA* and *LAI* (Appendix 2 and Appendix 4). Error bars displayed in the *x* direction show the maximum error expected in the measurement of *B* from recharge transects. These are calculated from possible overestimates and underestimates of the extent of the root zone influence and the relative increase in recharge at the boundary of the root zone influence. Details of these calculations with specific reference to each site are given in Appendix 2 and a compilation of all experimental errors is given in Appendix 4. A summary of the site data, results and errors is given in Table 2.

Table 2 Summary of leaf area measurements, predicted *B* and measured *B* for belts and block edges. The sites are sorted in order of increasing climate wetness.

Site	Average annual rainfall (mm yr^{-1})	Eo (mm yr^{-1})	Vegetation type	Width of vegetation (m)	LLA (m^2 m^{-1})	LAI (m^2 m^{-2})	Tree height (m)	Width of surface expression (m)	Width of reduced recharge (m)	B predicted from leaf areas (m)	B measured from recharge (m)
Kimba 33° 15' S 136° 50'E	300	2250	Rem belt	7	11	0.56	4.5	20	<28	20 ±4	26.6 ±4
Kimba 33° 15' S 136° 50'E	300	2250	Rem block edge	6	6.5	0.56	4.5	26	31	12 ±2.4	25.5 ±1.5
Parilla 34° 31' S 140° 39'E	345	1900	Rem block edge	4	12	0.74	6	21	>30	16 ±3.5	>28
Parilla 34° 31' S 140° 39'E	345	1900	Plant'n edge	5	71	1.21	16	52	67	59 ±12	60 (small error)
Walpeup 35° 07' S 141° 59'E	343	2000	Rem belt	8	25	0.6	8	40	50	42 ±8.4	40 ±2
Dergholm 37° 21' S 141° 12'E	701	1500	Rem block edge	15	38	0.95	14	39	47	40 ±7.7	35 ±5

Explanatory notes for Table 2.

Width of vegetation for a belt is the width of the belt, measured stem to stem.

Width of vegetation for a block edge is the width of the strip of enhanced edge growth measured stem to stem.

Width of surface expression is the width of vegetation plus the distance to the apparent edge of the root zone (multiplied by 1 for a block edge and by 2 for a belt) as indicated by change in soil surface or soil cover.

Width of reduced recharge is the width of vegetation plus the distance to a significant increase in recharge (multiplied by 1 for a block edge and by 2 for a belt).

B predicted from leaf areas is $B = LLA/LAI$ where *LLA* is the Lineal Leaf Area (m^2 m^{-1}) of the belt or enhanced edge growth of the block and *LAI* is the Leaf Area Index *LAI* (m^2 m^{-2}) of local natural vegetation.

B estimated from recharge is the width of zero recharge that has the same recharge deficit as the width of reduced recharge.

Discussion

The recharge transect sites were remote and obtaining soil samples was hard work. For this reason, a minimum number of strategically placed profiles were dug at each site to attempt to efficiently describe each recharge transect. Chloride assays were not available until long after site visits however, with the benefit of hindsight, it is easy to see where additional profiles would aid interpretation of the transects. If time and resources had permitted, EM techniques (Cook and Williams, 1998) would have been a valuable adjunct to the chloride methods because they would have allowed a higher spatial resolution. This may have resulted in more coherent recharge transects and possibly smaller errors in the x direction.

At all sites it was attempted to obtain 2 profiles outside the influence of the root zone of the trees, usually by positioning them beyond the change in soil surface cover (weeds, crop, pasture etc.). Ideally, the two associated (higher) recharge values would have confirmed that the extent of the tree root zone had been exceeded. This condition was not always attained. However, the associations between recharge increases changes in surface cover allow relatively confident measurements of B. Also, the recharge values outside the root zones at Parilla and Walpeup are similar to other reports from those areas (3 – 13 mm yr^{-1}, O'Connell *et al.*, 1995; 3 – 5 mm yr^{-1}, Allison *et al*, 1990; 17 mm yr^{-1}, Williamson, 1998). In addition, given the abrupt changes in recharge at the edges of the root zone influence, the calculation of B from recharge transects was shown to be relatively insensitive to whether or not the transects defined the edge of the root zones exactly (see Appendix 2).

Recharge transects show the likely extent of lateral roots, but the time taken for them to reach maximum extension is not known. In the case of remnant vegetation, the position of roots of edge trees may not have changed since clearing. In the case of a plantation (Figure 27) however, lateral roots would take some time to reach maximum extension as the trees grew. If root extension occurs slowly, then one could expect that some recharge could occur during this time, and the transition, as depicted by the abrupt change in recharge at the edge of the root zone (Figure 30) would be gentler. Using root growth rates of 20 mm d^{-1} (Wilson, 1967) the salmon gum roots would reach their maximum extension of 50 m in about 6 years and 10 months. It is quite possible that an episodic recharge event did not occur over that period (Hume *et al.*, 1998). Although this is somewhat inconclusive, the abrupt change shown in Figure 30 is possible.

The most likely areas of over simplification in the approach relate to soil evaporation and run off. There is no available data for forest floor evaporation in the study areas; neither is it known if it is similar to that beneath isolated tree belts. One can safely assume that evaporation will increase with distance from the edge of belts but the integrated effect is unknown (this is investigated in more detail in the next chapter). The effects of run off were minimised by careful site selection although it is unlikely that they were completely removed. The remnant block edge sites at Parilla and Kimba sloped away from the trees such that run off may have been significant during intense rainfall events, leading to the under-prediction of *B* (Figure 31). In both these cases the predicted *B* from leaf areas was smaller than that from recharge transects, as would be expected if run off was significant.

Another key assumption made when developing the *ENOR* approach (Chapter 4) was that the long-term average contribution of the crops and pastures (within *B*) was small. Although this was not measured, Figure 31, together with field observations of growth near trees confirm that this was a valid assumption, except possibly in the case of the Kimba tree belt. The under prediction of *B* for that site could be attributed to the presence of some perennial grass understorey, the leaf area of which was not taken into account.

The predictions for the plantation edge at Parilla, the remnant belt at Walpeup, and the remnant block at Dergholm are suitably accurate for application to agroforestry systems. When the Parilla and Kimba block edge sites are excluded (because of runoff), Table 2 shows that a working error of less than 20% can be expected when predicting *B*.

Conclusions

This chapter has shown two things:

1. The *ENOR* concept is a useful simplification of a complex below ground interaction between trees and soil water.
2. The approach for predicting *ENOR* width *B* (Equation 12) was valid over a range of water-limited climates, and requires no below ground measurements. Care needs to be taken when applying the approach where runoff is significant.
3. The 'worst case' error associated with the prediction of *B* is modest, and although it is difficult to quantify a confidence interval, a working error of less than 20% is suitably conservative.

The approach is likely to oversimplify some of the water balance aspects of isolated tree elements, however, it appears that leaf areas are an integrated expression of the area they hydrologically occupy in the landscape. The *ENOR* concept allows a binary representation

of agroforestry systems (Equation 14) and, combined with predictions of *B* from leaf area (Equation 12), a practical means for estimating the recharge control potential of low rainfall agroforestry systems.

Summary

This chapter has tested the *ENOR* approach using measured recharge transects at two tree belt sites and four block edge sites. It is illustrated, using site photographs and leaf area transects, that tree growth was significantly enhanced at the edges of blocks, by factors of about 1.5 to 3, relative to mid-block growth and for distances of 5 – 15 m in from block edges. The calculation of *ENOR* width *B* from recharge transects is explained using one belt and one block edge example. *B* calculated from all six transects is compared with *B* predicted from leaf area measurement (Equation 12). It is shown that the *ENOR* approach can be applied to tree belts to predict *B,* and the worst-case error is unlikely to be greater than 20%.

Chapter 6

Testing the *ENOR* approach using water balance measurements

The contents of this chapter are also described in a manuscript submitted for publication to *Water Resources Research* (see Ellis *et al.*, in press).

Introduction

The *ENOR* approach developed in Chapter 4 sought to describe the zone hydrologically occupied by a belt of trees in terms of recharge. The approach was tested against measured recharge transects in Chapter 5, and found to predict the results within reasonable limits. This chapter tests the *ENOR* approach from a water balance perspective.

Recharge is one component of the water balance, and although it is usually a relatively small one, it can be calculated by difference, if the remaining water balance components are known (and errors are small). This is relatively simple for systems that can be considered one-dimensional such as a uniform forest or crop; all water balance components are normalised to area. For a belt of trees however, the area hydrologically occupied is also an unknown and the water balance components cannot be normalised in this way. In this case therefore, a more useful way to look at the water balance of a belt of trees is to set recharge zero and solve the water balance for *ENOR*. This gives a relationship that can be tested experimentally, and provides another viewpoint from which

to consider the new approach. This chapter first derives an expression for B in water balance terms, and then describes an experiment used to obtain the necessary measurements to calculate B for a tree belt (in water balance terms), and to compare it with B predicted from leaf area measurements.

ENOR in water balance terms

The water balance-based concept of *ENOR* (Figure 32) defines it as the hypothetical zone that catches enough rainfall to account for the other water balance components: transpiration T; interception I; soil evaporation E; and change in soil storage ΔS. Recharge, by definition, does not exist within the *ENOR* zone. E will vary spatially, but over a long time step will be a constant value. Applying the water balance, and expressing water balance components in appropriate units, gives Equation 16 for *ENOR* area A (Figure 32)

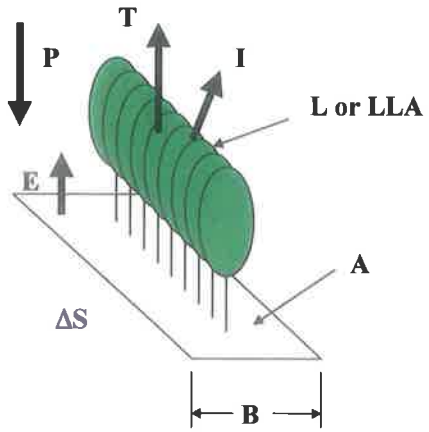

Figure 32 Schematic diagram defining *ENOR* in water balance terms. *ENOR* has area A, the area required to catch enough rainfall P to account for: transpiration T; interception I; soil evaporation E; and change in stored soil water ΔS, which will be zero over long periods of time. B is the width of area *ENOR* area A for linear agroforestry elements such as alley farming belts.

$$A = \frac{T + I}{P - E - \Delta S} \tag{16}$$

where: T transpiration (L); I is interception (L); P, E and ΔS are rainfall, evaporation and change in soil water storage, respectively (mm), yielding A in m^2. Over long periods ΔS will be small. If this concept is applied to a linear agroforestry tree element such as a belt, Equation 17 is used

$$B = \frac{T + I}{P - E - \Delta S} \tag{17}$$

where: T transpiration (L per m of belt); I is interception (L per m of belt); P, E and ΔS are rainfall, evaporation and change in soil water storage, respectively (mm), yielding B in metres. Again, over long periods ΔS will be small and can be omitted.

It is important here to consider the implications of the water balance Equation 17 when combined with the *ENOR* approach developed in Chapter 4 (Figure 20; Equation 12). If ΔS is assumed small and Equation 17 is applied to both isolated (belt) and non-isolated (block) cases then the following must hold.

$$\left(\frac{T+I}{P-E}\right)_{isolated} = \left(\frac{T+I}{P-E}\right)_{non-isolated} \tag{18}$$

This is not tested explicitly in this study, however a separate experiment is described that tests the null hypothesis that T_{isolated} and $T_{\text{non-isolated}}$ (from Equation 18) are equal. That is, the leaf efficiency (transpiration per unit leaf area, as coined by Hatton *et al.*, 1997) is the same for isolated trees as it is for trees in a block. Results from this experiment are used to support the approach.

Aim

To compare for a belt of trees: the *ENOR* width B predicted from leaf area measurements (Equation 12) with *ENOR* width B calculated using water balance considerations (Equation 17).

Experimental site

Tree belt water balance site

A tree belt was chosen for the water balance study using the following selection criteria: 'mature' trees that had come into equilibrium with and were not 'mining' soil water stored from before they were planted; trees were 'rain fed' only and did not have access to a water table; single, branchless stems to a height of at least 1 m (for ease of sap flow instrumentation); and minimal micro-relief in the surrounding soil surface so that runoff would be minimal; land was cropped on both sides of the belt; no stones at the surface or in the profile for ease of soil sampling and instrumentation.

The tree belt comprised two rows of 13 year old, single stemmed eucalypts planted in a north-south orientation on a private farm at Roseworthy, South Australia (Figure 33; $34^0$31'S, $138^0$41'E). The winter-dominated annual average rainfall was 443 mm; and annual average pan evaporation was 2000 mm. The western row was *E. occidentalis* and the eastern row was *E. leucoxylon*. The rows were 3.5 m apart; interrow stem spacing was

3 m, with one row staggered relative to the other; canopy width of the belt was about 8 m; tree height was 7 m to 9 m, with *E. leucoxylon* generally larger than the *Eucalyptus occidentalis* (Figure 34a; Figure 36). There was canopy closure within the *Eucalyptus leucoxylon* row but about 1 m between the *E. occidentalis* canopies and a canopy gap of 0.5 m to 1 m between rows (see Figure 36 for the tree layout).

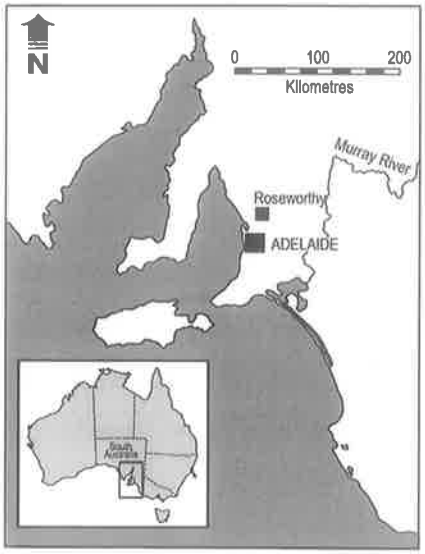

Figure 33 Southern South Australia showing the location of the water balance site at Roseworthy, on the northern Adelaide plains.

The tree root zone had a visible effect on crops up to 10.5 m from *E. occidentalis* stems (western side) and up to 13 m from *E. leucoxylon* stems (eastern side), giving a nominal root zone width of about 22 to 27 m. The topography was flat and the soil was a red *chromosol* with some variation to *calcarisol* across the site (Isbell, 1996) – loam from 0 m to 0.1 m deep, below which was a silty clay to at least 6 m with a bulk density of about 1.5 g cm^{-3}. Normally, winter crops were sown to within 2 m of tree stems on both sides of the belt but to simplify the experiment, the soil was kept bare 45 m each side of the belt, for a 40 m length of belt (Figure 34a). This negated the need to measure crop transpiration. Four immediately adjacent trees were chosen for sap flow measurements; two *E. leucoxylon* (L1 and L2) and two *E. occidentalis* (O1 and O2) (Figure 34b; Figure 36); the dimensions and leaf areas of the trees are given in Table 3. A fence was erected around the site to exclude stock that grazed the surrounding stubble over the summer period.

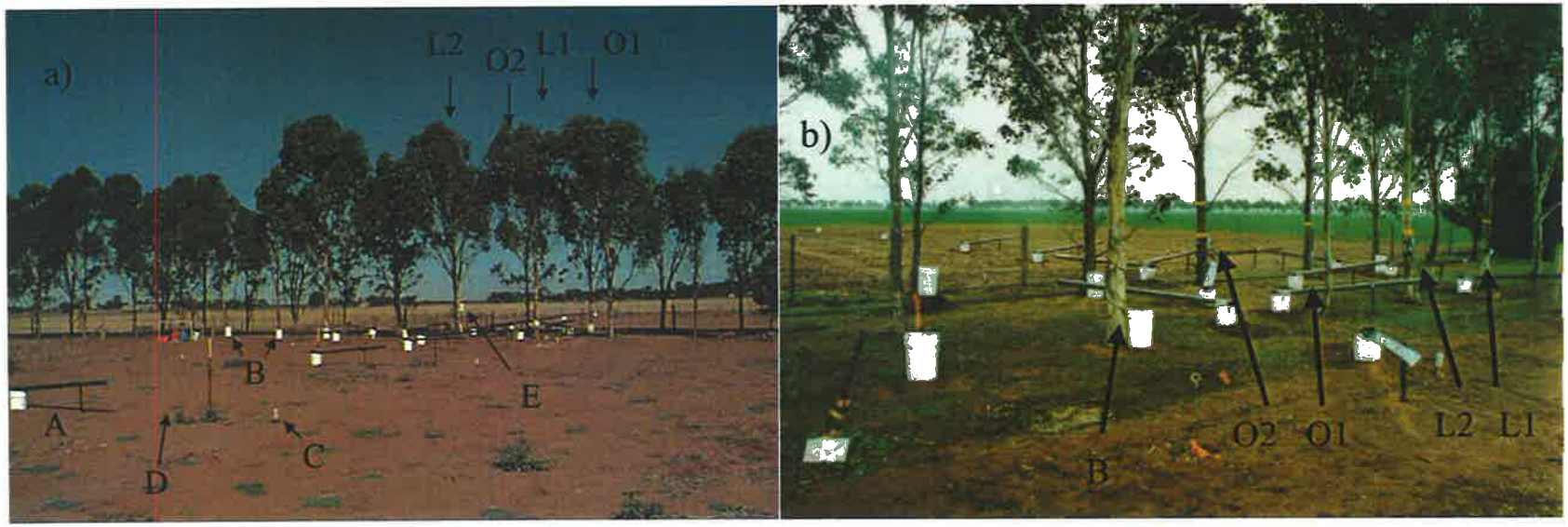

Figure 34 a) The water balance experimental site in summer, looking southwest and showing trough and bucket rain gauges (A); stem flow buckets (B); neutron moisture meter NMM access tubes (C); the four trees (L1, L2, O1, O2) from which transpiration was monitored; and the automatic weather station (E). The position of a microlysimeter is indicated (D).

b) The water balance experimental site in winter, looking southeast. Transpiration was measured using heat pulse sap flow meters installed in trees marked with yellow tape. The foreground row is *E. leucoxylon* (L1, L2) the far row is *E. occidentalis* (O1, O2). Stem flow buckets and rubber collection channel can be seen attached to stem (B).

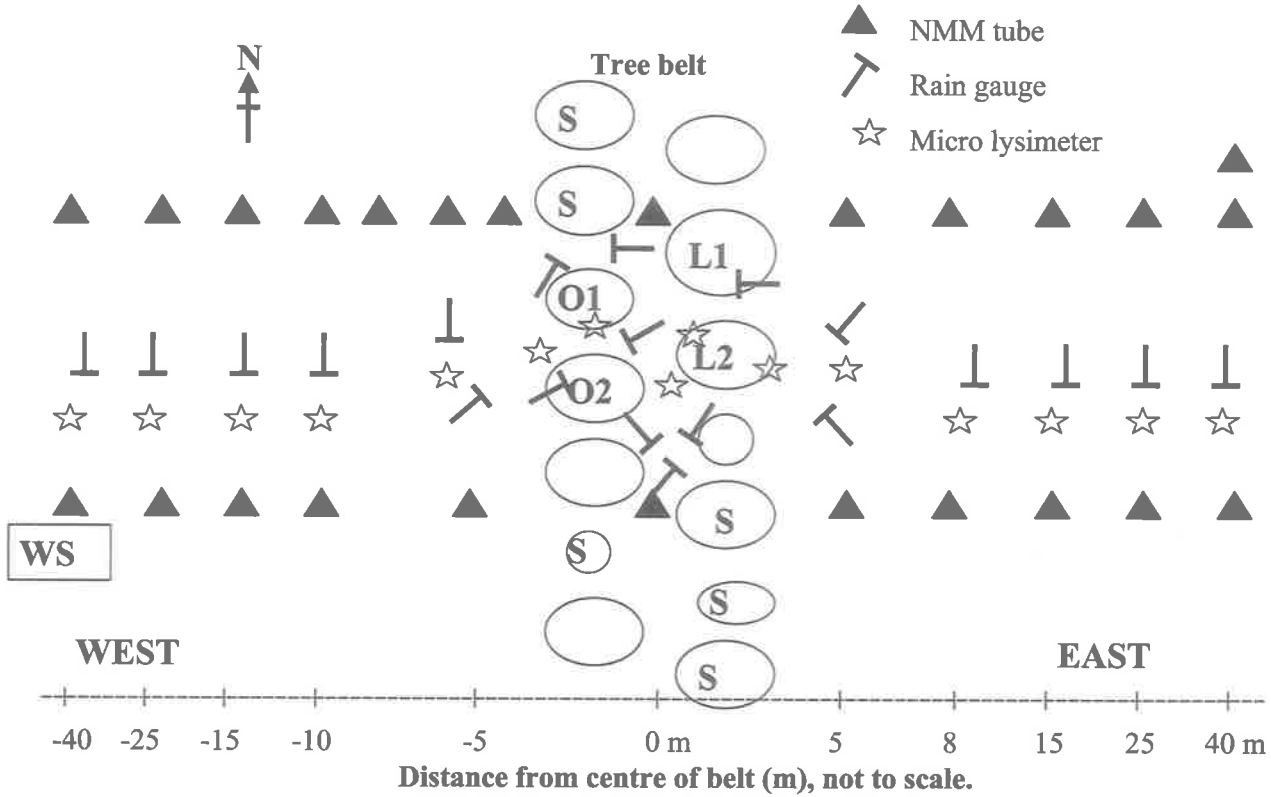

Figure 35 Tree belt water balance experimental site layout showing horizontal dimensions (not to scale). Open circles indicate tree canopies and approximate relative sizes. Four adjacent trees: O1; O2; L1; L2; were instrumented for sap flow. Two transects of neutron moisture meterNMM access tubes are shown as ▲ and one transect of microlysimeters as an open stars. Trough and bucket rain gauge position and orientation are shown as T. Stem flow measurements were made on trees labelled with S. WS is the automatic weather station.

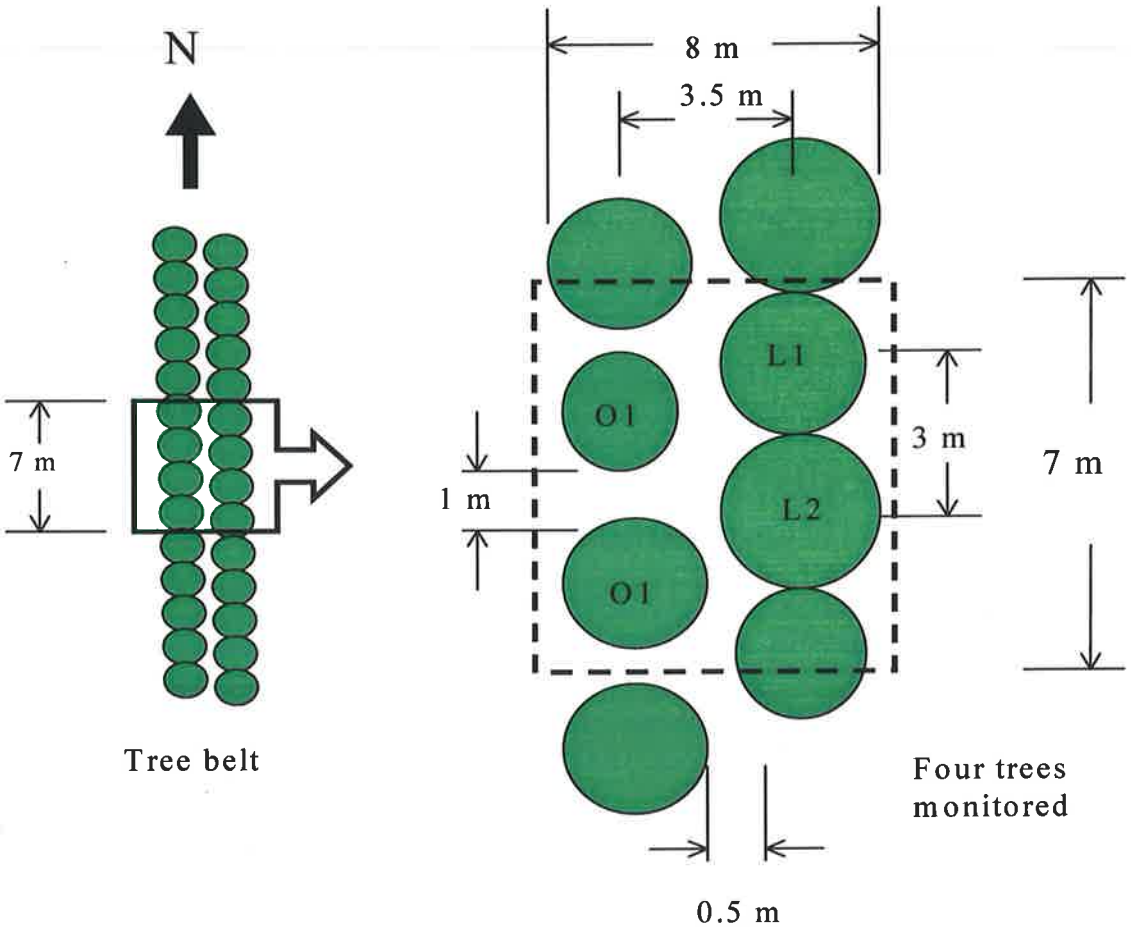

Figure 36 Detail of tree layout and dimensions of water balance experimental site. Crown width 8 m; row spacing 3.5 m; interrow tree spacing 3 m; 4 measured trees represented 7 m length of belt; interrow crown gap 0.5 m; canopy closure in *E. leucoxylon* row; 1 m gap in *E. occidentalis* row. Transpiration measurements were made on two *E. leucoxylon* (L1, L2) and two *E. occidentalis* (O1, O2).

Table 3 Dimensions and leaf areas of the four trees used for transpiration measurement at the water balance site.

Tree ID code	Species	Leaf area (m^2)		Average canopy diameter (m)	Canopy projected area (m^2)	Stem diameter (mm)	Sap wood area (cm^2)
		May 97	Jan 98				
L1	*E. leuc'n*	37	55	3.8	11.3	123	132
L2	*E. leuc'n*	34	46	5.1	20.3	187	140
O1	*E. occid's*	25	36	2.9	6.5	190	143
O2	*E. occid's*	20	27	3.7	10.5	153	98

Leaf efficiency site

The transpiration and leaf area of two isolated and two non-isolated trees (one example of each treatment is shown in Figure 37) were measured for 343 days from August 1997 at Roseworthy, South Australia, about 5 km south of the tree belt site.

Figure 37 Examples of each of the two isolated (left) and two non-isolated (right) trees (*E. largiflorans*) used for transpiration measurements in the leaf efficiency experiment.

All trees were *E. largiflorans* and were assumed to be of similar age as they were all natural remnants. Isolated trees were 50 m apart in a pasture paddock that was cleared about 100 years previously. Non-isolated trees were 20 m apart in an adjacent 5 ha block with about 80 stems per hectare and *LAI* about 0.8 m^2 m^{-2}. Figure 93 in Appendix 1 gives

an aerial view of the site and shows the relative positions of the four trees. Tree parameters are given in Table 4 and show the leaf areas of isolated trees were up to 9 times larger than those of non-isolated trees. This was considered to be due to a larger growing space (i.e. no perennial neighbours).

Table 4 Dimensions and leaf areas of the four remnant *E. largiflorans* trees used in the leaf efficiency experiment.

Tree	Leaf area (m^2)	Canopy projected area (m^2)	Tree height (m)	Stem diameter (mm)	Sap wood area (cm^2)
Isolated 1	206	130	10	510	661
Isolated 2	287	93	9	430	407
Non-isolated 1	30	24	6	210	134
Non-isolated 2	54	28	7	220	143

All trees were remnant natives and increased growth was therefore due to clearing of neighbouring trees allowing greater access to soil water. Agricultural fertilizers applied to surrounding crops are unlikely to have had a significant effect in the long term, being a secondary effect relative to the water limitations of the climate (Landsberg and Waring, 1997). Non-isolated trees were about 200 m from the isolated trees. Terrain was flat with similar soils to the tree belts site. Annual pasture surrounded isolated trees in spring 1997 and oats was sown during 1998. The under storey in the block was mainly annual grasses. In both isolated and non-isolated cases, actively growing understorey was only present between about June and October.

Methods

Leaf area

Tree leaf area was measured using the Adelaide (module) method (Andrew *et al.*, 1979) as described in Chapter 5, and in more detail in Appendix 2. The absolute leaf area (m^2) was used in the calculation of the leaf efficiency (Hatton *et al.*, 1998) of each tree. The *LLA* (m^2 m^{-1}) of the belt was measured for the 7 m length of belt that included only the four monitored trees, and for a 30 m length of belt that encompassed the four trees and extended 10 m to the north and 13 m to the south. At the water balance site, leaf areas were measured in May 1997 and again in January 1998. At the leaf efficiency site leaf areas were measured only once in June 1997. *LAI* (m^2 m^{-2}) of local remnant mallee

vegetation was measured at 5 sites in May 1997, within 10 km of the experimental site, and using quadrats with a minimum side length of 30 m.

Soil water storage

Twenty-four neutron moisture meter access tubes, constructed from 50 mm outside diameter steel tubing with 1.6 mm thick wall, were installed in a 60 mm diameter hole using the 'slurry' technique (Greacen, 1981). The tubes were arranged in two transects, 9 m apart of across the experimental site (Figure 35) to a depth of 6.0 m. The slurry was allowed to equilibrate with the surrounding soil for two weeks before measurements commenced. Neutron counts were taken using a CPN Hydroprobe™ , model 503DR, every 2 to 4 weeks at 16 depths: every 0.2 m to a depth of 1.2 m; every 0.5 m from 1.5 m to 5.5 m; and at 5.9 m. Standard counts were made in a 50 mm diameter steel tube immersed in a 200 litre drum of water.

Four access tubes were sacrificed for neutron probe calibration: 2 in late spring 1997; 2 in autumn 1998. In spring 'wet' samples were taken at the +40 m position on the transect (outside root zone) and 'dry' samples were taken at +5 m (inside root zone). In autumn a 'wet' samples were taken from a special sacrificial tube outside the root zone was wet up for a period of 2 weeks prior to sampling; 'dry' samples were taken at the centre of the belt. In both spring and autumn, 3 replicate soil samples were taken close to the access tube using a 75 mm diameter push tube in 0.5 m stages to 3 m deep. One replicate of samples between 3.0 m and 5.9 m, was taken in spring using a truck-mounted, hollow-stemmed auger and 43 mm diameter removable split core (Figure 129). This technique is often referred to as 'wire lining' because the split core is lowered and removed from the hollow-stemmed auger via a wire rope.

The neutron count ratio of all calibration samples was regressed against volumetric soil water content (r^2 = 0.71, n = 43; Figure 127). There was no significant trend with soil depth. A single relationship was therefore used for all depths to estimate volumetric water content θ from count ratio n ($\theta = 0.64n\text{-}1.95$). No attempt was made to adjust θ for the effect of soil textural variation across the site, since it primarily affects the offset, rather than the slope, of the relationship. $\Delta\theta$, rather than absolute θ, was the main concern.

At the beginning of the experiment, soil profiles inside the root zone were, without exception, drier than profiles outside the root zone of the trees (Figure 38). Trees appeared to have extracted water to a depth of at least 4 m. The site was not sampled specifically for roots; however roots were observed in soil cores up to 5.5 m deep, 5 m horizontally from the centre of the belt.

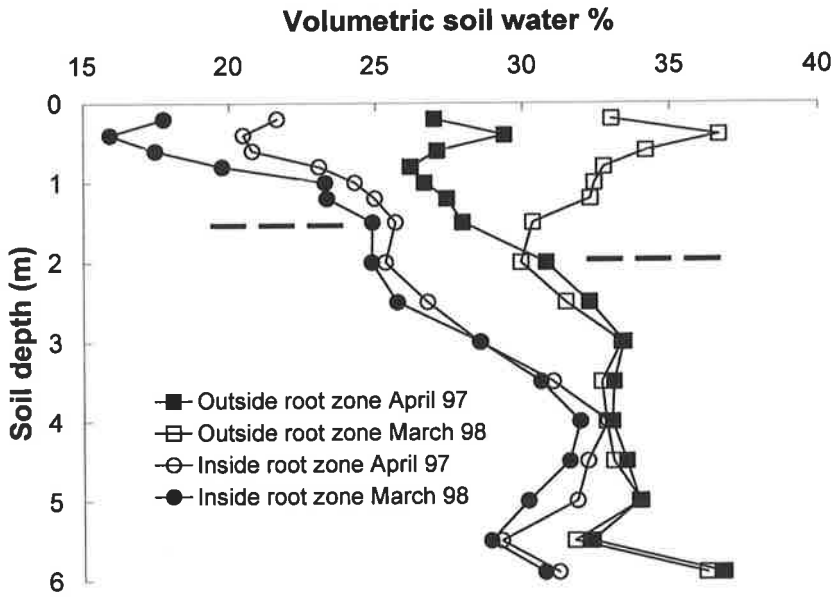

Figure 38 Examples of volumetric soil water profiles: outside the root zone in April 1997 (■); outside the root zone in March (□); inside the root zone in April 1997 (●); inside the root zone in March 1998 (○). Although not shown here, maximum recorded soil water content θ in the root zone was about 24% between 0.2 m and 0.4 m, both in May and September 1997. Dashed lines indicate depths above which ΔS was calculated and below which $\Delta\theta$ was less than E_θ, the standard count error.

During the experiment, soil profiles outside the root zone became wetter while profiles within the root zone became drier. A visual assessment of the soil water profiles outside the root zone showed apparently no significant change in water content with time deeper, than 1.5 m to 2.0 m (Figure 38). Within the tree root zone $\Delta\theta$ was relatively small, and the depth interval of water extraction was difficult to determine. An appropriate depth interval over which to calculate ΔS was determined to be that where $\Delta\theta$ was greater than the random count error (Bell, 1976)

$$E_\theta = \frac{s}{b} n \sqrt{\left(\frac{1}{c} + \frac{1}{w}\right)}, \tag{19}$$

where E_θ is the error on the volumetric water content %, s (= 2) is the number of standard deviations required for the confidence level; n is neutron count ratio; b is the slope of the calibration curve; c is the neutron count in the soil and w is the standard count in water.

To consider the largest possible E_θ at each depth, for each tube, E_θ was calculated using the largest n and the smallest c from the first and last measurements of that period. The

profile depth interval selected for calculation of ΔS was that over which all $\Delta\theta$ were greater than E_θ. For all tubes, this method identified a contiguous depth extending from the surface to a depth where $E_\theta > \Delta\theta$. At the lower end of this interval $\Delta\theta$ was between 1.4 and 1.5% *v/v*. Depths determined by this method were generally: 0 m to 2.0 m outside the root zone; 0 m to 1.5 m inside the root zone - the former being consistent with that established by visual appraisal of θ versus soil depth. ΔS at each depth was calculated as $\Delta\theta$ multiplied by half the vertical interval between points immediately higher and lower in the profile. Total ΔS for each profile on the transect was therefore the sum of ΔS over depth intervals where $\Delta\theta > E_\theta$.

Rainfall and throughfall

An automatic weather station (Measurement Engineering™) was positioned 45 m to the west of the belt for the entire 343 day measurement period from April 1997 to March 1998. Trough and bucket rain gauges were used to scale rainfall and throughfall across the rest of the transect. These were made from galvanised steel sheet, bent to form a trough, positioned to drain into 20 litre plastic buckets (Figure 126). They were installed across the east west transect (Figure 35) for 210 days from August 1997 to March 1998. At each position within the influence of the tree canopy (–5, -2.5, 0, 2.5, 5 m) 2 or 3 trough and bucket gauges were placed at different orientations, and at different positions beneath the canopies to estimate a mean value for each transect position. The position and orientation of each trough was chosen deliberately, rather than at random, in an effort to representatively sample rainfall and throughfall from canopies, canopy gaps and drip lines. Rainfall depth was measured using a calibrated dipstick. Linear regression of data from the most western trough and bucket gauge (10 m from weather station) against weather station measurements (6.6 mm < P < 35.0 mm; $y = 1.2x - 2.3$; $r^2 = 0.98$; n = 10; Figure 125) showed the trough and bucket gauge recorded about 16% less rainfall than the weather station. For this experiment the weather station rain gauge was assumed to be correct. Rain or throughfall measured at each position across the transect was expressed as a percentage of that recorded by the calibrated trough and bucket gauge. These percentages were used to scale the rainfall or throughfall to rainfall recorded by the weather station. This method extrapolated the shape of the rainfall/throughfall transect from the 210 day period to the whole 343 day period. The presence of the trees affected the amount of rainfall reaching the ground for at least 10 m either side of the belt centre, although the canopy extended only 4 m either side (Figure 40).

Stem flow

Rainfall intercepted by plant canopies is partitioned into interception loss and stem flow. Stem flow is intercepted rainfall that runs from the outside of twigs and branches to the main stem and eventually the ground (Prebble and Stirk, 1980). It often represents a proportionately small redistribution of water but can be up to 15% of rainfall in Australian native vegetation (Nulsen *et al.*, 1986). I therefore measured stem flow to allow a more accurate estimate of interception loss. Stem flow was difficult to collect from the main experimental trees due to the installation of sap flow instruments. Instead, three trees from each row were chosen, adjacent to the main trees, ranging from the smallest to the largest (Figure 35). A square rubber channel (1 cm x 1 cm) was attached to the stem in a helix, in a similar manner to that described by Crockford and Richardson (1990), and fed into a 20 litre plastic bucket (Figure 130). Stem flow volumes were recorded for 14 rainfall events between August 1997 and March 1998 using a calibrated dipstick (detail of construction is shown in Figure 130). A single relationship was used for both species: stem flow (L) per mm of rainfall for the whole period was regressed against tree leaf area: $y = 0.019x + 0.13$ ($r^2 = 0.67$, n = 6; Figure 131). This was used to scale the stem flow to leaf area of the section of belt comprising the 4 main trees.

Interception

The presence of the canopy affected the amount of rain reaching the ground up to 10 m from the belt centre - well outside the canopy (Figure 40). This was possibly due to rain shadow and change in airflow around the trees. I have chosen, however, to represent interception as an equivalent volume per unit length of tree belt, rather than varying with horizontal distance from the belt centre, since the latter is complex and of little benefit to the analysis.

I therefore define the term 'rainfall deficit' as being equal to the difference between rainfall, outside the influence of the canopy, and rainfall reaching the ground within the region affected by the canopy. Rainfall was not measured above the canopy so I assumed it to equal that recorded at the weather station. The partitioning of rainfall deficit into either interception or stem flow was assumed to be uniform across the 30 m width of apparent canopy influence. Therefore, at each position on the transect over this 30 m width, rainfall deficit was calculated as the depth of rain reaching the ground, minus total rainfall recorded by the weather station outside the influence of the tree canopy. Stem flow volume per metre of belt was estimated from the stem flow relationship (see previous section). This volume was expressed as an equivalent depth across the 30 m width of apparent influence of the canopy, and subtracted from the rainfall deficit at each point on

the transect, yielding interception loss (mm). An equivalent volume of interception per meter of belt, for each horizontal increment on the transect was calculated by multiplying the average depth of interception for each horizontal increment on the transect (trapezoidal method) by the width of that increment, and multiplied again by unity. The total volume of interception per metre of belt was the sum of individual volumes.

Transpiration

Greenspan Technology™ heat pulse sap velocity sensors (Swanson,1972) were installed in belt trees O1, O2, L1 and L2 to measure sap flux for 308 days - between May 1997 and March 1998 - as described in Hatton *et al.* (1995). Probes were inserted to sample sap velocity at four positions across the depth of sapwood. The inner (heartwood) boundary of sapwood was estimated by incremental measurement of sap velocity with depth (Hatton *et al.*, 1995). Wound diameter was set at 2.2 mm, the lower limit found by Hatton *et al.* (1990) in their water use study of eucalypts. Sap wood matrix and water contents were measured using the technique of Hatton and Vertessy (1990). However the data were discarded because water contents were highly variable (28% to 55%). It was suspected that the low values were due to moisture loss while sampling with a hole saw driven by a pistol drill, which heated the samples. Default values of 40% and 50% (Edwards and Warwick, 1984) for wood and water contents, respectively, were therefore used for all calculations. A sensitivity analysis showed that a 5% variation in these values gave a 7% variation in sap flux. Sap velocity was logged every 30 minutes for all trees and sap flux was calculated on a daily basis and converted to either: 30 day moving average (L d^{-1}); total volume (L) for the measurement period; transpiration per unit leaf area (L m^{-2}); or transpiration per metre of belt (L m^{-1}). Sap flux was calculated from average sap velocity multiplied by sapwood area – the weighted average technique (Hatton *et al.*, 1990). Average sap velocity is the sum of the four sampled velocities, weighted to the areas of the relevant sapwood annuli, relative to total sapwood area. A detailed description and worked examples of transpiration calculated from sap flow measurements is given in Appendix 2.

Figure 39 Heat pulse sap flow sensors installed in a tree at the water balance site.

Missing data days for each tree were: 40; 102; 37; 22 days; for O1; O2; L1; L2; respectively and were interpolated linearly as the mean of 10 days either side of the data gap. Transpiration per metre of belt was calculated by adding transpiration volume from each tree and dividing by the 7 m length of belt they occupied. Transpiration was also calculated by difference using P, I, E and ΔS measured at each position on the transect, assuming drainage to be zero. This assumption was checked, against estimates of drainage calculated using soil physical methods, and found to be valid (calculations are given in Appendix 2). An equivalent transpiration volume per metre of belt was calculated by summing average transpiration at each transect interval multiplied by the width of the transect interval.

Transpiration of trees in the leaf efficiency experiment was measured in the same way as for the tree belt. Data from one non-isolated replicate in 1997 was discarded due to suspected poor installation of the heat pulse probe – sap fluxes were extremely low and showed monotonic decrease in spring rather than an a dramatic increase. Probes in that tree were reinstalled in 1998 and from then on leaf efficiencies were similar to those of the neighbouring tree. Annual values of leaf efficiency were calculated from measured data only; no missing values were interpolated.

Soil evaporation

Given that the depth of soil wetting due to rainfall was clearly determined (Figure 38), soil evaporation E, outside the root zone, was determined from P - ΔS, assuming zero drainage

below this depth. Hydraulic conductivity at a depth of 3 m outside the tree root zone was estimated to be 1 $\times 10^{-3}$ mm d^{-1} using measured θ, θ_{sat} and % clay (Campbell and Shiozawa, 1992; Smettem *et al.*, 1999; Smettem and Bristow, 1999); calculations are shown in Appendix 2. This, combined with the apparent small hydraulic gradient at this depth confirmed that drainage would have been insignificant, about 1.5 mm yr^{-1}. E was therefore calculated using one replicate of rainfall and two replicates of ΔS at positions: – 40 m; -25 m; -15 m; 25 m; 40 m on the transect. For the 343 day measurement period there was 5% variation in evaporation between all these positions. Evaporation within the root zone was scaled to microlysimeter (Boast and Klute, 1986; Bond, 1998) measurements made at 15 positions across the transect of the tree belt (Figure 35), over an 81 day period in spring 1997. Microlysimeter construction and installation is described and in Appendix 2. All 15 microlysimeters were weighed, remade and replaced every 24 to 48 hours or after rain. The shallow depth and short measurement periods were chosen because soil water content changed rapidly within the tree root zone, due to the additional water extraction by the trees. Outside the root zone, average microlysimeter evaporation on the eastern and western sides was, respectively, 84% and 80% of that calculated by P - ΔS over the same 81 day period. Microlysimeter measurements were abandoned at the end of spring as weather conditions dried. Installation was not possible due to hard soil conditions, and wind-blown soil was deposited in the top of the microlysimeters.

Evaporation from each microlysimeter inside the root zone was expressed as a percentage of average microlysimeter evaporation outside the root zone. These percentages were multiplied by total average evaporation (P - ΔS for the 343 day period) outside the root zone to estimate total evaporation at each position within the root zone. Evaporation from both eastern and western sides of the belt was scaled in this manner, independently from each other. This method extrapolated the shape of the evaporation transect for the 81 day spring period to the whole of the 343 day period.

Results

Leaf area

Leaf areas of the four main trees in the belt are shown in Table 3. The *LLA* (m^2 m^{-1}) of the 7 m belt section comprising the four main trees was the same as *LLA* of a 30 m section on both occasions: 17 m^2 m^{-1}; and 23 m^2 m^{-1} in May and January, respectively. The 25% growth during the experiment was probably the combined effects of an unusually wet summer as well as the absence of normal competition from adjacent crops. The average *LAI* of remnant vegetation calculated from measurements at five local sites; 0.8 m^2 m^{-2},

Sdev = 0.1. Leaf areas from the trees used in the leaf efficiency experiment are shown in Table 4.

Rainfall, stem flow and interception

Rainfall recorded at the weather station was 497 mm for the 343 day period. This was about 50 mm more than average; 100 mm fell over summer. Rainfall reaching the ground was reduced by 25% at the centre of the belt, and between 5% and 10% up to 11 m outside the canopy (Figure 40).

Stem flow volume was estimated to be 253 litres per metre of belt from the stem flow calibration and using 497 mm rainfall and using an average *LLA* of 20 m^2 m^{-1} (the average of the May and January *LLA* measurements). This volume translates to a depth of 32 mm over the projected belt width, about 6% of rainfall, and 8 mm over the 30 m width of apparent interception. Interception was calculated to be 1370 litres per metre of belt for the 343 day period and was distributed across the transect as shown in Figure 41. Equivalent interception depths were 171 mm over the projected canopy width and 46 mm over the apparent effective width of interception (30 m).

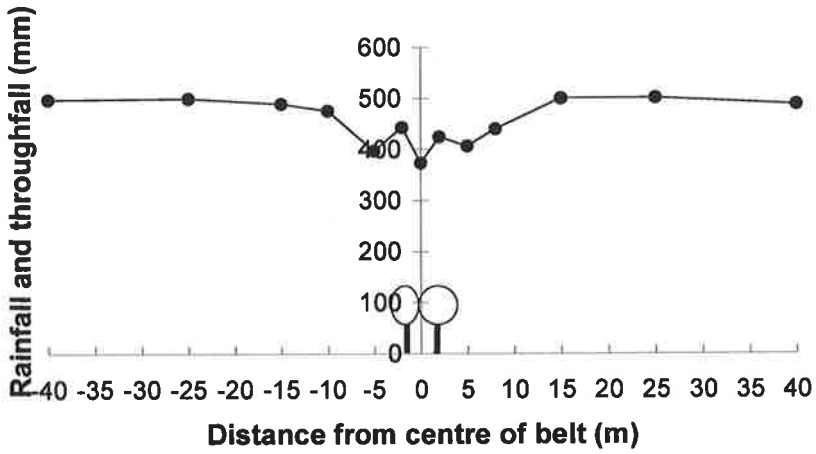

Figure 40 Transect of rainfall (outside the canopy) and throughfall (under the canopy) for a distance of 40 m either side of the tree belt.

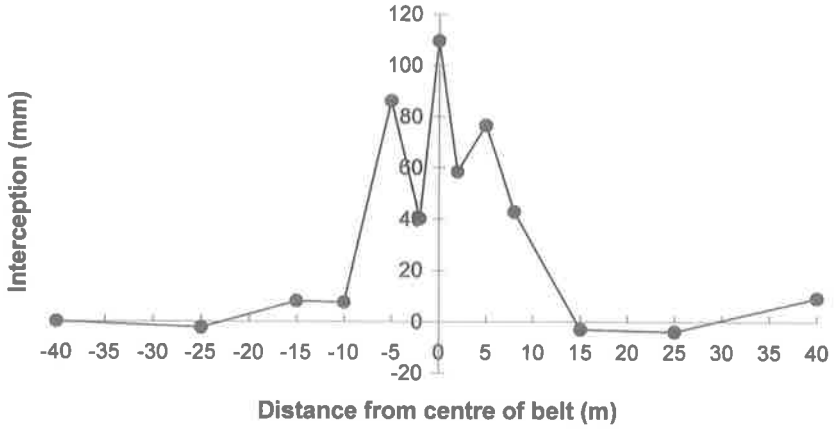

Figure 41 Transect, across the belt of trees, of interception calculated from rainfall, throughfall and stem flow measurements.

Transpiration

Figure 42 shows a 30-day moving average of leaf efficiency for the four main trees. Trees on the western side had about twice the leaf efficiency of eastern trees during spring and summer. Leaf efficiencies for the 343-day measurement period were 260; 217; 127; 160 litres m^{-2} for O1; O2; L1; L2, respectively. Total transpiration volumes for this period were 8056; 5109; 5829; 6409 litres for O1; O2; L1; L2, respectively.

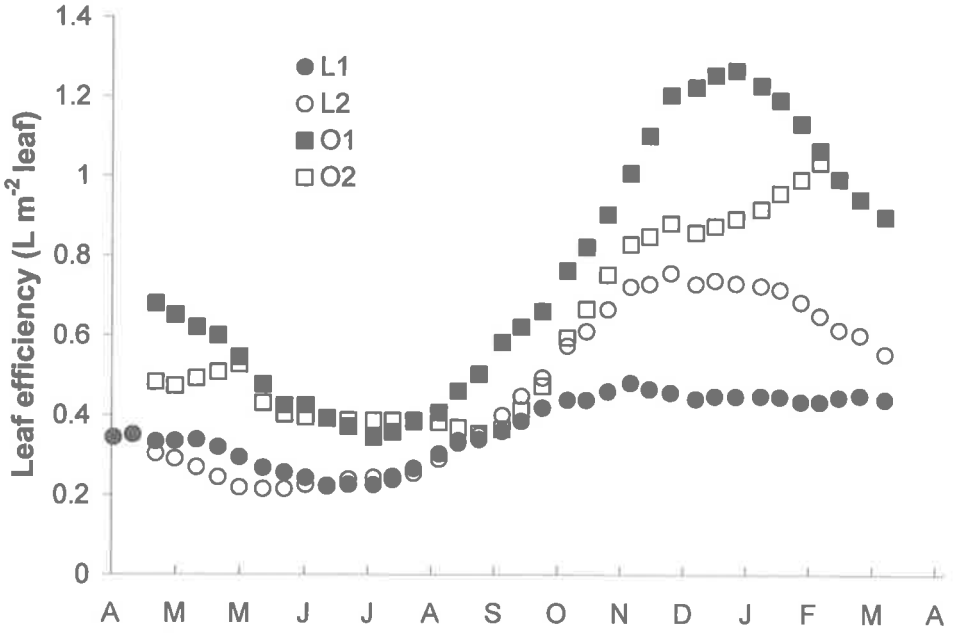

Figure 42 Leaf efficiency of the four trees in the water balance experiment, measured between May 1997 and March 1998.

Transpiration per metre of belt was 3629 L m^{-1} for the 343-day period; equivalent to a depth of 454 mm and 134 mm over the projected canopy width and nominal root zone width (27 m), respectively. On a projected canopy area basis, average transpiration for the period was 1.2 mm d^{-1}; average potential evaporation calculated using the Penman combination equation (Meyer, 1999) for the same period was 3.4 mm d^{-1}. Run-on and ponding was observed on the western side of the belt between –5 m and –10 m from the belt centre, following large rainfall events in spring and summer. On the eastern side however, water was observed to run off and pond off-site on the same occasions. The canopies of the western trees were smaller and lower than those of the eastern trees and not in a position to intercept more radiation. Higher leaf efficiency of these trees was therefore unlikely to be due to higher leaf irradiance. Wind roses recorded by the on-site weather station showed nothing to suggest that transpiration from the western trees would have been aerodynamically enhanced relative to the eastern trees. The higher leaf efficiency of trees in the western row was therefore attributed to a better water supply, due to local ponding.

To indicate the likely horizontal distribution of water extraction by the trees, and also to check measured transpiration, transpiration was calculated by difference, assuming recharge to be small. This assumption was ratified in the same manner described the soil evaporation section, using measured θ, θ_{sat} and % clay from 2 m deep (Campbell and Shiozawa, 1992; Smettem *et al.*, 1999; Smettem and Bristow, 1999); drainage was estimated to be in the order of 1×10^{-5} mm d^{-1} (Appendix 2). Figure 43 shows T for each position across the transect where all water balance components were available, and calculated as $T = P - E - I - \Delta S$. Negative transpiration at –10 m position is a possible indication of run-on at this point. Total transpiration by difference was 4104 L per metre of belt.

This was equivalent to 513 mm over the canopy width and 152 mm over the 27 m width of the nominal root zone. Transpiration estimated by difference was therefore 13% greater than that measured by heat pulse. I chose to assume that the heat pulse measurements of T were correct but have given due consideration to the 13% difference between methods when discussing possible errors.

Figure 44 shows the 10-day moving average of leaf efficiency (transpiration per unit leaf area) from the leaf efficiency experiment, for isolated and non-isolated trees, over a 12 month period. The 'isolated' trace represents the average of two replicates for the whole

period. The 'non-isolated' trace represents one replicate during 1997 and 2 replicates during 1998. Error bars show one standard deviation either side of the mean.

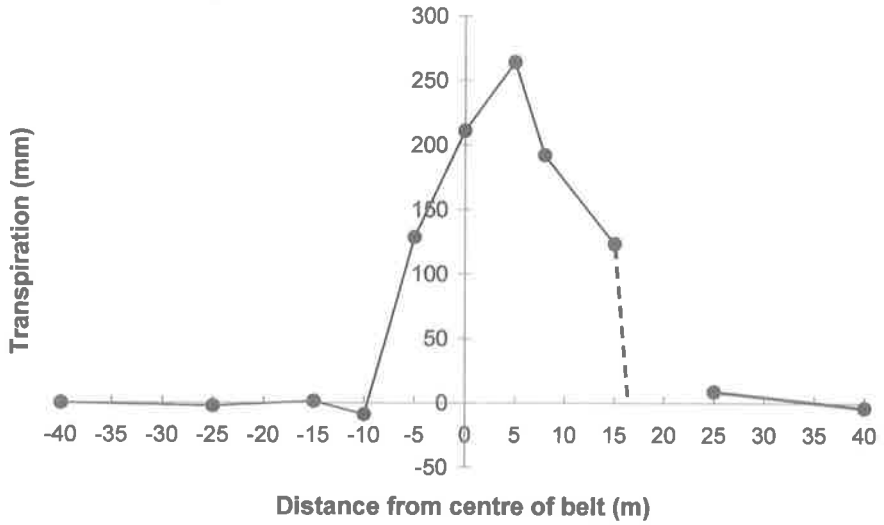

Figure 43 Transpiration transect from the water balance site, calculated by difference.

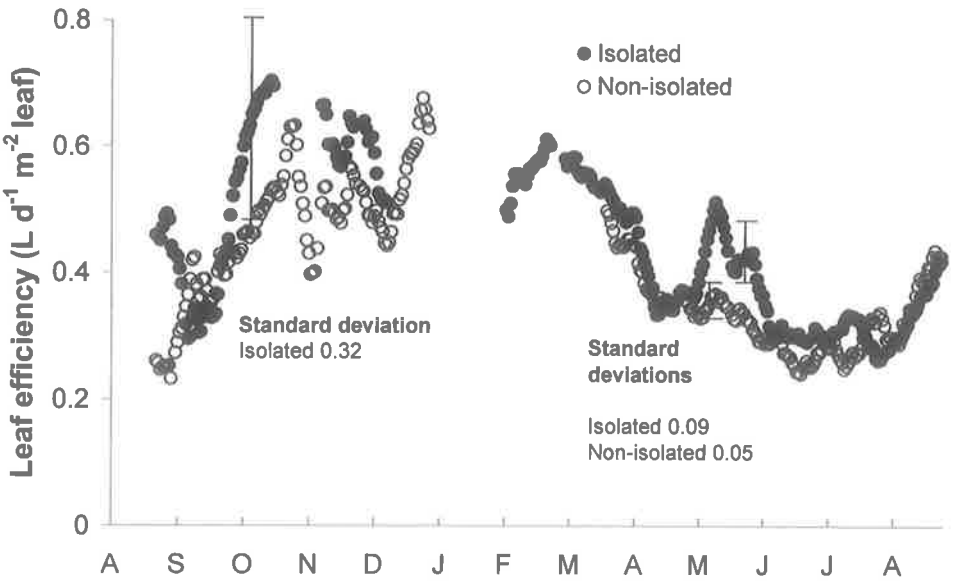

Figure 44 Average leaf efficiency of the 'isolated' and 'non-isolated' treatments from the leaf efficiency experiment. Errors bars show standard deviations from the mean of two replicates.

In the spring of 1997, there were differences in leaf efficiency greater than 100% between the two isolated trees with no obvious explanation. The tree with the higher leaf efficiency, Isolated 2, had a lower *LAI* compared to Isolated 1 (see Table 4; leaf area per canopy projected area), possibly causing an increase in average leaf irradiance, and therefore higher leaf efficiency. There was no evidence to suggest that the tree had greater access to soil water as with the tree belt experiment. Maximum average leaf efficiencies were similar to those measured in the tree belt experiment during 1997 spring and summer, ranging from about 0.4 to 1.1 L d^{-1} m^{-2}. Winter values of leaf efficiency were similar for both experiments, about 0.35 to 0.4 L d^{-1} m^{-2}, for all treatments. Given the similarity in long-term average values of leaf efficiency I found no reason to reject the null hypothesis that $T_{isolated} = T_{non\text{-}isolated}$ over the 12 month measurement period. This experiment is not completely conclusive, however, and this generalisation is unlikely to be valid over periods of one to two months, especially in spring.

Soil water storage

Figure 45 shows the mean value of ΔS calculated from the two transects of neutron moisture metre access tubes. Each point represents the mean of two values at each position on the transect and error bars represent one standard error either side of the mean. Average ΔS outside the root zone was 76 mm (Sdev 14 mm), respectively. Inside the root zone average ΔS was 5 mm, with large increases close to the edge. Directly beneath the canopy average ΔS was –22 mm (Sdev 8 mm). The coarser horizontal resolution of access tube placement on the eastern side was due to the presence of overhead power lines, which restricted access of the truck-mounted drilling rig during installation.

The influence of the root zone appears to cease between 10 and 12 m on the western side, corresponding with above ground observations of soil drying and significant changes in remaining stubble from previous crops. On the eastern side, the surface expression of the extent of the root zone differed between the two access tube transects by about 2 m either side of the +15 m position. This was reflected in the largest variation in ΔS at this point. A discontinuous function, comprising three linear relationships, was fitted to the data to allow calculation of an equivalent average ΔS for any width between –12.5 m and +25 m (see following section 'Calculating *ENOR*').

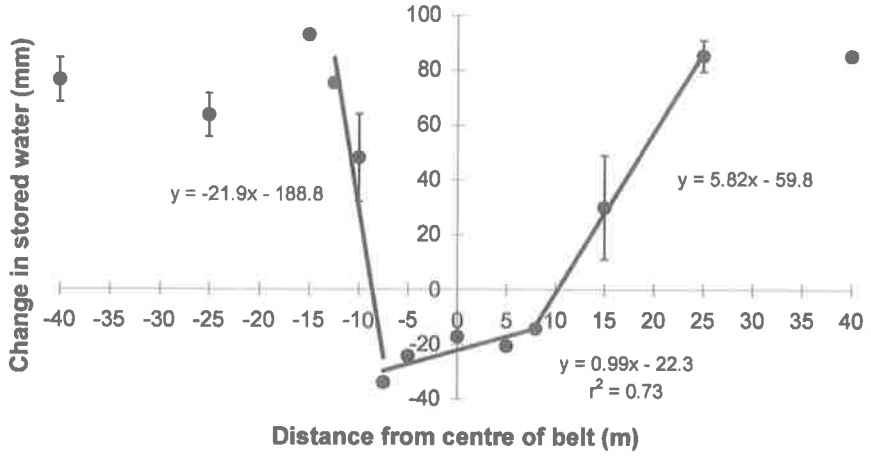

Figure 45 Change in stored water ΔS across the belt of trees. Error bars show the standard deviation from the mean of two replicates. Where error bars are not visible they are smaller than the data point symbol. ΔS was approximated by discontinuous linear functions.

Soil evaporation

The evaporation transect (Figure 46) shows that average bare soil evaporation outside the root zone accounted for 428 mm (Sdev = 10 mm) of the 497 mm rainfall. In the centre of the belt evaporation was about 200 mm due to less rainfall reaching the ground and more soil water used by the trees. A discontinuous function, comprising five linear relationships was fitted to the data to allow calculation of an equivalent average evaporation across any width between –10 m and +15 m.

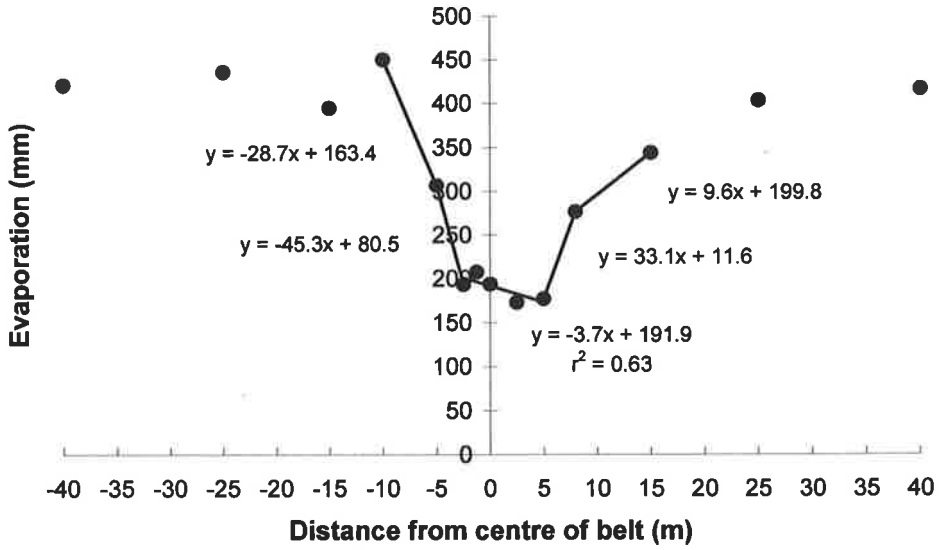

Figure 46 Soil evaporation transect across the belt of trees. Values outside the root zone were calculated as the difference between *P* and *ΔS*. Values inside the root zone were scaled to microlysimeter measurements. *ΔE* was approximated by discontinuous linear functions.

Calculating *ENOR*

From leaf areas

Using May 1997 *LLA* and *LAI* measurements and Equation 12, *B* for the belt of trees was predicted; $B = 17/0.8 = 21.3$ m. *B* was not calculated for January 1998 because *LAI* was not measured then.

From water balance

Equation 17 was rearranged to define a water balance, which was set to zero (Equation 20) and placed as a formula in a spreadsheet on a personal computer. *T* and *I* were set in separate cells as 3629 and 1370 L per metre of belt, respectively, and *P* was set at 497 mm as measured in the experiment.

$$B(P - E - \Delta S) - T - I = 0 \qquad (20)$$

The discontinuous functions fitted to ΔS and *E* were integrated with respect to horizontal distance from the belt centre. Average values of ΔS and *E* over any chosen horizontal width were calculated simultaneously as the integral of each function over the same width *B* (centred on the belt), divided by *B*. *B* was then iterated manually until Equation 20 was satisfied, at which point *B* was 19.8 m; average *E* and ΔS over width *B* were 262 mm and –18 mm, respectively.

Error analysis

The main points of the error analysis are summarised below. For a detailed error analysis of each component, see Appendix 4.

Due to the labour involved in data collection, measurements from the tree belt experiment were not spatially replicated except for leaf area and ΔS. The crosschecks performed within the data set promote confidence in the measurements. However, independently of this, I considered the possible errors associated with the calculation of B as being of 3 types: errors associated with each measurement technique; errors associated with interpolation of data; errors associated with extrapolation of data. For each measurement the largest corresponding errors were: $LLA \pm 10\%$; $LAI \pm 12.5\%$; $T \pm 13\%$; $I \pm 15\%$; $P \pm 10\%$; $E \pm 10\%$; $\Delta S \pm 50\%$ (Appendix 4). These were used to test the effect of worst-case combinations of errors on both the prediction of B from leaf area measurements (Equation 12) and the calculation of B from water balance measurements (Equation 17).

Maximum and minimum (worst-case scenario) predicted B (Equation 12) were calculated respectively by: 1) using the largest LLA and the smallest LAI; 2) the smallest LLA and largest LAI measurement. This allowed the calculation of the smallest possible B using the smallest numerator and the largest denominator (and *vice versa*) and gave $17 \text{ m} \leq B \leq 26.7$ m. A similar approach was used to determine maximum and minimum B according to water balance measurements (Equation 17). This was done by choosing the largest possible values for T, I and ΔS (ΔS was negative) and the smallest possible values for P and E, so as to combine the largest numerator and smallest denominator. The smallest possible value of B was calculated using the smallest T, I and ΔS, and the largest P and E. This gave $13.0 \text{ m} \leq B \leq 34.1$ m, the maximum value being physically impossible given the root zone width of 27 m.

Discussion

The *ENOR* approach (Chapter 4) tested here was developed from considerations of equilibrium between vegetation and climate, using tree leaf area as an indicator of those conditions. Such equilibria are often notional in practice, given that climatic conditions vary considerably from year to year. I discuss, below, the implications of this with respect to the water balance experiment.

In this experiment I have compared predictions from annual average leaf area, albeit calculated from only 2 measurements, with an area of hydrologic occupation calculated from water balance measurements made in the same year. The site was also significantly

perturbed from average annual conditions because of the higher than average rainfall but also, more importantly, by the exclusion of crops from the tree root zone. The combined effects of the two perturbations were probably reflected in the 25% canopy growth over the measurement period. If the tree growth had not fully responded to the higher than average water supply, one would expect that the root zone would have become wetter over the measurement period. This was not the case, and in fact the root zone continued drying slightly during autumn. I am confident, therefore, that the leaf area and water balance measurements fairly represented their respective influences over the measurement period.

As indicated when deriving the water balance expression for *ENOR* in the second section of this chapter, the approach also requires that Equation 18 must hold. Here I explore the likelihood of this. The leaf efficiency experiment showed that, for the purposes of this argument, long-term average leaf efficiency was not significantly different for isolated and non-isolated trees. Taylor *et al.* (2001) measured the transpiration of a blue gum (*E. globulus*) over a two-week period in spring and showed that it was enhanced by 10%, at the edge of a blue gum plantation, due to advected energy. My data shows that this probably also occurred in the isolated trees in spring and autumn (Figure 44). Over long periods, however, it appears that leaf efficiency does not vary hugely between isolated and non-isolated situations. Therefore, for the same leaf area, T_{isolated} can be considered approximately equal to $T_{\text{non-isolated}}$. A corollary to this is that aerodynamic enhancement of T in the isolated case is not significant and that, for the same reasons, I_{isolated} will be similar to $I_{\text{non-isolated}}$. Also, P will be identical for both sides of Equation 18, therefore if Equation 18 is true, E_{isolated} must equal $E_{\text{non-isolated}}$. In the water balance experiment annual E_{isolated} was determined to be 262 mm ±10%, slightly more than half of rainfall. I am not aware of any long-term measurements of $E_{\text{non-isolated}}$ in mallee vegetation for comparison. $E_{\text{non-isolated}}$ can, however, be estimated (Cooper *et al.*, 1983) although the technique is sensitive to k^*, the canopy light extinction coefficient. Using this technique, together with $k^* = 0.42$ (Vertessy *et al.*, 1993), $E_{\text{non-isolated}}$ was estimated to be 303 mm, indicating that E_{isolated} and $E_{\text{non-isolated}}$ are probably not hugely dissimilar, although I expect the error to be larger than 10%. This is not a rigorous test of Equation 18, however, it serves to show that it is likely to approximate reality, and therefore supports the *ENOR* approach.

Conclusions

This chapter has shown *ENOR* width $B = 21 \pm 7$ m, predicted from leaf area measurements (Equation 12), compared favourably with *ENOR* width $B = 20 \pm 7$m calculated from the water balance (Equation 17) over a period of almost a year. The error analysis I have

imposed on this experiment has been severe, and must be taken in context with the many crosschecks of calculations by different methods, and the demonstrated close agreements in such cases. I suggest that conservative use of the *ENOR* approach should therefore include a possible error of no more than 20%.

Scientists contemplating studies of tree belts or block edges should heed the importance of the horizontal resolution of measurements near root zone edges, so that the root zone extent can be accurately determined. With the benefit of hindsight, I recommend that the extremities of the root zone be first approximated from above ground observation of changes in surface cover. The positions of measurements along a transect should then be chosen so that the nominal root zone edge is bracketed by at least 4 closely spaced measurements.

Summary

This chapter has tested the *ENOR* approach from a water balance perspective. A mathematical definition of *ENOR* in water balance terms is derived, and it is noted that this, when applied within the *ENOR* approach, implies that the relative proportions of the water balance components are similar (normalised to leaf area) for tree belts (isolated) and forests (non-isolated).

An experiment is described where all the components of the water balance were measured along a transect transverse to and spanning a 13 year old eucalypt tree belt. A second experiment is described that tests the hypothesis that long term average leaf efficiency (transpiration per unit leaf area, Hatton *et al.,* 1998) is equal for both isolated and non-isolated situations.

The results and accompanying error analysis of the first experiment show that *ENOR* calculated from water balance measurements agreed well with that predicted from leaf area measurements. The second experiment, while not completely conclusive, showed that leaf efficiency was higher in isolated trees for short periods in spring and autumn, however the hypothesis of equivalent long-term average leaf efficiency could not be rejected.

Chapter 7

Estimating Leaf Area Index *LAI* of natural vegetation

Preliminary findings from this chapter were presented at the *Envirowater99 – 2nd Inter-Regional Conference on Environment, Water* (Ellis *et al.*, 1999). This chapter also forms the basis for a paper that has been submitted to the *Australian Journal of Botany* (Ellis and Hatton, in press).

Introduction

Chapters 5 and 6 have shown that predictions of *ENOR* for a tree belt can be made from *LAI* and *LLA* measurements (Equation 12). This chapter and the next respectively provide methods for estimating *LAI* and *LLA* where rapid application of Equation 12 is required for testing the effects of alley farming in catchment management scenarios, or where *LAI* and *LLA* data are not available. This chapter deals specifically with the prediction of *LAI*.

A variety of models exist for predicting eucalypt plantation growth (Landsberg and Waring, 1997; Battaglia and Sands, 1997) and for predicting *LAI* in eucalypt plantations (Battaglia *et al*, 1998). Plantations usually comprise species exotic to the site and are fertilised. While the growth of natural vegetation communities may be governed by similar physical principles as plantations, the limits to growth are usually lower for ecological reasons. Natural vegetation in water-limited environments has been shown to be

conservative in itswater use to ensure survival through drought periods (Eagleson, 1982; Eagleson and Tellers, 1982) and is not represented well by plantation models. In addition, forest growth models are too complex for the task of predicting *LAI* for practical application of the *ENOR* model, and require numerous species and site input parameters.

Around the world, physical characteristics of natural vegetation have been shown to be dependent on local climate. Simple climate parameters such as rainfall and evaporation are readily available at large spatial scales for most of Australia. In this chapter, *LAI* measurements from 43 natural eucalypt sites across southern Australia are collated and used to explore simple relationships between *LAI* and climatic indices calculated from rainfall and evaporation measurements. The merits of several indices are compared with respect to: the usefulness of each; the accuracy of *LAI* predictions; and the physical significance of the relationships, particularly in terms of boundary conditions.

Relating *LAI* to climate

Several studies have demonstrated that the structure of natural vegetation communities, and the structure of the plants within the communities reflect local climatic conditions (Specht, 1972; Budyko, 1974; Grier and Running, 1977; Ghotz, 1982; Specht and Specht, 1989). Budyko (1974) and Ghotz (1982) show that climate and water balance can determine the rates of primary production of natural vegetation. Plants capture radiative resources via their leaves. It therefore follows that leaf area and hence *LAI* will also be related to climate (Grier and Running, 1977; Ghotz, 1982; Specht and Specht, 1989).

Grier and Running (1977) plotted leaf area index against rainfall for coniferous forests in North American and fitted a linear relationship with $r^2 = 0.84$. The relationship did not fit well in high rainfall (> 1000 mm yr^{-1}) areas and overestimated *LAI*. They went on to show a much better correlation ($r^2 = 0.99$) between *LAI* and a water balance index that added soil water storage to growing season precipitation and subtracted open pan evaporation. Negative values indicated evaporation in excess of available water while positive values indicated the converse. Specht (1972) presented a linear relationship between canopy projective cover of natural Australian plant communities, and an evaporative coefficient *k* which relates monthly transpiration to available water. Specht and Specht (1989) subsequently showed that *k* could be estimated from annual pan evaporation E_0, and then showed a curvilinear relationship between *k* and over storey *LAI*.

Budyko and Efimova (1968) presented data to support the notion that natural vegetation cover is an indicator of the combined energetic status of the land surface and the climate. Budyko (1974) subsequently expressed: *"the productivity of natural vegetation under*

conditions of sufficient moisture depends on the radiation balance at the earth's surface". He then constructed a family of curves relating measured annual biomass increments of natural vegetation in the (then) USSR to a climatic of a radiative dryness index $R/\lambda P$ where: R is net annual radiation at the earths surface, λ is the latent heat of the vaporisation of water; and P is average annual rainfall. The different curves represented changes in production potential with changes in latitude (and hence radiation) at the earth's surface, showing maxima at values of $R/\lambda P = 1$, and tending toward zero at high values of $R/\lambda P$. Bazilevich *et al.* (1970) presented data to show that at the positions of the maxima of Budyko and Efimova's (1968) earlier work were incorrect and occurred at lower and higher values of $R/\lambda P$ for higher and lower values of R, respectively (Figure 47).

R/λ closely approximates potential evaporation (Budyko, 1974), which is highly correlated ($r^2 = 0.98$) with pan evaporation E_0 (Budyko, 1974). Therefore Budyko's (1974) radiative index of dryness can then be replaced by the analogous water balance terms

$$\frac{R}{\lambda P} \approx \frac{E_0}{P} \qquad (21)$$

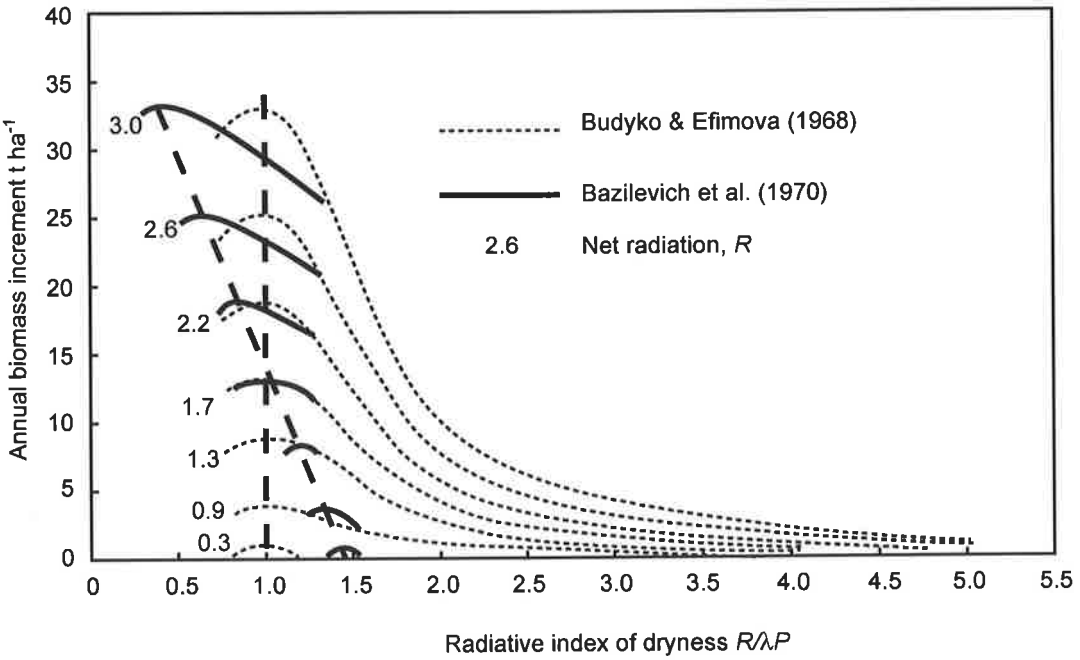

Figure 47 The relationships between annual biomass increment and radiative index of dryness $R/\lambda P$ for a range of radiation balance R (G J m^{-2} yr^{-1}) (Budyko and Efimova, 1968; Bazilevich *et al.*, 1970). For latitudes 30^0 – 40^0 S, $R \approx$ 2.6 G J m^{-2} yr^{-1}.

Table 5 shows 43 measurements of *LAI* of natural eucalypt vegetation from southern Australia (latitudes –30 to –40 degrees) used in the construction of Figure 48a to d and Figure 49 a and b. Six sites were measured for this study; the remaining 37 have been obtained from the literature. The Adelaide (module) method of leaf area estimation (Andrew *et al.*, 1979; Appendix 2) was used in all cases except those of Pook (1984) and Carbon *et al.* (1979a) who used litter fall traps and the method of Carbon *et al.* (1979b), respectively. P and E_0 were obtained from 'Data Drill' the Queensland Department of Natural Resources historical meteorological data surfaces (/www.dnr.qld.gov.au/silo/).

These data have been used to investigate the relationship between *LAI* and the following: long-term average annual rainfall P (Figure 48a); long-term average annual potential evaporation E_0 (Figure 48b); a simplified version of Grier and Running's water balance index P - E_0 (Figure 48c); Specht and Specht (1989) evaporation coefficient k (Figure 48d); Budyko's climatic dryness index E_0/P (Figure 49a); and a climatic wetness index, the inverse of the latter, P/E_0 (Figure 49b).

Results

Figure 48a and b shows that *LAI* is strongly correlated (r^2 = 0.76) with rainfall but very weakly (r^2 = 0.26) with pan evaporation. The modified Grier and Running index $P - E_0$ (Figure 48c) provides a slightly stronger relationship with *LAI* (r^2 = 0.57). The data set shows a very poor match with Specht and Specht's (1989) evaporation coefficient k. Evaporative coefficient k values (Figure 48d) for each of the 43 sites were calculated using Equation 22 (this is equation 7, p195 of Specht and Specht (1989).

$$k = 0.0045 + \frac{71.57}{E_0} \qquad (22)$$

The solid curvilinear line (Figure 48d) has been graphically reproduced from Figure 10 of Specht and Specht (1989), rather than the quadratic equation the authors quote in the caption as being the equation fitted to their data.

It should be noted that their quoted quadratic equation (LAI = 1.37 - 73.76k + 1136k^2; Specht and Specht, 1989) describes their data over their measured range only and does not satisfy the boundary condition of small *LAI* at low values of k.

Table 5 Natural vegetation *LAI* measurements from southern Australia with site coordinates and local annual average rainfall and evaporation.

Source	Latitude (deg. min.)	Longitude (deg. min.)	P (mm)	E_0 (mm)	*LAI*
Carbon *et al.* (1979a)	-32° 20'	116° 03'	1104	1625	2.1
Carbon *et al.* (1979a)	-33° 50'	115° 55'	993	1221	1.8
Carbon *et al.* (1979a)	-33° 10'	116° 25'	833	1480	1.4
Carbon *et al.* (1979a)	-34° 12'	116° 00'	953	1453	1.3
Dunin *et al.* (1985)	-35° 36'	150° 17'	1174	1607	3.0
Ellis (this study)	-33° 15'	136° 50'	283	2003	0.45
Ellis (this study)	-35° 07'	141° 59'	332	1676	0.6
Ellis (this study)	-35° 17'	140° 39'	359	1749	0.75
Ellis (this study)	-36° 45'	142° 15'	439	1481	0.8
Ellis (this study)	-34° 31'	138° 41'	424	1807	0.8
Ellis (this study)	-37° 21'	141° 12'	662	1369	1.07
McVicar *et al.*, (1996)	-31° 57'	148° 52'	568	1864	2.07
McVicar *et al.*, (1996)	-31° 58'	148° 52'	568	1864	2.05
McVicar *et al.*, (1996)	-31° 59'	148° 59'	596	1813	2.09
McVicar *et al.*, (1996)	-31° 52'	148° 42'	552	1893	1.47
McVicar *et al.*, (1996)	-31° 44'	150° 04'	902	1442	1.86
McVicar *et al.*, (1996)	-31° 44'	149° 59'	831	1508	2.46
McVicar *et al.*, (1996)	-31° 40'	149° 38'	610	1796	1.7
McVicar *et al.*, (1996)	-31° 11'	149° 21'	711	1810	1.89
McVicar *et al.*, (1996)	-31° 01'	149° 19'	609	1918	1.68
McVicar *et al.*, (1996)	-31° 01'	149° 13'	624	1909	2.03
McVicar *et al.*, (1996)	-31° 16'	149° 05'	882	1724	2.59
McVicar *et al.*, (1996)	-31° 31'	145° 59'	370	2210	0.71
McVicar *et al.*, (1996)	-31° 29'	145° 37'	328	2201	0.59
McVicar *et al.*, (1996)	-31° 37'	144° 19'	248	1968	0.36
McVicar *et al.*, (1996)	-31° 42'	143° 44'	252	1835	0.13
McVicar *et al.*, (1996)	-31° 35'	143° 23'	240	1817	0.13
McVicar *et al.*, (1996)	-31° 54'	141° 37'	217	2207	0.1
McVicar *et al.*, (1996)	-31° 53'	141° 47'	202	2188	0.18
McVicar *et al.*, (1996)	-31° 47'	142° 10'	195	2149	0.1
McVicar *et al.*, (1996)	-31° 43'	142° 42'	220	1984	0.46
McVicar *et al.*, (1996)	-31° 32'	143° 17'	237	1839	0.17
Pook (1984)	-35° 30'	150° 18'	1170	1620	2.76
Roberts (2001)	-37° 29'	149° 35'	929	1356	3.7
Silberstein *et al.* (1999)	-33° 30'	116° 00'	953	1453	2
Vertessy *et al*, (1998)	-37° 51'	145° 36'	1400	1265	4.0
Walker *et al.*, (1998)	-33° 06'	147° 26'	447	1747	0.22
Walker *et al.*, (1998)	-35° 52'	146° 43'	568	1535	0.72
Walker *et al.*, (1998)	-34° 34'	147° 58'	608	1422	0.75
Walker *et al.*, (1998)	-35° 01'	149° 09'	670	1298	1.1
Walker *et al.*, (1998)	-34° 30'	148° 26'	613	1297	1.71
Walker *et al.*, (1998)	-35° 32'	147° 23'	828	1389	1.53
Walker *et al.*, (1998)	-35° 40'	147° 32'	730	1415	1.68

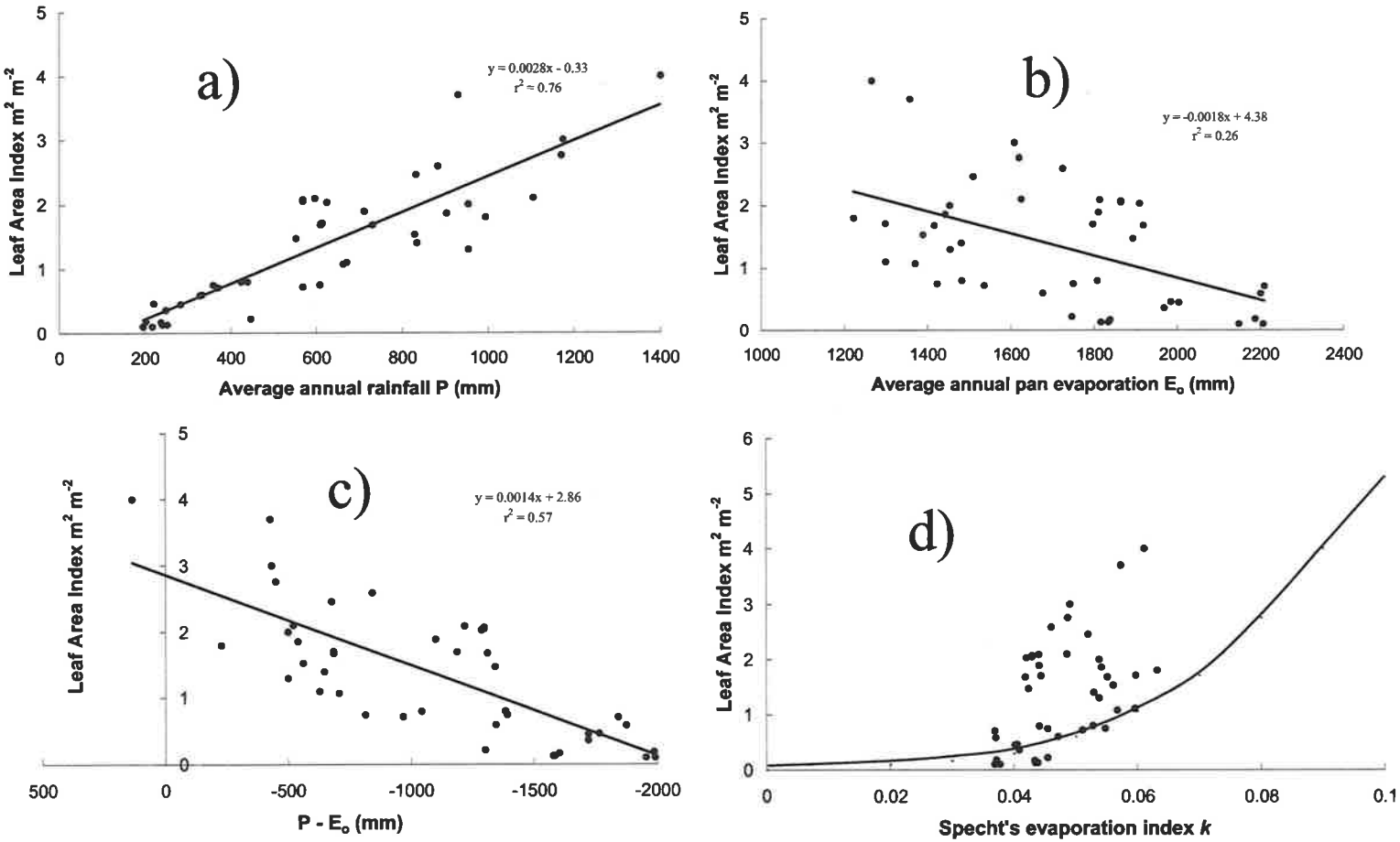

Figure 48 a) *LAI* versus *P;* b) *LAI* versus E_0 c) *LAI* versus P-E_0, and d) *LAI* versus Specht's evaporation coefficient k, where k is estimated from E_0 (k = 0.0045 + 71.57/ E_0, Specht and Specht, 1989) and the solid curvilinear line is that fitted by Specht and Specht (1989) to *LAI* measurements from 34 eucalyptus-dominated sites around Australia.

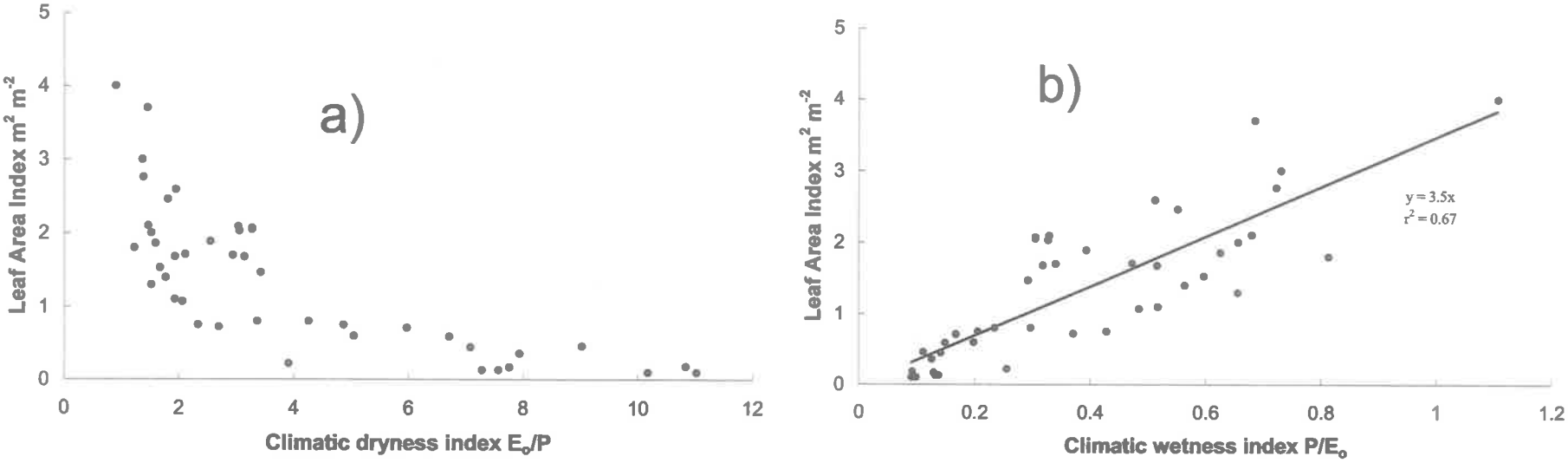

Figure 49 a) *LAI* of southern Australian natural vegetation (latitudes –30 to –40 degrees) versus Budyko's climatic index of dryness (Budyko, 1974) expressed in analogous water balance terms. b) *LAI* of southern Australian natural vegetation (latitudes –30 to –40 degrees) versus a climatic wetness index P/E_0.

Figure 49 shows *LAI* from the 43 sites (Table 5) versus Budyko's (1974) index of climatic dryness. The scatter plot exhibits a similar shape to the curves of annual vegetative production increment of Budyko and Efimova (1968) and Bazilevich *et al.* (1970) (Figure 47); *LAIs* are high at low values of climate dryness and appear to asymptote to zero as the climate becomes drier. This supports the notion that vegetative production of natural vegetation is proportional to *LAI* since it is leaf area that captures radiative resources. Given the roughly hyperbolic shape of Figure 49a, the same *LAI* data were then regressed (and forced through the origin) against the inverse of the index of dryness; P/E_0 (Figure 49b) The regression coefficient (r^2 = 0.67) shows that there is a reasonably strong relationship although not as strong as when rainfall alone was used (Figure 48a; r^2 = 0.76). Ellis *et al.* (1999) also tested *LAI* vs P/E_0 with a smaller and more polarised data set and reported a stronger linear trend (r^2 = 0.91) and smaller slope of 2.9 compared with 3.5 (Figure 49b).

Choosing an appropriate index

The criteria used to select an appropriate index for estimating *LAI* are as follows:

1. The index must use only easily procurable inputs;
2. The index must be algebraically simple;
3. The index must return an *LAI* estimate within measurable and acceptable limits;
4. The relationship between *LAI* and the index must be intuitively obvious;
5. The relationship must have (at least implicitly) calculable and logical boundary conditions.

Using the above criteria E_0, k, P-E_0 and E_0/P can be rejected immediately as being inappropriate indices for predicting *LAI*: E_0 does not meet criteria 3, 4 and 5; k does not meet 3 and 5; P-E_0 fails to meet 4 and 5; and E_0/P fails to meet criterion 2. This leaves P and P/E_0 which will be examined in turn with respect to the first four criteria. Criterion 5, boundary conditions, will be dealt with separately.

Local rainfall records are possibly the most universally available climate statistic in Australia, and least prone to measurement error. Using rainfall P alone is very simple and would appear to return the smallest uncertainty (r^2 = 0.76, SE_{yx} = 0.5). A standard error of 0.5 *LAI* would represent an absolute error of 50% to 25% along an annual average rainfall gradient from 400 to 1000 mm. For approximations at the landscape scale this is an

acceptable error. It is intuitively obvious that *LAI* should increase with increasing *P* as shown in Figure 48a. Annual average rainfall *P* therefore satisfies criteria 1 to 4.

The climate wetness index P/E_0 (Figure 49b) is less precise than *P* alone for predicting *LAI* (r^2 = 0.67, SE_{yx} = 0.6); producing a likely absolute error of 60% to 30% along an annual average rainfall gradient from 400 to 1000 mm. Annual average pan evaporation data is less readily available than rainfall and often prone to measurement error. Again it is intuitively obvious that *LAI* should increase with increasing climate wetness as demonstrated in Figure 48b. The climate wetness index P/E_0 therefore also satisfies criteria 1 to 4, although less convincingly than *P*.

Boundary conditions

The apparent threshold rainfall (~ 200 mm, Figure 48a) below which there is negligible *LAI* is often the case in arid environments as a large proportion of the rainfall evaporates directly from the soil surface. A negative y intercept for the fitted relationship between *LAI* and *P* is therefore acceptable and there is no good reason for the trendline to be forced through the origin. In the case of P/E_0, fitting an unforced trendline only minimally altered the slope of the relationship (-3%). In arid climates E_0 is usually much greater than rainfall (Table 5) and therefore the wetness index would be small. It is therefore acceptable that P/E_0 versus *LAI* should go close to or through the origin.

The upper boundary conditions are less definite. The two plots (Figure 48a; Figure 49b) both beg the questions: "what is the maximum *LAI,* and under what climatic conditions is likely to occur?". In both cases the answer is unlikely to be straightforward due to confounding factors: 1) as rainfall and climate wetness increase, radiation becomes a limiting factor to plant growth and water availability becomes non-limiting; 2) wetter climates are often associated with mountainous terrain where incident radiation is dependent on hill slope aspect (Budyko, 1974); 3) more cloud accompanies wetter climates, increasing the relative proportion of diffuse light and allowing a denser spatial arrangement of leaves for optimal light capture (Horn, 1971; Roderick *et al.*, 2001); and 4) wetter climates often occur at higher altitudes which, in the extreme (above the snow line), become too cold for plant growth (Budyko, 1974). It is likely however, that the fitted linear relationships between *LAI* and both *P* and P/E_0 approximate what is in reality probably asymptotic, approaching a maximum *LAI* as *P* and P/E_0 go to infinity.

It is difficult to estimate the upper boundary condition of *LAI* versus *P*, but it is possible for P/E_0 . This can be done by estimating the value of P/E_0 for which biomass is maximum at latitudes $30^0 - 40^0$ S and substituting it into Equation 23 from Figure 49b

$$LAI = 3.5\frac{P}{E_0} \tag{23}$$

Budyko (1974) lists mean components of heat balance at the surface of the earth for a range of latitudes. For latitudes $30^0 - 40^0$ S mean annual *R* for land is 2.6 G J m^{-2} yr^{-1}. There will be some error associated with using a mean value of *R* since it will vary with land surface, but not greatly between dense vegetation covers (Budyko, 1974; Oke, 1978). A more recent data source (Sellers *et al.,* 1995) gives an average value (for years 1987-88), for latitudes $30^0 - 40^0$ S on the Australian continent, 11% higher than that of Budyko (1974). The standard deviation was greatest (about 10%) for 35^0 S, but was only 3% overall. Dunin *et al.* (1985) recorded *R* about 30% higher than that of Budyko (1974) for Kioloa, $35^0$60'S, $150^0$28'E, on the New South Wales coast however this appears to be an extreme value.

For *R* = 2.6 G J m^{-2} yr^{-1} Bazilevich *et al.* (1970) give a maximum biomass increment at $R/\lambda P$ = 0.6 (Figure 47). Given that $R/\lambda P$ is analogous to E_0/P (Equation 21) then this maximum should occur at a wetness index P/E_0 of 1.67. This then gives a maximum *LAI* = 5.8 (Equation 23) for latitudes $30^0 - 40^0$ S. This compares favourably with *LAI* estimations of *E. regnans* forest of 5.7 - 6.2 (Berringer, 1994) made using the Li-Cor™ light interception plant canopy analyser (Welles and Norman, 1991). These measurements were made in 8 year old regrowth and would be considered to represent close to maximum values of *LAI*. Vertessey *et al.* (1998) report the highest *LAI* for mature forest in Table 5 of 4.0, also *E. regnans* forest.

Two checks can be made on the feasibility of this method for estimating the upper boundary condition: one is to calculate maximum *ET* from a semi-empirical relationship between the ratio of evaporation to precipitation (*ET/P*) and radiative index of dryness $R/\lambda P$ (Budyko, 1974); the second check is to solve this relationship for *P* and E_0 and compare them with expected values. Budyko (1974) presents Equation 24 when illustrating the dependence of *ET/P* on $R/\lambda P$, as part his investigations of geographic associations of energy and water balances.

$$ET = \frac{R}{\lambda}\tanh\frac{\lambda P}{R} \tag{24}$$

ET will approach a maximum of R/λ as $\lambda P/R$ approaches infinity. Using R = 2.6 G J m^{-2} yr^{-1} (Budyko, 1974) and λ = 2.4 M J kg^{-1} (Oke, 1978) maximum *ET* will be 1083 mm yr^{-1} for latitudes 30^0 – 40^0 S. One can also expect that maximum *ET* will occur when biomass and *LAI* are at a maximum, at $\lambda P/R$ = 1.67 as before (Bazilevich *et al.*, 1970). Budyko's Equation 24 (Budyko, 1974) therefore estimates that *ET* will be 1009 mm yr^{-1} at this point. These two estimates of *ET* are in close agreement.

Budyko's (1974) Equation 24 can be solved for *P* (Equation 25) and hence estimate the rainfall at which the maximum *LAI* may occur

$$P = \frac{R}{\lambda} \tanh^{-1} \frac{\lambda ET}{R} \qquad (25)$$

Some circularity emerges if *ET* is set to the maximum value of 1083 mm yr^{-1} as calculated above since $\lambda ET/R$ then becomes unity, for which the $\tanh^{-1}$ function is undefined. If *ET* is set to the 'rule of thumb' 1000 mm yr^{-1}, the rainfall, *P* is calculated to be 1744 mm yr^{-1}. This is a reasonable maximum value to expect for the high rainfall zones of southern Australia, which are heavily forested. If this value for *P* is substituted into the trendline fitted to *LAI* versus *P* (Equation 26; Figure 48a)

$$LAI = 0.0028P - 0.33 \qquad (26)$$

then the maximum *LAI* is estimated to be 4.7. This is 19% lower than that estimated when combining Equation 25 and Figure 49b; and 24% lower than the maximum recorded LAI in southern Australia for *E. regnans* (Berringer, 1994).

Given the several confounding factors as rainfall and climate wetness increase, the methods used to check the boundary conditions of Equation 23 serve to illustrate that the upper end of the relationship is in the right 'ballpark', rather than exact. *LAI* values interpolated from the relationship should provide reasonable predictions.

Discussion

The notion that natural vegetation evolves to reflect soil available water is not a new one, and has been demonstrated (Specht, 1972; Grier and Running, 1977; Specht and Specht, 1989). The challenge faced in this chapter was to determine an appropriate index, derived from gross climate parameters – one that did not require any estimates of less accessible parameters such as soil water storage or other local hydrologic characteristics.

Most natural vegetation communities comprise an evergreen and an annual vegetation component. The *LAI* of both of these components will depend on recent climatic conditions; in dry years the annual vegetation may not even germinate. The long-term

average of the sum of annual and perennial *LAI* components is likely to bear a very strong relationship to long-term average climatic conditions, but not in individual years. The growth of the annual vegetation will only reflect recent conditions, but by its very nature however, the evergreen (and hence perennial) vegetation must evolve to survive inter-storm or drought periods (Eagleson, 1982; Eagleson and Tellers, 1982). For these reasons, although the *LAI* of the perennial vegetation will fluctuate seasonally with climate, the fluctuations will be attenuated relative to climate fluctuations, and will always bear some relationship to long-term average climatic conditions.

Therefore, in the absence of long-term data on total *LAI* of natural communities, in this chapter, only the evergreen component of natural vegetation *LAI* is considered. For the purposes of *ENOR* application, it is assumed that this represents the *LAI* that is in equilibrium with the climate, such that recharge is very small (although it is acknowledged that there will be some seasonal variation).

Clearly E_0, $P - E_0$ and k, although easily obtainable, are not strongly related to the *LAI* from the data set used (Table 5). It would appear that the weak relationship between *LAI* and $P - E_0$ (Figure 48c) may have been improved if stored water was taken into account as with Grier and Running (1977), however this would have defeated the purpose of the exercise. Particularly interesting is the lack of agreement between the Table 5 data set collated from southern Australia and Specht and Specht's (1989) relationship, derived for the whole of Australia. I can offer no explanation for this but note that the *LAI* measurements used by Specht and Specht (1989) were mostly calculated from litter fall traps data rather than from visual estimation methods as used for the measurements in Table 5. and that there may be some bias between the techniques. Seasonal perturbations from 'normal' climatic conditions could not cause such a major difference between the two data sets given the associated large spatial and temporal ranges. Such an effect is likely to change the position of individual points or groups of points but a general trend is unlikely.

Conclusion

This chapter has confirmed that there exists a strong relationship between local climatic conditions and the *LAI* of natural vegetation in southern Australia. As an appropriate index for the purposes of estimating *LAI* for predicting *B* for a tree belt (Equation 12) the climate wetness index P/E_0 satisfied the 5 criteria used to select an appropriate index. Although

the upper boundary condition cannot be readily assessed using P in isolation, it appears that it is also a useful index for the purpose, and possibly more precise than P/E_0 .

Summary

This chapter investigates simple methods for estimating the *LAI* of natural vegetation as an input parameter to the *ENOR* model when data is not available. *LAI* measurements of natural vegetation made during this study (Chapters 5 and 6), were used together with *LAI* measurements from other studies conducted in southern Australia, to investigate relationships between *LAI* and indices of climate derived from gross climate parameters, and a water balance index (Specht and Specht, 1989).

A poor relationship was found between *LAI* and k but strong relationships were found between *LAI* and both P and P/E_0 . Criteria are established for selection of an appropriate index, with particular attention paid to boundary conditions. It is concluded that P as an index may be a more precise predictor of *LAI,* however the relationship between *LAI* and P/E_0 has more readily testable, and feasible, boundary conditions. The use of either index is appropriate for predicting *LAI* as an input parameter for the *ENOR* model.

Chapter 8

Estimating Lineal Leaf Area *LLA* of tree belts

The contents of this chapter and the next chapter have been combined and published as a CSIRO Technical Report (see Ellis *et al.*, 2001).

Introduction

Chapter 7 described the development of a method for estimating *LAI* from a simple climate index for use as the denominator in Equation 12. This chapter provides a scheme for estimating the numerator of Equation 12, *LLA* of a tree belt.

As discussed in Chapter 3, agroforestry models and isolated tree growth models are either insufficiently advanced to be used for predicting tree belt growth parameters such as *LLA*, or are prohibitively complex for an application such as this. An almost universally limiting factor is lack of knowledge regarding tree belt root growth and distribution. While the *ENOR* approach has provided a method for simplifying this issue, it cannot be used to predict the growth of tree belts, as it requires knowledge of the *LLA* in the first place. In Australia, the best-documented attempt to model the growth of tree belts was made by McJannet (1999), using process-based model TOPOG (Dawes *et al.,* 1997). McJannett (1999) however, assumed that there was no lateral spread of roots from the tree belts. The modelled belt growth was enhanced relative to plantation growth, but due mainly to

assumed run-on from upslope. This epitomises the dilemma that is constantly confronted in such situations: the model was not capable of describing the interface zone but the applied simplification omitted the effect of lateral roots, the dominant characteristic of tree belts. A more suitable model such as WaNulCAS (Van Noordwijk and Lusiana, 1999; ICRAF, 2001) could have been used but, as discussed in Chapter 3, the resources required to obtain input parameters become extreme, and there remains the problem of site-specific, and largely unknown, growth characteristics of tree roots.

In the absence of belt growth models that can be practically applied over a wide range of species and site conditions, and so that *ENOR* to be more widely used, this chapter describes a survey of typical farm tree belts in key catchments of the Murray Basin. Site characteristics and species are tabulated and a scheme is devised for visually estimating *LLA* from site photographs. *B* for each site is also calculated as additional information but it is noted that it is specific to the site. For a particular *LLA*, *B* will vary depending on the local *LAI*.

Site selection

Figure 50 shows the location of the 27 sites used in this survey, the selection of which involved the following considerations.

Alley farming is a relatively recent development in Australian landscapes. Although in excess of 10 000 ha of alley farms have been planted in Western Australia (Stirzaker and Lefroy, 1997), there is much less in other states, and what exists is at relatively immature stages of growth.

Primarily, tree belts were sought and located, where possible, on alley farms, but many of the sites used were fence-line or windbreak plantings. Initially, it was hoped to select sites of the same tree species (e.g. *E. cladocalyx* was planted widely on farms, rural towns and schools in some areas) and also of similar stages of maturity. In this regard little uniformity was found, with the added complication that tree belts varied in width from one to many rows.

The Murray Basin covers a large area and cannot be represented in full by this exercise. The criteria for the selection of *LLA* sites was focussed to represent: catchments in the Basin that are of significant interest in the short-term with regard to salinity; Focus Catchments already identified for study by other projects; a climate gradient (and hence a potential *LAI* gradient).

The project budget necessitated restriction of sites to within about half a days drive of CSIRO Land and Water Laboratory, ACT.

Catchments

Local and intermediate sized catchments (Coram, 1998) on the South-western Slopes of NSW are of significant interest in terms of future land use for salinity mitigation due to their relatively quick (decades) hydrogeologic response times and salt loads (Coram *et al*, 2000). The Upper Billabong Creek catchment is one of the Land and Water Audit (LWRRDC, 1999) focus catchments for these reasons, and due to the significant interest in tree planting from the farming community.

Contacts

Contact was made with farmers via the Murrumbidgee Landcare Association (http://www.landcareweb.com/lcdirectory/Murrumbidgeelca.html) and the Murrumbidgee Catchment Management Committee (http://www.murrumbidgee-catchment.org.au/).

Tree age

ENOR approach was developed and tested on mature eucalypts species (Chapters 5 and 6) where trees were remnant; a 70 year old plantation; and a 13 year old belt. The approach is not easily applicable to young plantings growing on stored water, so relatively arbitrary minimum age of 10 years was set for sites in this survey. This allowed a compromise between the paucity of mature tree belts of this age, and the need to gather data. The implications of calculating *B* for young belts is discussed in the next chapter.

Exceptions to this age limit were the *E. polybractia* (oil mallee) plantation (Site 10, Figure 60) grown in belts 3 m apart, and the LRAF trials (Sites 3,4 and 9; Figure 53, Figure 54 and Figure 59). These examples were included as they represent an established enterprise but their age must be considered when interpreting results.

Siting

The *ENOR* model was developed where trees are rain-fed only and runoff is negligible. Sites in this project were therefore chosen wherever possible on flat land and, away from the influence of creeks and groundwater or likely run-on. This excludes more than 90% of tree belts found in rural areas as they are often planted adjacent to roadways, which significantly affect the local surface hydrology and the tree root zone.

These issues are of significant concern to the siting of tree belts for plot-scale investigations but need not be a serious limitation to the application of *ENOR,* at catchment to regional scales. Although not corroborated except in the 'flat land' context, *ENOR* approach implies that the leaf area of a tree belt represents its equivalent width of

occupation in the landscape, independent of the source of water. This point is covered in more detail in the discussion section.

Tree health

In general, only healthy tree belts were selected for *LLA* measurement. Site 27 (Figure 77) had sustained significant insect attack and leaves were relatively sparse. This is reflected in calculated *B* equal to 5 m, which is less than the belt width of 6 m (Table 6).

Belt sections containing dead or missing trees were included if it was apparent that the trees had died or been removed a 'long time ago' and therefore belt growth had 'stabilised'. This was often apparent if the growth of adjacent trees had compensated for the missing tree. Site 26 (Figure 76) included a recently deceased tree but the effect of this was considered to be negligible as *LLA* was estimated from a 180 m length of belt.

Trees with greater than about 5% dieback (estimated visually), indicated by dead branches or dead segments of stem, were avoided.

Understorey

All sites except Site 24 (Figure 74) were considered to have insignificant understorey and it was not measured. This was either due to grazing or growth suppression by the trees. The effect of the pasture growth at Site 24 (Figure 74) may be reflected in the calculated *B* equal to 12 m, which was identical to the belt width

Length of belt selected

Where belts were relatively short (less than 40 m) *LLA* was estimated from the whole belt, excluding the 'end' trees. These trees usually showed relatively enhanced growth due to access to a greater land area than other trees in the belt (as with edge effects in Chapter 5). Where belts were long (greater than 100 m) and tree growth was relatively even, a 20 m to 40 m section was selected for *LLA* measurement. Where belts were greater than 40 m long and growth varied significantly with length, the method of estimating *LLA* from stem diameters was used (see Stem diameter – leaf area relationships, next section; and also Appendix 2 – inferring *LLA* from stem diameter).

When is a belt a belt?

Tree belts are planted in the landscape in a variety of widths and lengths. A site was judged to be a tree 'belt' when it its length was greater than 10 times its width and tree spacing and growth stage were such that trees were judged to be occupying a contiguous linear strip in the landscape. Where the combined effects of intra-row tree spacing and growth stage was such that trees appeared to not be affected by their neighbour, it was not considered a belt.

In water-limited environments, blocks of eucalypt trees usually show an edge strip of growth that is enhanced relative to that at mid-plantation. The width of such strips has been reported to vary between 5 m and 15 m (McJannett, 1999; Albertson *et al.,* 2000; Chapter 5). A belt was therefore considered to comprise any number of rows of trees, as long as: it was certain that the root zones of rows met or overlapped; and the belt was not more than two widths of 'enhanced edge' growth wide. It is worth noting that typical alley farm designs use belt widths of 5 to 10 m, and hence edge effects are not likely to be an issue.

Typically sites varied between single rows or up to five rows 2 m apart. Site 22 (Figure 72) was 16 m wide with obvious enhanced growth at the edges but it was considered that the enhancement of growth (due to the proximity of the edge) reached to the belt centre.

How many sites?

Early in the study it became clear there was little consistency in age, species or width within the sites available, and it was pointless specifying sample sizes in search of such relationships, and that the *LLA* data would represent a survey exercise. The number of sites was therefore determined by budget restrictions.

Leaf area measurement

Lineal Leaf Area *LLA*

As with experiments in chapters 5 and 6, leaf area was measured using the Adelaide (module) method (Andrew *et al.*, 1979) and is described in full in Appendix 2. Lineal Leaf Area *LLA* (m^2 m^{-1}) was calculated by dividing the leaf area (m^2) by the length of the tree belt (m).

Stem diameter and leaf area relationships

Tree belt lengths varied from tens to hundreds of metres. In the latter case, the belts often covered a range of growing conditions (soil type, depth etc.), and was reflected in changes in tree size along the belt length. For the scale of interest to this project, the longer the length of belt over which *LLA* is averaged, the better the representation of the expected *LLA* for that catchment (for that particular species and age). Measurement of *LLA* using the module method for belt lengths greater than about 40 m was considered prohibitively time-consuming (greater than ~1.5 hrs). However, to efficiently obtain a representative measurement in such cases, leaf area was scaled to stem diameter as this has been shown to be a useful method for eucalypts (Vertessy *et al.*, 1995).

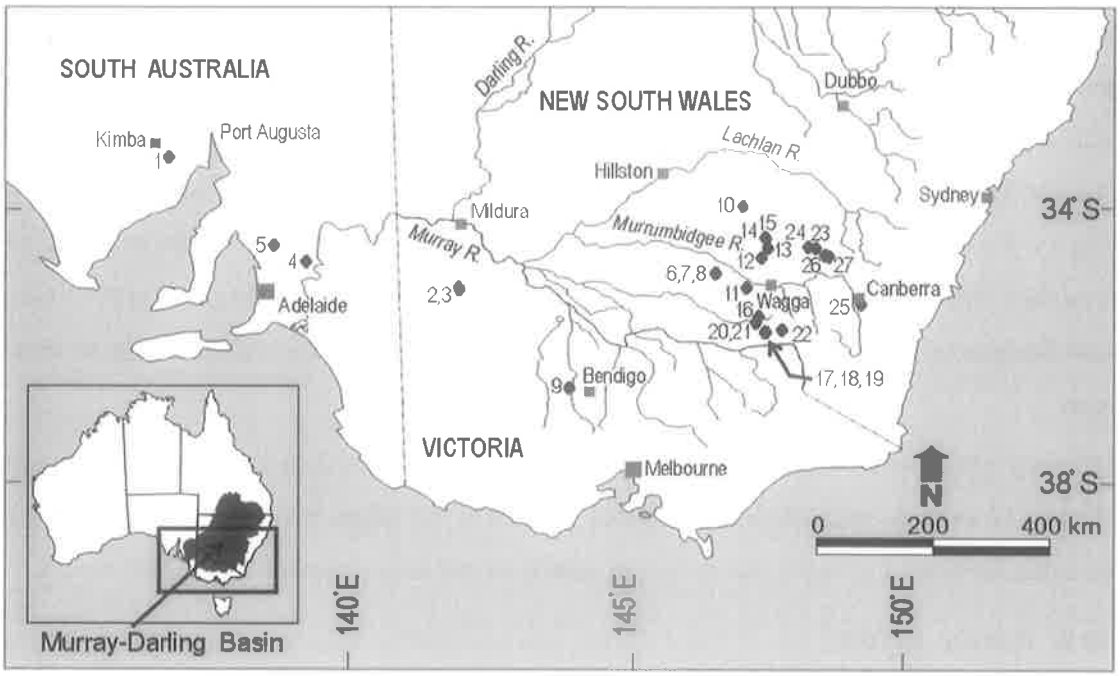

Figure 50 Southeastern Australia and the Murray-Darling Basin (inset) showing the location of the 27 *LLA* measurement sites used in this survey.

Where long belts also comprised a large range of tree sizes, about 12 trees were chosen to evenly represent the range from the smallest to the largest. Both the stem diameters (below all leaf-bearing branches) and number of leaf modules were measured on the selected trees. A second-order polynomial relationship was fitted to the data; the stem diameters of all the remaining trees in the belt were then recorded and the mean number of modules per tree was calculated from the polynomial relationship. Total leaf area and *LLA* were then calculated as described above. This method was evaluated (Figure 100) on a 40 m length of *E. globulus* (Site 25, Figure 75). *LLA* predicted from the stem diameters was found to be within 10% of that from counting the modules of all the trees.

Nine sites were measured using the stem diameter method; coefficients of the fitted polynomial relationships are shown in Table 7 and include the data of Vertessy *et al.* (1995) for 15 year-old *E. regnans*. When the data set was viewed as a whole, there was only a relatively weak relationship between stem diameter and leaf area ($r^2 = 0.54$) and preliminary attempts to make generalisations were made by adjusting for tree age. Although further investigation is required, it is worth noting that, when the remnant sites were excluded (because it is difficult to assign an age), along with two *E. globulus* Sites 20 and 25 (Figure 70 and Figure 75), the relationship $y = 0.0084x^2 + 1.36$ ($r^2 = 0.82$, n = 120) was fitted to stem diameter (mm) versus leaf area (m^2) x age (yr). *E. globulus* is considered to be a profligate user of resources compared to other eucalypt species and

tends to maintain a high leaf area under conditions when other species have reduced their leaf area in response to dry conditions (pers. comm. Michael Battaglia, CSIRO Forests and Forest Products). This may justify treating *E. globulus* separately but it would require further investigation.

Results

Typical tree belts and LLA measurements

The purpose of the photographs and accompanying *LLA* measurements is to provide an appreciation of the likely range of *LLA* of tree belts and to allow an estimation of *LLA* for hypothetical tree belts/alley farms. Readers should note the following:

- Site numbers correspond with those in Table 6 and have been sorted in order of ascending increasing climate wetness (P/E_0) that roughly corresponds with increasing local *LAI*. Sites 1, 2 and 5 (Figure 51, Figure 52, Figure 55) are from Chapters 5 and 6; Sites 3, 4 and 9 (Figure 53; Figure 54; Figure 59) are the MDBC Low Rainfall Alley Farming Trial sites planted in 1997-98. The remaining sites were measured specifically for this survey.
- Unless otherwise specified, the following site photographs were taken at the time of measurement – between May and September 2000.
- To give an appreciation of scale, operators in the photographs are holding a 4 m staff.
- Photograph captions include: species; type, orientation and location of planting.
- The *LLA* ($m^2\ m^{-1}$) of each site is given and ranked: 5 – 15 small; 16 – 30 medium; 31 – 45 large; 46 – 65 very large; >66 extremely large. Note that the rank refers to the magnitude of the *LLA*, not the physical dimensions of the trees.
- The length of belt used to measure *LLA* is given.
- The method used at each site is indicated: either 'module' counts only (Andrew *et al.*, 1979); or 'stem diameter/leaf area' relationship (Hatton *et al.*, 1995; Vertessy *et al.*, 1995).
- Further site details are given in Table 6 and include: age; belt width; canopy width; latitude; longitude; local rainfall and evaporation; local *LAI*; width of visually discernible root influence; and *B*.

Figure 51 Site 1 Remnant *E. socialis* north-south oriented fence line planting at "Cooinya" south east of Kimba, SA. November 1998.

***LLA* = 11 m^2 m^{-1} – small.**
Length of belt measured = 20 m.
Method used –'module' only.

Figure 52 Site 2 Remnant *E. dumosa* (Chapter 5) north-south oriented fence line at the Wakefield's property near Walpeup, Vic. October 1997.

***LLA* = 25 m^2 m^{-1} – medium.**
Length of belt measured = 30 m.
Method used –'module' only.

Figure 53 Site 3. *Atriplex nummularia* and *Atriplex amnicola* north-south oriented alley farm trial at the Mallee Research Station, Walpeup, SA.

***LLA* = 13 m^2 m^{-1} – small.**
Length of belt measured = 10 m.
Method used – 'module' only.

Figure 54 Site 4 *Atriplex nummularia* and *Acacia saligna* north-south oriented alley farm trial at Pallamana, north of Murray Bridge, SA.

***LLA* = 42 m^2 m^{-1} – large.**
Length of belt measured = 10 m.
Method used – 'module' only.

Figure 55 Site 5 *E. leucoxylon and E occidentalis* (Chapter 6) north-south oriented windbreak on the Selleck's property near Roseworthy, SA.

***LLA* = 17 m^2 m^{-1} – medium.**
Length of belt measured = 30 m.
Method used –'module' only.

Figure 56 Site 6 *E. maculata* belt in a north west-south east oriented alley layout at "Avondale", Sandigo south east of Narrandra, NSW. The belt is one of several (see Site 7) planted in an effort to reduce a saline seep a few kilometres away.

***LLA* = 22 m^2 m^{-1} – medium.**
Length of belt measured = 20 m.
Method used – 'module' only.

Figure 57 Site 7. *camaldulensis* (right) belt in a north west-south east oriented alley layout at "Avondale", Sandigo south east of Narrandra, NSW. Site 6 can be seen on the far left.

***LLA* = 16 m^2 m^{-1} – medium.**
Length of belt measured = 20 m.
Method used – 'module' only.

Figure 58 Site 8 *E. cladocalyx* east-west fence line planting at "Avondale", Sandigo south east of Narrandra, NSW.

***LLA* = 19 m^2 m^{-1} – medium.**
Length of belt measured = 112 m.
Method used – 'module' only.

Figure 59 Site 9 *E. leucoxylon, E. camaldulensis, E. maculata, E. microcarpa, Acacia salicina* north-south oriented alley farm trial at Bridgewater-on-Loddon, near Bendigo, Vic.

***LLA* = 14 m^2 m^{-1} – small.**
Length of belt measured = 20 m.
Method used – 'module' only.

Figure 60 Site 10 *E. polybractia* (blue mallee) 18 mth old regrowth following harvest in a north-south oriented oil mallee plantation at "Tumbledown" south of West Wyalong, NSW. Rows are 3 m apart.

***LLA* = 5 m^2 m^{-1} – very small.**
Length of belt measured = 20 m.
Method used – 'module' only.

Figure 61 Site 11 *E. dawsioni* and *E. dwylerii* north-south fence line planting at "Truro" east of Wagga Wagga, NSW.

***LLA* = 15 m^2 m^{-1} – small.**
Length of belt measured = 466 m.
Method used – 'stem diameter/leaf area'.

Figure 62 Site12 Belt of an unidentified eucalypt species in a north-south oriented wide-spaced alley (200 m between belts) at "Waerawi", west of Old Junee, NSW.

***LLA* = 11 m^2 m^{-1} – small.**
Length of belt measured = 20 m.
Method used – 'module' only.

Figure 63 Site 13 *E. sideroxylon* north-south oriented fence line planting at "Carinya', west of Old Junee, NSW.

***LLA* = 14 m^2 m^{-1} – small.**
Length of belt measured = 77 m.
Method used – both: 'stem diameter/leaf area'; and 'module' only.

Figure 64 Site 14 *E. microcarpa* north-south oriented fence line planting at Temora Research Station, north of Temora, NSW.

***LLA* = 17 m^2 m^{-1} – medium.**
Length of belt measured = 75 m.
Method used – 'module' only.

Figure 65 Site 15 *E. largiflorans* northeast-southwest oriented fence line planting at Temora Research Station, north of Temora, NSW.

***LLA* = 16 m^2 m^{-1} – medium.**
Length of belt measured = 70 m.
Method used – 'module' only.

Figure 66 Site 16 *E. saligna* and *E. botrioides* east-west windbreak at "Jayfields" north of Holbrook, NSW.

***LLA* = 54 m^2 m^{-1} – very large.**
Length of belt measured = 80 m.
Method used – 'stem diameter/leaf area'.

Figure 67 Site 17 *E. polyanthemos* remnant belt on a north-south fence line at "Ardrossan", south east of Holbrook, NSW.

***LLA* = 25 m^2 m^{-1} – medium.**
Length of belt measured = 55 m.
Method used – 'stem diameter/leaf area'.

Figure 68 Site 18 *E. melliodora* and *E. sideroxylon* north-south oriented row, planted for stock shelter at "Killandaye" south east of Holbrook, NSW.

***LLA* = 24 m^2 m^{-1} – medium.**
Length of belt measured = 33 m.
Method used – 'module' only.

Figure 69 Site 19 *E. melliodora* north-south oriented row planted for stock shelter at "Killandaye" south east of Holbrook, NSW.

***LLA* = 24 m^2 m^{-1} – medium.**
Length of belt measured = 48 m.
Method used – 'module' only.

Figure 70 Site 20 *E. melliodora* and *E. globulus* north-south windbreak at "Mima" north of Holbrook, NSW.

***LLA* = 62 m^2 m^{-1} – very large.**
Length of belt measured = 66 m.
Method used – 'stem diameter/leaf area'.

Figure 71 Site 21 *E. melliodora* and *E. cladocalyx* north-south windbreak at "Mima" north of Holbrook, NSW

***LLA* = 19 m^2 m^{-1} – medium.**
Length of belt measured = 43 m.
Method used – 'module' only.

Figure 72 Site 22 *E. albens, E. mannifera* and *E. dives* remnant windbreak oriented east-west at "Highfields", west of Rosewood NSW.

***LLA* = 102 m^2 m^{-1} – extremely large.**
Length of belt measured = 110 m.
Method used – 'stem diameter/leaf area'.

Figure 73 Site 23 *E. globulus* council planting oriented north-south, east of Harden, NSW.

***LLA* = 29 m^2 m^{-1} – medium.**
Length of belt measured = 135 m.
Method used – 'module' only.

Figure 74 Site 24 *E. camaldulensis* discharge planting (valley floor seep) oriented north-south at "Oxton Park", northwest of Harden, NSW. Note significant understorey growth.

***LLA* = 16 m^2 m^{-1} – medium.**
Length of belt measured = 148 m.
Method used – both: 'stem diameter/leaf area'; and 'module' only.

Figure 75 Site 25 *E. globulus* council planting, oriented north-south at Chifley, ACT. Photographed December 2000.

LLA = 45 m^2 m^{-1} – large.
Length of belt measured = 185 m; 40 m
Method used – both: 'stem diameter/leaf area'; and 'module' only (calibration site).

Figure 76 Site 26 *E. globulus* east-west oriented fence line planting at "Emu Flat" north of Yass, NSW.

LLA = 17 m^2 m^{-1} – medium. Note gaps in the belt which have affect the average LLA.
Length of belt measured = 180 m.
Method used – 'stem diameter/leaf area'.

Figure 77 Site 27 *E. camaldulensis* east-west oriented windbreak at "Bobbara Creek" west of Binalong, NSW. There was significant insect leaf damage.

***LLA* = 7 m^2 m^{-1} –small.**
Length of belt measured = 66 m.
Method used –'module' only.

Site data and calculation of *B*

The *LLA* measurements for the 27 sites are listed in Table 6, together with local *LAI* values estimated using Equation 23. *B* values were calculated from Equation 12 and are presented as additional information; the main purpose of the survey is to provide an appreciation of the likely range of *LLA* values and a means for approximating *LLA* in the absence of either data or measurable tree belts. Table 6 also lists site specifications including the type of planting, age, species, dimensions, climate. The width of visible root influence on adjacent pasture or crop has also been approximated where possible. In most cases no effect was discernible. Sites have been sorted with increasing *LAI*, which corresponds with increasing climate wetness.

Table 6 Site specifications and *LLA* measurements, modified from *Ellis et al.* (2001d). Data is sorted with increasing climate wetness, which approximately follows increasing *LAI*. *B* is calculated from Equation 12. Sites 1, 2 and 5 are from Chapter 5. Sites 3, 4 and 8 are the Murray Darling Basin Commission Low Rainfall Alley Farming trial sites. For all sites *LAI* was estimated using Equation 23.

Site [a]	Species [b]	Type of planting [c]	Age (y)	Width stem to stem (m)	Tree height (m)	Canopy width (m)	Latitude (deg, min)	Longitude (deg, min)	Average annual rainfall (mm)	Average annual evaporation (mm)	Local *LAI* (m^2 m^{-2})	*LLA* (m^2 m^{-1})	Width of visible root influence [d] (m)	*B* (m)
1	*so*	R	<60	7	4.5	9	33°15'	136°50'	300	2250	0.47	11	20	20
2	*du*	R	<60	8	8	10	35°07'	141°59'	343	2000	0.6	25	40	42
		F												
3	*nu*	A	3	10	1.0	10	35°09'	142°00'	343	2000	0.6	13	1.5	22
	am				0.5									
4	*nu*	A	3	6	1.9	6	35°01'	139°19'	300	1900	0.55	42	2	64
	sa				3.2									
5	*le*	W	13	4	9	8	34°31'	138°41'	443	2000	0.78	17	24	21
	oc	F												
6	*ma*	A	10	8	8	10.5	34°55'	146°36'	432	1826	0.83	22	NV	32
7	*ca*	A	10	8.5	8	11	34°55'	146°36'	432	1826	0.83	16	NV	23
8	*cl*	F	28	3	14	10	34°55'	146°36'	432	1826	0.83	19	11	27
9	*sa*	A	3	10	1.9	10	36°33'	143°57'	425	1800	0.83	14	2	54
	le													
	ca													
	ma				3.9									
	mi													
10	*pa*	P	1.5	S	1.8	1.6	33°57'	147°05'	455	1753	0.91	5	NV	7
11	*dw*	F	12	3	9	7	35°07'	147°10'	516	1790	1.01	15	NV	18
12	*?*	A	6	3	4.2	5.6	34°42'	147°26'	506	1753	1.01	11	NV	14
13	*si*	W	25	4	6	9.5	34°33'	147°33'	510	1760	1.01	14	20	17
14	*mi*	F	50	S	13	7.5	34°25'	147°31'	505	1717	1.03	17	NV	20
15	*la*	F	45	S	12	15.8	34°24'	147°30'	509	1717	1.04	16	NV	19
16	*bo*	W	10	11	8	14	35°32'	147°23'	575	1717	1.17	54	2.5	55
	sa													
17	*po*	R	<70	8	17	24	35°45'	147°31'	588	1680	1.23	25	13	25
		F												
18	*me*	W	15	S	9	7	35°45'	147°30'	597	1680	1.24	24	6	23
	si													
19	*me*	W	15	S	7	6.5	35°45'	147°30'	597	1680	1.24	24	8	23
20	*me*	W	40	9	12	21	35°37'	147°20'	699	1680	1.46	62	8	51
	gl													

Table 6 (Continued)

Site [a]	Species [b]	Type of planting [c]	Age (y)	Width stem to stem (m)	Tree height (m)	Canopy width (m)	Latitude (deg, min,)	Longitude (deg, min)	Average annual rainfall (mm)	Average annual evaporation (mm)	Local *LAI* (m^2 m^{-2})	*LLA* (m^2 m^{-1})	Width of visible root influence [d] (m)	*B* (m)
21	*me cl*	F	40	9	13	18	35°37'	147°20'	699	1680	1.46	19	5	15
22	*al man di*	R W	<70	16	16	27	35°43'	147°49'	673	1607	1.47	102	NV	84
23	*gl*	C	30	S	12	11	34°33'	148°25'	625	1424	1.54	29	NV	23
24	*ca*	D	15	12	7	16.5	34°32'	148°17'	666	1461	1.6	16	NV	12
25	*gl*	C	20	4	16	13	35°30'	149°00'	662	1424	1.63	45	NV	33
26	*gl*	F	24	S	10	13	34°41'	148°39'	666	1424	1.64	17	NV	13
27	*bl*	W	11	6	6.5	11	34°39'	148°35'	676	1424	1.66	7	NV	5

Notes for Table 6:

[a] Site number corresponds with photographs.

[b] Most sites were eucalypt species: *E. albes (al); blakeli (bl); botryoides (bo); camaldulensis (ca); cladocalyx (cl); dives (di); dumosa (du); dwylerii (dw); globules (gl); largiflorans (la); leucoxylon (le); maculata (ma); mannifera (man); melliodora (me); microcarpa (mi); occidentalis (oc); polyanthemos (ps); polybractia (pa); saligna (sa); sideroxylon (si); socialis (so).* Sites 3, 4 and 8 included *Atriplex* spp: *nummalaria (nu); amnicola (am)* and *Acacia saligna (sal).* The eucalypt species at site 12 were not identified.

[c] Type of plantings: belt in an alley farm system A; fence line F; plantation P; windbreak W; council C; discharge area D; remnant R.

[d] NV means effect/extent of tree roots was not visible.

Additional remarks

Following on from the discussion in Chapter 3 regarding spatial and temporal variation of processes within the root zone, and the expression of these as tree/crop competition, it is worth noting the limited indications of root zone extent (from visible effects of trees on adjacent pasture or crop) that were possible during this survey. Many factors influence the

presence and extent of such an effect including soil water conditions in the root zone of the crop or pasture, and their stage of development. Because of this, the temporal distribution of rainfall can have a large influence. The best indication of the extent of the tree root zone can be seen in very dry conditions during which the trees usually compete aggressively for soil water at the expense of the other species (see Chapter 5). Under certain conditions towards the end of spring and during summer, or when the soil is waterlogged, annual pastures can be seen to grow better beneath the tree canopies. Table 6 shows that in most cases it was impossible to discern an effect of the trees on adjacent species, and where one could be estimated, there were large differences between the estimated width of influence and predicted *B*. Some authors have expressed the extent of influence of a tree belt on crops as a function of tree height (Hall *et al.,* 2000) however only very weak relationships were found between *B* and tree height in this study.

Due to the disparate nature of the sites in terms of species, age, climate and belt width, the *B* values calculated, although interesting, are site-specific and are not the main purpose of the survey. In the absence of suitable growth models, the site photographs and accompanying *LLA* values serve as a guide for estimating *LLA* when applying the *ENOR* model to hypothetical or planned alley farms. The next chapter briefly revises the *ENOR* model and provides worked examples of its application.

Summary

This chapter describes a survey of 27 farm tree belts and alley farming trial sites in the Murray Basin and presents the data as a guide for users of the *ENOR* model. Selection criteria are presented for the sites used in the survey, as well as the methods used to measure *LLA* directly, or to estimate *LLA* from stem diameter/leaf area relationships. For each site a photograph is provided and is accompanied by the *LLA* value measured at the site. This allows users of the *ENOR* model to make realistic estimates of the *LLA* they might expect for hypothetical alley farms.

Chapter 9

Model application

The contents of this chapter and the previous chapter have been combined and published as a CSIRO Technical Report (see Ellis *et al.*, 2001).

Introduction

This chapter brings together the approach described in chapter 4, the methods for estimating *LLA* and *LAI* in chapters 7 and 8, and provides procedures for applying the *ENOR* model. The *ENOR* approach is summarised and a map is presented of potential long-term average *LAI* of natural vegetation for the Murray Darling Basin, developed from P and E_0 data and the climate wetness index Equation 23. Worked examples of hypothetical alley farms are presented showing how to use *ENOR* to: 1) estimate recharge from an alley farm; 2) design an alley farm to result in a prescribed level of recharge.

Some practical implications of the application of both alley farms and the *ENOR* model are discussed in relation to: catchment response to reduced recharge; the productivity of alley farms; the application of *ENOR* to young and non-eucalypt systems; and coppicing and root pruning practices. The errors associated with predictions and designs are quantified and compared for cases where *LLA* and *LAI* are: 1) directly measured; 2) estimated.

Summary of *ENOR* conceptual model and approach from Chapter 4

Model description

The *ENOR* approach developed in Chapter 4 can be summarised as follows (note: equation numbers relate to Chapter 4):

Recharge from an alley farm is expressed as Relative Recharge *RR*

$$RR = \frac{\text{recharge from alley farm}}{\text{recharge from conventional farm}} = 1 - \frac{B}{W} \qquad (13)$$

where B (m) is the Equivalent No Recharge (*ENOR*) width of the tree belts and W (m) is the centre-to-centre spacing of the tree belts (Figure 78).

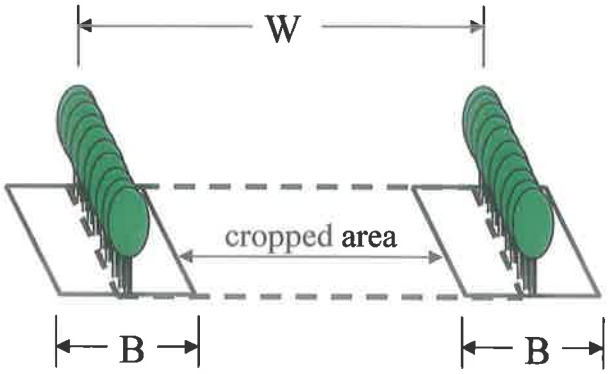

Figure 78 *ENOR* width *B* and belt spacing *W* for an alley farm.

B can be calculated from leaf area measurements

$$B = \frac{LLA}{LAI}, \qquad (12)$$

where: *LLA* is the Lineal Leaf Area of the tree belt (m^2 m^{-1} belt); and *LAI* is the leaf area index of local natural vegetation (m^2 m^{-2}).

If the magnitude of recharge from the conventional farming system *RC* is known, an average recharge from the alley farm *RA* can be calculated

$$RA = RC \times RR. \qquad (15)$$

Model inputs

The four model inputs are as follows:

1. Lineal Leaf Area *LLA* (m^2 m^{-1}) of the tree belt(s), equal to the leaf area (m^2) per unit length (m) of belt;

2. Leaf Area Index *LAI* of natural vegetation where Leaf area index (m^2 m^{-2}) of a block of vegetation is equal to the ratio of plant leaf area (m^2) to the ground area (m^2) it covers;
3. The centre-to-centre belt spacing of the alley farm *W;*
4. An estimate of recharge from the conventional farming system *RC.*

If *RC* is not known, typical values are available from the technical report of Petheram *et al.* (2001) that is available on line at http://www.clw.csiro.au/publications/technical2000/. If data is not available *LLA*, *LAI* and *W* can be estimated as described below.

Leaf Area Index of natural vegetation *LAI*

As shown in Chapter 7, *LAI* can be estimated for a site using Equation 23 if the long-term average annual rainfall *P* and pan evaporation E_0 is known

$$LAI = 3.5\frac{P}{E_0}. \qquad (23)$$

P and E_0 can be obtained from the Bureau of Meteorology weather maps (Australian Bureau of Meteorology, 2000).

To facilitate rapid approximation of *LAI* a map (Figure 79) was generated for the whole of the Murray Darling Basin using a GIS package and Equation 23 (derived for latitudes 30 to 40 S). The Basin extends between latitudes 25^0S and 37^0S and the implications of the extrapolation of Equation 23 (to the whole Basin) are addressed in the discussion section of this chapter.

LAI was evaluated at a grid cell resolution of 36 seconds, which represents about 1 km, over the MDB. The inputs required were:

- A Digital Elevation Model (DEM) – used in the generation of rainfall and evaporation surfaces;
- A rainfall surface;
- A pan-evaporation surface;

The resulting DEM, rainfall and evaporation maps are shown in Appendix 5.

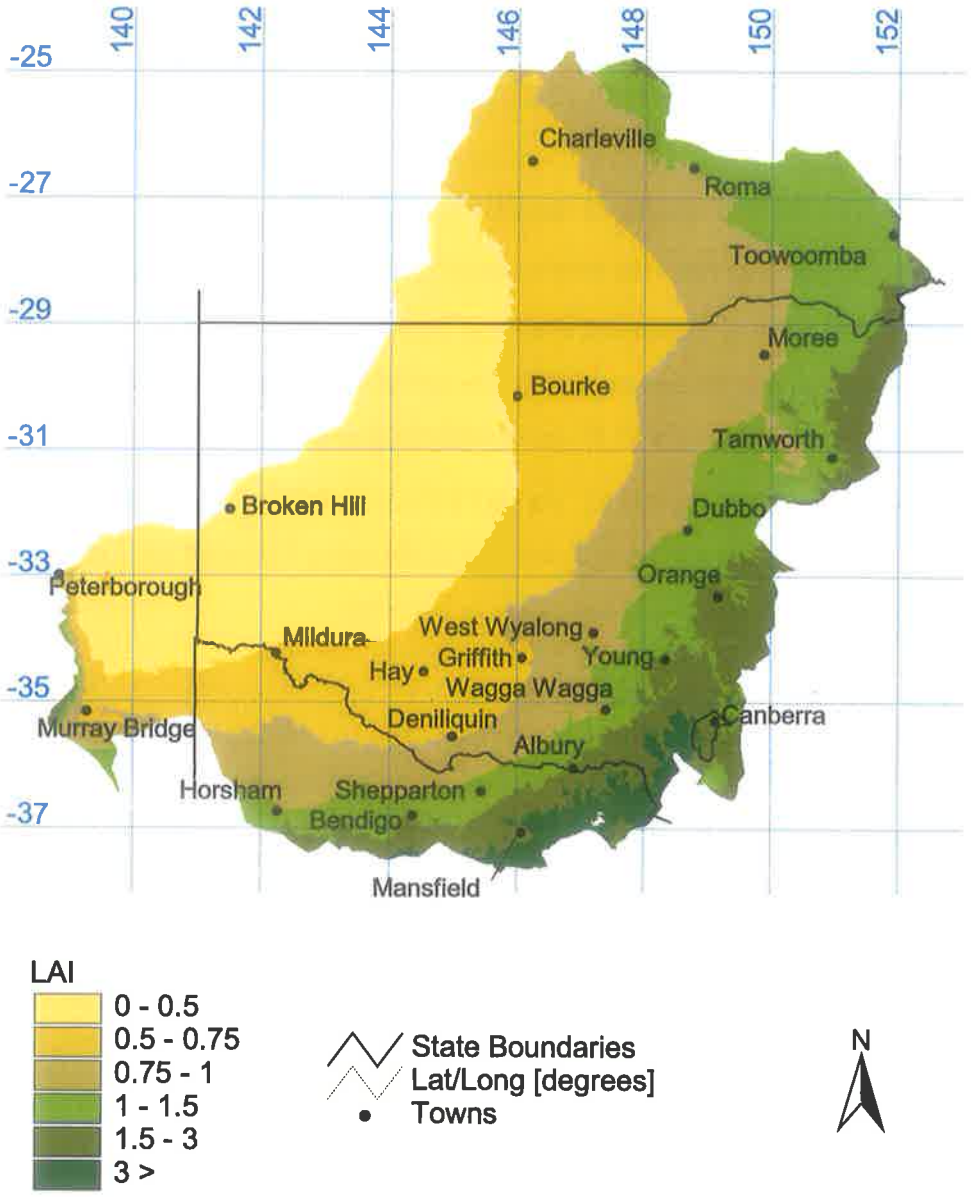

Figure 79 Map of the Murray Darling Basin showing estimated Leaf Area Index *LAI* for natural vegetation derived using Equation 23. Ellis *et al.* (2001) included a similar map but it was derived using a coefficient of 2.9 (Ellis *et al.*, 1999) instead of 3.5.

Lineal Leaf Area of tree belt *LLA*

The paucity of alley farms and appropriately sited tree belts will necessitate the estimation of *LLA* in many cases. A scheme was developed in Chapter 8 to allow estimates to be made by inspecting the site photographs of typical tree belts and deciding on an *LLA* rank and range:

- small 5 – 15 m^2 m^{-1};
- medium 16 – 30 m^2 m^{-1};

- large 31 – 45 m^2 m^{-1};
- very large 46 – 65 m^2 m^{-1};
- extremely large >66 m^2 m^{-1}.

Note: the rank refers to the magnitude of the *LLA*, not the physical dimensions of the trees.

Belt spacing *W*

W is the centre-to-centre spacing of tree belts (Figure 78). If this measurement is not available from an existing site, typical values range between 50 m and 200 m. Typically, this dimension is determined as a multiple of the width of the farmer's seeding and/or harvesting machinery.

Procedures for applying the model

Procedure 1 - Calculating recharge from an alley farm

1. estimate *LLA* for tree belts (Chapter 8);
2. estimate local *LAI* (Figure 79 or Equation 23);
3. calculate *B* (Equation 12)

$$B = \frac{LLA}{LAI};$$

4. choose centre-to-centre belts spacing *W* and calculate the percentage recharge reduction *RR* (Equation 13)

$$RR = 1 - \frac{B}{W};$$

5. calculate average recharge *RA* from the alley farm (Equation 15)

$$RA = RR \times RC.$$

Example 1 – calculating recharge

An alley farm is to be planted in a cropping paddock 50 km west of Wagga Wagga (35°10'S 147°30'E). The farmer uses 10 m wide seeding equipment and wants to be able to sow the crop between the belts with 4 passes of the seeder. Assume tree belts will be 10 m wide, therefore the centre-to-centre spacing of the belts *W* would be 50 m. What relative recharge *RR* can be expected once the belts have matured? What will be the average recharge *RA* from the alley farm if recharge from the crop *RC* is 50 mm yr^{-1}?

1. choose a medium belt (Chapter 8) with an *LLA* = 20 m^2 m^{-1};
2. using Figure 79 estimate local *LAI* = 1.0;

3. using Equation 12 calculate $B = \frac{20}{1} = 20\text{m}$;

4. using Equation 13 calculate relative recharge $RR = 1 - \frac{20}{50} = 0.6$;

5. using Equation 15 $RA = 0.6 \times 50 = 30\text{mm yr}^{-1}$.

If an alley farm near Wagga Wagga comprised tree belts similar to Sites 9, 18 and 21 Chapter 8) spaced at 50 m intervals (measured centre-to-centre), the recharge from the paddock would be 60% of that from a conventional farming system.

Procedure 2 - Designing an alley farm to meet a recharge target

To design an alley system that will result in a prescribed recharge reduction, steps 1 to 3 are followed in the same way as above but Equation 13 in step 4 is solved for W rather than RR.

Example 2- designing an alley farm

If *E. cladocaylix* is intended for use in an alley farm 100 km north of Albury (36°00'S, 147°00'E), what centre-to-centre belt spacing W would be required to reduce recharge to 20% of that from the conventional farming system? What proportion of the paddock would be left for crop or pasture production?

1. estimate $LLA = 40\ \text{m}^2\ \text{m}^{-1}$, similar to Site 25 (Figure 75, Chapter 8), belts 4 m wide;
2. from Figure 79, $LAI = 1.3$ at Albury;
3. calculate $B = \frac{40}{1.3} = 31\text{m}$;
4. rearrange Equation 13 and calculate $W = \frac{B}{1-RR} = \frac{31}{1-0.2} = 39\text{m}$;
5. if the tree belts were 4 m wide then the proportion of the paddock remaining for crop and pasture would be $\frac{39-4}{39} = 0.9$.

If recharge from a cropping paddock near Albury is to be reduced by 80% using 4 m wide sugar gum (*E. cladocaylix*) belts, the belts would need to be placed every 39 m (measured centre-to-centre) across the paddock. The tree belts would occupy about 10% of the total land area.

Discussion

Catchment response

The eventual impact of such a recharge reduction on either dryland salinity or stream salinity levels depends to a large degree on the type of catchment being considered. Investigations of catchment responses to changes in land use are at an early stage of development. Current research is aimed at intensively modelling the response of representatives of several catchment types (Coram, 1998; Coram *et al.*, 2000) so that generalisations may be made regarding the likely response of similar catchments. Dawes *et al.*, (2001) and Stauffacher *et al.*, (2000) give examples of such studies in two catchment types. Whatever modelling technique is used, however, recharge estimates made using the *ENOR* model will be required for inputs to groundwater models.

Productivity

The compromise between crop production and recharge control is a difficult issue, requiring consideration at different scales of time and space. The loss of production due to tree competition is significant, relatively immediate and localised. However the recharge reduction benefits from trees are not immediate. They are long-term and usually off site – lower in the catchment. The production costs of not controlling recharge, and hence salinity, are very large and very long-term. There is consequently a lot of interest in developing productive tree species that can offset crop yield losses due to tree competition, and still provide some recharge reduction. Some eucalypt mallee species have high leaf oil concentrations and can provide a commercially viable return, depending on production costs. The productivity of fodder shrubs, such as saltbush is also under investigation for agroforestry in southern Australia (Knight *et al.*, 2001). Tree belts can add value to a rural landscape in other was such as stock and crop shelter (Nuberg *et al.*, 1998), biodiversity and amenity.

Ignoring the intrinsic value of the trees momentarily, if there is a requirement to reduce recharge in a catchment by, say, 50%, tree plantings are the most effective method for doing so. 50% recharge reduction can be achieved by planting a single block of trees covering half the catchment; or the whole the catchment with an alley farm where *B/W* equal to 0.5 (from Equation 14). The block planting will also undoubtedly reduce catchment crop production by at least 50%. The alley belts will cover less than 50% of the ground area; crop production loss could also be as high as 50%, but is likely to be much less. Stirzaker *et al.*, (2001a and b) propose a complementarity index *CI*, the ratio of *ENOR* to an equivalent no yield zone, as a means for quantifying this compromise. The

authors also show that when $CI > 1$ there is a crop yield incentive for choosing an alley farm configuration rather than a single block. When $CI = 1$ there is no yield advantage from an alley configuration. *CI* is unlikely to ever be less than 1.

Application to young and non-eucalypt systems

The *ENOR* model is a static representation of mature systems and does not address the hydrological implications of dynamic agroforestry systems involving young trees. In such instances, leaf efficiencies are likely to be different from those of mature trees, and the trees are likely to be 'mining' soil water stores. Given the long-term nature of the hydrological issues involved, the transient phase of young agroforestry systems could be seen to be of secondary concern compared to steady state conditions, although this deserves further consideration.

Knight *et al.* (2001) reported rapid growth of 6 m wide belts old man of salt bush *Atriplex nummlaria* and *Acacia saligna* (Site 4; Figure 54) in the three years following planting on a deep sandy loam. *LLA* was 42 m^2 m^{-1} and the local *LAI* was 0.66, giving an *ENOR* of 64 m (Equation 12). This required the untested assumption that both the young shrub belts and the local remnant eucalypt had similar leaf efficiency. Surface lateral roots were observed about 20 m either side of the belt but soil water extraction was measured no further than 4 m either side of the belt edge. This gives a 'water extraction zone' of about 14 m, less than one quarter of the predicted *ENOR*. The overestimation of *ENOR* is what would be expected in a situation where the plants had access to a water source other than rainfall. In this case, Knight *et al.* (2001) found the belts had access to stored soil water.

The site was previously used for conventional cropping for about 100 years and recharge was estimated using the chloride profile technique to be in the order of 20 mm yr^{-1}. Roots were found in soil samples from up to 13 m deep and neutron moisture meter measurements showed that water had been extracted to a depth of 8 m. Approximately 500 mm of water had been extracted directly below the belts, below 2 m in the profile. This can be considered to be water that would otherwise eventually have added to the water table (60 m below the surface), because conventional crops would never have accessed it. It would be expected that once the shrubs had reached steady state and ceased to expand their root zone, they would reduce their leaf area such that the predicted *ENOR* more closely matched the root zone. It is also likely that at this stage the shrubs would be more actively competing for rainfall with adjacent crops. The significance of the 500 mm of 'saved' recharge depends on the spacing of the shrub belts. This represents 14 years of equivalent average recharge prevented from reaching the water table, over a 3-year period.

If belts spacings were 50 m or 100 m this would only be the case for 28% to 14% of the landscape. If, however, the whole of the landscape were planted to perennial shrubs on, say, a 3-year rotation with crops it seems possible that recharge could be eliminated from the landscape. This is assuming the shrub roots could 'catch up to' and use all the recharge that occurs during the cropping phase. The implications of this transient phase need to be considered in future groundwater modelling exercises (see Chapter 2).

In this study I have considered only eucalypt species because of the availability of mature stands that are old enough to have developed stable chloride profiles, and because of the generalities that can be made regarding leaf efficiencies (Hatton *et al.*, 1998). Also, for preliminary investigations with regard to the recharge reduction potential of agroforestry systems, it is likely that eucalypts will provide the upper limits in the long term because of their size, adaptability and longevity. The method should apply, however, to any species, as long as leaf area data from mature sites is available.

Cultural practices

Australian farmers sometimes limit the extension of lateral tree roots into crops by 'deep ripping' but it is not yet normal practice in low rainfall areas, possibly due to the cost of the operation. 'Ripped' trees do not grow as large as 'non-ripped' trees and produce less leaf. In the long term, the area hydrologically occupied by the trees would still be proportional to leaf area, and *ENOR* approach would still apply. The appraoch would predict that a greater area of 'ripped' belts (measured stem to stem) would be required to reduce recharge by the same amount as 'non-ripped' belts. It follows therefore, that if the belts were ripped close to the edge trees, the total area of 'ripped' belts would approximate the total *ENOR* of 'non-ripped' belts. It is also likely that the root zone of a 'ripped' belt, as defined by the rip lines, would closely approximate the *ENOR* of that belt. The merits of the 'ripped' and 'non-ripped' systems would then be compared on the bases of productivity and management but will not be discussed further here.

It is not known to what extent *ENOR* approach can be applied to coppicing practices, which involves the periodic removal of all leaves for enterprises such as oil mallee harvesting. Commercial oil mallee producers at West Wyalong, NSW typically harvest the trees every 12 to 18 months (Site 10; Figure 60, Chapter 8). This introduces two new unknowns: the comparative efficiency of the regrowth leaves relative to local mature vegetation; a representative long term average leaf area. *ENOR* was applied to Site 10 which had an $LLA = 5\ m^2\ m^{-1}$; a local *LAI* estimated to be 0.8 which yields *B* equal to 7 m. This value is more than twice the belt spacing of 3 m. It is unlikely that this discrepancy is

due to errors. Although uncorroborated, this is an indication that the system was not in equilibrium, but was 'mining' soil water stored during a period of low leaf area.

Errors

A more detailed error analysis (Chapter 5 and 6; and Appendix 4) has shown that a maximum error of about 20% can be expected when estimating *B*, and hence *RR*, using field measurements of *LLA* and *LAI*.

Additional uncertainty is introduced if *LLA* and *LAI* are estimated, rather than measured. In reality, *LLA* will depend upon: tree species; growth stage; climate; site conditions; belt width; and cultural practice. *LLA* values measured from the survey sites are therefore only a guide. Until better data sets and predictive tree belt growth models are available, one could expect error in estimating *LLA* to be as high as 50% but it is impossible to quantify. Chapter 7 showed that a standard error (S.E.yx) of ±0.6 for *LAI* when it is estimated from the climate index (Equation 23, Figure 79), producing an absolute error of 60% to 30% along an annual average rainfall gradient from 400 to 1000 mm. The total error possible for *B* could therefore be about 100%. The prediction made in Example 1 (above) therefore would be $RA = 30 \pm 30$ mm yr^{-1}, although this would be an extreme situation.

If Equation 12 is applied using an actual measurement of *LLA,* but with *LAI* was estimated using Equation 23 or Figure 79, then it is possible that additional error could be introduced because of the effects of seasonal climate variation. This error is also difficult to quantify but it is likely that if the *LLA* was measured under drought conditions, and *LAI* was predicted, then *B* will be under predicted, and *vice versa*.

Conclusion

The *ENOR* model allows relative recharge *RR* predictions to be made rapidly, and without the need for below ground measurements. Input parameters can be easily estimated using the methods in this and the previous chapter. The likely prediction errors are known and are within acceptable limits. The *ENOR* meets both of the original aims of the study (see Chapter 1). The model is, however, a preliminary method for making such predictions and the following limitations apply:

1. *ENOR* approach was developed for water-limited conditions;
2. the model has been tested on eucalypt species only;
3. it has been developed and tested on mature systems only;

4. equation 23, for the prediction of *LAI,* was derived for use between latitudes 30° and 40° S and application of the relationship may be inaccurate for areas of the Basin outside this zone, such as south central Queensland.

It is likely that future alley farming systems will incorporate both immature trees and non-eucalypt species. If interest in alley farming continues to grow, the *ENOR* approach should be tested on a range of species and on transient systems. Preliminary results (Knight *et al.,* 2001) in this regard are encouraging.

Summary

This chapter gives procedures and worked examples of the application of *ENOR* to hypothetical alley farms in the Murray Darling Basin. Recharge is estimated from a given alley geometry; and an alley farm is designed to result in a prescribed recharge. A detailed discussion is given of the applications, the limits of the *ENOR* model, the implications of cultural practices and the errors involved in the application of the model.

Chapter 10

Conclusions

Introduction

In this thesis I have developed a simple and robust model for estimating recharge from alley farms in the southern Murray Basin. The motivation for doing so was the need to assess the likely long-term impact of alley farms on recharge, and their impact on dryland salinity. By reviewing the methods used for measuring and modelling of recharge from conventional farms and forests, together with reviews on agroforestry modelling and previous key studies, it became clear that a new approach was required for alley farms. This is due principally to the complex spatial and temporal distributions of plant/soil/water interactions within tree belts themselves. I therefore presented the *ENOR* concept for approximating the width B (m) of the zone hydrologically occupied by tree belts, and showed that this allowed the representation of alley farms using the simple *ENOR* model.

This thesis concludes with a reiteration of the original aims and a summary of the thesis findings, by examining in turn: the *ENOR* approach and model; the testing of the approach; and the application of the model. The thesis hypotheses are then reviewed in light of the findings, and some potential future research directions are outlined.

Reiteration of the original aims

To develop a model for:

1. Predicting groundwater recharge from alley farming systems in the Murray Basin;
2. Designing alley farms that will result in a prescribed recharge reduction.

Thesis findings

The *ENOR* conceptual model

Recharge is a difficult quantity to both measure and model, even in relatively spatially homogeneous systems such as 'pure' forest plots or 'pure' agricultural crops. The spatial heterogeneity of alley farming systems adds further complexity and prompted the development of the 'Equivalent No Recharge' *ENOR* concept (Figure 21). The width B (m) of the *ENOR* approximation, for a tree belt, is an abstract width within which recharge is zero, and is a powerful tool for summarising the overall effect of complex spatial distributions. The *ENOR* approximation negates the need to consider:

1. The manner in which water extraction patterns (and hence recharge patterns) vary within the tree belt root zone in both the vertical and horizontal directions;
2. The actual point value, or average value, of recharge below a tree belt.

The *ENOR* concept also simplifies the representation of recharge from an alley farm to a binary system comprising alternate units of: tree belts, characterised by width B of no recharge; and crop/pasture, characterised by the recharge RC from that conventional system. This binary model, named the *ENOR* model, allows a simple calculation of relative recharge, and absolute recharge, from the alley farm (Equation 14; Equation 15) for a given tree belt spacing W.

Scaling *B* to leaf area

The approach for scaling B to the tree belt leaf area was derived by extending the principles of eco-hydrological optimality theory (Eagleson, 1982) of natural plant communities, to tree belts. The resulting approach (Equation 12) predicted that B for a tree belt was equal to the ratio of leaf area of the tree belt (normalised to belt length) LLA (m^2 m^{-1}) to the LAI (m^2 m^{-2}) of the local natural vegetation. This requires the assumptions: that recharge from the natural vegetation was very small in comparison to recharge from conventional farming systems; the tree belt overwhelmingly dominates the zone it occupies; and that runoff is small.

The approach for estimating B has the significant attribute that it requires no measurements from below ground.

Testing the *ENOR* approach

The above approach was tested in two separate experiments:

1. In Chapter 5, long-term average recharge measurements using chloride profiles (Walker *et al.*, 1991) were used calculate B for mature tree belts and compared with B predicted from leaf area measurements (Equation 12). Predictions were shown to be sufficiently accurate for practical applications (Figure 31), except for two sites where B was under-predicted, possibly due to runoff from the site.
2. In Chapter 6, an expression for B in terms of the water balance (Equation 17) was derived. All components of the water balance were measured over a 343-day period and used to calculate B (19.8 m), which compared well with B predicted from leaf area measurements (21.3 m).

Chapters 5 and 6 conclude that the *ENOR* approach is a simple and robust method of estimating B. A rigorous error analysis (Appendix 4) undertaken in both experiments showed conservative use of the approach should include an error of about 20%. This error could possibly have been reduced if EM techniques (Cook and Williams, 1998) had been used as an adjunct to the chloride profiles, allowing greater horizontal resolution in the recharge transects. It is also noted that the possible implications of seasonal climatic variations (e.g. drought) need to be considered if *LLA* and *LAI* measurements are significantly separated either in time or space. If measurements are made within a few days and a few kilometers of each other, this is not a concern.

Applying the *ENOR* model and estimating input parameters

The National Action Plan for Salinity and Water Quality (Agriculture, Forests and Fisheries Australia, 2000) is undertaking to establish target outputs for selected catchments in Australia, and to develop catchment management plans to meet those targets. Alley farming is one of the land management options for reducing recharge from agricultural lands, however alley farms are relatively rare and their hydrologic effects at the catchment scale are unknown. As an input to groundwater flow models and catchment management plans therefore, the *ENOR* model is likely to be used to estimate the recharge from hypothetical alley farms or to design alley farms such that that average recharge is a specified value. The methods developed in Chapters 7 and 8 allow the estimation of both *LAI* and *LLA* respectively from gross climate parameters and from photographs of typical farm tree belts. Following the application of these methods and the model, using worked

examples, Chapter 9 concludes that the *ENOR* model can be applied in this way to make recharge estimates (with measurable errors), and to design alley farms when used within the following limits:

1. water-limited plant growth conditions;
2. eucalypt species only;
3. mature systems only.

However, Chapter 9 discusses results from the MDBC LRAF trials that suggest the application of the *ENOR* model to non-eucalypt belts, and to young tree belts, should still provide useful indications regarding their role in the overall water balance of a catchment.

Estimates of absolute, rather than relative, recharge from an alley system require an estimate of recharge from the accompanying cropping system *RC* (Equation 15). *RC* can vary significantly at the paddock scale (Cook *et al.*, 1989) and users of the ENOR approach should endeavour to use an *RC* that is representative of the area under consideration.

Assumptions

Small recharge under natural vegetation

The assumption that recharge from natural vegetation in southern Australia is small, in comparison to recharge from agricultural systems, is valid in the large majority of cases (Allison *et al.*, 1990; Cook *et al.*, 1992; Kennett-Smith *et al.*, 1992a; Kennett-Smith *et al.*, 1992b; Walker *et al.*, 1992). Where this assumption does not hold (e.g. Carbon *et al.*, 1982), an *ENOR* can still be calculated if the recharge from the natural vegetation is known, or alternatively, the Equivalent Recharge Zone *ERZ* concept could be used to replace *ENOR*.

Trees hydrologically dominate the area they occupy

In light of the complications of describing the interactions between trees and crops in alley farming systems, the point is made in Chapter 4 that, over long time scales (years) in southern Australia, tree belts overwhelmingly dominate the zone that they hydrologically occupy. This greatly simplified the approach to the problem and allowed the assumption that the long-term average effects of annual crops and pastures (within that zone) was small. The results of the experiments confirm that this was a valid approach but also highlight the instances where the assumption did not hold (e.g. the tree belt at Kimba, Chapter 5). Caution should be observed, therefore, if the same approach is used in wetter climates where crop production in the tree root zone can be significant.

Runoff was small

Assuming runoff to be small is a valid approach for much of the southern Murray Basin, particularly the Mallee region where hillslopes are not a common feature. The experiments described in Chapters 5 and 6 however, emphasise the significance of this assumption when making investigations at the plot scale. Despite the care with which sites were selected, the effects of runoff were observed in the 'recharge transect' experiment (Kimba and Parilla remnant mallee block sites, Chapter 5); and both runoff and run-on were observed at the 'water balance' site (Chapter 6). In addition, it appears that both runoff and run-on influenced *LLA* and the resulting prediction of *B* from Equation 12. It would appear that where runoff occurred, the *LLA* reflected a drier climate than the local conditions, and *vice versa* in the case of run-on. While this is intuitively reasonable, it stresses the need for also addressing the surface hydrology where alley farms are to be considered for hillslopes (see 'Future Research', this chapter).

Review of hypotheses

Two hypotheses were proposed in Chapters 5 and 6 and are reviewed below in light of the findings of the thesis. The hypothesis central to the approach for predicting *B* from leaf area was presented in Chapter 4:

1. *The hydrologic effect of an isolated tree element in the landscape is equivalent to the hydrologic effect of a certain area of uniform vegetation within a block. The size of that area can be scaled to the LAI, or the leaf area L, of the isolated tree element, relative to the LAI of the uniform block.*

The hydrologic effect of something, measured at the landscape scale, can be thought of as its combined contribution to ΔS, run off and recharge. For this study where ΔS and runoff are small, this reduces to its contribution to recharge. In tackling this problem I have used the *ENOR* (an *absence* of recharge) to define this contribution. The results of the 'recharge transect' experiment (Chapters 5) and the 'water balance' experiment (Chapter 6) provide strong evidence to support this hypothesis. However this must be viewed in light of the derivation of the water balance definition of *ENOR* (Chapter 6). For the above hypothesis to hold, Equation 18 must also be true; the ratio $\frac{T+I}{P-E}$ must be the same for both the local natural vegetation and the isolated tree belt, when considering equal leaf areas in both cases. Equation 18 was not tested explicitly but was investigated piecemeal: P would be equal in both cases; in Chapter 6 E was estimated to be similar in both isolated and no-isolated cases; I was not measured for the non-isolated case but is considered to be driven

by atmospheric demand in a similar fashion to *T*. Although not intended as a rigorous test of Equation 18, a second hypothesis (relating to *T*) was proposed and tested as an adjunct to the first:

2. *Long-term average leaf efficiency (transpiration per unit leaf area) of an isolated tree is equal to that from a non-isolated tree growing in a community.*

The results of the 'leaf efficiency' experiment described in Chapter 6, although indicating definite differences in leaf efficiency between treatments in the short term, do not allow a rejection of the hypothesis. It is concluded in Chapter 6 that, this is further evidence that first hypothesis is a valid approximation of reality.

Future research

Testing of the *ENOR* model at catchment scale

In this study I have developed a model that is applicable at any scale, but I have only tested it at the plot scale. Ultimately we want to know the hydrologic effects of alley farming at the catchment scale, and at the scale of the groundwater systems that are contributing to dryland salinity. If such a study were undertaken, two significant time delays must be considered: the time required for the tree belts to reach maturity (years to decades); the time required for the groundwater system to respond and/or equilibrate (decades). It is conceivable that a site suitable for such a study may arise in coming decades during the course of the implementation of catchment management plans. The costs of establishing tree belts over such a large area would have to be justified by the perceived long-term intrinsic value of the trees and/or the resource protection (via salinity control) they would afford. Large areas of oil mallee belts have been planted in Western Australia with both such outcomes in mind, and it is possible that an area suitable for testing the *ENOR* model at a larger scale could be identified. It would be essential however, that groundwater data was available from a period before the implementation of the tree belts.

Predicting the growth of tree belts

Chapter 8 provides, in the absence of a tree belt growth model, a scheme for estimating realistic ranges for the magnitude of *LLA*. The number, type, maturity and geographical distribution of the 'typical' farm tree belts that are available for description and measurement, limit the widespread application of this scheme. For a more detailed appraisal of both the productivity and the hydrologic effect of alley farms, better approximations of the likely growth rates and leaf areas of tree belts are required, for a wide range of species, and for a wide range of soil types and climates. Forest growth

models are available (Battaglia and Sands, 1997; Landsberg and Waring, 1997), as are some models for describing isolated trees (Landsberg and McMurtrie, 1984) and models that describe agroforestry systems (Van Noordwjik and Lusiana, 1999; Lawson *et al.*, 1995). With regard to the growth of tree belts specifically, the practical application of these models to large areas is limited by their requirement for relatively large numbers of site-specific and species-specific input parameters. I therefore believe a new and more focussed approach is required.

The broad question to be answered here is "How big will tree belts grow?"; a more focussed question is "By how much will tree belt growth be enhanced, relative to the growth in the centre of a plantation?". In asking this question we are also asking how trees respond to a change in growing space; our current knowledge requires us to assign a growing space (root zone dimensions) to a tree belt before we can model its growth. The problem is, in most cases, we can only guess at the growing space, or work backwards from top growth as the *ENOR* approach does. This is a significant limitation to describing any land use system that incorporates spaced trees, and will remain so until such time that there is a comprehensive data base on tree root distributions, or efficient methods for predicting them.

Understanding the implications of runoff/run-on for tree belts on hill slopes

This study has not considered the implications for alley farms planted on hill slopes, however there is a pressing need to do so, given the possible effects of revegetation of water supply catchments (Vertessy and Bessard, 1999).

Critical to the drought tolerance of Australian natural vegetation systems is their ability to 'internally' redistribute surface water (Nulsen *et al.*, 1986). In low rainfall areas, some natural vegetation systems such as mulga (*Acacia aneura*) have evolved to comprise regular, linear zones or 'bands' (Greene *et al.*, 2001), each of which performs a unique role in either shedding runoff to the lower zone, or storing the run-on for use by either annual or perennial vegetation. In this regard, there is a need for methods to optimise alley farm designs for sloping land in Australia, and in other countries (Droppelmann *et al.*, 2000a and b).

Concluding remarks

Over the next ten years, targets for levels of land and stream salinity will be set and monitored in 20 to 50 major catchments in the around Australia (Agriculture, Forests and Fisheries, 2000); six of these catchments are in the southern Murray Basin. Target setting

will be a first stage of the development of catchment management plans for the large-scale management of dryland salinity. In each case, the catchment management plan will need to reflect a compromise between primary production and protection of resources and infrastructure both within, and downstream of, the catchment.

Groundwater flow models will be used to test the effects of a suite of land management options aimed at reducing recharge from agricultural land, or for prescribing target recharge values that will result in a 'design' groundwater discharge. Alley farming is one land management option for reducing recharge, and this thesis describes the development of the *ENOR* model that can be used to: estimate recharge from alley farms; and to design them to result in a prescribed recharge. In this way *ENOR* satisfies both of the original aims of this study. Further, the *ENOR* model requires a maximum of six input parameters, none from below ground; it is simple and effective, and will be a useful tool in the development of catchment plans for the management of dryland salinity.

Bibliography

Agriculture, Forests and Fisheries (2000) National Action Plan for salinity and Water Quality, http://www.affa.gov.au/docs/nrm/actionplan/action-plan-intro.html.

Agriculture Western Australia (2001) Alley farming network, Greening Australia, http://www.agric.wa.gov.au/agency/Pubns/farmnote/1996/f06396.htm#alley

Albertsen, T., Eckersley, P., Blennerhassett S., Moore R. and R. Hingston (2000) Bluegum Timberbelt design for alley farming. Rural Industries research and Development Corporation publication No 99.

Allison, G. B., and M. W. Hughes (1972) Comparison of recharge to groundwater under pasture and forest using environmental tritium. *Journal of Hydrology*, 17:81-95.

Allison, G. B., and M. W. Hughes (1978) The use of environmental chloride and tritium to estimate total recharge to an unconfined aquifer. *Australian Journal of Soil Research*, 16:181-195.

Allison, G. B., and M. W. Hughes (1983) The use of natural tracers as indicators of soil-water movement in a temperate semi-arid region. *Journal of Hydrology,* 60:157-173.

Allison, G. B., Cook, P. G., Barnett, S. R., Walker, G. R., Jolly, I. D., and M. W. Hughes (1990) Land clearance and river salinisation in the western Murray Basin. *Journal of Hydrology,* 119:1-20.

Anderson, L.S., Muetzelfeldt, R.I. and F.L. Sinclair (1993) An integrated research strategy for modelling and experimentation in agroforestry, *Commonwealth Forestry Review* 72(3):166-174.

Anderson, L.S., and F.L. Sinclair (1993) Ecological interactions in Agroforestry systems, *Agroforestry Abstracts,* 6:57-91.

Andrew, A. H.; Noble, I. R., and R. T. Lange (1979) A non-destructive method for estimating the weight of forage shrubs, *Australian Rangelands Journal*, 1:777-782.

Arah, J. and M. Hodnett, (1997) Approximating soil hydrology in agroforestry models, *Agroforestry Forum,* 8(1):17-20.

Armstrong, D. and K. Narayan, (1998) Using groundwater responses to infer recharge, *In* (Eds L Zhang and Glen Walker) *Studies in catchment hydrology – the basics of recharge and discharge*, CSIRO Publishing, Collingwood, 1998.

Australian Bureau of Meteorology (2000) Australian Climate Averages (Web Page). URL http://www.bom.gov.au/climate/averages/.

Barnes, C.J., Jacobsen, G. and G.D. Smith (1994) The distributed recharge mechanism in the Australian arid zone, *Soil Science Society of America Journal*, 58:31-40.

Barnett, S.R., (1989) The effect of land clearance in the Mallee region on River Murray salinity and land salinisation, *Journal of Australian Geology and Geophysics*, 11:205-208.

Barnett S.R. (1990) Murray Basin hydrogeological investigation – Mallee region groundwater modelling exercise. South Australia Department of Mines and Energy, Report Book 90/36.

Barnett, S.R, Henschke, C, Hatton, T.J. and P. Cole (1996) Dryland Salinity in South Australia. Primary Industries of South Australia.

Barnett, S.R., Yan, W., Watkins, N.R., Woods, J.A. and K.M. Hyde (2000) Murray-Darling Basin Salinity Audit – groundwater modelling to predict future salt loads to the River Murray in SA, Department for Water Resources in South Australia, Primary Industries and Resources South Australia, 98/2420.

Barrett, D. (1992) Ecophysiological bases for the distribution of rainforest and Eucalypt forest in Southeastern Australia. Ph.D. thesis, Australian National University, Canberra. 177 pp.

Battaglia, M. and P.J. Sands (1997) Modelling site productivity of Eucalyptus globulus in response to climatic and site factors, *Australian Journal of Tree Physiology*, 24:831-850.

Battaglia, M., Cherry, M.L., Beadle, C.L., Sands, P.J. and A. Hingston (1998) Prediction of leaf area index in eucalypt plantations : effects of water stress and temperature, *Tree Physiology*, 18:521-528.

Bazilevich, N. I., Rodin, L. Ye., and Roznov, N. N. (1970) Geographical aspects of biological productivity. *In Proceedings of the Fifth Congress of the Geographical Society USSR,* Leningrad, 1970.

Beech, A. (1996) CSIRO Method Sheet CS9602-05.2-1, CSIRO Adelaide, 1996.

Bell, J. P. (1976) Neutron Probe Practice. Natural Environment Research Council, Institute of Hydrology, Wallingford, UK; *Rep.* 19, Second Edition, 82 pp.

Berringer, J. (1994) Preliminary evaluation of leaf area index using the LICOR LAI-2000 plant canopy analyser in a *Eucalyptus regnans* forest, Unpublished data.

Bicknell, D. (1991) The role of trees in sustainable agriculture, *In Proceedings from a National Conference on the Role of Trees in Agriculture*, Albury, Victoria, Australia, October 1991.

Boast C.W. and A. Klute (1986) Evaporation from bare soil measured with high spatial resolution, in *Methods of soil analysis, Part 1. Physical and mineralogical methods*, edited by A. Klute, Madison, pp. 889-900, American Society of Agronomy, Inc., Wisconsin, USA, 1986.

Bohm W.(Ed.) (1979) Methods of studying plant roots, Springer-Verlag, London, 394 pp.

Bond, W, (1998) Soil physical methods for estimating recharge, *In* (Eds L Zhang and Glen Walker) Studies in catchment hydrology – the basics of recharge and discharge, CSIRO Publishing, Collingwood, 1998.

Booth, TH (2000) The biophysical environment of the Murray darling Basin and potential for tree growth. *In* Restoring Tree Cover in the Murray-Darling Basin, (Eds.) S. Nambiar, R. Cromer, A. Brown, CSIRO Forestry and Forest Products, Canberra, pp 3-8.

Brown, C.M., (1989) Structural and stratigraphic framework of groundwater occurrence and surface drainage in the Murray Basin, south eastern Australia, Bureau of Mineral Resources Journal, 11:2/3, 127-146.

Brown, C.M and A.E. Stephenson (1991) Geology of the Murray Basin, southeastern Australia, Bureau of Mineral Resources Bulletin, 235, Australian Government Publishing Service, Canberra, 430 pp.

Budyko, M. I., and Efimova, N. A. (1968) The utilization of solar energy by natural vegetation cover in the USSR. *Bot. Zh.* 23(10).

Budyko, M. I. (1974) Climate and Life. New York. Academic Press. 508 pp.

Burke, S. (1991) The effects of shelter belts on crops at Rutherglen, *In Proceedings from a National Conference on the Role of Trees in Agriculture*, Albury, Victoria, Australia, October 1991.

Campbell, G.S. (1974) A method for simply determining soil hydraulic properties from moisture retention data, *Soil Science*, 117:311-314.

Campbell, G. S., and S. Shiozawa (1992) Prediction of hydraulic properties of soils using particle-size distribution and bulk density data,, *In Proceedings of the Conference on Indirect methods for estimating the hydraulic properties of unsaturated soils*, Riverside, California, October 11 1989-October 13 1989.

Carbon, B.A., Bartle, G.A and A.M. Murray (1979a) A method for visual estimation of leaf area, *Forest Science,* 25:53-58.

Carbon, B.A., Bartle, G.A and A.M. Murray (1979b) Leaf area index of some eucalypt forests in south-west Australian, *Australian Forest Research,* 9(4):232-326.

Carbon, B. A., Roberts, F. J., Farrington, P., and J. D. Beresford (1982) Deep drainage and water use of forests and pastures grown on deep sands in a Mediterranean environment. *Journal of Hydrology, Netherlands*, 55, 53-64.

Cassell, D.K. and A. Klute (1986) Water Potential: tensiometry, *In* Klute, A. (Ed.) *Methods of Soil Analysis, Part 1. Physical and mineralogical Methods,* Agronomy Mongraph No. 9 (2nd edition), American Society of Agronomy – Soil Science Society of America, Madison, USA, pp. 563-596.

Choudhury, B.J. and J.L. Monteith (1988) A four-layer model for the heat budget of homogeneous land and surfaces, Q.J.R. *Meteorol. Soc*, 114:373-398.

Cleugh, H.A., Miller, J.M., Bohm, M. and R.T. Prinsley (Ed.) (1998) Direct mechanical effects of wind on crops, *Agroforestry Systems*, Special Issue. Windbreaks in support of agricultural production: review of papers from the Australian Windbreaks Program, 41:85-112.

Cleugh, H.A. and R.T. Prinsley (Ed.) (1998) Effects of windbreaks on airflow, microclimates and crop yields, *Agroforestry Systems*, Special Issue. Windbreaks in support of agricultural production: review of papers from the Australian Windbreaks Program, 41:55-84.

Closs, R.L. (1958) The heat pulse method for measuring rate of sap flow in a plant stem, *N.Z. J. Science,* 1:281-288.

Cook, P.G. (1989) Estimating regional groundwater recharge in the western Murray Basin for inclusion in a groundwater model, Centre for Groundwater Studies, CSIRO Division of Water Resources, Report No. 11.

Cook, P.G., Walker, G.R. and I.D. Jolly, (1989) Spatial variability of groundwater recharge in a semiarid region, *Journal of Hydrology,* 111:195-212.

Cook, P.J. (1990) The effect of soil type on groundwater recharge in the Mallee region, Report No. 28 Centre for Groundwater Studies, CSIRO Division of Water Resources, South Australia.

Cook, P.G., Walker, G.R., Jolly, I.D., Allison, G.B. and F.W. Leaney (1990) Localised recharge in the vicinity of the Woolpunda groundwater mound, CSIRO Centre for groundwater Studies Report No. 30, Adelaide.

Cook, P. G., Jolly, I. D., Hughes, M. W., Beech, T. A., and CT. Fiebiger (1992) CSIRO Technical memorandum 92/8, CSIRO Division of Water Resources.

Cook, P.G, Telfer, A.L. and G.R. Walker (1993) Potential for salinisation of groundwater beneath mallee areas in the Murray Basin, Centre for Groundwater Studies Report No. 42, Engineering and Water Supply report No. 93/6, 15 pp.

Cook, P.G. and B.G. Williams (1998) Electromagnetic Induction Techniques, *In* (Eds L Zhang and Glen Walker) *Studies in catchment hydrology – the basics of recharge and discharge*, CSIRO Publishing, Collingwood, 1998.

Cook, P.J. and A.L. Herczeg (1998) Groundwater chemical methods for recharge studies, *In* (Eds L Zhang and Glen Walker) Studies in catchment hydrology – the basics of recharge and discharge, CSIRO Publishing, Collingwood, 1998.

Cooper, P. J. M., J. D. H. Keatinge, and G. Hughes (1983) Crop evapotranspiration - a technique for calculation of its components by field measurements, *Field Crops Research*, 7:299-312.

Coram, J.E. (1998) National classification of catchments for land and river salinity control, LWRRDC Final Report AGS-1A, Land and Water Resources Research and Development Corporation, Canberra, Australia.

Coram, J.E., Dyson, P.R., Houlder, P.A., and W.R. Evans (2000) Australian groundwater flow systems contributing to dryland salinity, Report by Bureau of Rural resource Sciences for the Dryland Salinity Theme of the national Land and Water resources Audit, Canberra, Australia.

Crab, P. (1997) Murray-Darling Basin Resources, Murray-Darling Basin Commission.

Cooperative research Centre for Plant-Based Management of Dryland Salinity (2001), www.isr.gov.au/crc/

Crockford, R. H. and D. P. Richardson (1990) Partitioning of rainfall in a eucalypt forest and pine plantation in southeastern Australia: II stemflow and factors affecting stemflow in a dry sclerophyll eucalyptus forest and a pinus radiata plantation, *Hydrological Processes*, 4:145-155.

Dawes W.R., Zhang L., Hatton T.J., Reece P.H., Beale G.T.H. and I. Packer (1997) Application of a distributed parameter ecohydrological model (TOPOG-IRM) to a small cropping rotation catchment, *Journal of Hydrology,* 191:67-89

Dawes, W. D., Walker G. R., and M. Stauffacher (2001) Practical modelling for management in data-limited catchments, *Mathematical and Computer Modelling,* 33:625-633.

Divakara, B.N., Mohan Kumar, B., Balachandran, P.V. and N.V. Kamalam (2001) Bamboo hedgerow systems in Kerala, India: root distribution and competition with trees for phosphorus, *Agroforestry Systems,* 51:189-200.

Duncan, W.J., Thom, A.S. and A.D. Young (1970) Mechanics of fluids, Edward Arnold, Great Brittain, 725 pp.

Dunin, F.X., McIlroy, I.C., O'Loughlin, E.M., Hutchison, B.A., and Hicks, B.B. (1985) A lysimeter characterization of evaporation by eucalypt forest and its representativeness for the local environment- the forest-atmosphere interaction. *In Proceedings of the forest environmental measurements conference*, held at Oak Ridge, Tennessee, October 23-28, 1983. Dordrecht, Netherlands. D. Reidel Publishing Company.

Dunin, F.X., Williams, J., Verburg, K. and B.A Keating (1999) Can agricultural management emulate natural ecosystems in recharge control in south eastern Australia? *Agroforestry Systems*, 45:343-364.

Dunin, F. X., White D. A., Hatton T. J. and T. W. Ellis (2001) Evapotranspiration characteristics of woody communities, natural and exotic, across southern Australia, *In Proceedings of the MODSIM Conference*, Canberra, August 2001.

Eagleson, P. S. (1982) Ecological optimality in water-limited natural soil-vegetation systems.1 Theory and hypothesis, *Water Resources Research,* 18, 352-340.

Eagleson P.S., and Tellers T.E. (1982). Ecological optimality in water-limited natural soil-vegetation systems. 2. Tests and applications. *Water Resources Research,* 18:341-354.

Eagleson, P. S., and R. I. Segarra (1985) Water-limited equilibrium of savanna vegetation systems. *Water Resources Research*, 21:1483-1493.

Edwards, W. R. N. and N. W. M. Warwick (1984) Transpiration from a kiwifruit vine as estimated by the heat pulse technique and the Penman-Monteith equation, *New Zealand Journal of Agricultural Research*, 27, 537-543.

Ellis, T.W., T. J. Hatton and I.K. Nuberg, (1999) A simple method for estimating recharge from low rainfall agroforestry systems. *In* (Eds A. Musey, L. Santos Pereira and m. Fritsch) *Envirowater99, 2nd Inter-Regional Conference on Environment-Water, 1-4 September, Laussane*, Switzerland. Presses Polytechnique et Universitaires Romandses, Laussane, 1999.

Ellis, T.W., T. J. Hatton and I.K. Nuberg (in press) An ecological optimality approach for predicting deep drainage from alley farming systems in water-limited environments, submitted to *Water Resources Research*, 2002.

Ellis, T. W., and Hatton, T.J (in press) Relating *LAI* of natural vegetation to climate indices in southern Australia, *Australian Journal of Botany,* submitted March 2002.

Ellis, T.W. and Y. Bessard, (2001) Estimating recharge form alley farms: applying the *ENOR* model within the Murray-Darling Basin –Full Report, CSIRO Land and Water Technical Report 3/01.

Evans, W.R. (1988) Preliminary Shallow groundwater Map of the Murray Basin, (1:1 000 000 scale map), Bureau of Mineral resources, Canberra.

Evans, W.R and J.R. Kellett (1989) The hydrogeology of the Murray Basin, southeastern Australia, *Bureau of Mineral resources Journal of Australian Geology and Geophysics,* 11:147-166.

Evett S.R., Warrick A.W. and A.D. Matthias, Wall material and capping effects on microlysimeter temperatures and evaporation, Soil Science Society of America Journal. 59(2): 329-336, 1995.

Francis, P., 1992, Alley farming challenge for sustainable cropping, *Australian Farm Journal*, 64-69.

George, R.J, Nulsen, R.A., Fedosian, R and G.P Raper (1999) Interactions between trees and groundwater in recharge and discharge areas – a survey of Western Australian sites, *Agricultural Water Management*, 31:91-113.

Gholz, H.L. (1982) Environmental limits on above ground primary production, leaf area, and biomass in vegetation zones of the Pacific northwest, *Ecology,* 469-481.

Gibbons, F.R. and R.G. Downes (1964) A study of the land in south-western Victoria, Soil Conservation Authority, Victoria, 289 pp.

Good, M. (1994) A revegetation strategy for the Murray Mallee district, Primary Industries, South Australia, State Print, South Australia, 247 pp.

Greacen, E. L. (1981) Soil Water assessment by the neutron method, Rep. CSIRO Division of Soils Adelaide, 140 pp, CSIRO, East Melbourne, Victoria, Australia.

Greene, R.S.B., C. Valentin, Esteeves, M. (2001) Runoff and erosion processes, *In Banded vegetation patterning in arid and semi-arid environments, ecological processes and consequences for management*, Springer-Verlag, in press.

Gregory, P.J. (1996) Approaches to modelling the uptake of water and nutrients in agroforestry systems, *Agroforestry Systems,* 34:51-65.

Grier, C. C., and S. W. Running (1977) Leaf area of mature northwestern coniferous forests: relation to site water balance. *Ecology,* 58, 893-899.

Gunn, R.H. and D.P. Richardson (1979) The nature and possible origins of soluble salts in deeply weathered landscapes of eastern Australia, *Australian Journal of Soil Research,* 17:197-215.

Hall D.J.M., Sudmeyer R.A., McLernon C.K., and R.J. Short. (2000) Characterisation of a windbreak system on the south coast of Western Australia III - Water balance and hydrology. *Agroforestry Systems* (submitted).

Hatton T.J., Catchpole E.A., and R.A. Vertessy (1990) Integration of sapflow velocity to estimate plant water use, *Tree Physiology*, 6:201-209.

Hatton T.J. and R.A. Vertessy (1990) Transpiration of plantation Pinus radiata estimated by the heat pulse method and the Bowen ratio, *Hydrological Processes*, 4:289-298.

Hatton, T.J. and W.R. Dawes (1993) TOPOGIRM 2. example simulations, CSIRO Division of Water Resources, Technical Memorandum 93/6, February 1993.

Hatton, T.J., Dawes, W.R. and J. Walker (1994) Predicting the impact of land use change on salinity – the role of spatial models, *In Proceedings of resource Technology '94*, Melbourne, Australia, September 26-30, 1994.

Hatton, T. J. Moore, S. J., and P. H. Reece (1995) Estimating stand transpiration in a *Eucalyptus populnea* woodland with heat pulse method: measurement errors and sampling strategies, *Tree Physiology,* 15:219-227.

Hatton, T. J., Taylor, P. J., Reece, P., and K. L. McKewan (1997) 'Is water use efficiency constant among eucalypts in water limiting environments?' *Tree Physiology*, 18, 529-536.

Hatton, T.J. (1998) Catchment scale modelling, *In* (Eds L. Zhang and G. Walker) *Studies in catchment hydrology – the basics of recharge and discharge*, CSIRO Publishing, Collingwood, 1998.

Hatton, T.J. and R. Salama (1998) Is it feasible to restore the salinity-affected rivers of western Australia?, *In Proceedings of the Second Stream Management Conference, 8-11 February, Adelaide, South Australia,* Cooperative Research Centre for Catchment Hydrology, Canberra.

Herczeg, A.L., Dogramaci, S.S. and F.W.J. Leaney (2001) Origin of dissolved salts in a large, semi-arid groundwater system: Murray Basin, Australia, *Marine and Freshwater Research, 52, 41-52.*

Hingston, F.J and Gailitus V. (1976) The geographic variation of salt precipitated over Western Australia, *Australian Journal of Soil Research*, 14:319-335.

Horn, H.S. (1971) The Adaptive Geometry of Trees, Princeton University Press, Princeton, NJ., 502 pp.

Hume, I., Mitchell, D. C., Milthorpe, P. L., Tea, M., O'Connell, M., and L. Zhang, (1998) Episodic recharge under crops and shrubs in the mallee zone - Final Report, Report No. NRMS - M4025.

Hutchinson, M.F., H.A. Nix, D.J. Houlder and J.P. Mcmahon (1998). ANUCLIM Version 1.6 User Guide. Centre for Resource and Environmental Studies, Australian National University, Canberra, 53 pp.

Hutchinson, P.A. and W.J. Bond (2001) Routine measurement of the soil water potential gradient near saturation using a pair of tube tensiometers, *Australian journal of Soil Research,* Volume 39, in press.

Hutton, J.T. and T.I. Leslie (1958) Accessions of non-nitrogenous ions dissolved in rainwater to soils In Victoria, *Australian Journal of Agricultural Research,* 9:492-507.

Hutton, J.T (1976) Chloride in rainwater in relation to distance from ocean, *Search*, 7:207-8.

ICRAF (2001) International Centre for Research in Agroforestry web site, WaNulCAS, a model for nutrient and light capture in agroforestry systems, www.icraf.cgiar.org/sea/AgroModels/WaNulCAS/index.htm.

Isbell, R. F. (1996) Australian soil classification, CSIRO Publishing, Collingwood, Australia, 143pp.

Johnson, C.D., (1987) Preferred pathway water flow and localised recharge in a variable regolith, *In* A.J. Peck and D.R. Williamson *(Eds.) Hydrology and salinity in the Collie River Basin*, Western Australia, J. Hydrology, 94: 129-142.

Jolly, I. D., Cook, P. G., Allison, G. B., and M. W. (1989) Hughes, Simultaneous water and solute movement through an unsaturated soil following an increase in recharge, *Journal of Hydrology (Amsterdam),* 111:391-396.

Jose, S., Gillespie, A.R., Seifert, J.R. and D.J. Biehle (2000) Defining competition vectors in a temperate alley cropping system in midwestern USA, *Agroforestry Systems,* 48:41-59.

Kang, B.T., Reynolds, L and A.N. Atta-Krah (1990) Alley Farming, *Advances in Agronomy*, 43: 315-359.

Kennett-Smith, A. K., Budd, G. R., and G. R. Walker (1992a) Groundwater recharge beneath woodlands cleared for grazing, south western New South Wales. Rep. 92/1, CSIRO Division of Water Resources, Adelaide.

Kennett-Smith, A. K., Cook, P. G., and R. Thorne (1992b) Comparison of recharge under native vegetation and dryland agriculture in the big desert region of Victoria, *Rep. 46*, Centre for Groundwater Studies, CSIRO Adelaide.

Knight J.H. (1999) Root distributions and water uptake patterns in eucalypts and other species. *In* Landsberg, J. (Ed) The Way Trees Use Water. Water and salinity Issues in Agroforestry No.5, RIRDC Publication No. 99/37, RIRDC, Canberra, pp 66-102

Knight, A., Blott, K., Portelli, M., and C. Hignett, (2001) The use of tree and shrub belts to control recharge in 3 dryland cropping systems, *Australian Journal of Agricultural Research*, submitted.

LWRRDC Land and Water Resources Research and Development Corporation (1999) Management Plan 1998 – 2003, Land and Water research and Development Corporation, 130 pp.

Landsberg J.J. and McMurtrie, R. (1984) Water use by isolated trees, *Agricultural Water Management,* 8:223-242.

Landsberg, J.J and R.H. Waring, (1997) A generalised model of forest productivity using simplified concepts of radiation-use efficiency, carbon balance and partitioning, *Forest Ecology and Management,* 95:209-228.

Landsberg, J. J. (1999) Tree water use and its implications in relation to agroforestry systems, Rural Industries Research and Development Corporation, Rep. 99/37.

Laut, P., Heyligers, P.C., Keig, G., Loffler, E., Margules, C., Scott, R.M. and M.E. Sullivan, Environments of South Australia – Province 4, Eyre and yorke Peninsulas, CSIRO, 1977.

Lawson, G.J., Crout, N.M.J., Levy, P.E., Mobbs, D.C., Wallace, J.S., Cannell, M.G.R. and R.G. Bradley (1995) The tree-crop interface: representation by coupling of forest and crop models, *Agroforestry Systems*, 30:199-221.

Lefroy, E. and P.Scott (1994) Alley Farming - new vision for Western Australian farmland, *Journal of Agriculture*, 35(4), 119-126.

Lefroy E.C., Stirzaker R.J., Hobbs R.J., O'Connor M.H. and J.S. Pate (1999) Agroforestry for water management in the cropping zone of southern Australia, *Agricultural Water Management,* Special issue: Agriculture as a mimic of natural ecosystems. Edited papers from a workshop held in Western Australia, 2-6 September 1997, 277-302.

Lefroy E.C., Pate J.S. and R.J. Stirzaker (2001a) Growth, water use efficiency, and adaptive features of the tree legume tagasaste (*Chamaecytisus proliferus* Link.) on deep sands in south-western Australia, *Australian Journal of Agricultural Research,* 52:221-234.

Lefroy E.C., Pate J.S. and R.J. Stirzaker (2001b) Influence of tagasaste (*Chamaecytisus proliferus* Link.) trees on the water balance of an alley cropping system on deep sand in south-western Australia, *Australian Journal of Agricultural Research*, 52:235-246.

Lewis, F. (1998) Modelling episodic recharge in the Western Australian wheat belt, Resource Management Technical Report 168, 120 pp, Agriculture Western Australia, Perth.

Macintyre, B.D., Riha, S.J., and C.K. Ong (1996) Light interception and evapotranspiration from hedgerow agroforestry systems, *Agricultural and Forest Meteorology*, 81:1/2, 31-40.

Marshall, D.C. 1958. Measurement of sap flow in conifers by heat transport. *Plant Physiology*, 6:385-396.

Marshall T.J., Holmes J.W. and C.W. Rose (1996) Soil Physics, 3rd Ed., Cambridge University Press, Cambridge, UK, 453 pp.

McJannet, D.L., (1999) Hydrologic analysis and growth performance of break of slope plantations, PhD Thesis, Monash University, Clayton, Victoria.

McMurtrie, R. and L. Wolf (1983) A model for competition between trees and grass for radiation, water, nutrients, *Annals of Botany,* 52:449-458.

McVicar, TR, Walker, J, Jupp, DLB, Reece, PH (1996) Relating *AVHRR* vegetation indices to *in situ* leaf area index measurements, CSIRO Division of Water Resources, Technical Memorandum 96.5.

MDBC (1999) The Murray Darling Basin Commission salinity and drainage strategy – ten years on, The Murray Darling Basin Commission.

MDBC (2000) Murray-Darling Basin Commission Strategic Investigation and Education Program, http://www.mdbc.gov.au/action_room/pdf/investigations_projects.pdf

Meyer, W. S. (1999) Standard reference evaporation calculation for inland Australia, CSIRO Land and Water Technical Report 35/98, CSIRO Publishing, Australia.

Monteith, J.L. and M.H. Unsworth (1990) Principles of Environmental Physics, 2nd Ed., Edward Arnold, London, 291 pp.

Muetzelfeldt, R.I., and F.L. Sinclair (1993) Ecological modelling of agroforestry systems, *Agroforestry Abstracts,* 6(4):208-247.

Norman, C.P. (1995) Effect of groundwater pump management on reclaiming salinised land in the Goulburn Valley, Victoria, *Australian Journal of Experimental Agriculture,* 35:215-222.

Northcote, K.H. (1979) A factual key for the recognition of Australian soils, CSIRO, Adelaide, South Australia, 122 pp.

Nuberg, I. K., and Evans, D. G., (1993) Alley cropping analog forests for soil conservation in the dry uplands of Sri Lanka, *Agroforestry Systems*, 24:247-269.

Nuberg, I.K. (1998) Effect of shelter on temperate crops - a review to define research for Australian conditions, *Agroforestry Systems*, 41:3-34.

Nulsen, R. A.; Bligh, K. J.; Baxter, I. N.; Solin, E. J., and D. H. Imrie (1986) The fate of rainfall in a mallee and heath vegetated catchment in southern Western Australia, *Australian Journal of Ecology,* 11, 361-371.

O'Connell, M. G., O'Leary, G. J., and M. Incerti (1995) Potential groundwater recharge from fallowing in north-west Victoria, Australia, *Agricultural Water Management*, 29, 37-52.

Oke, T. R. 1978. Boundary layer climates. Methuen, London, 372pp.

Ong C, and C.K., Ong (1994) Alley cropping - ecological pie in the sky?: Agroforestry Today, v. 6, p. p8-10.

Ong, C.K., Deans, J.D., Wilson, J., Mutua, J. Khan, A.A.H. and E.M. Lawson (1999) Exploring below ground complementarity in agroforestry using sap flow and fractal techniques, *Agroforestry Systems,* 44:87-103.

Peck, A.J. (1977) development and reclamation of secondary salinity. *In* (Eds J.S. Russell and E.L. Greacen), *Soil Factors and Crop Production in a Semi-Arid Environmant*, University of Queensland Press, Brisbane.

Petheram, C, Zhang, L.,Walker, G. and R. Grayson (2000) Towards a framework for predicting impacts of land-use on recharge: a review of recharge studies in Australia, *CSIRO Land and Water Technical Report 28/00, September 2000.*

Petheram, C, Zhang, L.,Walker, G. and R. Grayson (2001) Towards a framework for predicting impacts of land-use on recharge: a review of recharge studies in Australia, *Australian Journal of Soil Research*, submitted.

PMSEIC (1999) Dryland salinity and its impact on rural industries and the landscape, Prime Minister's Science, Engineering and innovation Council Occasional Paper No. 1, Department of Industry, Science and resources, Canberra.

Pook, E.W. (1984) Canopy dynamics of Eucalyptus maculata Hook. II. Canopy leaf area balance, *Australian Journal of Botany*, 32:405-413.

Pook, E.W. (1985) Canopy dynamics of Eucalyptus maculata Hook. III Effects of drought, *Australian Journal of Botany*, 33:65-79.

Prebble R.E. and G.B. Stirk (1980) Throughfall and stemflow on silverleaf ironbark (*Eucalyptus melanophloia)* trees, *Australian Journal of Ecology*, 5:419-427.

Richards, L.A. (1931) Capillary conduction of liquids through porous mediums, *Physics*, 1:318-333.

Ringersma, J. and A.F.S. Sikking (2001) determining transpiration coefficients of Sahelian vegetation barriers, *Agroforestry Systems,* 51:1-9.

Ringrose-Voase, A.J., Paydar, Z, Huth, N., Banks, R., Cresswell, H.P., Keating, B.A., Young, R., Bernardi, T., Holland, J. and I. Daniels (1999) Modelling deep drainage under different land use systems. 2 Catchment-wide application. *In Proceedings of MODSIM 99.*

Ringrose-Voase, A.J. and H.P. Cresswell (2000) Measurement and prediction of deep drainage under current and alternative farming practice. A final report prepared for the Land and Water Resources Research and Development Corporation, CSIRO Land and Water Consultancy Report.

RIRDC (1999) Commercial prospects for low rainfall agroforestry, Project No. AGT – 4A 99/152, Rural Industries Research and Development Corporation, http://www.rirdc.gov.au/reports/AFT/99_152.doc.

RIRDC (2000) Rural Industries Research and Development Corporation, Agroforestry and Farm Forestry Sub-program, http://www.rirdc.gov.au/programs/aft.html

Roderick, M.L., Farquar, G.D., Berry, S.L. and I.R. Noble (2001) On direct effect of clouds and atmospheric particles on the productivity and structure of vegetation, *Oecologia,* submitted 1 June 2001.

Rowan, J. N., and R. G. Downs (1963) A study of the land in north-western Victoria, Soil Conservation Authority, Victoria, 116 pp.

Schroth, G. (1999) A review of below ground interactions in agroforestry, focussing on mechanisms and management options, *Agroforestry Systems,* 43:5-34.

Sellers, P. J., Meesen, B. W., Hall, F. G., Asrar, G., Murphy, R. E., Schiffer, R. A., Bretherton, F. P., Dickinson, R. E., Ellingson, R. G., Field, C. B., Huemmrich, K. F., Justice, C. O., Melack, J. M., Roulet, N. T., Schimel, D. S., and Try, P. D. (1995) Remote sensing of the land surface for studies of global change: Models - algorithms - experiments. Remote Sensing Environment, 51:3-36.

Simunek, J., Sejna, M. and M. Th. Van Genuchten (1999) Hydrus 2D Program for simulating water flow and solute transport in two-dimensional, variably saturated media, www.ussl.ars.usda.gov/MODELS/HYDRUS2D.HTM.

Silberstein R.P., Sivapalan, M. and A. Wyllie (1999) On the validation of a coupled water and energy balance model at small catchment scales, *J. Hydrology*, Vol. 220,3-4:149-168.

Sillon, J.F., Ozier-Lafontaine, H. and N. Brisson (2000) Modelling daily root interactions for water in a temperate grass and alley cropping system, *Agroforestry Systems,* 49:131-152.

Slavich, P.G., Smith, K.S., Tyerman, S.D., Walker, G.R. and P. Thorburn (1999) Water use of grazed salt bush plantations with saline water, *Agricultural Water Management,* 39:2/3, 169-185.

Smettem, K.R.J. (1998) Deep drainage and nitrate losses under native vegetation and agricultural systems in the Mediterranean climate region of Australia, Occasional Paper RAPPS02/98,Land and Water resources research and Development Corporation, Canberra, 43pp.

Smettem K.R.J., and K.L. Bristow (1999) Obtaining soil hydraulic properties for water balance and leaching models from survey data. 2. Hydraulic conductivity, *Australian Journal of Agricultural Research,* 50:1259-1262.

Smettem K.R.J., Y.M. Oliver, L.K. Heng, K.L. Bristow and E.J. Ford (1999) Obtaining soil hydraulic properties for water balance and leaching models from survey data. 1. Water retention, *Australian Journal of Agricultural Research*, 50:283-289.

Smith, D. M., Jarvis, P. G., and J. C. W. Odongo (1997) Energy budgets of windbreak canopies in the Sahal. *Agricultural and Forest Meteorology*, 86(1-2):33-49.

Specht RL. (1972). Water use by perennial evergreen plant communities in Australia and Papua New Guinea. *Australian Journal of Botany*, 20:273-299.

Specht RL, and Specht A. (1989). Canopy structure in Eucalyptus-dominated communities in Australia along climatic gradients. *Acta Oecologica, Oecologia Plantarium*, 10:191-213.

Stauffacher, M., Bond, W., Bradford, A., Coram, J., Cresswell, H., Dawes, W., Gilfedder, M., Huth, N., Keating, B., Moore, A., Paydar, Z., Probert, M., Simpson, R., Stefanski, A., and G. Walker (2000) Assessment of salinity management options for Wanilla, Eyre Peninsula: Groundwater and crop water balance modelling, CSIRO Land and Water Technical Report 1/00.

Stephenson, A.E. (1986) Lake Bungunnia – a Plio-Pleistocene megalake in southern Australia, *Palaeoecology*, 57:137-156.

Stephenson, A.E. and C.M. Brown (1989) The ancient Murray River system, Bureau of Mineral Resources, *Journal of Australian Geology and Geophysics*, 11:(2-3), 387-395.

Stirzaker, R., and Lefroy, E. C. (1997), Alley farming in Australia - current and future directions. A report for RIRDC, Research paper No 97/29.

Strizaker, R.J., Cook, F.J., Knight, J.H. and P. Thorburn (Ed.) (1999) Where to plant trees on cropping land for control of dryland salinity: some approximate solutions, *Agricultural Water management, Special issue: interactions between plants and shallow, saline water tables - implications for the management of salinity in Australian Agriculture,* 36:2(3), 115-133.

Stirzaker, R.J., Lefroy, E.C., Keating, B. and J. Williams (2000) A Revolution in Land Use: emerging land use systems for managing dryland salinity, CSIRO Land and Water, Canberra, 24 pp.

Stirzaker, R.J., T.W. Ellis and E.C. Lefroy, (2002) Mixing trees with crops and pastures, *In* Stirzaker, R.J., Vertessy, R.A. and Sarre A. (Eds), *Trees, Water and Salt: an Australian guide for using trees to achieve healthy catchments and productive farms*, RIRDC/LWRRDC/FWPRDC Joint Venture Agroforestry Program.

Stirzaker, R.J. (2001) Planting over saline water tables, *In* Stirzaker, R.J., Vertessy R.A., and A. Sarre (*Eds*) *Trees, Water and Salt – an Australian guide to using trees fro healthy catchments and productive farms*, Rural Industries research and Development Corporation, in press.

Stirzaker, R.J., E.C. Lefroy and T.W. Ellis, (2002) Belts of trees in the cropping landscape; the tradeoff between drainage and yield, *Agricultural Water Management*, 53:187-199.

Swanson, R. H. (1972) Water transpired by trees as indicated by heat pulse velocity, *Agricultural Meteorology*, 10:277-281.

Swanson, R.H. and D.W.A. Whitfield (1981) A numerical analysis of heat pulse velocity theory and practice. *J. Exp. Bot.* 32:221-239.

Tanner, C.B. (1967) Measurement of evapotranspiration. *In* Hagen (Ed.) *et al., Irrigation of Agricultural Lands,* Agronomy Monograph no. 11, American Society of Agronomy – Crop Science Society of America – Soil Science Society of America, Madison, USA, pp. 534-574.

Taylor, P. J., (1999) The potential of interception belts in the management of dryland salinity. Dissertation, Department of Agronomy and Farming Systems, Faculty of Agricultural and Natural Resource Sciences, University of Adelaide.

Taylor, P.J., Nuberg, I.K. and T.J. Hatton (2001) Enhanced transpiration in response to wind effects at the edge of a blue gum (*Eucalyptus globulus*) plantation, *Tree Physiology,* 21, 403-408.

Taylor, S. (1996) Dryland Salinity – introductory extension notes, 2nd edition, Department of Land and Water conservation of New South Wales, Sydney, 63 pp.

Thornley, J. H. M., and I. R. Johnson (1990) Plant and crop modelling: a mathematical approach to plant and crop physiology, Oxford, UK: Oxford University Press, 669 pp.

VanDenbeldt, R. J., Brenner, A.J., and F. L. Sinclair (1990) Tree/crop Interactions in Agroforestry Systems, *In* Proceedings , 19th IUFRO World Congress, Montreal, Canada, 5-11 August, 1990, p292-303.

Van Noordwijk, M., Spek, L.Y. and P. Purnomosidhi (1995) Quantifying shallow roots – tree geometry makes root research easy, R*esearch*, April-June 1995, 9-11.

Van Noordwijk, M. and Lusiana, B. (1999) WaNuLCAS, a model of water, nutrient and light capture in agroforestry systems, *Agroforestry Systems* 43: 217-242.

Vertessey, R. A., T. J. Hatton, P. J. O'Shaughnessy., and M. D. A. Jayasuriya (1993) Predicting water yield from a mountain ash forest catchment using a terrain analysis based on a catchment model, *Journal of Hydrology*,150:665-700.

Vertessy, R.A., Benyon, R.G., O'Sullivan, S.K. and P.R.Gribben (1995) Relationships between stem diameter, sapwood area, leaf area and transpiration for young mountain ash forest, *Tree Physiology*, 15:559-567.

Vertessy, R., Watson, F., O'Sullivan, S., Davis, S., Campbell, R., Benyon, R., and Haydon, S. (1998) Predicting water yield from mountain ash catchments, Report No. 98/4. Cooperative Research Centre for Catchment Hydrology, CSIRO Publishing.

Vertessy, R.A. and Y. Bessard (1999) Anticipating the negative hydrologic effects of plantation expansion: results from a GIS-based analysis on the Murrumbidgee Basin, Cooperative Research Centre for Catchment Hydrology Report 99/6, CSIRO Canberra, pp 63-67.

Wagenet R.J. (1986) Water and solute flux. *In* Klute (Ed.) *Methods of Soil Analysis, Part 1. Physical and mineralogical Methods,* Agronomy Mongraph no. 9 (2nd edition), American Society of Agronomy – Soil Science Society of America, Madison, USA, pp. 1055-1088.

Walker, G. R., Jolly, I. D., and P. G. Cook (1991) A new chloride leaching approach to the estimation of diffuse recharge following a change to land use, *Journal of Hydrology,* 128: 49-67.

Walker, G. R., Cook, P. G., Jolly, I. D., Hughes, M. W., and G. B. Allison (1992) Diffuse groundwater recharge in the western Murray Basin, Rep. No. 6, CSIRO Water resources Series.

Walker G.R., (1998) Using soil water tracers to estimate recharge, *In* (Eds L Zhang and Glen Walker) *Studies in catchment hydrology – the basics of recharge and discharge,* CSIRO Publishing, Collingwood, 1998.

Walker, G., Gilfedder, M. and John Williams (1999) Effectiveness of current farming systems in the control of dryland salinity, CSIRO Land and Water, Canberra, 16 pp.

Walker G.R. and L. Zhang (2001) Plot-scale models and their application to recharge studies, *In* L. Zhang and G. Walker (Eds), *Studies in Catchment Hydrology – the basics of recharge and discharge*, CSIRO Publishing, Collingwood, Australia, in press.

Walker, G.R. Zhang, L., Ellis, T. W., Hatton, T.J. and C. Petheram, (2001) Towards a predictive framework for estimating recharge under different land uses: review of modelling and other approaches, *Hydrogeology*, 10:68-90.

Walker, J., Bullen, F. and F.G Williams (1993) Ecohydrological changes in the Murray-Darling Basin – the number of trees cleared over the last two centruries, *Journal of Applied Ecology,* 30, 265-273.

Walker, J. Sharpe, P.J.H., Penridge, L.K. and H. Wu (1989) Ecological field theory: concept and field tests, *Vegetatio,* 83:81-95.

Walker, J., Dowling, T., Fitzgerald, W., Hatton, T., Mackenzie, D., Milloy, B., Nicoll, C., O'Sullivan, A., and Richardson, P. (1998) Final report on the National Landcare project - Evaluating the success of tree planting for degradation control. CSIRO Publishing.

Welles, J.M. and J.M. Norman (1991) Instrument for indirect measurement of canopy architecture, *Agronomy Journal,* 83:818-825.

Williams, J., Hutchings, T., Lefroy, E.C. and P. Price (1998) Redesign of Australian plant production systems R&D program operating plan, Occasional Paper RAPPS01/98, Land and Water Resources Research and Development Corporation, Canberra, 16pp.

Williamson, D. R. (1998) Land degradation processes and water quality effects: water logging and salinisation, *In* J. Williams, R. A. Hook, and H. L. Gascoigne (Eds.), *Farming Action- catchment reaction* (pp. 162-187). Collingwood, Victoria, Australia: CSIRO Publishing.

Wilson, B. F. (1967) Root growth around barriers, *Botanical Gazette*, 128:79-8.

Wood, W.E. (1924) Increase of salt in streams following destruction of native vegetation, *Journal of Royal Society of Western Australia,* 10:35-47.

Zhang, L., and W.R. Dawes (1998) WAVES – an integrated energy and water balance model, CSIRO Land and Water Technical Report No. 31/98.

Zhang, L. and G.R Walker *Eds* (1998) The basics of recharge and discharge – studies in catchment hydrology, CSIRO Land and Water, Canberra, in press.

Zhang, L., Dawes, W.R., Slavich, P.G., Meyer, W.S., Thorburn, P.J., Smith, D.J. and G.R. Walker (1999) Growth and ground water uptake responses of lucerne (*Medicago sativa)* to changes in ground water levels and salinity: lysimeter, isoltope and modelling studies, *Agricultural Water Management,* 39:2/3, 265-282.

Zhang, L., Dawes, W.R., Hatton, T.J., Hume, I.H., O'Connell, M.G., Mitchell, D.C., Milthorthpe, P.L. and M. Yee (1999) Estimating episodic recharge under different crop/pasture rotations in the Mallee region. Part 2. Recharge control by agronomic practices, *Agricultural Water Management*, 42:237-249.

Appendix 1 – site descriptions

Introduction

This appendix provides descriptions of the landform, soil and natural vegetation of the experimental sites used in the experiments described in Chapters 5 and 6, as well as photographs and site details that relate directly to the experiments.

Recharge transect sites (Chapter 5)

Soil descriptions given in this section have been converted to the Australian Soil Classification (Isbell, 1996) from a combination of field data and soil descriptions from other surveys (Rowan and Downes, 1963; Gibbons and Downes, 1964; Laut *et al.* 1977). The sites appear in the same order as in Table 1 and Table 2.

Kimba

Recharge transects were measured at two sites: **a remnant belt** (Figure 82); and **a remnant block edge** (Figure 83). These were separated by about 2 km, on the property "Cooinya" (owner Ms Sue Murphy) approximately 30 km south east of the township of Kimba 33^0 15' S 136^0 50'E on the Eyre Peninsula, South Australia. Laut *et al.* (1977) categorise the landscape in Province 4, Eyre and Yorke Peninsulas under "Kimba Environmental Association – 4.3.16" and describe the association:

> *"A gently undulating calcreted plain with occasional low quartzitic hills, partly mantled with sand sheets and dunes" (Figure 80).*

Figure 80 Aerial view of partly cleared dune/swale land forms near Kimba, South Australia.

Natural vegetation was mainly mallee communities dominated by *Eucalyptus socialis* and *E. gracilis* (Figure 81).

Figure 81 Remnant undisturbed mallee on a dune formation near Kimba, South Australia. *LAI* of the overstorey was 0.47.

The association comprises 2 land units: hill; dune; and plain (swale). Hills are typically 30 m high and uncleared. Dunes are typically 5 m to 10 m high, 1 km in width and several kilometres long. Generally only the swales were cleared for grazing, about 60 years previous, and vegetation is retained on the dunes to prevent wind erosion.

The **remnant mallee belt** of *E. socialis* (Figure 82) was orientated north-south across an east-west oriented dune. The recharge transect (Figure 110) extended east from the belt along the crest of the dune. Laut *et al.* (1977) describe dune soils of these systems as having uniform, loose, coarse textured brownish sand; Uc5.11 (Northcote, 1979). This translates to a Hypercalcic, Calcarasol under the Australian Soil Classification (ASC) (Isbell, 1996). The soil was deep and well-drained, changing gradually from a sandy loam and a clay loam at about 10 m deep.

Figure 82 Hand augering profiles for soil water and chloride analyses at the remnant mallee belt of *Eucalyptus socialis* on a dune at 'Cooinya' near Kimba South Australia.

The **remnant block edge of mallee**, *E. socialis* and *E. gracilis* (Figure 83), was oriented east-west, on the southern edge of a block, on the southern toe of an east-west oriented dune. At the toe of the dunes soils make a transition over a distance of about 10 m to a red duplex soil: Dr2.23 (Northcote, 1979); Calcic, Red, Chromosol (Isbell, 1996). While a clear distinction is difficult, the vegetation was considered to be wholly on the dune and the root zone in the swale. The depth to B horizon varied from 0.5 m at the vegetation edge to 0.2 m at a horizontal distance of 25 m. Below the B horizon the soil alternated between a loamy clay and a clay sand to a depth of about 6 m. The (apparent) root zone was almost devoid of vegetation or litter. This changed abruptly to substantial annual grass growth at the edge, which in turn tapered off over the next several metres. It appeared that the grass at the edge benefited from run off from the bare root zone. The recharge transect measured at this site is shown in (Figure 111).

Figure 83 The remnant block edge of mallee, *E. socialis* and *E. gracilis* near Kimba, South Australia. Tree growth was enhanced by a factor of about 1.5, relative to mid-block growth (see mid-block Figure 81), for a distance of about 6.5 m in from the block edge. Note zone of strong competition between trees and annuals and apparent high runoff towards the foreground where competition lessens and ceases near the orange tape reel. The growth of annuals in the foreground is apparently enhanced by run-on.

Parilla

Two recharge transects were measured at Parilla: the salmon gum (*E. salmonophloia*) **plantation edge** (Figure 87); and the **remnant mallee block edge** (Figure 85 and Figure 86). Both sites were on the property of Mrs Hazeldeane, about 6 km northwest from the township of Parilla in South Australia Parilla 34^0 31' S 140^0 39'E. Laut *et al.* (1977) name the "Pinnaroo Environmental Association 2.3.4" in Province 2 Murray Mallee, and describe the region:

> *"A gently undulating sandy plain with low parallel dunes and locally, small outcrops of calcrete"* (*Figure 84*).

The association comprises 2 land units: dune; and plain (swale). Although mostly cleared, the native vegetation is predominantly white mallee (*E. dumosa*) and other mallees. The understorey is generally absent due to grazing. Dune soils are described as: deep uniform

Figure 84 Aerial view of Murray Mallee region near Parilla. Remnant vegetaion remains along roadsides and other small patches. The dune-swale formation can be seen throughout and is most obvious near the bottom of the picture.

coarse, Uc5.11 (*Northcote*, 1979); or Regolithic, Hypercalcic, Calcarosol (Isbell, 1996). Swale soils are: shallow brown gradational calcareous, Gc1.12 (Northcote, 1979); or Rendic, Hypercalcic Calcarosol with a clay loam B horizon (Isbell, 1996).

The dune soil profile generally comprised a sandy loam interspersed with bands of clay loam about 0.5 m thick at 4m, 8 m and 12 m deep, reflecting the sedimentary origins of the soil. The swale soil profile comprised 0.2 m to 1 m of sandy loam overlying a loamy clay B horizon about 1.5 m thick, below which was alternate bands of clay loam and sandy loam.

The **remnant mallee block** (Figure 85) grew on the next dune 200 m to 300 m to the north of the **salmon gum plantation**. The dune was 10 m high, about 100 m wide and about 1 km long. The edge of the mallee block approximately coincided with the southern toe of the dune (Figure 86). The apparent root zone, judged by change in weed cover, extended about 20 m from the block edge, into the swale. The recharge transect is shown in Figure 112.

Figure 85 Aerial view of remnant mallee (*E. dumosa*) block edge at Parilla, South Australia. The edge strip of enhanced growth can be seen clearly and the length of edge measured is indicated. The *LAI* away from the edge effect was 0.76.

Figure 86 Remnant mallee *E. dumosa* block edge at Parilla, South Australia. Tree growth was enhanced by a factor of about 2, relative to mid-block growth, for distance of about 4 m in from the block edge.

The **salmon gum plantation** (Figure 87) recharge transect measured was on the southern, east-west oriented edge of the plantation in the swale between two east-west oriented dunes. The plantation edge was close to the toe of a dune that was: 6 m high; 150 m wide; and about 1 km in length. The apparent root zone of the edge trees extended about 50 m up the north face of the dune, as indicated by the change in soil cover. The plantation was part

of a species trial planted in the early 1900s. Surrounding natural vegetation was cleared at about the same time. The recharge transect is shown in (Figure 113).

Figure 87 Aerial view of the salmon gum (*E. salmonophilia)* at Parilla, South Australia, looking west. Enhanced growth is obvious at both north and south edges of the block. The recharge transect extended south from the southern edge. The *LAI* of mid-plantation was 1.21.

Walpeup

The **remnant mallee belt** was on a north-south oriented fence line on Mr and Mrs Wakefield's property about 5 km northeast from the Victorian Department of Agriculture Mallee Research Station, near the township of Walpeup, in north west Victoria Walpeup 35^0 07' S 141^0 59'E. Surrounding natural vegetation was cleared about 50 years previous to the experiment. The site and surrounding area is on an 60 km^2 'island' of Boigbeat land system (Rowan and Downes, 1963) in a large expanse of the, lower, Central Mallee land system. The land unit is described:

> *"...the landscape is composed of a plain on which there is a dense array of hummocks, typically one quarter of a mile (400 m) across.*
>
> *The more northerly areas of the land system also have distinctive native vegetation in which pine, belar (Casuarina cristata), buloke (C. luehmanii) or pine (Callitris preissii)-belar-buloke woodlands predominate amongst smaller proportions of mallee".*

The belt (Figure 88 and Figure 23) was on the north face of a hummock where soils are described as Group A sandy loams (Rowan and Downes, 1963) or Hypercalcic Calcarasols (Isbell, 1996).

Figure 88 Aerial view looking south toward the Walpeup remnant tree belt site, marked with arrow. A ground view of the site is shown in Figure 23.

A particle size distribution of the top 1.4 m is given in Figure 89. Below 1.4 m soil texture was generally a sandy loam with clay loam bands up to 0.5 m thick at 3 m, 8 m and 11 m. The recharge transect (Figure 114) extended eastward from the belt, approximately in the horizontal plane.

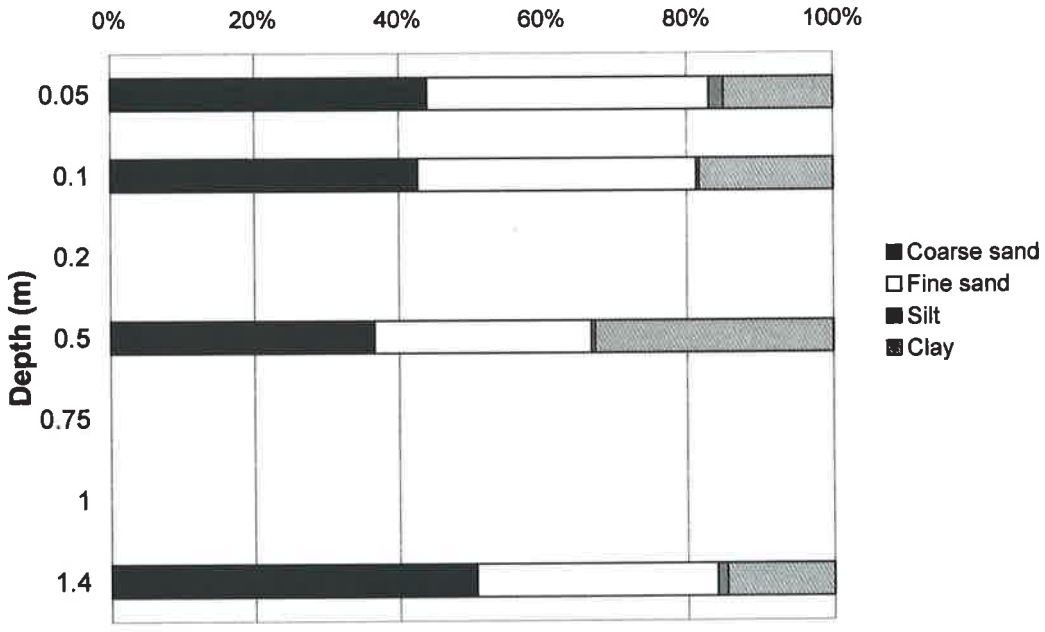

Figure 89 Particle size distribution of a Group A sandy loam, to 1.4 m deep, modified from Rowan and Downes (1963).

Dergholm

The Dergholm recharge transect (Figure 115) site was on a property belonging to Mr Simpson, about 7 km east from the township of Dergholm, Victoria. The **remnant vegetation block edge** (Figure 90) ran east-west on the boundary between farm land and the southern edge of the Dergholm State Park Dergholm 37^0 21' S 141^0 12'E.

Figure 90 Remnant vegetation edge at Dergholm Victoria. Tree growth was enhanced by a factor of about 2, relative to that at mid-block growth (*LAI* = 0.95), for a distance of about 15 m in from the block edge. The competition zone between the trees and the pasture can be seen to wane towards the left of the photograph.

Gibbons and Downes (1964) describe the area under the Kanawinka Land System as:

> *Gentle dunes and sheets of white acid sands overlying swampy laterized table lands and dissected tablelands.*

The land unit was gentle dunes of acid white sands classified as a Kowree sand (Gibbons and Downes, 1964) or Aeric, Podosol (Isbell, 1996). The coarse sand is up to 15 m deep with a laterite basement. Natural vegetation was dry schlerophyll forest of stringy bark (*E. baxteri*), pink gum (*E. fasciculosa)* and yellow gum (*E. leucoxylon*) up to 16 m high. The understorey was relatively sparse grasses and heaths. The farm land was cleared about 40 years prior to the experiment. The soil at the remnant block site matched well with the description given by Gibbons and Downes (1964):

...a dark grey coarse A_1 horizon overlying a very light grey coarse sand with a B horizon of brown sand.

Figure 91 gives the particle size distribution measured by Gibbons and Downes (1964) in the top 1.7 m. Below this depth the soil texture was a relatively uniform coarse sand with red mottled bands, to a depth of at least 8 m.

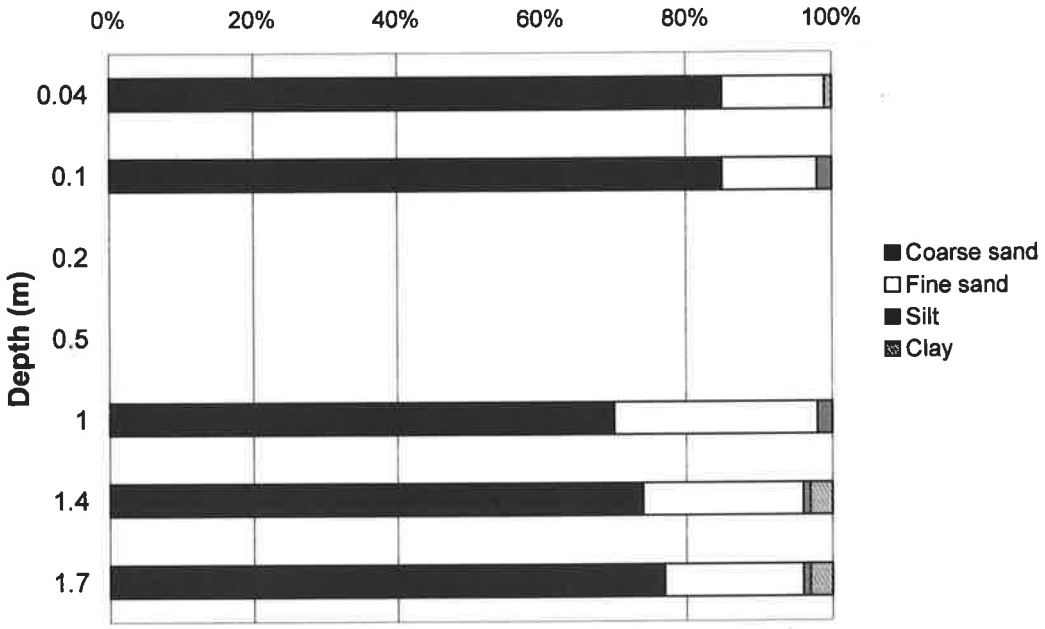

Figure 91 Soil particle size distribution of the top 1.7 m near the Dergholm site, modified from Gibbons and Downes (1963).

Water balance and leaf efficiency sites (Chapter 6)

The **water balance site** (Figure 92; Figure 34) was on the property of Mr Robert Selleck, approximately 8 km north west from Roseworthy Campus of the University of Adelaide, South Australia. The **leaf efficiency site** (Figure 93; Figure 37) was about 1 km southwest from the Roseworthy Campus 34°15'S, 138°41'E. The local landform is classified by Laut *et al.* (1977) as 4.6.6 "Mallala Environmental Association", occurring in Province 4, Eyre and Yorke Peninsulas. This association comprises 2 land units: a dominant undulating plane; and a minor dune land unit. Natural vegetation was mostly cleared around the turn of the century but patches of *E. largiflorens* and mixed mallee species remain on the plain while most dunes are still vegetated with *Callitris preissii*. The understorey is minimal in such patches, due to grazing, comprising mainly summer grasses and weeds.

Both the **water balance site** and **leaf efficiency site** were situated on the plane where soils are dominantly gradational calcareous loams (Gc1.12) with some red duplex (Dr2.23)

(Northcote, 1979), or Calcic, red Chromosol with some Supracalcic, Red, Chromosol (Isbell, 1996).

Figure 92 The water balance site, in the year following the experiment, viewed from the air and looking northwest. The dashed line indicates the 90 m x 40 m rectangular area that was kept bare for water balance measurements on both sides of the belt.

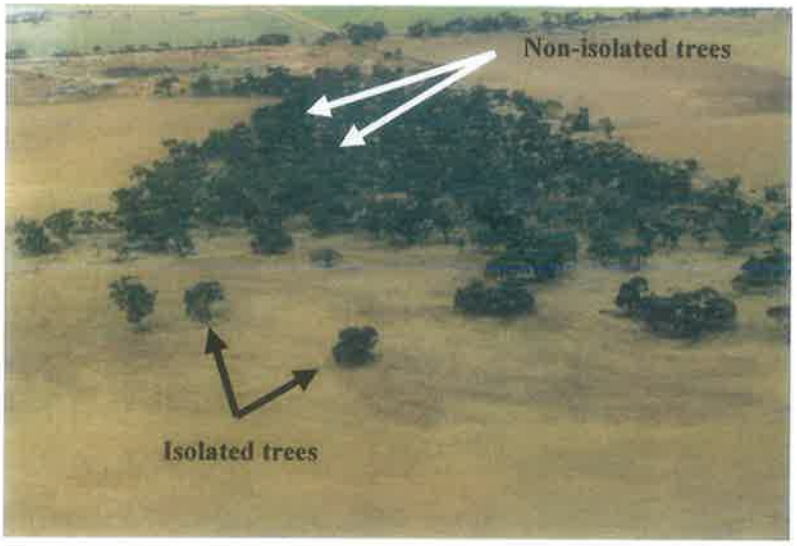

Figure 93 Aerial view of leaf efficiency site at Roseworthy South Australia, looking south east. Positions of the 2 isolated trees and the two non-isolated trees are shown.

Figure 94 shows the particle size distribution to a depth of 5.9 m at the water balance site. Soil particle size was not measured at the leaf efficiency site however the soil was very similar to that at water balance site.

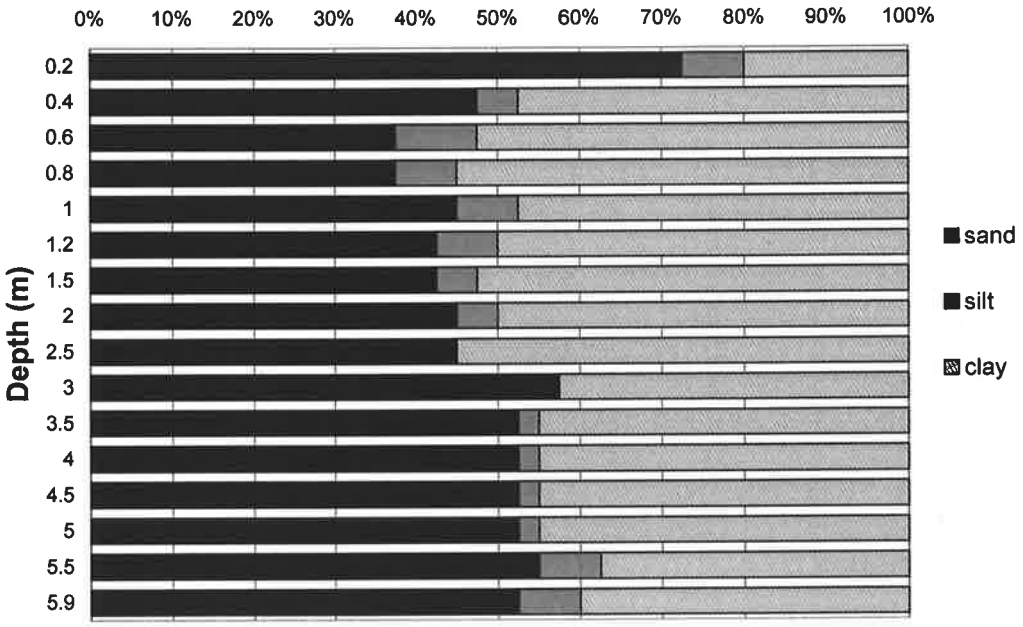

Figure 94 Soil particle size distribution from water balance site.

Appendix 2 methods and calculations

Introduction

This appendix provides additional and more detailed descriptions of methods, apparatus and calculations (where appropriate) for methods used in Chapters 5, 6, 7 and 8. The measurement of ΔS (using the neutron moisture meter NMM) is not covered in this appendix as it is described in detail in Chapter 6. Appendix 2 gives the NMM calibration data. For each of the recharge transect sites (Chapter 5) the chloride profiles are shown in this appendix, in the same order as in Table 1 and Table 2. The resulting recharge transects and *ENOR* measurements are then shown in the subsequent section in the same order.

Leaf area estimation

Tree leaf areas were estimated for the experiments described in Chapters 5, 6 and 8. Leaf areas were either expressed as: absolute area L (m^2); Leaf Area Index LAI (m^2 m^{-2}); or Lineal Leaf Area LLA (m^2 m^{-1}). In all cases leaf areas were estimated using a modified version of the Adelaide (module) method (Andrew *et al.*, 1979). In the cases of LAI and LLA, L was divided by the ground area of the quadrat, or the length of the tree belt, respectively.

The Adelaide (module) method (Andrew *et al.*, 1979) was developed for estimating the biomass of fodder shrubs. It requires two operators to inspect the plant(s) and agree on a branch, or collection of branches (module), of which the total foliage of the plant(s) can be estimated to be a multiple. Once identified, the module is removed from the plant and carried with the operators as they move between plants. Each operator records an estimate of the equivalent number of modules that comprise each plant. The foliage is stripped from the module, weighed, and multiplied by the module count (the average count from two operators) to give the foliage mass for each plant.

Figure 95 Canopy of salmon gum (*E. salmonophloia*), viewed from below, showing the "clumpy" or modular nature of eucalypt foliage that makes it suitable to the Adelaide (module) technique (Andrews *et al.*, 1979).

The Adelaide (module) method (Andrew *et al.*, 1979) was modified for this project in the following ways: eucalypt tree canopies were used rather than fodder shrubs (Figure 95); the estimated number of modules in each canopy was calculated from the average of three estimates made by each of the two operators; the leaf area of the module was determined by electronic planimetry.

Following module counting, leaves were stripped from the module and sealed in a plastic bag. Leaf area of the module was calculated from the average area of three 100 g sub samples of leaf using Equation 27.

$$Module\ area\ (m^2) = \frac{average\ area\ of\ sub\ samples\ (m^2) \times total\ mass\ of\ leaf\ (g)}{100} \qquad (27)$$

Modules varied in size from about 1 kg to 4 kg mass of leaf. The area of 100 g sub samples varied between 0.18 m^2 to 0.25 m^2.

For *LAI* measurements, quadrats were marked out as rectangles using a tape and optical square. Branches attached to stems inside the quadrat (but hanging outside the quadrat) were not counted, and *vice versa*. For *LLA* measurements, the ends of the length of tree belt considered were marked as close as possible to mid-way between canopies.

Module counting – bias between operators

A total of four operators were used for *LLA* measurement by the Adelaide (module) method (Andrew *et al.*, 1979). The same two operators (Operators 1 and 2) were used for all leaf area estimations made in Chapters 5 and 6. An initial period of training was

required for the selection of appropriate modules and comparison of count estimates. Bias between operators 1 and 2 was measured and found to be small (Figure 96). Operators 1, 3, 4 and 5 were used for the leaf area measurements in Chapter 8. The counts made by each operator were compared with counts made by Operator 1 at the same sites (Figure 97; Figure 98; Figure 99). Any associated bias was shown to be small.

Calibration

This method was calibrated by defoliating three entire tree canopies and comparing leaf area estimates made by the module method and by weighing and sub sampling the entire canopies. This procedure is described in Appendix 3.

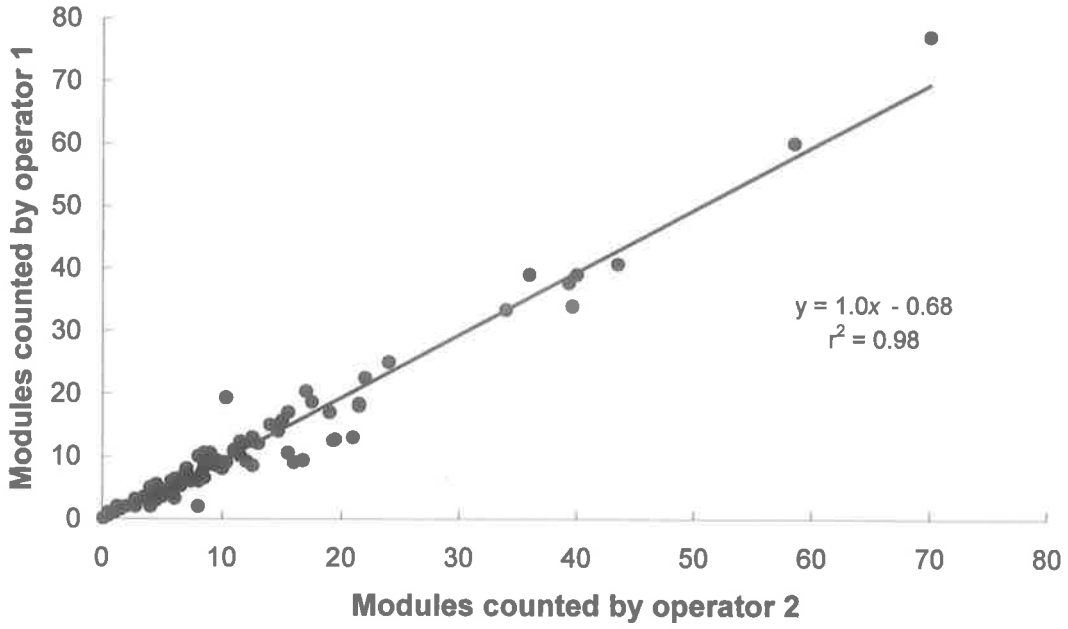

Figure 96 A comparison of module counts, by the two operators used in Chapters 5 and 6, from 89 stems of native eucalypt at Dergholm, in a 612 m^2 quadrat. The fitted line has a slope of 0.97 indicating, on average, an insignificant bias between operators.

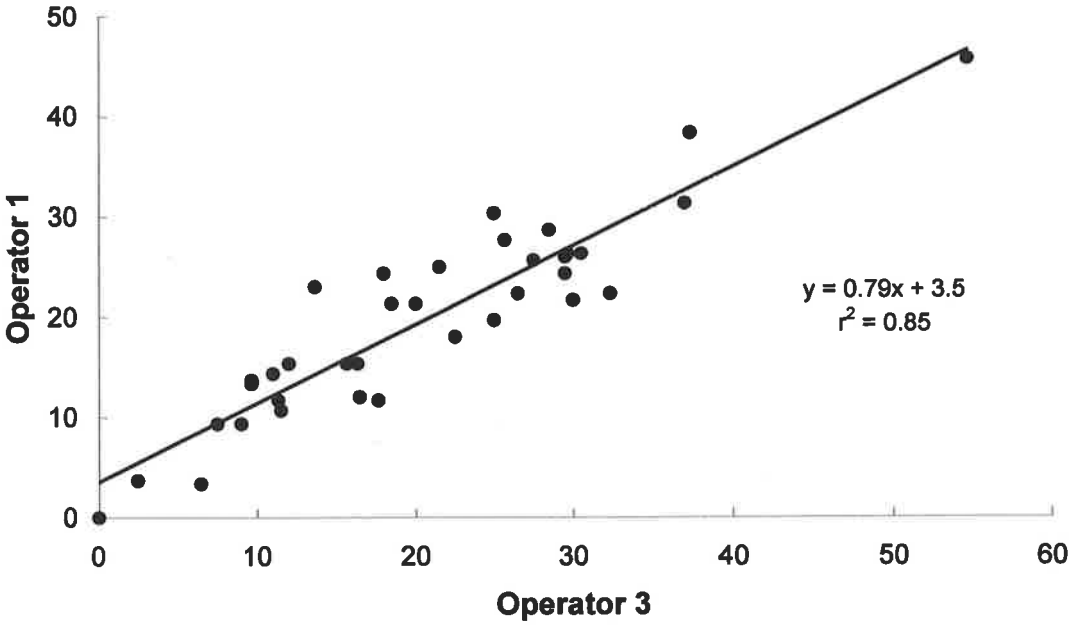

Figure 97 Bias between module counts made by Operators 1 and 3 at Site 25 Chapter 8.

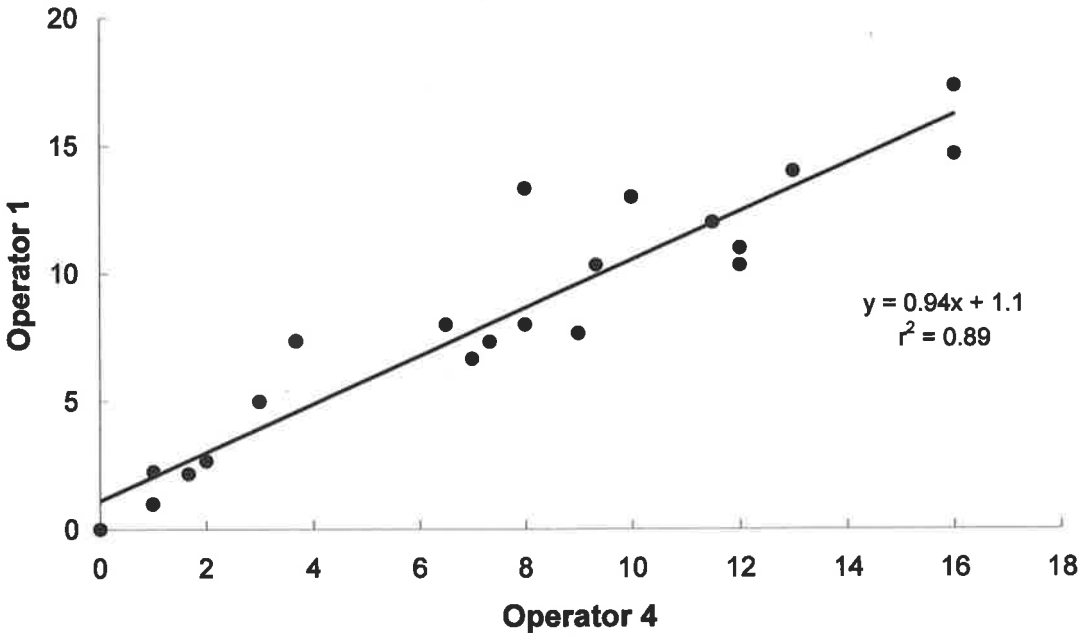

Figure 98 Bias between module counts made by Operators 1 and 4 Site 26 Chapter 8.

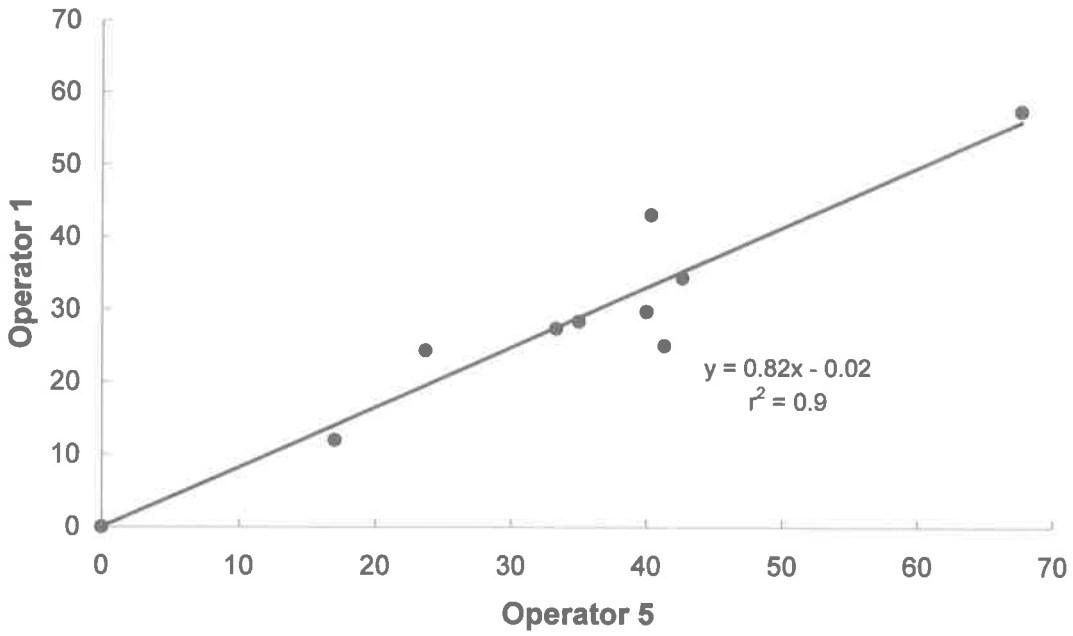

Figure 99 Bias between module counts made by Operators 1 and 5 at Site 13, Chapter 8.

Inferring *LLA* from stem diameter

There is often a strong relationship between stem diameter and leaf area of eucalypt trees (Vertessy *et al.,* 1995). This was used to obtain an average *LLA* of lengthy belts (>40 m), relatively quickly, without having to count the modules on all trees.

The method was tested by fitting a 2nd order polynomial relationship to stem diameter vs leaf area for 10 trees ranging between the smallest and largest in a 100 m long belt of *E. globulus* at Chifley, ACT (Site 25, Figure 75). The average number of modules, per metre of belt, for a 40 m section of the same belt, was then calculated from; the average stem diameter, of the same section; and the fitted relationship (Figure 100). This method predicted an average *LLA* of 44.8 m^2 m^{-1}. All the modules of the same section were then counted, giving an average *LLA* of 48.4 m^2 m^{-1}.

Table 7 gives the coefficients from regression equations used to estimate leaf area from stem diameter.

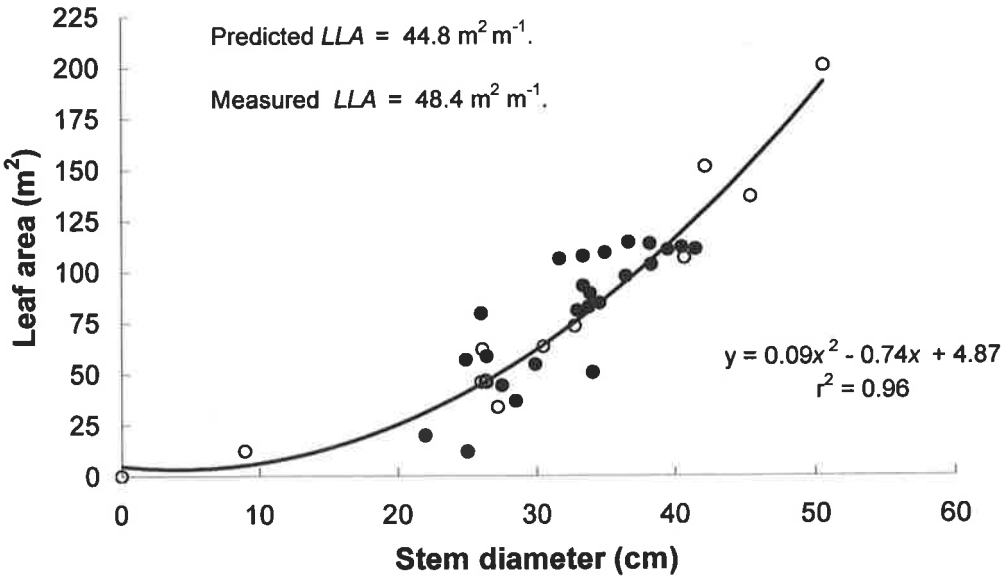

Figure 100 Evaluation of the method for estimating average *LLA* from stem diameter on *E. globulus* at Chifley, ACT (Site 25, Figure 73). A relationship was fitted to stem diameter and leaf area data for ten trees ○ ranging between the smallest and the largest. The average *LLA* for a 40 m section of the belt was estimated to be 44.8 m^2 m^{-1} using the fitted relationship and the average stem diameter of all trees in the 40 m section ●. *LLA* was then calculated from measured leaf area and found to be 48.4 m^2 m^{-1}.

Table 7 Coefficients from regression equations used to estimate leaf area from stem diameter. Site photographs and descriptions can be found in Chapter 8.

Site number (see Chapter 8)	Coefficients for regression equation: $y = ax^2 + b$, y = stem diameter (mm), x = leaf area (m^2)			Number of trees in sample
	a	b	r^2	n
11	0.00013	0.25	0.62	13
13	0.00044	0.04	0.78	33
16	0.0025	-0.16	0.93	14
17	0.00015	0.092	0.93	9
21	0.000003	0.35	0.62	12
22	0.00010	0.089	0.91	20
24	0.00057	0.065	0.84	14
25	0.00084	-0.044	0.96	12
26	0.0027	0.062	0.93	13
Vertessy *et al.* (1995)	0.0015	-0.019	0.91	21

Recharge

Chloride mass balance technique

The chloride mass balance technique for estimation of recharge is described by Allison and Hughes (1978) and was used to estimate recharge at some sites described in Chapter 5. The mass balance technique is applicable where conditions have reached a steady state, and is of most use in areas where there has been no change in land use for a long period, and hence the chloride concentration profile in the soil has stabilised. For this project the technique was applied in the root zones of remnant vegetation and a 70-year-old plantation. For sites that have been perturbed and have not yet reached a new steady state, the Transient Chloride Method (Walker *et al.,* 1991) was used. This technique is described in the next section.

The chloride ion Cl^- occurs naturally in precipitation and dryfall, its mean annual concentration C_p can be estimated using an empirical relationship between C_p and distance from the coast in south-eastern Australia (Hutton, 1976)

$$C_p = \frac{0.99}{\sqrt[4]{d - 0.23}}, \qquad (28)$$

where: C_p (m mol L^{-1}) is the total mean annual chloride concentration of the precipitation and dryfall; d is distance from the coast in kilometres, measured in the direction most likely to contribute oceanic chloride. *Cp* can be converted to m g L^{-1} by multiplying by 35.45, the atomic mass of chlorine. Table 8 shows the approximate distance of each recharge measurement site (Chapter 5) from the coast and the associated *Cp* calculated from Equation 28.

Table 8 Approximate long term average chloride concentration of precipitation and dryfall *Cp* at recharge measurement sites.

Site	Distance from coast (km)	*Cp* (m g L^{-1}) X 1000
Kimba	150	10.0
Parilla	150	10.0
Walpeup	250	8.8
Dergolm	150	10.0

Other sources of Cl^- are considered negligible except where potassium chloride fertilisers are applied. Allison and Hughes (1978) reported two such cases where it was necessary for

this to be taken into account. Although no farm records were available for sites in this study, the assumption of zero or negligible application of potassium chloride in those areas is a safe one, as it would be an unusual practice. Export of chloride from sites in livestock tissue is negligible but can be large in cases of extreme wind and water erosion.

Plant roots extract soil water but leave behind chloride, concentrating it in the root zone. Over a long period (at least decades) of unchanged land use, the chloride concentration of water draining below the root zone stabilises to a constant value C_d. The mass balance therefore gives

$$PC_p = DC_d, \tag{29}$$

where P is annual average rainfall, D is average annual recharge and C_d is the chloride concentration of the recharge water. Equation 29 is therefore solved for D

$$D = \frac{PC_p}{C_d}. \qquad \text{(Equation 4, Chapter 3)}$$

Allison and Hughes (1978) go on to derive a correction factor of 0.9 for the right hand side of Equation 4 to allow for deviations in values of the annual values of D and C_d from annual means (Equation 30).

$$D = 0.9 \times \frac{PC_p}{C_d}. \tag{30}$$

Figure 101 shows the chloride profile from the root zone of the remnant mallee belt at "Wakefield's", Walpeup. The profile exhibits the characteristic pronounced 'bulge' at about 2 m deep. The chloride concentration of the soil water draining below the root zone C_d, is approximately 8500 mg L^{-1}. Although this profile is insufficiently deep to show that this value stabilises with depth, the other deeper profiles in the transect (Figure 108) show a similar C_d value. In the method used by Allison and Hughes (1983, 1987), the position of the chloride bulge was used to approximate the position of the chloride 'front'.

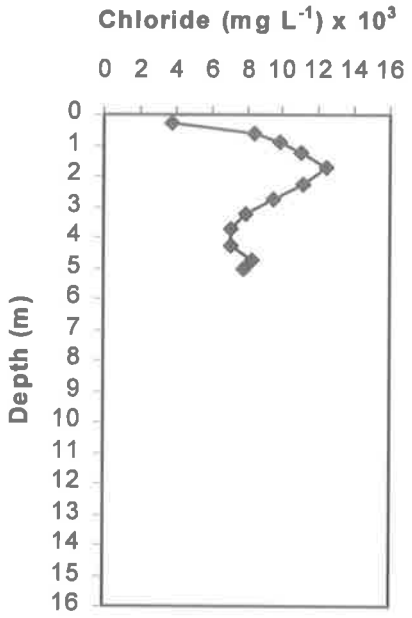

Figure 101 Chloride profile from the root zone of remnant mallee belt at "Wakefield's", Walpeup, Victoria. Such a profile is typical of an non-leached soil under remnant vegetation, showing a chloride 'bulge' at about 2 m.

Recharge beneath the root zone of the mallee was calculated using the chloride mass balance technique (Allison and Hughes, 1978) and Equation 30. Using: P; C_p; and C_d equal to 343 mm yr^{-1}; 48.8 mg L^{-1}; and 8500 mg L^{-1}, respectively, D is calculated as 0.32 mm yr^{-1}.

Transient chloride technique

The transient chloride technique (Walker *et al.*, 1991) is a generalised version of the chloride front displacement technique (Allison and Hughes, 1978, 1983), and hence is also called the "generalised chloride front displacement technique". It is used to estimate recharge under land use situations that have been perturbed from equilibrium and have not yet reached a new steady state. It also avoids the need to assume piston flow and remains valid even if the chloride profile becomes distorted (and a chloride front is not obvious). The technique identifies the position of the 'effective' chloride front, from chloride and water balance considerations, defining it as the depth at which Equation 31 is satisfied.

$$\int_0^{Zef} \theta \, dz = \int_0^{Zd} \theta (1 - \frac{C}{C_d}) \, dz , \qquad (31)$$

where: θ is the soil water content (v/v%); C is the chloride concentration of the soil water (mg L^{-1}); C_d is the chloride concentration of the soil water at the depth at which it

stabilises to an constant value (mg L^{-1}); Z_d is the depth at which C_d stabilises (m); and Z_{cf} is the depth of the effective chloride front. Figure 102 illustrates the logic behind the technique, using an idealised soil water/chloride profile as an example. Flow is 'non-piston' as represented by the curved, solid line. The horizontal dashed line represents the position of the effective chloride front Z_{cf}, the sum of soil water above this line being equal to the left hand side of Equation 31. The right hand side of Equation 31 calculates the equivalent depth of 'new' water (the area above the solid line). This is done by summing total soil water to depth Z_d, and subtracting from it, the equivalent depth of 'old' water (area below the solid line).

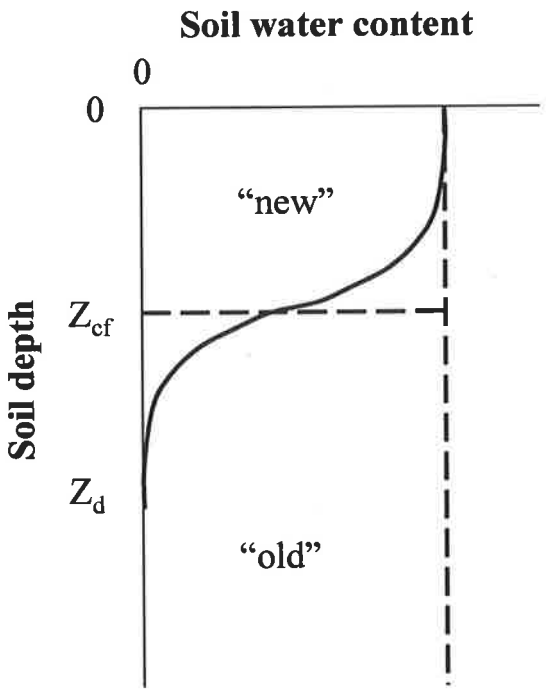

Figure 102 An idealised soil water profile, following leaching. For conceptual simplicity, soil water content does not vary with depth. 'New' water (above the solid line) has infiltrated and displaced 'old' water as it moves downward.

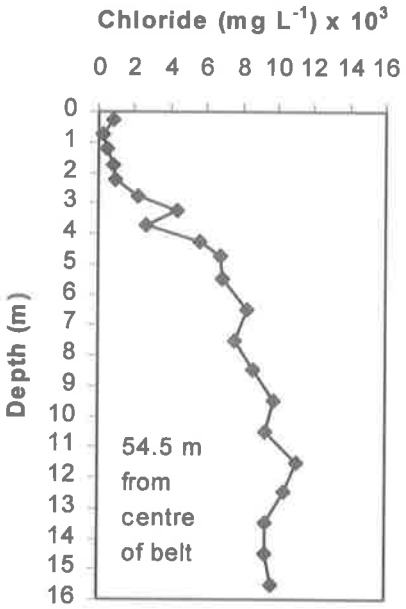

Figure 103 Soil chloride profile from outside the root zone of the remnant mallee belt at "Wakefield's", Walpeup, Victoria. The profile is obviously leached relative to Figure 101. The 'new' position of the chloride front is not obvious but can be calculated (Equation 31).

Figure 103 shows a classic example of a real soil profile that has been leached following clearing of natural vegetation, and has not yet reached a new equilibrium. As described by Walker (1998), the depth at which Equation 31 holds can be relatively easily determined using an electronic spreadsheet. Integrations were performed by trapezoidal approximation on the sampling interval. Table 9 shows soil chloride and soil water data from the profile in Figure 103. Note: the increase in soil water from the surface to 6 m deep; the stabilisation of soil chloride at depth; the stabilisation of column 5 below 7 m. The effective depth of the chloride 'front' is located using Equation 31. The condition is satisfied, in this case, at a depth of 4 m, at which point the value in column 4 (565) approximately equals the (stabilised) value in column 5 (567).

In the case of the leached profile, recharge is calculated as the total soil water between the position of the effective chloride front, and the position it most likely was before land clearing. The non-leached profile, Figure 101 is most likely representative of the pre-clearing condition. The generalised chloride front displacement technique (Walker *et al.*, 1991) shows that Z_{cf} for a non-leached profile can be approximated as 1/3 of the depth to the chloride bulge. If this is approximated to be about 1 m in the "Wakefield's" case (Figure 101), total recharge since clearing in this case is 565 mm – 213 mm = 352 mm.

Since the land had been cleared for about 50 years then the average annual recharge rate is about 352/50 = 7 mm yr^{-1}.

Where a local non-leached site is not available for comparison, Z_{cf} must be estimated. Walker *et al.* (1991) present a relationship between % clay in the top 2 m of the soil profile and Z_{cf}. Unfortunately % clay was not measured for this experiment. However, it is relatively safe, in low to medium rainfall environments, to assume that the effective chloride front would occur within the top 1 m of the profile (pers. comm. Ian Jolly, CSIRO Land and Water). While the calculation of recharge, using the generalised chloride front technique, is somewhat dependent on this assumption, the calculation of *ENOR* from recharge transects is relatively insensitive to it. This is explained in detail in Appendix 2, with specific reference to each site and each recharge transect.

Table 9 Soil chloride and water data from the profile in Figure 103. The effective chloride front has been located at a depth of 4 m where the value in the 4th column approximates the value in the 5th column. The depth of the chloride front under natural vegetation is about 1 m (Figure 101). The amount of recharge is therefore the water stored between 1 m and 4 m in the 4th column: 565 – 213 = 352 mm. This spread over 50 years since clearing gives 7 mm yr^{-1}.

Depth (m)	Soil water chloride (mg L^{-1})	Soil water content (vol %)	$\int_0^{Zcf} \theta\, dz$ (mm)	$\int_0^{Zd} \theta(1-\frac{C}{C_d})\, dz$ (mm)
0.0	765	2	50	46
0.5	230	18	140	134
1.0	480	18	213	204
1.5	858	11	267	253
2.0	939	10	317	298
2.5	2146	10	363	334
3.0	4353	9	409	360
3.5	2701	10	479	410
4.0	5603	18	565	447
4.5	6784	17	671	480
5.0	6906	26	862	537
6.0	8289	13	962	552
7.0	7627	7	1024	567
8.0	8629	5	1070	572
9.0	9839	4	1112	572
10.0	9298	4	1155	574
11.0	11073	4	1193	570
12.0	10322	3	1226	568
13.0	9329	3	1262	570
14.0	9293	4	1297	572
15.0	9683	3	1329	572

Soil chloride and soil water profiles

This section presents the soil chloride from all transects investigated in Chapter 5. Soil water profiles are included to augment interpretation of the chloride profiles. Recharge values are plotted as recharge transects in the next section.

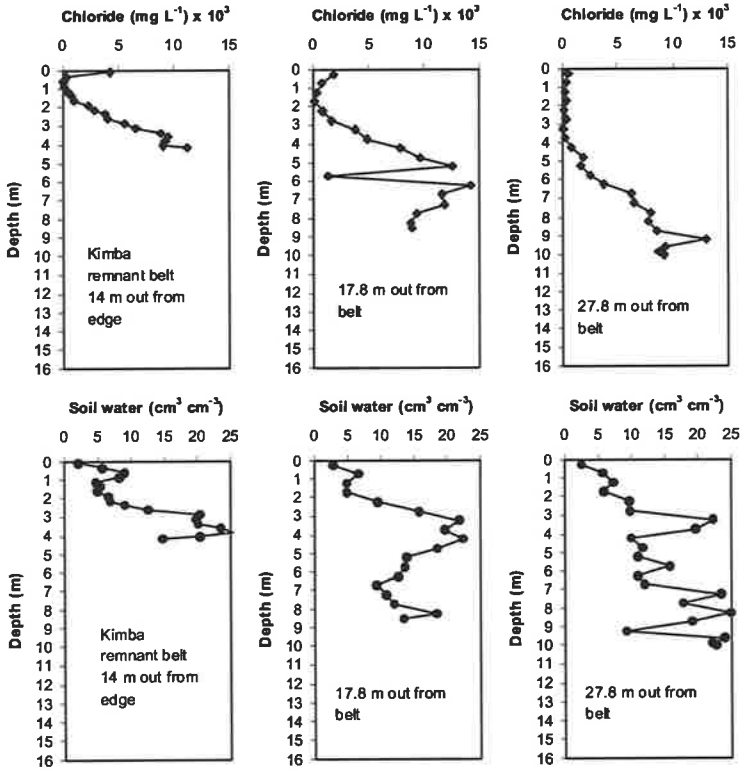

Figure 104 Soil chloride and soil water profiles from a *remnant belt* at "Cooinya", Kimba South Australia (Figure 82). Leaching and associated soil water storage increases with distance from the belt. Soil samples were unprocurable closer to the belt due to hard soil conditions and dry sandy soil that could not be retrieved with the auger. Figure 110 shows the recharge transect for the site.

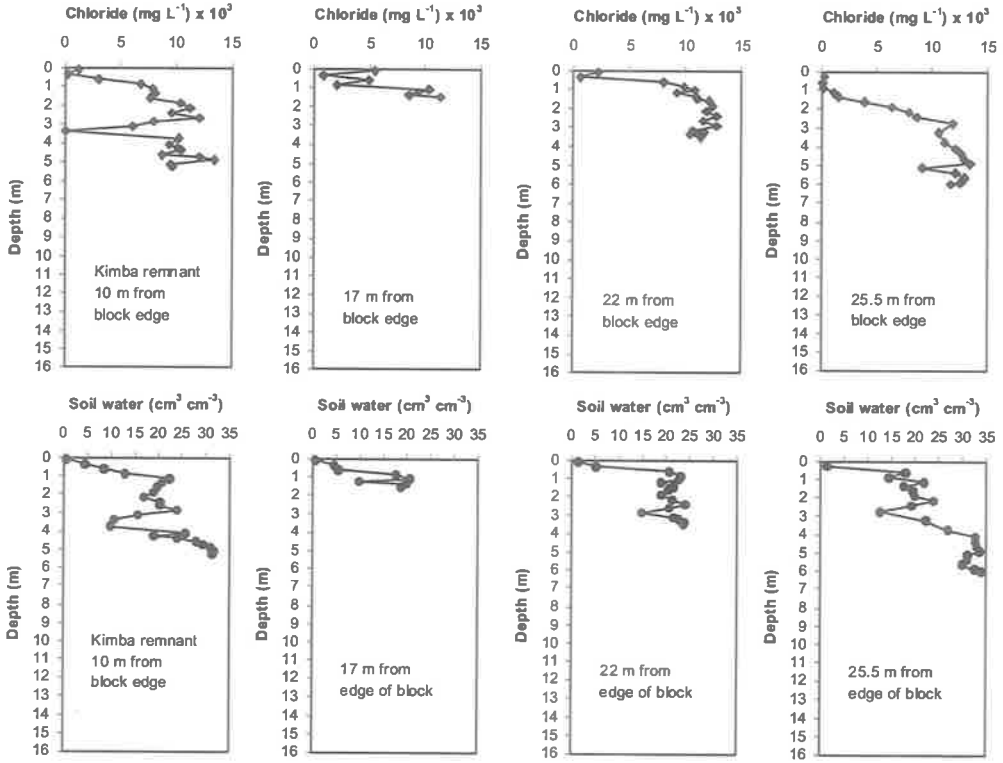

Figure 105 Soil chloride and soil water profiles from a *remnant block edge* at "Cooinya", Kimba, South Australia (Figure 83). The vegetation edge coincided with the base of the dune so the transect extended into the swale. Some leaching can be seen at both 10 m and 25.5 m from the block edge, exhibiting a variation in the recharge transect (Figure 111) compared to the other sites.

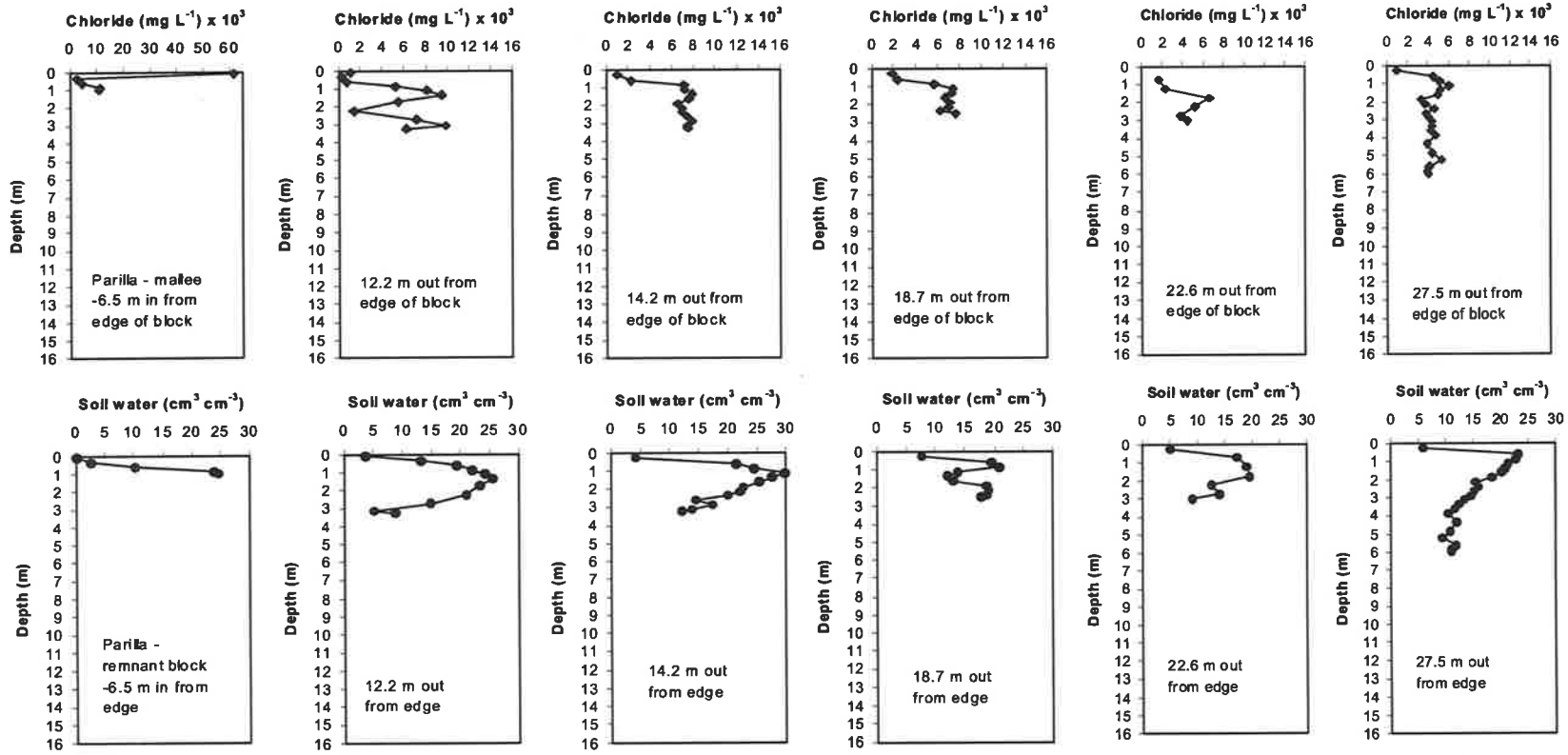

Figure 106 Soil chloride and soil water profiles from the *remnant block edge* at Parilla, South Australia (Figure 85). While chloride concentrations are much higher directly under and near the vegetation, no significant leaching could be detected further from the block. It would appear the influence of the trees on recharge extended at least 27.5 m although a change in surface cover was obvious at about 25 m horizontally from the block (Figure 112).

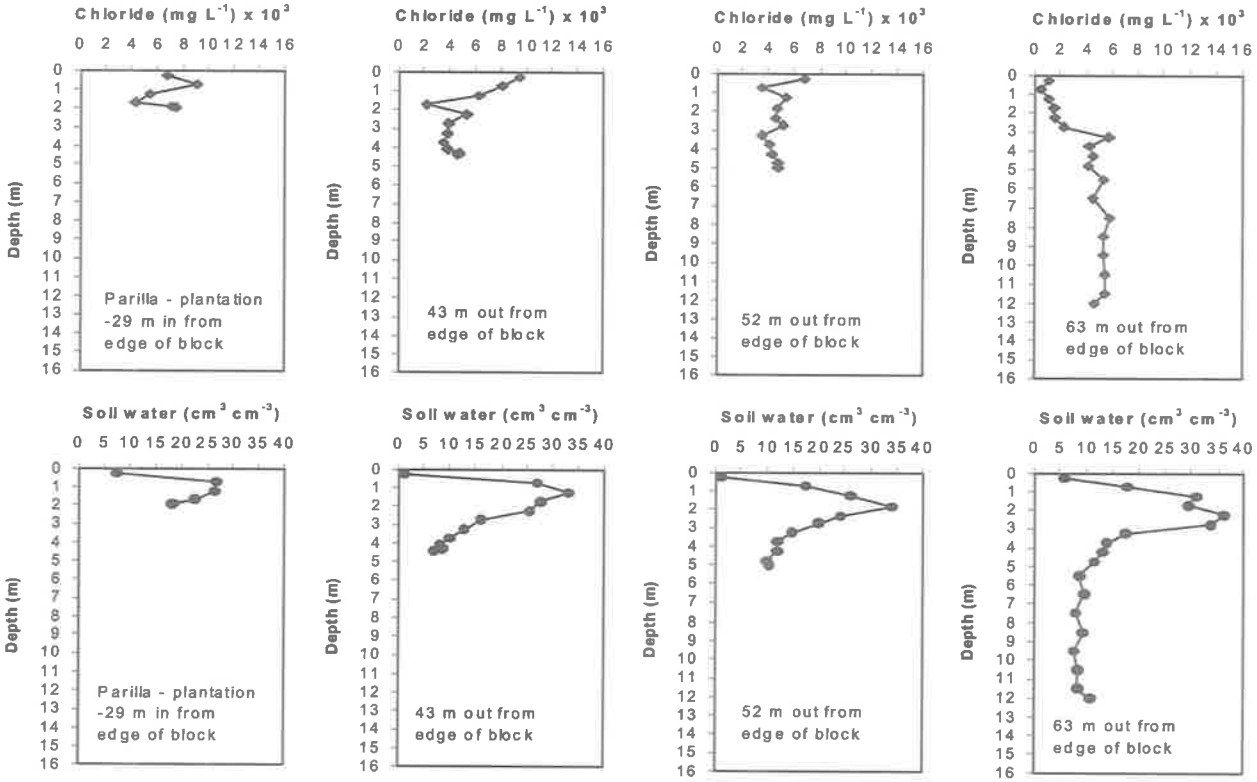

Figure 107 Soil chloride and soil water profiles from the salmon gum *plantation edge* at Parilla, South Australia (Figure 87). Horizontal distances are measured from the block edge rather than from the inner edge of the 5 m wide strip of enhanced edge growth. Significant leaching is evident at 63 m from the block with much lower chloride concentrations from 0 m to 2 m deep compared to the other profiles. Stored soil water progressively increases with horizontal distance from the block. Figure 113 shows the recharge transect for the site.

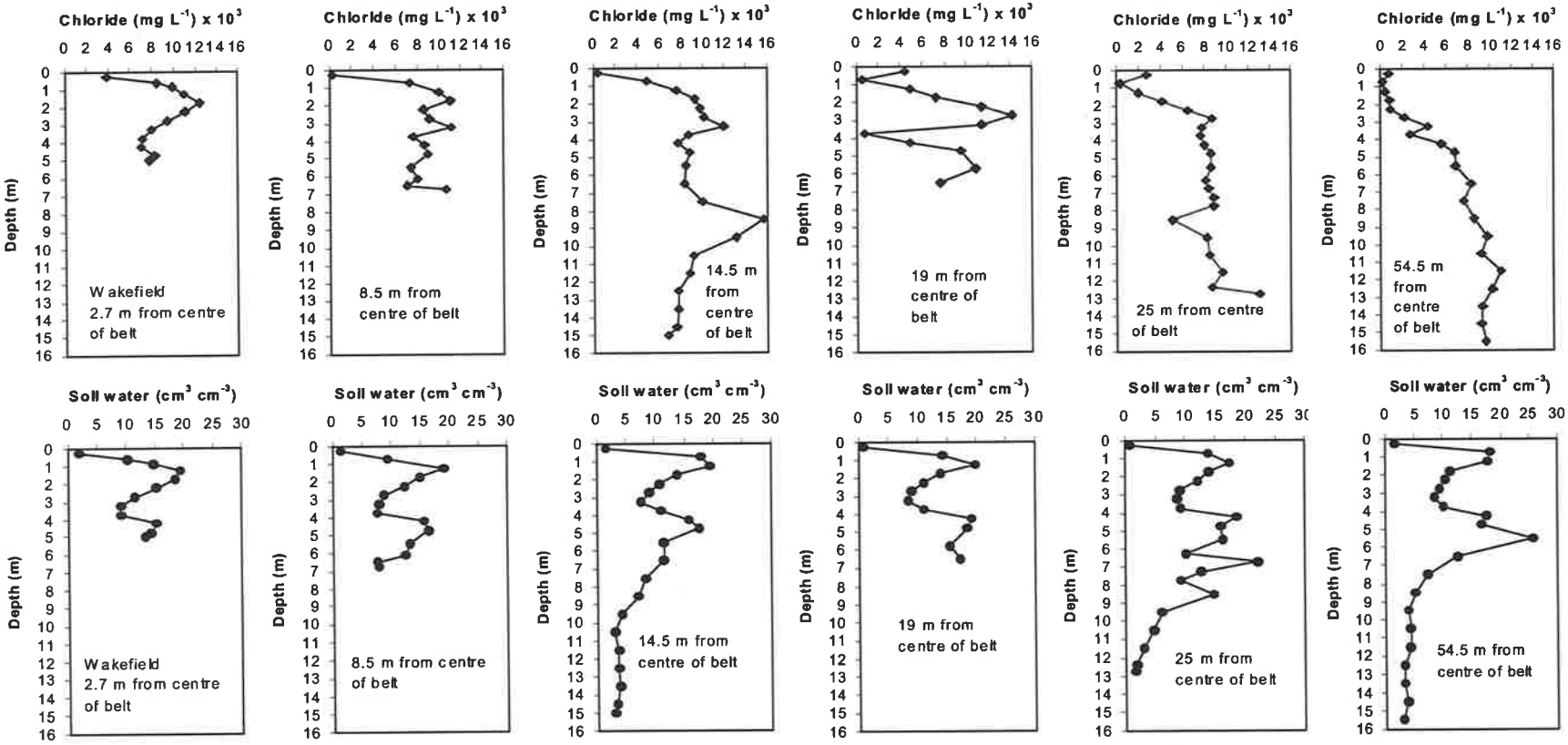

Figure 108 Soil chloride and soil water profiles from "Wakefield's" *remnant belt* at Walpeup, Victoria (Figure 88). The level of leaching of the chloride profile, relative to the non-leached profile at 2.7 m from the belt, can be seen to progress with horizontal distance from the tree belt. The associated increase in water stored below 3 m is obvious at 25 m and 54.5 m from the belt. Figure 114 shows the recharge transect for the site.

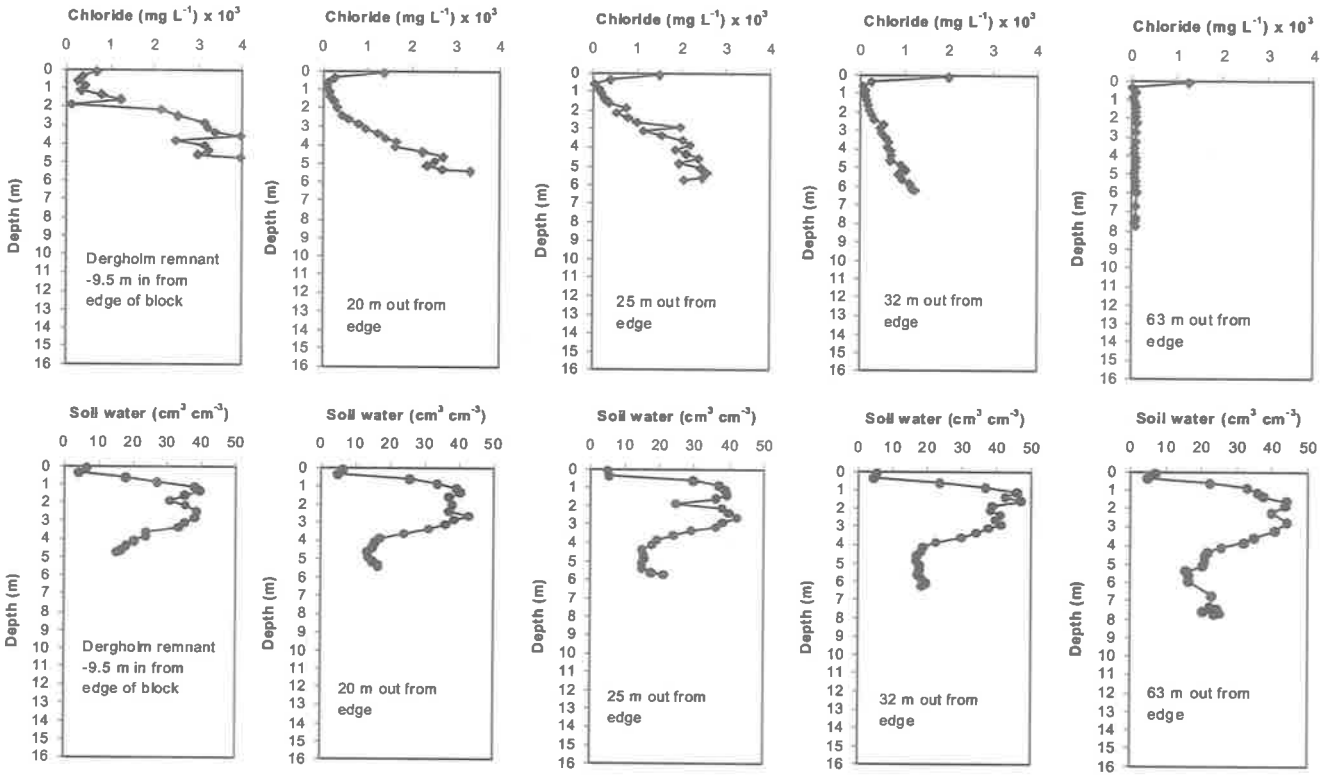

Figure 109 Soil chloride and soil water profiles from a remnant *block edge* at Dergholm, Victoria (Figure 90). Leaching in the pasture paddock is large (as is shown 63 m from the block edge) due to high sand content of the soil and 701 mm average annual rainfall. Profiles were not deep enough to reach the displaced chloride fronts at 25 m, 32 m and 63 m. Minimum values only can therefore be calculated at these positions. This however, does not seriously effect the estimation of *B* (Figure 115).

Recharge transects

This section presents the recharge values calculated from the soil chloride profiles in the previous section, represented as recharge transects for each of the profiles investigated in Chapter 5. The order of presentation is the same as that in the previous section. Additional comments regarding the transects accompany each figure; "Change in surface cover" refers to the point on the transect at which there was an obvious change in the long-term soil surface cover of pasture, weeds, stubble etc. This is used as additional information, when required, for estimating the extent of the root zone influence. A detailed explanation of the calculation of B and the associated errors for each transect is given in Appendix 4.

The following assumptions were applied when plotting the recharge transects in the previous section. Possible errors resulting from these assumptions are reflected in the calculation of B for each site (Appendix 4).

1. Chloride profiles were positioned to allow adequate definition of the transition from (low) recharge within the root zone to (higher) recharge beyond the influence of the root zone.
2. Where a chloride profile was insufficiently deep (due to hard soil conditions) to obtain a C_d value, it could be estimated from other nearby profiles.

Where a chloride profile was no obtainable beneath remnant vegetation, recharge was calculated by the mass balance technique.

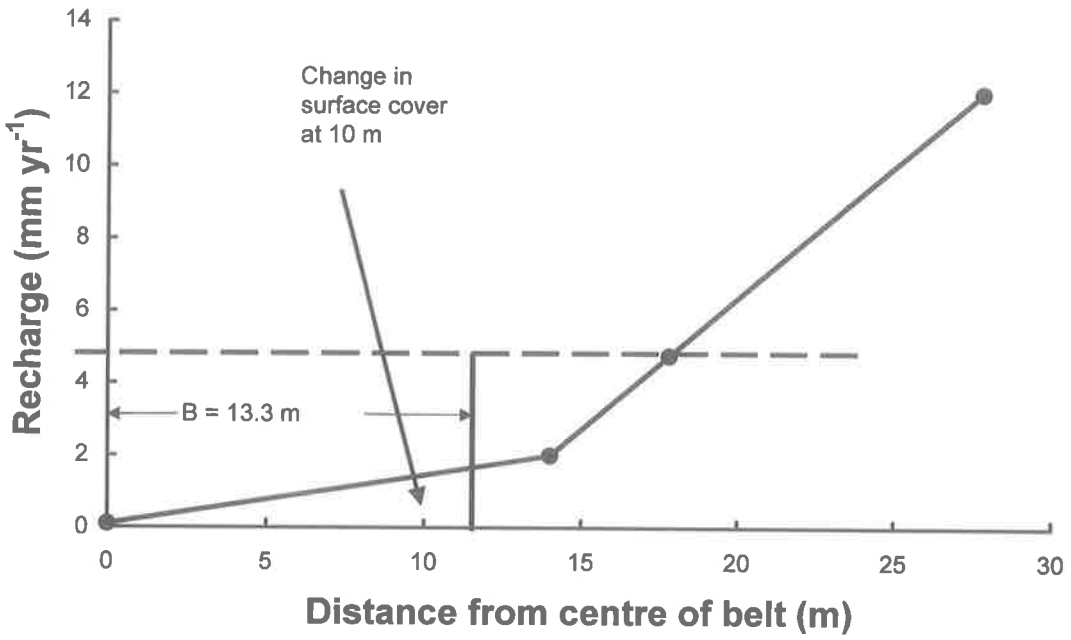

Figure 110 Recharge transect from a 7 m wide (stem to stem) *remnant belt* at Kimba, South Australia. Recharge values were calculated from soil chloride profiles. Horizontal distances are measured from the centre of the belt.

Comments: The site is shown in Figure 82; the chloride profiles are shown in Figure 104. No chloride profiles were obtainable within, or close to, the tree belt because of very dry, hard, sandy soil that could not be extracted with the auger. It was assumed that recharge in this zone was dominated by the presence of the trees and recharge was estimated using the mass balance method. The three remaining data points make a rigorous calculation of B difficult. Recharge outside the influence of the trees was assumed to be 5 mm yr^{-1}, at 17.8 m from the belt centre. B was calculated to be 13.3 ± 1.8 m for one side and was assumed to be symmetrical on the other, giving a total B of 26.6 ±4 m. Rationale for this decision is discussed in Appendix 4 in the error analysis.

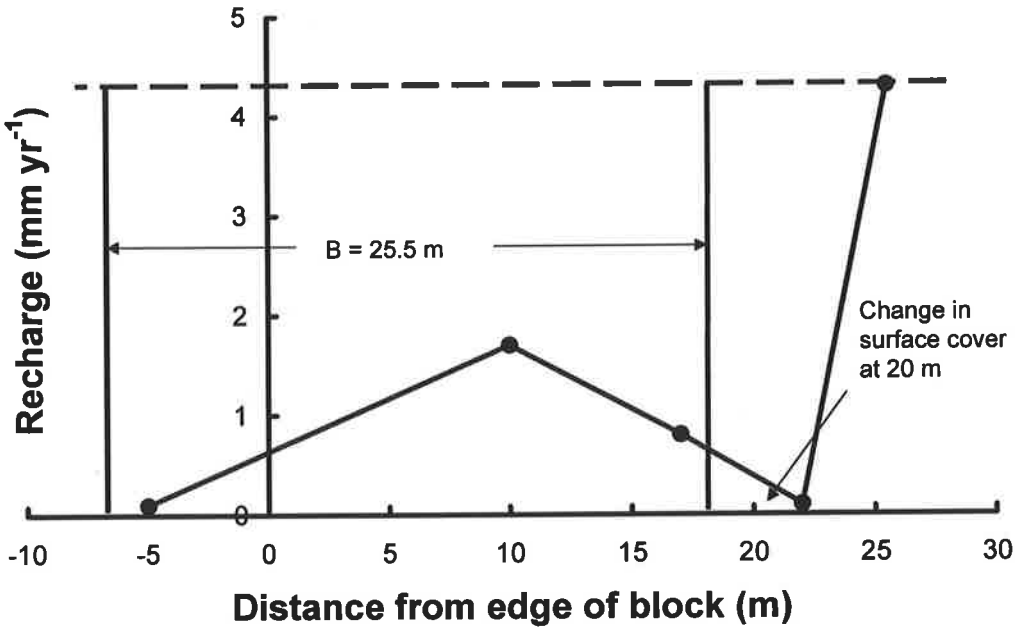

Figure 111 Recharge transect from the *remnant block edge* at Kimba, South Australia. Recharge values were calculated from soil chloride profiles. Horizontal distances are measured from the block edge.

Comments: The site is shown in Figure 83; the chloride profiles are shown in Figure 105. A chloride profile was not obtainable from within the vegetation due to hard, dry, sand soil conditions that made only surface samples procurable. The surface soil was wind-blown deposition and therefore was considered to be an unreliable indicator of soil chloride. It was assumed that recharge in this zone was dominated by the presence of the trees and recharge was estimated using the mass balance method. Rationale for this assumption is discussed above under 'Mass balance technique'. *B* was calculated to be 25.5 ±1.5 m.

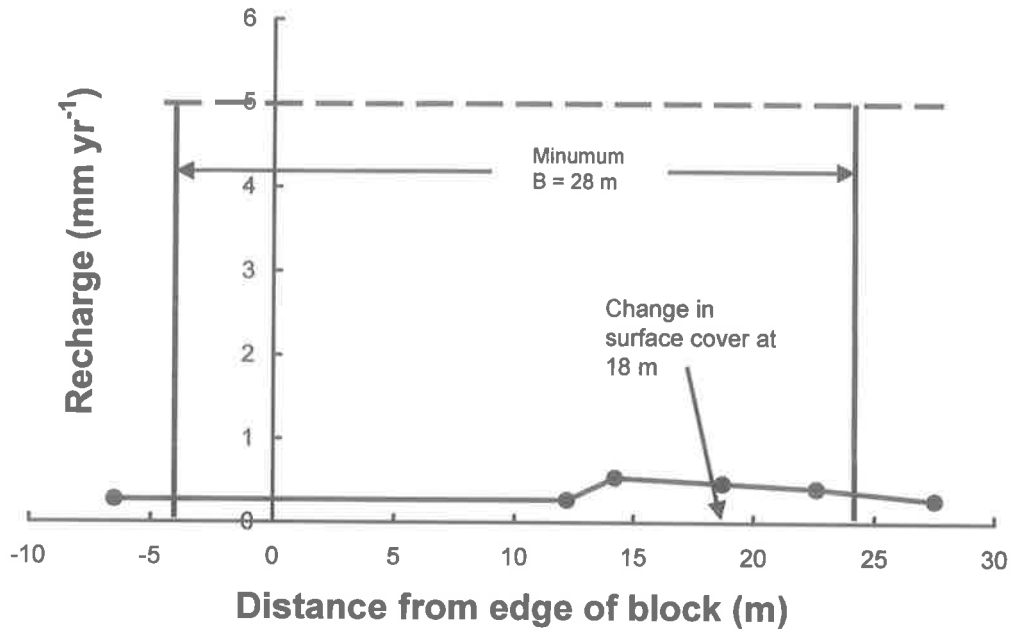

Figure 112 Recharge transect from *remnant block edge* block at Parilla, South Australia calculated from chloride profiles. Horizontal distances are measured from the edge of the block.

Comments: The site is shown in Figure 85; the chloride profiles are shown in Figure 106. No chloride profiles appear to have been sited beyond the influence of the tree roots and therefore only a minimum *B* can be calculated. *B* extends 24 m from the edge of the block, and includes the 4 m width of enhanced edge growth, therefore giving a value of 28 m. This was calculated assuming that recharge outside in the cropping zone was 5 mm yr^{-1}; this calculation is not very sensitive to the magnitude of the assumed value.

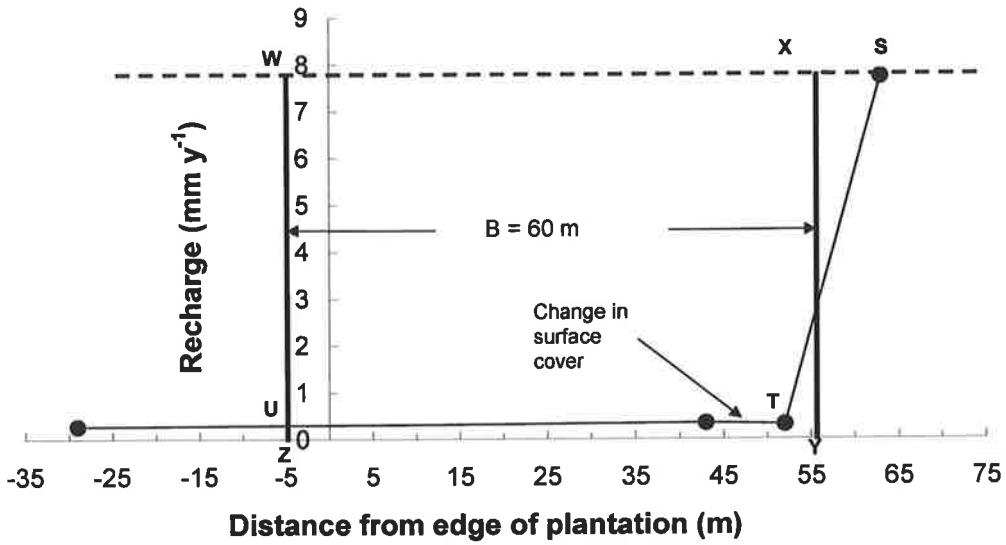

Figure 113 Recharge transect from the *plantation edge* at Parilla, South Australia. Recharge values were calculated from chloride profiles. The horizontal distance is measured from the edge of the plantation.

Comments: The site is shown in Figure 87; the chloride profiles are shown in Figure 107. The 60 m *B* is calculated from the inner edge of the 5 m edge strip of enhanced growth, such that the area of rectangle WXYZ is equal to the area of the trapezium WSTU. The *B* therefore extends 55 m from the edge of the block. No error was attached to this estimate (see Appendix 4).

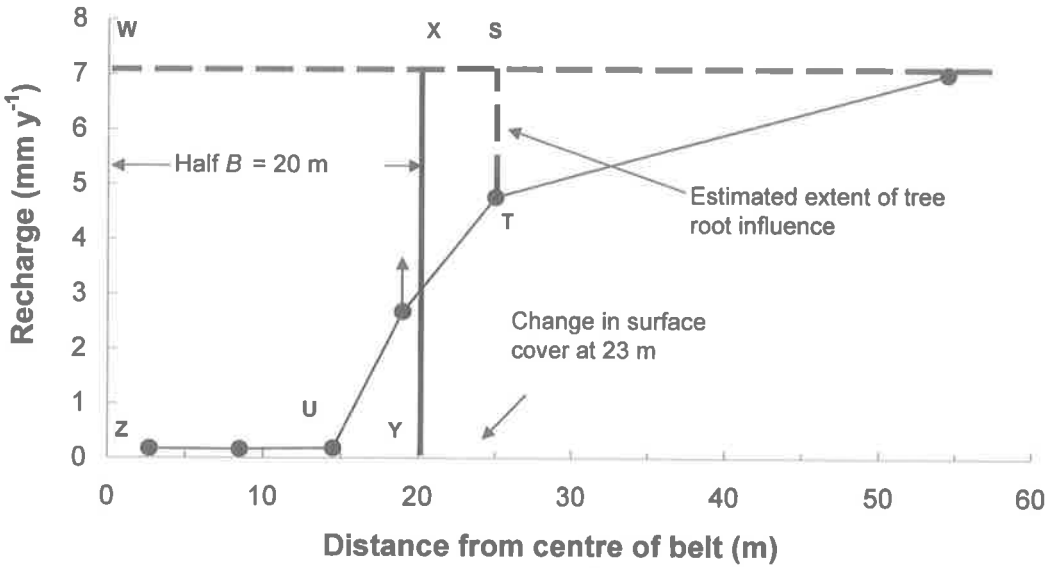

Figure 114 Recharge transect from one side of an 8 m wide *remnant belt* at "Wakefield's", Walpeup, Victoria Recharge values were calculated from chloride profiles. Horizontal distances are measured from the centre of the belt.

Comments: The site is shown in Figure 88; the chloride profiles are shown in Figure 108. The profile at 18 m was insufficiently deep to calculate the full recharge value so the upward arrow denotes the data point representing the minimum value, although is would be close to the value shown. Cropping zone recharge was taken as 7 mm yr^{-1}; the edge of the influence of the tree roots was assumed to be at 25 m (line ST) given the change in ground cover at this point (Table 2). *B* was calculated to be 20 ±1 m such that rectangle WXYZ has equivalent area to WSTUZ. This value is relatively insensitive to the assumed extent of the root influence. This transect represents only half of the *B* for the belt since below ground effects are assumed symmetrical on the other side of the belt. *B* for the whole belt is therefore 40 ±2 m.

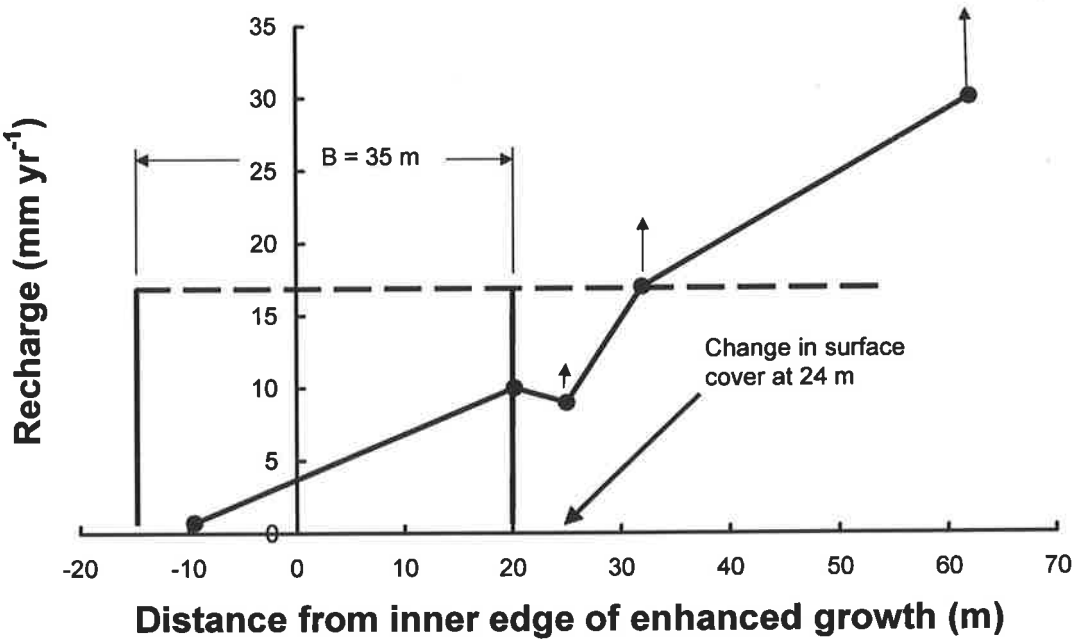

Figure 115 Recharge transect from the remnant block edge at Dergholm, Victoria. Recharge values were calculated from chloride profiles. Horizontal distances are measured from the edge of the block.

Comments: The site is shown in Figure 90; the chloride profiles are shown in Figure 109. Upward arrows on data points at distances 25 m, 32 m and 63 m denote profiles that were insufficiently deep (due to hard soil conditions) to calculate the whole recharge value. These three data points therefore represent the minimum recharge at these points. Recharge outside the influence of the trees was assumed to be 17 mm yr^{-1} (32m from the block edge) but was probably higher. Calculation of *B* is relatively insensitive to this assumed value, especially given that the slope of the recharge transect is steeper than shown. In hindsight, more data points were required within the root zone of the trees (between 0 m and say 20 m), their absence leading to a likely overestimate of *B*. The strip of enhanced edge growth was 15 m wide and *B* was calculated to be 35 ± 5 m, therefore extending 15 ±5 m from the belt edge.

Soil physics - estimates of K_{unsat}

In the water balance experiment (Chapter 6) drainage below 2 m was assumed to be negligible for two reasons: to allow the efficient calculation of evaporation E by difference outside the root zone ($E = P - \Delta S$); for comparing measured transpiration T with transpiration calculated by difference ($T = P - E - I - \Delta S$), applied over the root zone. This assumption was shown to be valid using the following calculations.

From Bond (1998) Darcy's law for unsaturated flow q in soil can be written as:

$$q = \frac{-K_\theta[\Delta h_\theta + \Delta z]}{\Delta z} \qquad \text{(Equation 2, Chapter 3)}$$

where q is flow rate (mm d^{-1}) and θ refers soil water content; K_θ and h_θ are hydraulic conductivity and suction, both dependent on water content; z is soil depth (m). If $\Delta h(\theta)$ is close to zero then $q \approx -K$. This condition could be considered to be approximated at a depth of about 2 m because at this point: θ does not vary greatly with depth in March 1998, when the profile is wettest (Figure 38); soil texture is relatively constant with depth (Figure 94).

Campbell (1974) showed that K (cm min^{-1}) could be estimated from moisture retention data

$$K = K_s\left(\frac{\theta}{\theta_s}\right)^{2b+3} \qquad (32)$$

where: K_s is saturated hydraulic conductivity; θ_s is saturated water content; and b is an exponent estimated from Equation 33 (Smettem *et al.*, 1999):

$$b = \frac{1}{[-0.25\log(\%clay) + 0.5]} \qquad (33)$$

Smettem and Bristow (1999) derived an expression for K_s (mm hr^{-1}):

$$K_s = 9.7\times10^9 a h_b^{-2} \qquad (34)$$

Where h_b (mm) is the to bubbling pressure head (Smettem *et al.*, 1999) and can be estimated from b

$$h_b = 43.5\times b \qquad (35)$$

Combining Equations 32, and 34, and accounting for the differences in units, gives an expression for K (mm hr^{-1}) in terms of h_b

$$K = \frac{10}{60} \times 9.7 \times 10^9 a h_b^{-2} \left(\frac{\theta}{\theta_s}\right)^{2b+3} \quad (36)$$

Smettem and Bristow (1999) give a = 3.7×10^{-5}; % clay at a depth of 2 m is about 50% (Figure 94), therefore b and h_b are 13.3 and 578 mm, respectively; θ at a depth of 2 m is about 30% and 25% outside and inside the root zone, respectively; θ_s was measured to be about 40% during the 'wet' calibration for the neutron moisture meter. Using Equation 36, K at a depth of 2 m was estimated to be 1.2×10^{-6} mm hr^{-1} and 5.0×10^{-9} mm hr^{-1}, outside and inside the root zone, respectively. Both of these values are negligible and equate to 0.01 and 4 x 10^{-5} mm yr^{-1}.

Transpiration measurement using heat pulse sap flow

Sapflux (volume flow per unit time) is the product of xylem sapflow velocity (sapflux density) and the cross sectional conducting wood area of the tree. The heat pulse, or *compensation*, method measures sapflow velocity by timing the progression of a small pulse of heat injected into the conducting wood of the tree. This is described in detail in "Sapflow Measurement with the Greenspan Sapflow Sensor: Theory and Technique" document on the Greenspan® website.

http://www.greenspan.com.au/saptheory.pdf

The following italicised text and equations is a modified excerpt from the afore-mentioned document, reproduced here with kind permission from Greenspan Technology Pty Ltd. Calculations have been performed using data from the water balance experiment (Chapter 6). This provides an example calculation of instantaneous sap flux from initial heat pulse times, through to instantaneous sap flux. Transpiration is then calculated as the total sap flux over a period, estimated from instantaneous sap fluxes measured and logged at 30 min intervals and downloaded periodically (Figure 118). Transpiration is later expressed as a flux density; either mm d^{-1} m^{-2} leaf, or mm d^{-1} m^{-2} ground area.

> *The Sapflow Sensor utilises two probe sets, each with a heater probe and two sensor probes (Figure 116). The upstream sensor probe is located 5 mm below the heater probe and the downstream probe is 10 mm above the heater probe. On each sensor probe there are one or two thermistors (sensors). The first thermistor is positioned 5 mm from the end of the probe, the second is 5 mm behind the first. Thermistors are paired on the vertical plane to facilitate the measurement of sap flow velocities.*

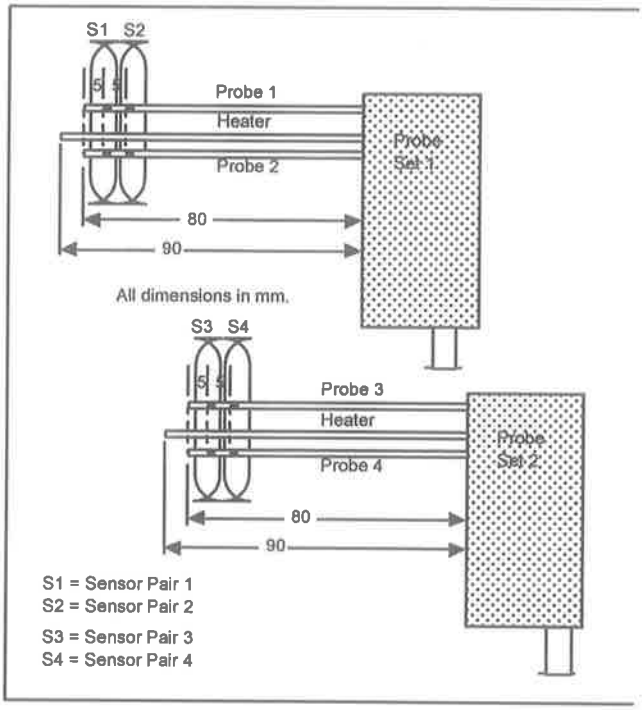

Figure 116 Schematic diagram of Greenspan heater probe sets.

The time taken for a pulse of heat to reach any point downstream is a function of both the conduction of the heat through the wood (i.e. diffusion) and the convection of the pulse by moving sap. Following the release of a pulse of heat from the heater probe, the closer upstream probe p2 warms with diffusion. Warming of p2 by convection cannot occur as sapflow direction is from p2 to the heater probe. The upstream probe warms above the baseline temperature where both sensor probes are in equilibrium (Figure 117) and there is a positive difference in temperature between the upstream probe and the downstream probe p2. The temperature difference p1-p2 peaks and then as the pulse moves downstream, with diffusion and any convection, declines as p2 warms. The differential returns to zero at T2, where the system has returned to a balance. If convection is occurring the temperature differential will become negative as p1 cools and p2 continues to warm.

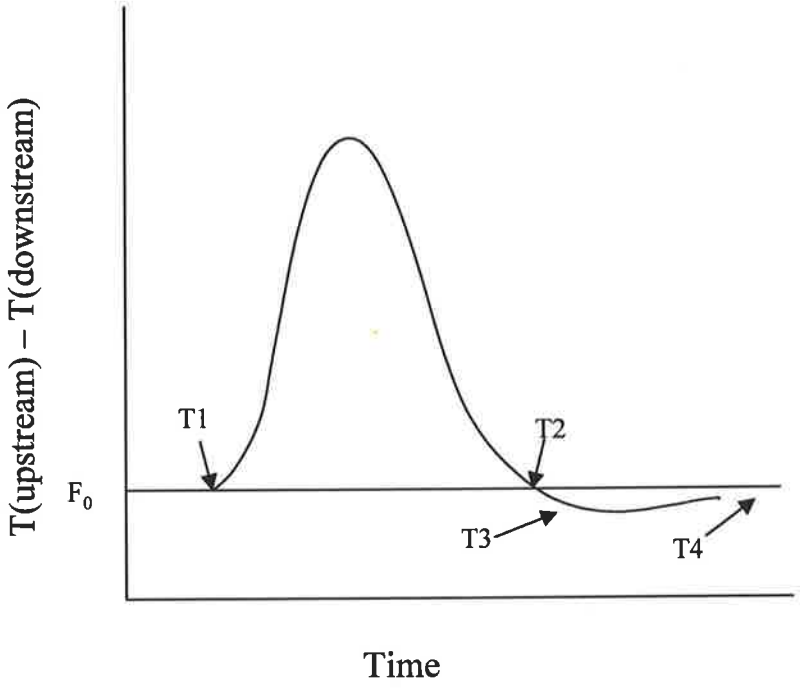

Figure 117 Change in the difference between the temperatures recorded at probes in upstream and downstream positions in the sapwood following the heat pulse at time T1.

Figure 118 Rebecca Sherman downloading heat pulse data from a Greenspan logger. Heater probes were installed and insulated with aluminium foil. Data was logged every 30 min and downloaded every 2 to 4 weeks.

Calculating Sapflow

Calculating the Heat Pulse Velocity

Heat pulse velocity is calculated from the time to reach T2, known as the heat pulse time (Figure 117). At this point the heat pulse has moved to a midpoint between the probes and the formula for heat pulse velocity V_h *is*

$$V_h = \frac{x_1 + x_2}{2t_0} \qquad (37)$$

where: x_1 *and* x_2 *represent the distances of the upstream and downstream sensors respectively from the heater, and* t_0 *is the time to T2, or the heat pulse time (*Closs, *1958).*

A negative value is assigned to x_1 *because of its position upstream from the heater probe.*

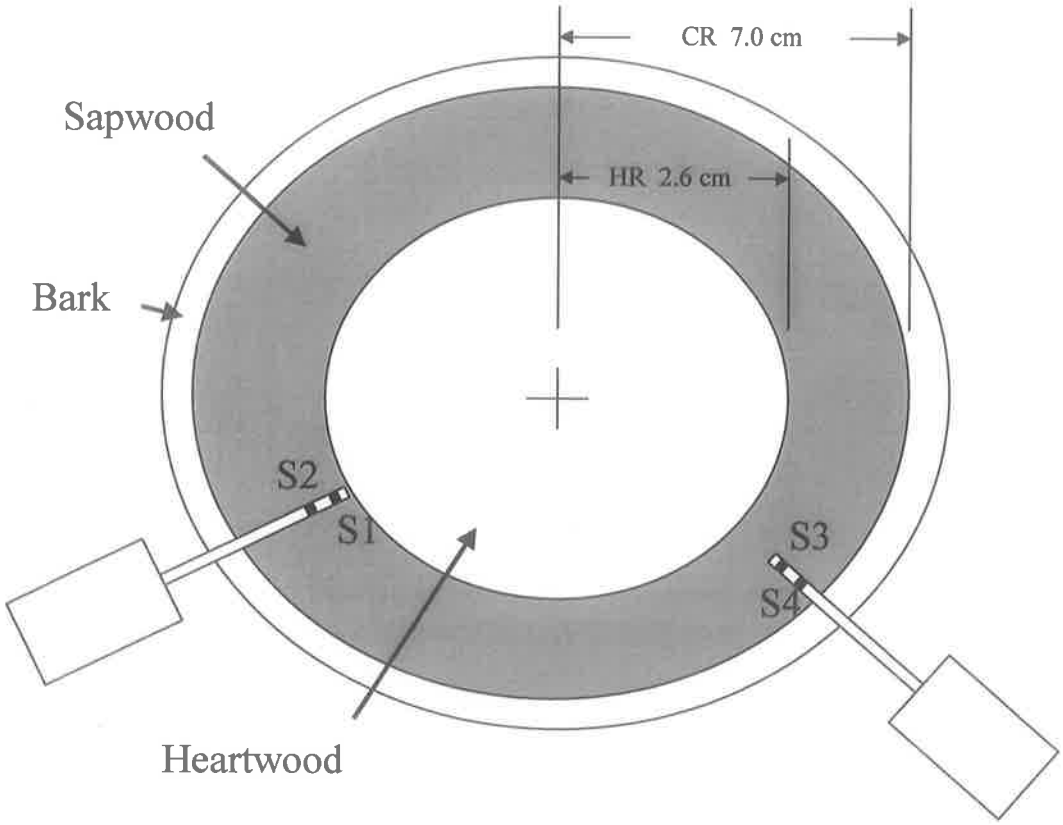

Figure 119 Cross-section of tree showing heartwood radius *HR* and cambium radius *CR*. Two probe sets are installed with two sensor pairs each (S1, S2, S3, S4) measuring sap velocity at four different sapwood depths.

To illustrate the calculations, data and tree parameters from tree L1 (Water balance experiment, Chapter 6) are used. Figure 119 shows 2 probe sets implanted in tree L1,

measuring sap velocity at 4 positions across the sapwood. Table 10 gives T2, and V_h at each point in the sapwood at one point in time on an autumn afternoon in 1997.

*Convection of the heat pulse is affected by the different thermal properties of the heater and sensor probes in comparison with wood, and by the damage to nearby xylem vessels due to drilling of the holes for probe insertion (*Barrett *1992). A numerical solution (*Swanson and Whitfield, *1981) is applied to correct heat pulse velocity V_h for wounding:*

$$V'_h = a_0 + a_1 V_h + a_2 V_h^2 \qquad (38)$$

where

V'_h is the corrected heat pulse velocity and the coefficients;

*where a_0, a_1, and a_2 are coefficients specific to a given wound diameter (*Swanson and Whitfield, *1981).*

The wound diameter was assumed to be equivalent to the probe diameter (0.22 cm). Greenspan® SAPCAL software provides values for a_0, a_1, and a_2 as –0.879, 2.544, and 0.005, respectively. Table x shows V'_h values calculated using V_h and the above wound coefficients.

Calculating the Sap Velocity

To convert the corrected heat pulse velocity V'_h to sap velocity Vs it must be translated on an areal basis. From Marshall *(1958),*

$$V_s = aV'_h \qquad (39)$$

*where **a** is the lumen area of the sapwood. Lumen area is not readily established without destructive sampling, and* Marshall *(1958) proposed further modifications, and together with work by* Edwards and Warwick *(1984), the following expression can be derived.*

$$V_s = V'_h\left(0.505F_m + F_w\right) \qquad (40)$$

Where F_m and F_w are, respectively, the sapwood volume wood and water fractions.

Table 10 Heat pulse times T2, heat pulse velocities V_h, and corrected heat pulse velocities V'_h at one point in time for tree L1 on at 2 pm, March 14 1997.

	S1	S2	S3	S4
T2 (sec)	100	73	94	149
V_h ($cm\ hr^{-1}$)	9.0	12.3	9.6	6.0
V'_h ($cm\ hr^{-1}$)	22.4	31.2	23.9	14.7
V_s ($cm\ hr^{-1}$)	14.6	20.4	15.6	9.6

Wood and water fractions were measured but were considered unreliable, possibly due to the heating of the sample during extraction from the tree, using a powered hole saw. Instead, default values were used: $F_m = 0.5$; $F_w = 0.4$.

Calculating the SapFlow Volume

The final point of interest to most workers is not sapflow velocity, but rather the volume of sap flow (or sap flux) through the stem. Sap flux in litres per unit time Q is a function of the velocity of sap flow and the area over which the flow occurs,

$$Q = \overline{V}_s A_s \tag{41}$$

where A_s is conducting wood (sapwood) area (Closs, 1958) and $\overline{V}_s$ is the average sap velocity. The simplest method of calculating $\overline{V}_s$ is by weighted area technique (Hatton *et al.,* 1990). The four point estimates of V_s are sampled from a sap velocity profile (Figure 120) across the sapwood which must be converted to an average sap velocity. The weighted area technique assigns each V_s to the area of sapwood it can be considered to represent.

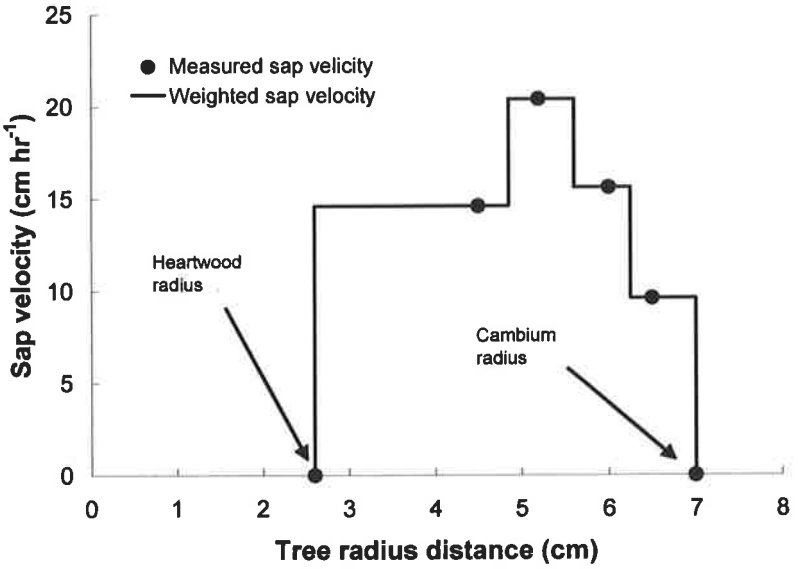

Figure 120 An instantaneous sap velocity profile from tree L1 (Water balance experiment, Chapter 6). Point velocities (•) from heat pulse measurements were converted to a weighted average (solid line), weighting factors are given in Table 10.

Weighting factors (Table 11) for each V_s are calculated from: cambium radius CR; heartwood radius HR; and sensor positions (Figure 119).

Table 11 Sensor positions of probes placed in tree L1 and associated weighting factors used to calculate $\overline{V}_s$ from point measurements of V_s.

	S1	S2	S3	S4
Sensor position on tree radius (cm)	4.5	5.2	6.0	6.5
Weighting factor	0.51	0.17	0.15	0.17

$\overline{V}_s$ is calculated:

$\overline{V}_s = (0.51 \times 14.6) + (0.17 \times 20.3) + (0.15 \times 15.6) + (0.17 \times 9.6) = 14.9$ cm hr^{-1}

Sapwood area A_s calculated from CR and HR (Figure 119) is about 0.13 m^2 therefore:

$Q = 0.13 \times 14.9 = 1.9$ litres hr^{-1}.

This is an example of an instantaneous sap flux in tree L1 at that point in time. The tree transpired for about 12 hours per day (approximately daylight hours) at this time of year. For the purposes of the example, if Q is assumed to be constant for the 12 hour period then

the daily sap flux would be about 23 litres d^{-1}. The leaf area of tree L1 was 46 m2 therefore the transpiration efficiency was 0.5 litres d^{-1} m^2 leaf.

Calculations of all sap flow calculations in this study were performed using a Microsoft Excel macro written by Peter Taylor (see Taylor, 1999).

Microlysimeter construction and installation

Soil conditions were often hard, so a metal construction was chosen for the microlysimeters, rather than PVC. Since the microlysimeter measurements were used for scaling evaporation in the root zone, relative to the more accurate P - ΔS, the thermal properties of the construction material were not a concern (Evett *et al.*, 1994). Inner rings were 50 mm long, 75 mm diameter brass tube with a 1.6 mm thick wall (Figure 121).

Figure 121 Microlysimeter installed. The inner ring was first pressed into the soil nearby, trimmed, sealed on the bottom face, and placed inside the outer ring, level with the surrounding soil surface.

The rings were pressed into the soil, rather than hammered (to minimise surface disturbance, Figure 122), using a lever anchored to a post, then dug out, trimmed and sealed on the bottom side with tight aluminium caps. They were then weighed and placed in a 100 mm diameter hole in the soil surface, lined with steel exhaust tubing. All 15 microlysimeters were weighed, remade and replaced every 24 to 48 hours or after rain. The shallow depth and short measurement periods were chosen because soil water content changed rapidly within the tree root zone.

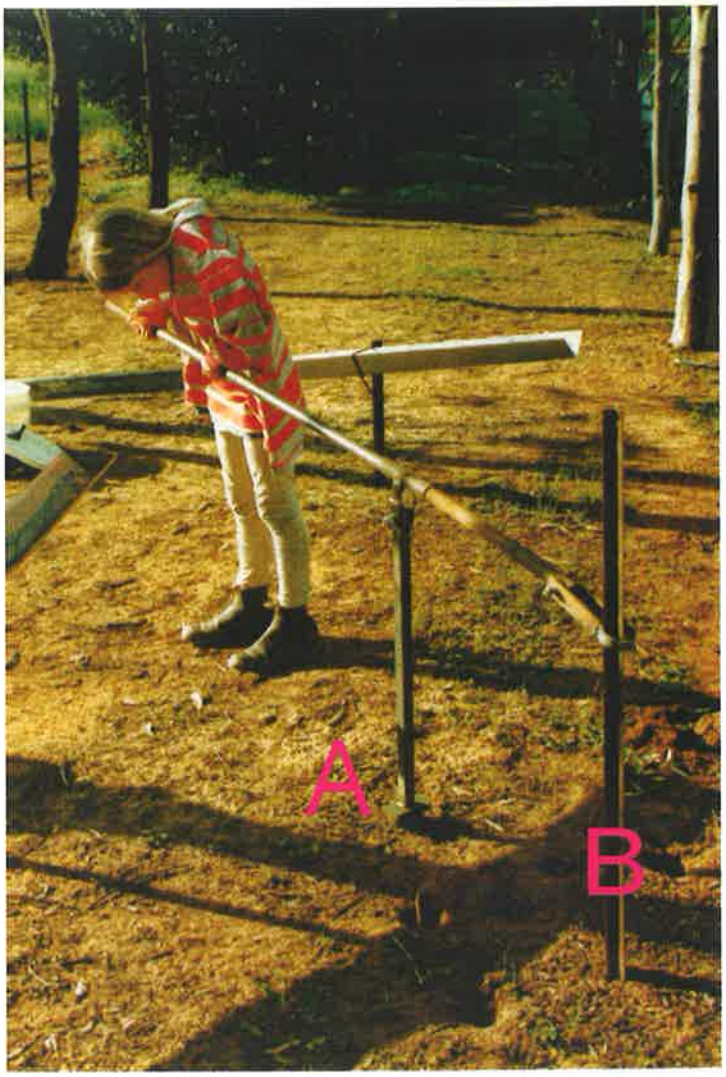

Figure 122 Hannah Ellis pressing the inner ring of a microlysimeter (A) into the soil using a lever mechanism with temporary anchor (B). Rings were subsequently removed, trimmed and weighed before placement in outer ring nearby (Figure 121).

Appendix 3 – calibrations

Introduction

This appendix shows the derived relationships and the apparatus used to calibrate: the Adelaide (module) method of leaf area estimation (Figure 123; Figure 124); rainfall trough and bucket gauges (Figure 125; Figure 126); neutron moisture meter (Figure 127; Figure 128); and stem flow apparatus (Figure 130; Figure 131).

Leaf area estimation

The leaf area of three trees was first estimated using the Adelaide (module) technique (Andrew *et al.,* 1979). The complete canopies were then destructively sampled (Figure 123), weighed, and the leaf area of each canopy was calculated from the average area of 3 sub samples measured using an electronic planimeter (Figure 124).

Figure 123 One of the three trees used to calibrate the leaf area estimation method *(*Andrew *et al.,* 1979*)* The picture shows the leafless branches of the 'middle-sized' tree, remaining after destructive sampling of complete canopy.

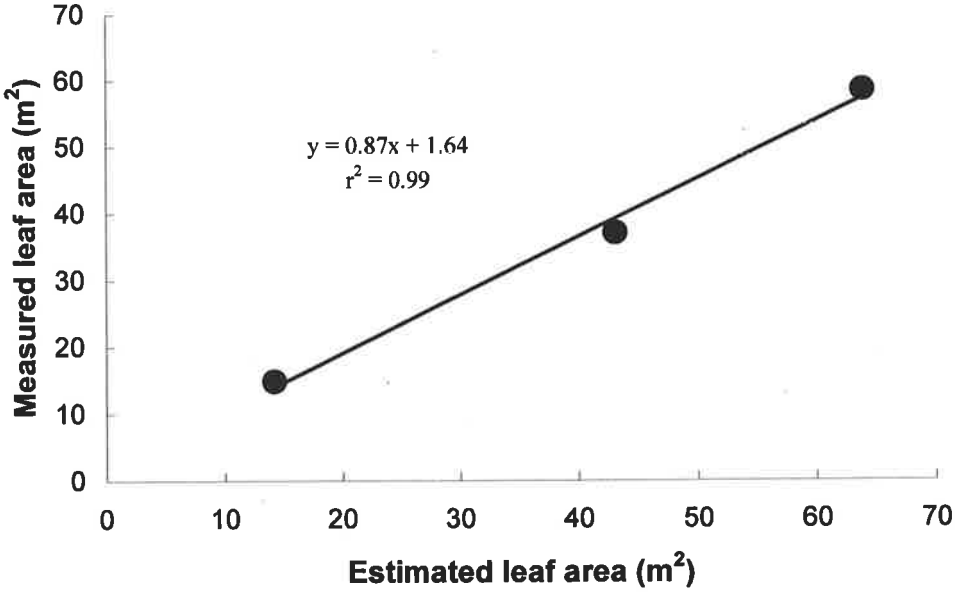

Figure 124 Calibration data for the Adelaide (module) method (Andrew *et al.* (1979) of leaf area estimation. Three complete tree canopies were destructively sampled.

Trough and bucket rain gauge

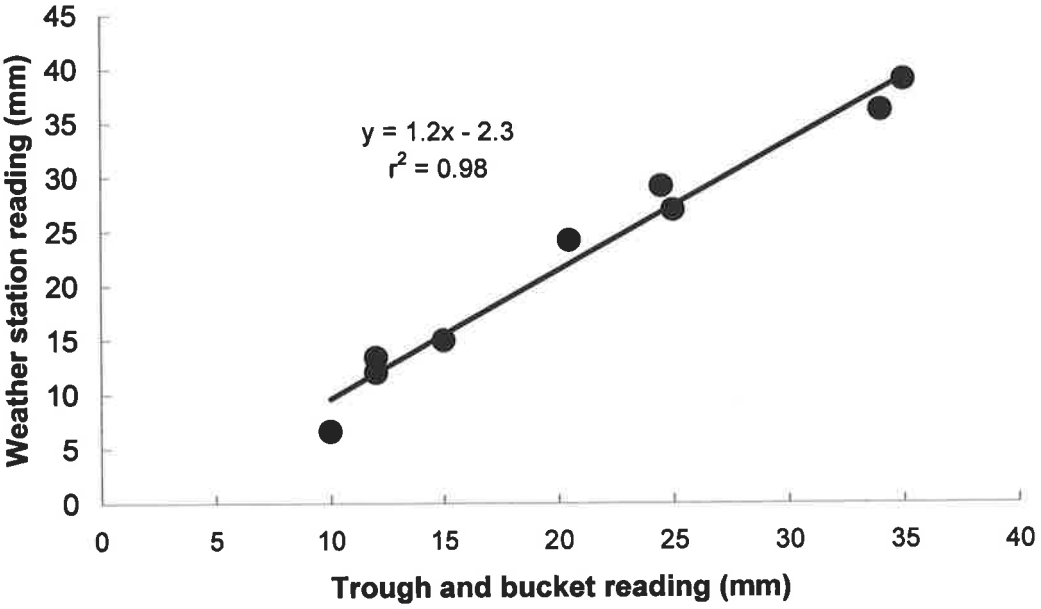

Figure 125 Data from the trough and bucket rain gauge calibrated against weather station tipping bucket gauge (Measurement Engineering Australia™).

Figure 126 Trough and bucket rain gauge were constructed from steel sheeting bent to form a 'V'-shaped channel, supported at one end by a post. The other end grained into a plastic funnel glued into the lid of a plastic 20 L bucket. Twenty identical gauges were used to measure rainfall and throughfall transects across the tree belt used in the water balance experiment. Placement, materials and dimensions of the gauges are provided in the Methods section of Chapter 6.

Neutron moisture meter NMM

The sampling strategy for the neutron moisture meter calibration (Figure 127) is described in Chapter 6. The procedure used for wetting the soil prior to 'wet' sampling is illustrated in Figure 128. The 'wire-line' sampling apparatus is shown in Figure 129.

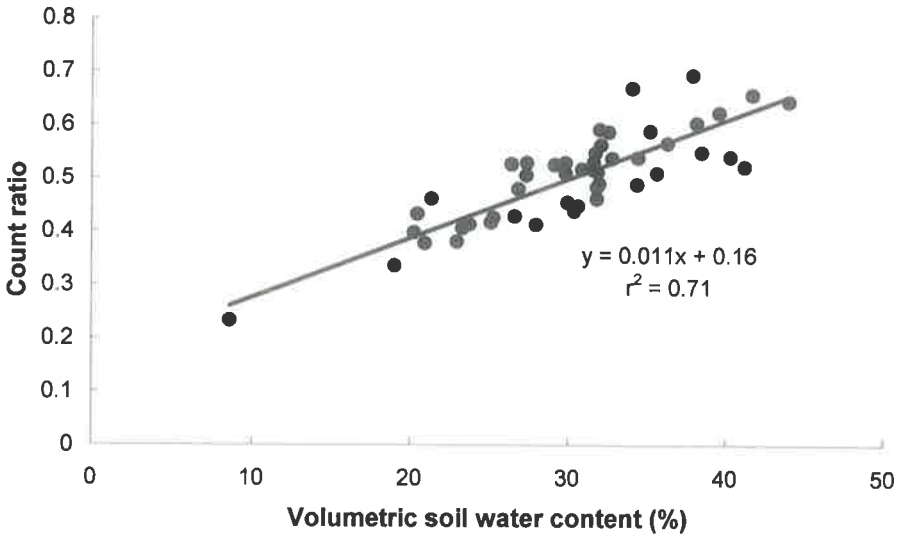

Figure 127 Neutron moisture meter calibration relationship from combined data gathered from 4 tubes. One relationship was used to represent all soil layers between the soil surface and a depth of 5.9 m.

Figure 128 George the dog (*Canis familiaris*) during the wetting-up of the soil surrounding the neutron moisture meter access tube, two weeks prior to soil sampling for 'wet' calibration.

Figure 129 Mr Thompson operating the CSIRO drilling rig with 'wire line' equipment, used for extracting soil samples both 'wet' and 'dry' neutron moisture meter calibration. Samples are taken using a 74 mm diameter, 1 m long split tube fitted to the tip of the hollow-stemmed auger and retrieved via a cable.

Stem flow

Stem flow is the small fraction of rainfall that runs down the outside of tree branches and is concentrated around the stem. Figure 130 shows a rubber channel attached to a tree stem at the water balance experimental site (Chapter 6) to catch stem flow and guide it into a bucket. Stem flow was not measured on the same trees as the transpiration measurements (L1, L2, O1, O2) because the installation of the sap probes interrupted flow down the stem. Figure 131 gives the relationship derived from measurements made on another 6 trees in the same belt, and used to scale stem flow to leaf area, and therefore estimate stem flow for L1, L2, O1 and O2.

Figure 130 Apparatus used to measure stem flow in water balance experiment. Rubber channel was attached to stem in a helix to direct flow into a bucket. Stem flow volume was measured using a calibrated dipstick.

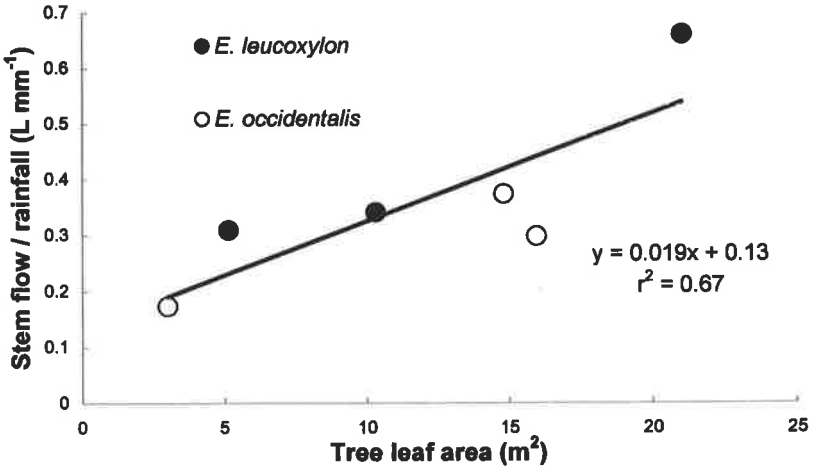

Figure 131 Relationship between stem flow and tree leaf area for the two species at the water balance experimental site. The fitted linear relationship was used to represent stem flow from both species.

Appendix 4 – error analyses

Introduction

This appendix considers, in turn, all significant likely errors associated with the measurements made in Chapters 5 and 6 that are used to calculate *B*. The largest likely error is selected and used to calculate the 'worst-case scenario' errors likely in the results of both experiments.

Recharge transect experiment

Leaf area

The Adelaide (module) technique for leaf area estimation (Andrew *et al.,* 1979) was calibrated of by the destructive sampling of three complete tree canopies (Appendix 3). Likely errors of this method were estimated to be less than 10% (Figure 124) and were similar to those of Hatton *et al.* (1995). Conversion to *LLA* and *LAI* values involved division by a measured length and area, respectively, for which the error is likely to be in the order of 1%. The maximum likely error for *LLA* and *LAI* was therefore assumed to be 10%.

Equation 12 was used to predict *B*, therefore maximum and minimum *B* values were calculated for each site by using respectively: the largest *LLA* and smallest *LAI*; smallest *LLA* and largest *LAI*. For the six sites this yielded: 20 ±4 m; 12 ±2.4 m; 16 ±3.5 m; 60 ±12 m; 42 ±8.4 m; 40 ±7.7 m; for the Kimba remnant belt; the Kimba remnant block edge; the Parilla remnant block edge; the Parilla plantation edge; the Walpeup remnant belt; and the Dergholm remnant block edge, respectively.

Chloride techniques

Reported errors associated with chloride techniques vary somewhat. When comparing the mass balance with a tritium tracer mass balance technique Allison and Hughes (1978) report a relative standard deviation of 15%. Walker *et al.* (1991) report a "*negligible*" difference between recharge calculated using the generalised chloride displacement technique and a profile water balance (Jolly *et al.,* 1989). However, while the accuracy of recharge estimates has some bearing on the calculation of *B* from recharge transects, a more critical factor is the positioning of the chloride profiles, as described in the following section.

Calculation of *B* from recharge transects

This section presents the rationale for the calculation of the *B* values and likely errors from the recharge transects calculated in Appendix 2, and which are summarised in Figure 31 and also in Table 2.

The error associated with the calculation of *B* from recharge transects arise from the designation of the following two values:

1) The recharge value outside the influence of the root zone;

2) The limit of the extent of influence of the root zone.

Due to the spacing of chloride profiles, these can be interpreted as having more than one possible value, therefore producing more than one *B* value. For each recharge transect therefore, the rationale for the designation of values for 1) and 2) above, are given together with the associated maximum and minimum *B*.

Remnant mallee belt, "Cooinya", Kimba (Figure 110): The influence of the root zone is unlikely to extend beyond about 18 m, and is probably shorter, given the change in surface cover at 10 m. Soil conditions were too dry and hard for soil sampling closer to the belt then 14 m. Recharge in the centre of the belt was estimated from mass balance to be in the order of 0.1 mm yr^{-1}. There are therefore two likely extreme values for *B*. One value is calculated assuming: the root zone influence ends at 18 m; recharge beyond its influence is about 4.8 mm yr^{-1} and linear decline in recharge toward the belt centre; the other value is calculated assuming the same recharge value outside the root zone influence but 0.1 mm yr^{-1} between the belt centre and 14 m. This gives an average half *B* of 13.3 ±1.8 m.

Remnant mallee block edge, "Cooinya", Kimba (Figure 111): The abrupt recharge increase beyond the root zone influence is relatively unambiguous at 25 m. As with the salmon gum plantation site, *B* is relatively insensitive to recharge remaining constant or increasing beyond 25 m. Recharge beneath the vegetation was about 0.1 mm yr^{-1}, calculated from chloride mass balance. As with "Cooinya" remnant mallee belt, it is likely that recharge is also small close to the trees and linear interpolation between 10 m and –5 m will result in a (possibly) underestimated *B*, equal to 24 m. If recharge is assumed to be 0.1 mm yr^{-1} in this zone then *B* will be 27 m. Average *B* can therefore be considered to be 25.5 ±1.5 m.

Remnant mallee block edge – Parilla (Figure 112): At the time of sampling, the outer two chloride profiles were considered likely to be outside the influence of the root zone. However, recharge values calculated from the profiles did not support this, allowing only a minimum *B* of 28 m to be calculated. This required an assumed recharge outside the

influence of the root zone. This was chosen to be 5 mm yr^{-1} rather than the 7 mm yr^{-1} at the close by salmon gum site since the mallee transect extended toward the swale (Rowan and Downs, 1963) rather than a dune, where higher values are expected (Kennett-Smith *et al.,* 1992b). Calculation of a minimum *B* is relatively insensitive to the assumed recharge value.

Salmon gum plantation block edge, Parilla (Figure 113): This recharge transect is relatively unambiguous. The main uncertainly surrounds whether recharge beyond the influence of the root zone is adequately represented at the outer most profile. The increase in recharge at the boundary of root zone influence is relatively sharp. Recharge is unlikely to drop below this value (beyond this point) and the calculation of *B* is relatively insensitive to whether it remains constant or increases. For these reasons any error associated with the calculation of *B* for this site is considered difficult to estimate and probably negligible.

"Wakefield's" remnant mallee belt, Walpeup (Figure 114): Recharge outside the influence of the root zone is taken to be 7 mm yr^{-1}. Although no information is available between the distances of 25 m and 54.5 m from the belt centre, it is safe to assume the influence of the root zone extends only to 25 m, and definitely beyond 19 m. It is unlikely, therefore, that *B* is greater then 21 m. If recharge outside the root zone is taken to be 4.7 mm yr^{-1} at 25 m, rather than 7 mm yr^{-1}, *B* is calculated to be 19 m. Assuming this to be the maximum likely uncertainty, and applying it to the whole belt (i.e. double the *B* shown for one side of the belt) then the *B* for "Wakefield's" site is 40 ±2 m.

Dergholm remnant block edge (Figure 115): This transect presents 2 obvious uncertainties: chloride profiles outside the influence of the root zone were insufficiently deep to calculate absolute recharge; recharge values within the influence of the root zone were poorly represented in space. Neither of these uncertainties however cause a large variation in the calculation *B*. Given that the increase in recharge outside the root zone would be steeper in reality than is represented in Figure 115, the designation of the boundary of root zone influence at 32 m is valid and renders the calculation of *B* relatively insensitive to the designated recharge value outside the root zone. Using a boundary at 32 m and recharge value of 17 mm yr-1 for outside the root zone, *B* is calculated as 30 m, a probable underestimate. If recharge between –10 m and 20 m is assumed similar to that at –10 m, then *B* is calculated to be 40 m. The resulting value for this transect is therefore approximately 35 ±5 m.

Water balance experiment

Due to the labour involved in data collection, measurements from the tree belt experiment were not spatially replicated except for leaf area and ΔS. The crosschecks performed within the data set allow confidence in the measurements. However, independently of this, I have considered the possible errors associated with the calculation of B as being of 3 types:

1. Errors associated with each measurement technique;
2. Errors associated with interpolation of data;
3. Errors associated with extrapolation of data.

For each measurement I have estimated the largest error from each of the above classes and tested the effect of worst-case combinations of errors on the calculation of B - both leaf area measurements (Equation 12) and water balance (Equation 17).

Leaf area

Leaf area estimations using the Adelaide (Module) method (Andrew *et al.*, 1979) were calibrated against destructive sampling of whole canopies (Ellis *et al,* in press) and estimated to be less than 10%. The canopy areas used in the calibration ranged between 14 m^2 and 64 m^2, bracketing all trees in the water balance experiment. Trees in the leaf efficiency experiment however, were up to 4.5 times as large as the largest calibration tree, with higher and denser canopies. The effect of this on leaf area estimations is unknown although it is expected that it would lead to underestimates of larger canopies. Given that leaf efficiencies of all trees are similar in winter, and also similar to those in the water balance experiment, the possible error in canopy leaf area estimation appears not to be an important issue in the leaf efficiency experiment. In the tree belt experiment, *LLA* estimates also rely on linear ground measurements to determine the relevant length of belt. Similar *LLA* values were obtained over belt lengths of 7 m and 30 m, on two separate occasions. I therefore believe that the method of estimating the beginning and end of the effective belt length occupied by the trees – midway between adjacent canopies – was effective and had small associated errors. The standard deviation from the five local *LAI* measurements was 0.1 $m^2\ m^{-2}$. *B* was predicted (Equation 12) using both *LLA* and *LAI* measurements performed within a short period of each other (May 97) to eliminate any seasonal bias. Average tree leaf area however, grew by about 25% between May 97 and January 98. New growth was also observed in local remnant vegetation, and although it was not measured a second time, it was assumed to grow by a similar amount. If this assumption was false and there was no change in local *LAI* during the year, the effect on

predicted B would be about 10%. This was tested using Equation 12 and an average LLA of 19 m^2 m^{-1} (assuming an LLA of 17 m^2 m^{-1} from May to October and a linear increase to 25 m^2 m^{-1} between October and March). A scenario of this kind is unlikely to be this extreme, so any associated error was assumed to be much smaller than 10%.

Transpiration

Hatton *et al.* (1995) calculated a 13% error in transpiration of eucalypts estimated from heat pulse velocity method. This represented the combined errors from: wound diameter; probe placement; volumetric wood and water contents. I examined the possible effects of poor probe installation because it occurred accidentally in our experiment.

Sap velocity was sampled at four positions across the sapwood, and is usually small at the outer (cambium) and inner (heartwood) boundaries of the sapwood, reaching a maximum somewhere in between. The accuracy of flux calculation using the weighted average technique (Hatton *et al.,* 1990) relies on the careful installation of probes to sample sap velocity uniformly across the sapwood. A probe arrangement that is skewed towards either the cambium or the heartwood can result in inappropriate weighting of sampled sap velocities, and inaccurate flux calculations. Skewed installation of probes occurred in two trees over one measurement period. In order to determine the resulting flux error, the effect of grossly skewed installation (only half the sapwood depth sampled) of probes was investigated using a spreadsheet and mock sap velocities and stem dimensions. Simulated sap velocities were zero at sapwood boundaries and distributed as a parabolic function of sapwood depth (Edwards and Warwick, 1984). Probe installations grossly biased toward the cambium boundary and the heartwood boundary caused flux overestimates of 15% and 11%, respectively, when compared with that from properly installed probes. Similar but less serious installation problems occurred once in 2 trees, for parts of spring and summer. I am confident, therefore, that there was less than 10% error in total transpiration due to poor installation.

Missing transpiration data was interpolated for: 12%; 24%; 11%; 6% of the measurement period for: O1; O2; L1; L2 respectively. For all trees except O2, missing data periods were less than a month and were relatively evenly distributed over the measurement period. O2 had 90 days of missing data in one block between July and September during which time transpiration was low and relatively uniform. There was about 20% decrease in the 10-day average transpiration values for O2, either side of this period whereas the transpiration of the other the trees increased by between 10% and 30%. Therefore the maximum likely error in O2 transpiration resulting from this interpolation would be: 15% over about one

quarter of the measurement period; during which time transpiration was about two thirds of average for that tree. The result was a possible 5% error in total transpiration of O2. Interpolation errors for the other trees would have been less than this.

In Chapter 6 the horizontal distribution of across the transect transpiration was also calculated by difference (Figure 43), assuming deep drainage to be zero. A value of total transpiration (by difference) was estimated to be 13% greater than that measured by heat pulse. Given this was the largest estimation of error, and that it is similar to that determined by Hatton *et al.* (1995), I have taken this as the largest most likely error.

Rainfall, interception and stem flow

The weather station rain gauge is purported to be ±2% accurate (Measurement Engineering Australia™). It used a 0.2 mm capacity tipping bucket mechanism that recorded 77 rainfall events during the experiment. Using a possible error of one 'tip' per event, this equates to 15.4 mm or 3%. The error involved in scaling trough and bucket rainfall data to weather station records would also be small ($r^2 = 0.98$; n = 10; 6.6 mm < P < 35.0 mm). The shape of the rainfall transect was extrapolated over a period of 123 days, during which time 25% of the total rain fell. The temporal variation of the shape of the rainfall transect was significant over a short time scale, close to the trees, and was dependent on wind direction. However when data from individual gauges over 10 week periods was regressed against that from the whole period there was good agreement (r^2 = 0.98) and extrapolation was considered to be a minor source of error. The maximum error of rainfall measurement was therefore considered to be less than 10%. Interception error comprised that from the rainfall troughs (about 10%) and that from the stem flow measurements. Stem flow error was about 33%, but because stem flow was small it represented only a 5% error in interception. Maximum interception error was therefore estimated to be 15%.

Evaporation

Evaporation from outside the root zone from P - ΔS was relatively consistent and gave Sdev = 5% for n = 4. By far the greatest uncertainty in total evaporation arises from the extrapolation of the relative root zone evaporation from spring, to the whole measurement period. However the likely error is difficult to determine. Although potential evaporation trebled during the 80-day microlysimeter measurement period, average root zone evaporation, relative to that outside the root zone, showed no trend with time and remained at about 0.6 (Stdev = 0.15, n = 37). Average evaporation outside the root zone was about 1 mm d^{-1} with a slight downward trend over spring. It would appear therefore,

that surface resistance, rather than atmospheric demand, dominated spring root zone evaporation. It is reasonable to assume that this was also the case in both winter and summer, given that the root zone remained relatively dry (Figure 45). Choudhury and Monteith (1988) related surface resistance directly to the depth of air-dry soil. It is likely that relative root zone evaporation was similar during winter and spring, but may have decreased over summer, but by how much is impossible to determine from the data. Assuming that I have overestimated root zone evaporation for the summer period (38% of the measurement period) by 50%, this equates to about a 10% error in total evaporation.

Soil water storage

ΔS was neither interpolated nor extrapolated, and was replicated twice. While errors were large towards the edges of the root zone, they were less than 5 mm between –7.5 m and 8 m positions (Figure 38; Figure 45). A weighted average of the maximum error in ΔS between –15 m and +15 m positions is about 10 mm. Because ΔS was small this represents about 50% error.

Worst-case scenarios

Using a possible 10% error in *LLA* and an *LAI* standard deviation of 0.1, two worst-case scenarios to considered for the prediction of *B* (Equation 12) were calculated by: 1) using the largest *LLA* and the smallest *LAI*; 2) the smallest *LLA* and largest *LAI* measurement. This allowed the calculation of the smallest possible *B* using the smallest numerator and the largest denominator (and *vice versa*) and gave 17 m ≤ B ≤ 26.7 m.

Table 12 Water balance component values and errors from the water balance experiment.

Component	Measured value (from Chapter 6)	% error (from this section)
T	3629 L	13
I	1370 L	15
P	497 mm	10
E	266 mm	10
ΔS	-17 mm	50

A similar approach was used for the water balance calculation using the values and errors shown in Table 12. Maximum and minimum B (from water balance Equation 17) were calculated by: 1) choosing the largest possible values for *T*, *I* and *E* and the smallest

possible values for P and ΔS (ΔS was negative), so as to combine the largest numerator and smallest denominator; and 2) the smallest possible value of B was calculated using the smallest T, I and E, and the largest P and ΔS. This gave 13.0 m $\leq B \leq$ 34.1 m, the maximum value being physically impossible given the root zone width of 27 m.

Appendix 5 – Digital Elevation Model (DEM), rainfall and evaporation surfaces for the Murray Darling Basin

Introduction

This appendix describes the 3 inputs (Digital Elevation Model DEM; rainfall; and evaporation) used to compose the map of potential long-term average *LAI* of natural vegetation in the Murray Darling Basin (Figure 79; based on Equation 23). Yves Bessard and Andrew Bradford, CSIRO Land and Water, Canberra performed all of this work.

Rainfall and evaporation maps were constructed from long-term mean annual rainfall and Class A pan evaporation surfaces extracted from the ANUCLIM/ESOCLIM, version 1.06 package (Hutchinson *et al.*,1998). The authors made use of the entire available records over the 1900-1975 period and use weighting factors to account for the differences in record length, attributing a larger weight to a station that has a longer record.

All maps have a 0.6 degree (~1 km) resolution.

Input 1 – Digital Elevation Model DEM

The following sheets of the 9 seconds (~250 m x 250 m) Auslig DEM were merged to obtain a DEM covering the entire MDB : SG55; SG56; SH54; SH55; SH56; SI54; SI55; SI56; SJ54; SJ55. That grid was resampled to a 0.6 degree cell size. A higher resolution would not have improved the accuracy of the input data, except for interpolation of rainfall surface in the more mountainous area where Equation 23 becomes less applicable. Choosing a coarser resolution also resulted in speeding up the computation and saving storage space. All the operations related to the assembling of the DEM (Figure 132) were performed in the following ArcInfo workspace.

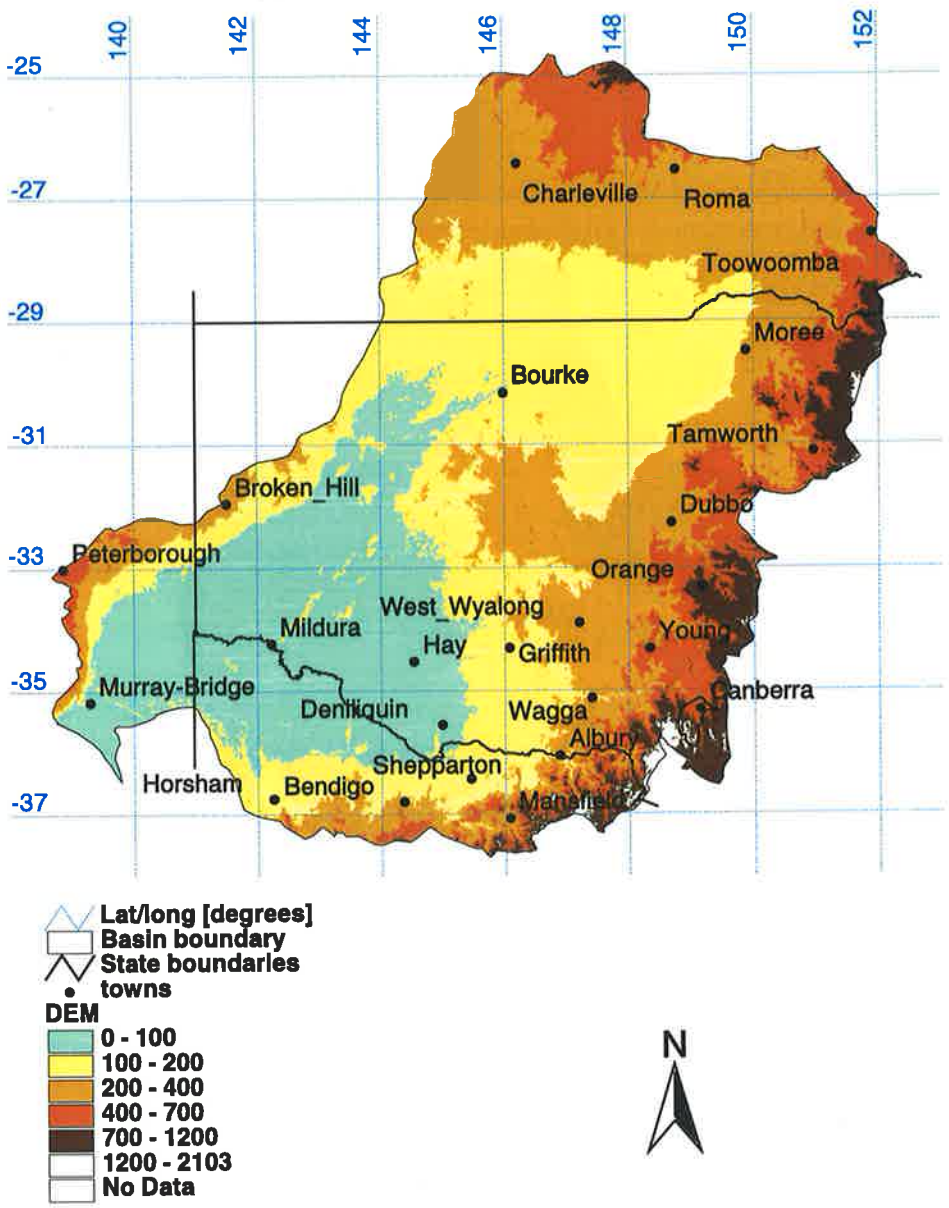

Figure 132 DEM of the Murray-Darling Basin. Elevation is shown in metres.

Input 2 - rainfall surface

Based on the DEM (Figure 132), a long term mean annual rainfall surface (Figure 133) was extracted from the climatic surfaces provided with the ANUCLIM/ESOCLIM package version 1.06 (Hutchinson *et al.*, 1998). Values were weighted according to record duration at each station. The interpolation parameters were latitude and longitude and the elevation above sea level.

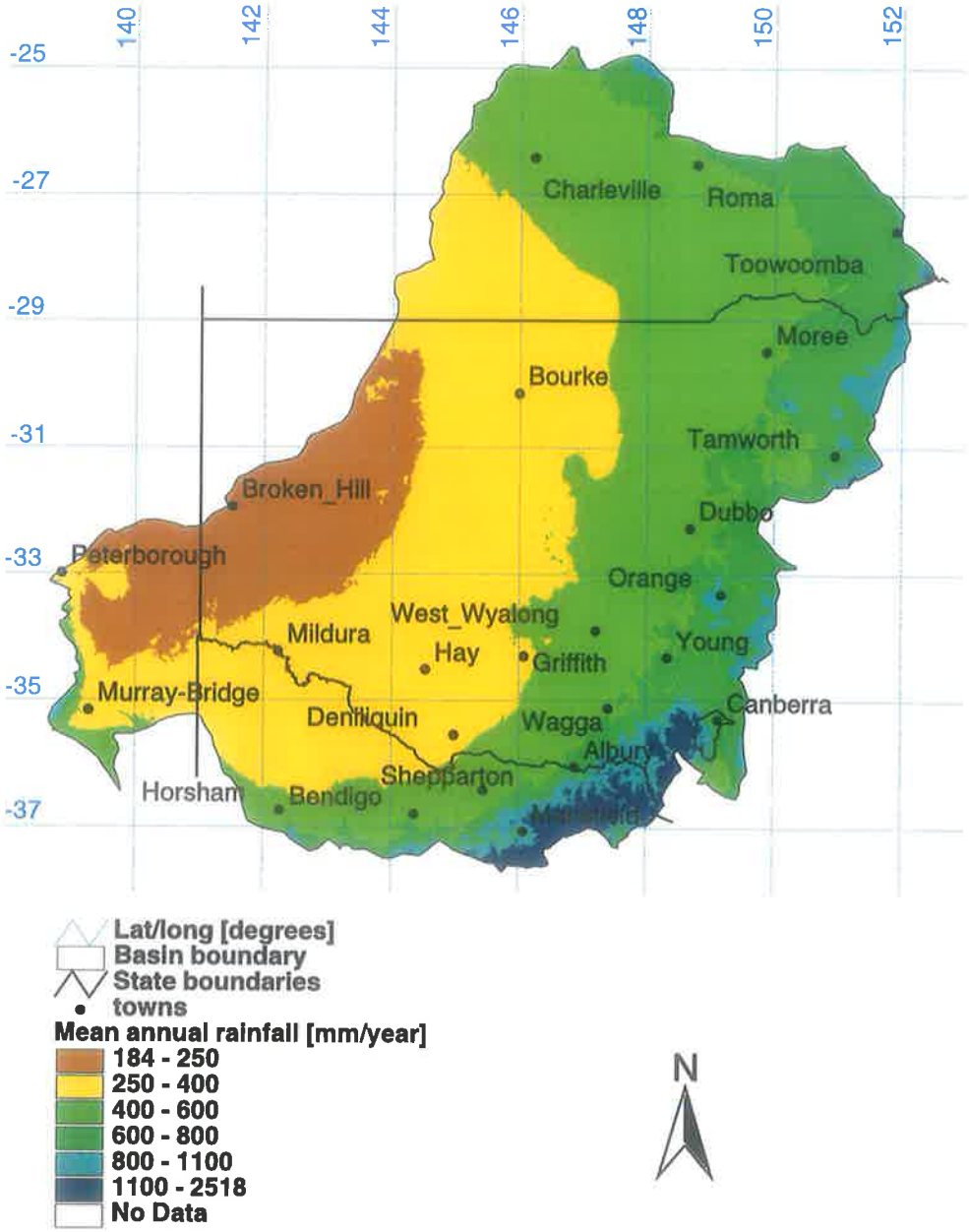

Figure 133 Rainfall map of the Murray-Darling Basin; mean annual long term values in mm yr^{-1}.

Input 3 - evaporation surface

As for the rainfall, a long-term mean annual evaporation surface (Figure 134) was extracted from ANUCLIM/ESOCLIM. Hutchinson *et al.*, (1998), used the Class A pan evaporation measurements as a surrogate for potential evaporation. As for the rainfall, the interpolation parameters were latitude, longitude and elevation.

Pan measurements were extracted from a number of meteorological stations within the Basin that had a record length of at least 5 years. These were used to check long term mean annual values and found to be consistent.

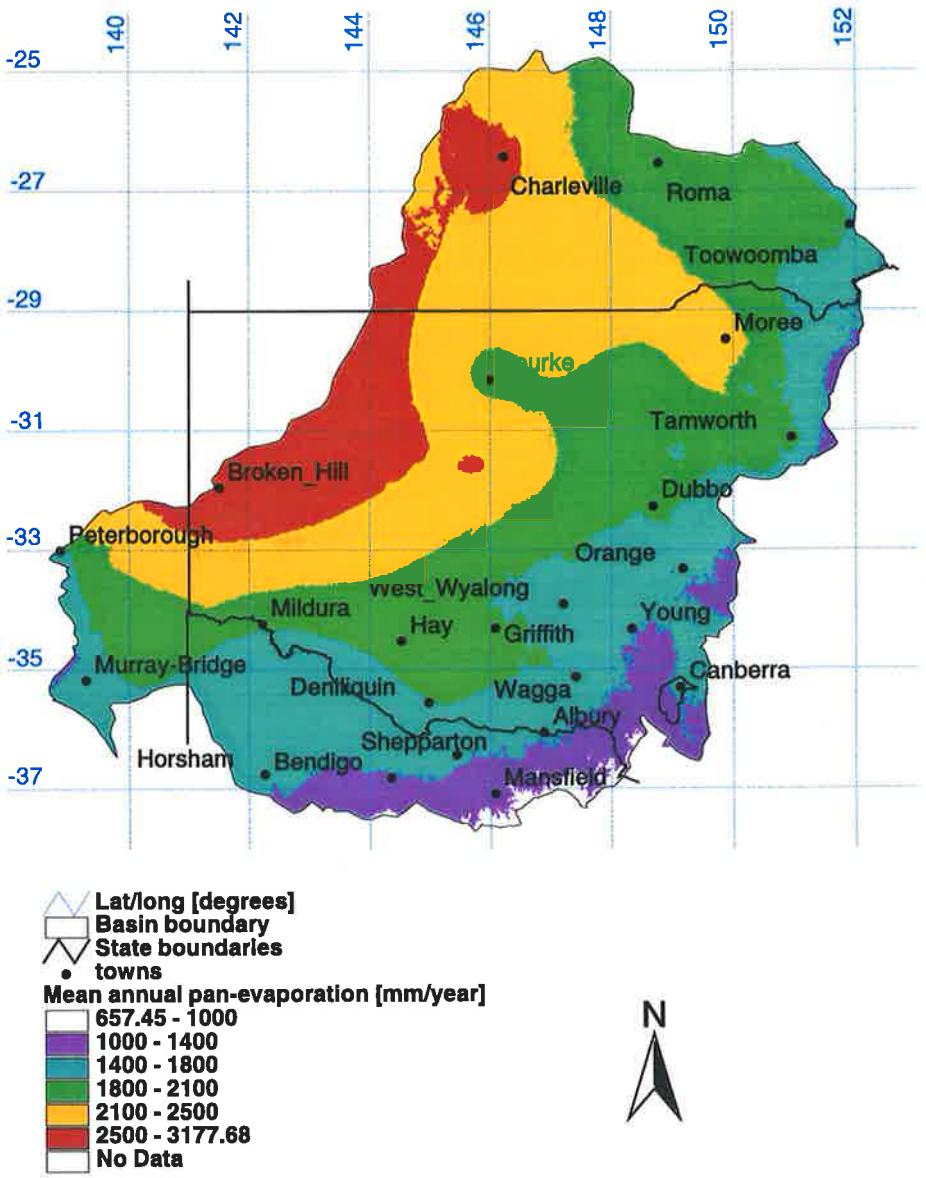

Figure 134 Pan-evaporation map of the Murray-Darling Basin; mean annual long term values in mm yr^{-1}.

The End